Experimental campaign on RC buildings typical of the Groningen region: Cyclic testing of precast wall connections

Emanuele Brunesi and Roberto Nascimbene

Eucentre

(European Centre for Training and Research in Earthquake Engineering)

Date   October 2015

Editors   Jan van Elk & Dirk Doornhof

General Introduction

In Groningen, many buildings have been constructed using pre-cast concrete elements. Often these buildings are not easily recognized as the pre-cast concrete elements making up the structural system are behind masonry veneers, giving the building a masonry appearance.

To better understand the seismic behaviour of the precast concrete panels commonly used in construction in The Netherlands (e.g. Heembeton and Alvon panels and Dycore floors) experiments were conducted. Especially, the connections between the panels are important to understand the seismic response of a pre-cast concrete building. This report describes these experiments on the pre-cast panels.

The results of these experiments are used in the modelling of pre-cast concrete index buildings (Ref. 1) and the preparation of fragility curves for these buildings (Ref. 2).

References

1. Numerical evaluation of the seismic response of the main typologies of non-masonry (non-URM) buildings that are found within the Groningen region – Report on structural modelling of non-URM buildings, Mosayk (H. Crowley, F. Bianchi, D. Cicola, R. Nascimbene, R. Pinho), Eucentre, (European Centre for Training and Research in Earthquake Engineering), October 2015
2. Development of v2 fragility and consequence functions for the Groningen Field, H. Crowley, R. Pinho, B. Polidoro, P. Stafford, October 2015.

Title	Experimental campaign on RC buildings typical of the Groningen region: cyclic testing of precast wall connections	Date	October 2015
		Initiator	NAM
Autor(s)	Emanuele Brunesi and Roberto Nascimbene	Editors	Jan van Elk and Dirk Doornhof
Organisation	Eucentre in Pavia (European Centre for Training and Research in Earthquake Engineering)	Organisation	NAM
Place in the Study and Data Acquisition Plan	Study Theme: Building fragility Comment: In Groningen, many buildings have been constructed using pre-cast concrete elements. Often these buildings are not easily recognized as the pre-cast concrete elements making up the structural system are behind masonry veneers, giving the building a masonry appearance. To better understand the seismic behaviour of the precast concrete panels commonly used in construction in The Netherlands (e.g. Heembeton and Alvon panels and Dycore floors) experiments were conducted. Especially, the connections between the panels are important to understand the seismic response of a pre-cast concrete building. This report describes these experiments on the pre-cast panels. The results of these experiments are used in the modelling of pre-cast concrete index buildings (Ref. 1) and the preparation of fragility curves for these buildings (Ref. 2).		
Directliy linked research	(1) Modelling of seismic response of buildings (2) Development of Fragility Curves (for non-URM buildings) (3) Risk Assessment		
Used data			
Associated organisation	NAM		
Assurance	Eucentre		

Nederlandse Aardolie Maatschappij B.V.

Schepersmaat 2, Postbus 28000, 9400 HH Assen

Experimental campaign on RC buildings typical of the Groningen region: cyclic testing of precast wall connections

EUCENTRE
FOR YOUR SAFETY.

Via Ferrata 1, 27100 Pavia, Italy
Tel. +39.0382.516911 Fax. +39.0382.529131
http://www.eucentre.it
email: info@eucentre.it

LAB AND TESTS RESPONSIBLE	DOCUMENT AUTHOR	REVIEWER
Filippo Dacarro	Emanuele Brunesi	Roberto Nascimbene
Signature	Signature	Signature

	Document type:	
Issue: 22/10/2015		File name: Precast_Panels-test_campaign_report.pdf
Revision: 06/03/2017	Technical report	
Revision:	pages: 189	Protocol EUC191/2014E – EUC319/2015U
Revision:		

Cite as:

Brunesi E., Nascimbene R. (2017). *Cyclic testing of precast panel connections for RC precast wall-slab-wall structure representative of the Groningen building stock.* Report EUC191/2014E – EUC319/2015U, European Centre for Training and Research in Earthquake Engineering (EUCENTRE), Pavia, Italy.

According to law, EUCENTRE Foundation trademark cannot be reproduced, copied or utilized, without the written permission of the EUCENTRE Foundation, which is the owner, except in accordance with established contract conditions pertaining to the production of this document.

This report, produced by the EUCENTRE Foundation, may be reproduced and/or released only in its entirety. Any partial reproduction must be authorized with the written consent by the Eucentre responsible of the project.

Table of contents

1   Introduction and framework of the research

The use of precast concrete in wall and framing systems is widespread in many European and non-European countries, particularly for what concerns single-story or low-rise residential and industrial buildings. Rapid and economical construction, high allowance for quality controls, and less labor required on-site have led the prefabrication of reinforced concrete (RC) elements to become an established technique worldwide in the past fifty years.

While the majority of Italian and European industrial facilities consist of reinforced precast concrete frames comprising continuous monolithic columns and pin-ended beams characterized by high flexibility and low resistance of beam-to-column and panel-to-structure connections, a wider set of solutions may be used for residential structures, depending on design target, building practice and seismicity of the area under investigation. Despite the vast variety of feasible structural schemes and solutions, the seismic response of all of them greatly depends on the behavior of the connection system, and the key role played by proper design and detailing of the joints is well established in the literature [FIB, (2003); FIB (2008); Englekirk (1982); Englekirk (1990); Englekirk (2003); Magliulo et al. (2008); Belleri et al. (2014); Brunesi et al. (2015)]. In the past decade, extensive research was undertaken to test traditional structural layouts and connections in quasi-static, pseudodynamic, and dynamic fashion [Rodríguez and Blandón (2005); Fischinger et al. (2009); Belleri and Riva (2012); Psycharis and Mouzakis (2012a); Psycharis and Mouzakis (2012b); Bournas et al. (2013a); Brunesi et al. (2015)].

Despite significant progress in research, the majority of actual structures have shown inadequate seismic performance [Iverson and Hawkins (1994); Muguruma et al. (1995); Sezen and Whittaker (2006); Adalier and Aydingun (2001); Ghosh and Cleland (2012)] when connections were insufficiently detailed and recent major earthquakes in Italy (May 20 and 29, 2012, Emilia seismic sequences) resulted in a similar scenario [Magliulo et al. (2013); Bournas et al. (2013b); Liberatore et al. (2013); Belleri et al. (2014)]. To point out the prevailing seismic vulnerabilities of precast systems and necessarily of its connections, a comprehensive review of typical solutions and current international design standards will be carried out. In particular, the most critical features and aspects of conventional design practice and inherent seismic performance will be examined in deep details and then synthesized to provide a background to the experimental program and numerical modeling conducted for a set of residential precast layouts that may be assumed as typical and representative examples of past and current Dutch building practice. Results from high-definition 3D solid models will be given and discussed as they will serve as a calibration of either experimental investigations or simplified beam-based modeling procedures that were defined to reproduce the seismic response of entire structural prototypes rather than structural subassemblies.

2 Precast structures and seismic performance: an overview

It is commonly recognized in any major code and standard that one of the prevailing objective in the design of earthquake-resistant structures, either precast or cast-in-place, is to reduce the lateral forces and to accept a certain level of damage in potential plastic hinge zones that are specifically designed and detailed for ductility. One of the main disadvantages of this approach, whether applied to conventional cast-in-place constructions or precast concrete buildings that are specifically designed to behave as "monolithic" is that the aforementioned sacrificial regions in the lateral force resisting system are likely to be sacrificed in moderate and strong earthquakes. Significant damage involving large residual lateral displacements and wide residual cracks is expected to occur with such systems; hence, the cost and consequences of damage after an earthquake can be significant to the building occupant. Uncoupling the energy dissipation mechanism from the structure is an ideal solution that was first conceived and implemented through seismic isolation. This solution, however, has generally been restricted in the United States and New Zealand to nationally significant structures.

Although structural walls are a common and cost-effective way of providing lateral force resistance to buildings in seismic areas of the world there has been a drive to make wall systems more economical. Historically, cast-in-place reinforced concrete has been the most commonly used method of construction for structural wall systems. More recently, there has been an increased use of precast concrete walls of either the tilt-slab or factory-built variety; their design being carried out to emulate the behavior of their cast-in-place counterparts.

Figure 1 schematically compares the response of a conventional reinforced concrete system, a fully prestressed precast concrete system and a partially prestressed (hybrid) concrete system.
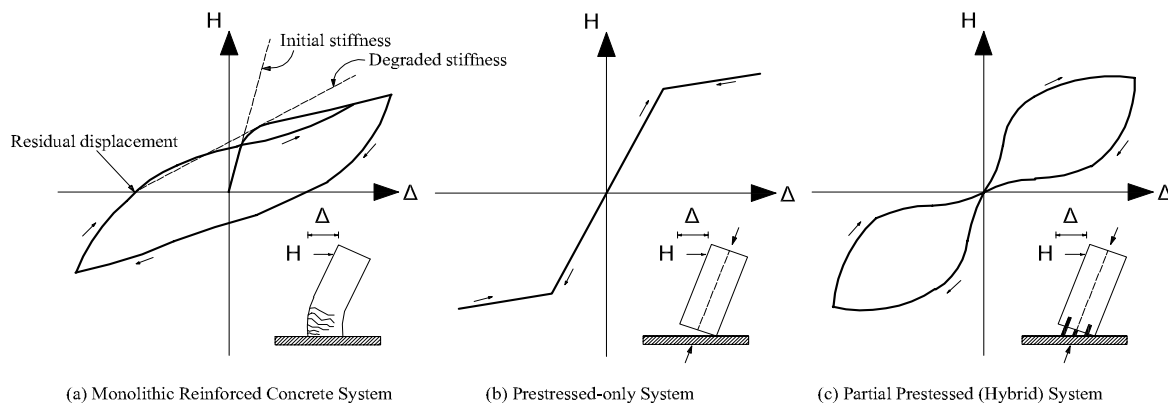

| (a) Monolithic Reinforced Concrete System | (b) Prestressed-only System | (c) Partial Prestessed (Hybrid) System |

Fig.1: Hysteretic response of various structural systems

Monolithic systems can dissipate large amounts of energy, but this is provided through structural damage that results in degradation in stiffness, as well as residual drift. In contrast, prestressed only systems dissipate little energy, which is expected to lead to displacement demands larger than for those systems in which energy dissipation can take place. Precast prestressed systems incorporating energy dissipators can be designed to combine the benefits from both systems, thus providing a good level of energy dissipation and showing self-centering characteristics as well as no damage.

Precast wall construction may emulate cast-in-place construction, with lapped reinforcing bars in concreted or grouted joints.

Fig.2: Lapped reinforcing bars in wall joints, emulating cast-in-place construction (Fib 27)

Alternatively they may be designed with discrete joints that are capable of dissipating energy through ductile connections or damping devices.

Fig.3: Wall panels with discrete joints and ductile connectors (Fib 27)

Limitations in crane capacity often require structural walls to be partitioned. Walls are usually partitioned horizontally, vertically or in both directions. The general aim when partitioning walls is to ensure that the horizontal connection between the wall segments does not influence the overall wall response by adding flexibility and/or by reducing the capacity. That is, horizontal connections

are deliberately made strong with good details to ensure that relative movement between the wall panels is minimized. Vertical connections, on the other hand, can be designed to provide flexibility and to dissipate energy. In some cases vertical connections are deliberately made overstrong to ensure monolithic behavior.
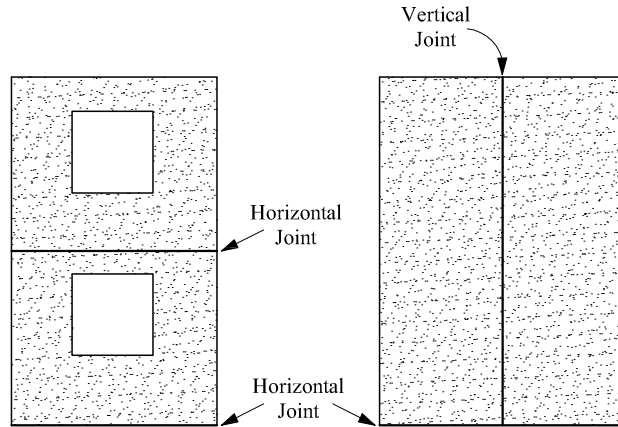

Fig.4: Examples of wall partitioning

Precast concrete structural walls are generally arranged to provide in-plane lateral force resistance primarily through three ways. They are by cantilevering from the foundation structure, through coupling with beams or other special devices, and by rocking about their foundation.
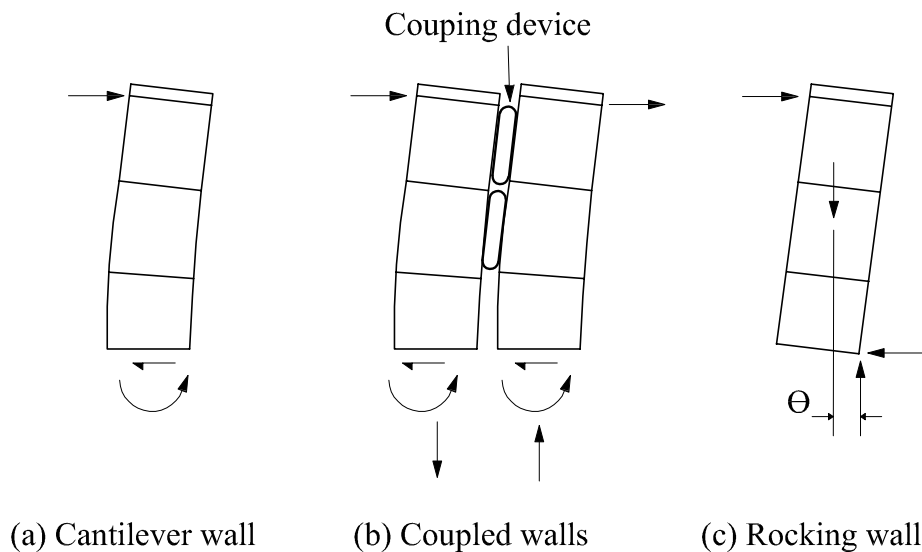

(a) Cantilever wall   (b) Coupled walls   (c) Rocking wall

Fig.5: Classification of precast concrete wall systems according to the in-plane lateral force

resisting mechanisms

Cantilever walls resist the overturning moment resulting from the lateral forces by bending. Coupled walls resist the overturning moment not only by bending of the individual walls but also through an axial force couple. Rocking walls resist overturning moment at the base of the walls through the couple arising from the eccentricity between the acting gravity load and the reaction at the wall-foundation interface. In some cases, rocking walls may be prestressed with unbounded tendons to increase the overturning moment capacity.

The connections are a key component of prefabrication. The ingenuity of the designers and the practical experience accumulated over the years are the basis of the wide range of solutions and theoretical justifications and practices introduced so far. The seismic response of a prefabricated structure depends almost entirely on the behavior of the connections, which must meet a number of requirements related to the project, the level of performance and other criteria. First of all, their main function is to transfer the force from a prefabricated element to the adjacent one, in order to ensure their mutual interaction. This interaction must be sought for the following reasons:

- Connect the individual components to the bearing structure

- To ensure effective global structural behavior desired, due to the interaction of the individual subsystems, such as diaphragms, shear walls, etc..

- Transfer the forces from their point of application to the stabilizing structure

The detailed design of the connections must also meet specific requirements relating to the construction, transport and assembly of individual structural components. In this sense, for example, is particularly important to assess the geometric tolerances.

As regards the transfer of forces, in the case of compression is necessary to take the necessary precautions to avoid contact between the irregular surfaces that may generate a concentration of efforts unwanted capable of causing breakages local or global prepaid than expected.

The actions of traction, instead, are transferred by resorting to various kinds of metal connectors. These connectors can be cast in so as to be continuous in the connection section, or anchored by means of special devices or special devices (overlap of reinforcing bars, tessellation, bolting).

The tensile strength of the connections is generally calculated according to the minimum value between the resistance of the cross section of the metal elements of connection (e.g. re-bars) and the maximum anchoring force of the latter, keeping in mind the various methods of anchoring previously mentioned.

The shear forces between adjacent elements in concrete can be transferred in several ways: through metal inserts embedded or anchored to the concrete by means of keys cutting or shaping of the sections to be connected. In reality there are several additional mechanisms related to friction and the aggregation of the inert, which are generally not covered by the rules, to the advantage of safety (to ensure the transfer of the shear action by friction, for example, is required constant presence of a compression force on the connection).

In the case of connection with protruding re-bars, shear force is transferred through the mechanism called "dowel action". The bars must have sufficient length so that it is verified their anchor, but at the same time must not be excessively long, to avoid instability problems for flexure. The resistance of such a connection is fundamentally dependent on the size of the bars and the concrete strength; the capacity decreases considerably if the shear action is supported by the bars at a certain distance (different position) compared to the section itself. In any case, special reinforcement should be arranged to withstand the potential high tensile stresses that arise at the interface.

Types of standard connections

In the following, a classification of different standard connection typologies will be given. From the point of view of the capacity to transfer actions, connections can be categorized as follows:

a) Hinged connections: this is the case of simply supported beams and vertical elements; this is a simple system of fast execution, in which the horizontal forces are transferred through metal inserts (protruding bars, plugs). They cannot transmit a bending moment.

b) Bending moment resistant connections: connections are able to reproduce the behavior of a cast in situ reinforced concrete system; in the past they were made by parties thrown (monolithic connections), but in the recent years many innovative solutions, even dry (as described in the following chapters) have been designed and implemented.

c) Torque-resistant connections: these systems are typically used for frame structures and the action of the torsion beam is generally converted into a bending action on the element to which the vertical beam is connected.

d) Suspended connections: this is the typical case of horizontal panels; this type of connections is prepared to transfer the weight of the panels to the foundations and at the same time to transmit the actions induced by the wind.

A series of highly detailed connections between structural elements and between the structural elements and non-structural elements can be found in Fip (1990). From a purely typological point of view, however, the connection systems generally used in prefabricated structures, not necessarily in a seismic zone, may be schematized as a function of the elements that are connected to each other.
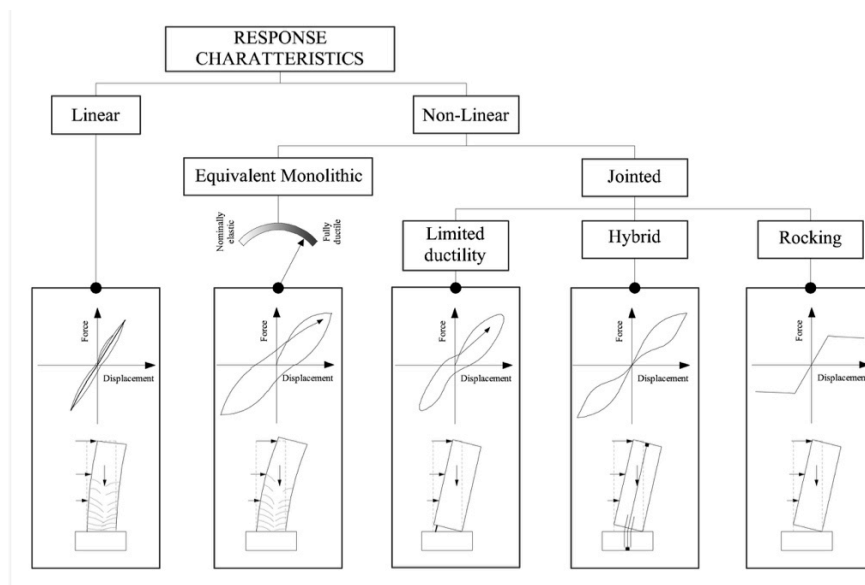

Fig.6: Classification of precast concrete wall systems according to the lateral force – lateral displacement response characteristics(fib Bulletin 27, 2003)

Two following classification may be provided according to their cyclic response:

- Linear response of connections based solely on strength capacity; they may or may not be monolithic. They may be designed to remain in the elastic range and locate the non-linearity in other parts of the structure, or simply their performance may be based only on the strength capacity (e.g. shear).

- Non-linear response of the systems:

  • Monolithic resistant to bending; these are the traditional cast in place connections, which comply with the principle of emulation ca in situ.

  • not monolithic resistant to bending; these systems are not continuous, they are made without casting in place, but they have flexure resistant, and can be divided into:

  - systems with limited ductility;

  - hybrid systems with post-tensioned cables and power dissipation based on the yield of reinforcement;

  - systems based on rocking mechanisms realized by means of post-tensioned cables and energy dissipation with additional devices.

Equivalent monolithic systems

These systems are designed to closely emulate the response of conventional cast-in-place reinforced or prestressed construction in terms of stiffness, strength, ductility capacity and energy dissipation characteristics. The equivalence between a precast concrete system and the cast-in-place counterpart should be determined through experimental work. For example, in Japan a precast concrete system is considered to be equivalent to a monolithic system if the drift of the precast system is within 80% to 120% of the cast-in-place counterpart and if the energy dissipation in the second loading cycle is no less than 80% of that obtained from the response of the cast-in-place counterpart.

Equivalent monolithic systems are designed to ensure that the overall lateral force-lateral displacement non-linear response is ascribed to the development of flexural plastic hinges in aprioristically selected regions of the frames. Such regions are detailed for ductility, depending on the expected local ductility demand. Other regions and elements within the structure are made overstrong to ensure they will always remain in the elastic range thereby avoiding the development of an unexpected and undesirable response and behavioral mechanism.

A major advantage of equivalent monolithic systems is that their design can generally follow the recommendations given in standards for seismic design of cast-in-place concrete systems. In equivalent monolithic systems, the ductility capacity of the system depends on the mechanism of inelastic deformation and on the ductility capacity of the critical section in the plastic hinge region. The ductility capacity of the system ranges from incipient or nominally elastic to fully ductile. The hysteretic response in equivalent monolithic systems depends primarily on the level of prestressing [Park and Thompson (1977), Thompson and Park (1980a and 1980b), Nishiyama (1990)]. The hysteretic response of frames composed of non-prestressed members is reasonably large and comparable to monolithic reinforced concrete framed structures. Equivalent viscous damping ratios of up to 25% are expected for this type of construction. On the other hand, fully prestressed frames have a relatively narrow hysteretic response, showing maximum equivalent viscous damping ratios of the order of 8%. The wall systems in this category are generally designed so that the non-linear response results from flexural plastic hinges in selected regions, usually placed at the base of the wall. Such regions are detailed for ductility in accordance with the expected ductility demand. As mentioned, the ductility of the system ranges from incipient or nominally elastic to fully ductile and the response of equivalent monolithic walls is usually characterized by large hysteresis loops, with

equivalent viscous damping ratios of up to 28% [Holden et al. (2003)]. In addition, these systems can be usually designed using recommendations given in standards for cast-in-place concrete walls.

Jointed systems

These systems are specifically designed so that the non-linear response takes place at aprioristically selected connection interfaces following a pre-determined mechanism of non-linear deformation. In jointed systems, all members are deliberately made overstrong to permit non-linear deformations to occur only at the level of the connections.

Hybrid and rocking systems are two jointed systems with distinct lateral force-lateral displacement response characteristics, as shown in Fig. 9. In hybrid frame systems, mild-steel reinforcement and unbonded prestressing tendons are combined at the critical connections to obtain a centered oriented hysteretic response that results in little or no residual lateral displacements. These systems present equivalent viscous damping ratios of up to 18%.

Rocking framed systems are usually characterized by a non-linear elastic response due to the elastic restoring force provided by the presence of the prestressing tendons. Rocking frame systems differ from hybrid systems because prestressing solely provides moment resistance at the connection. The source of energy dissipation is crushing of the compressed concrete at the end of the connection. Equivalent viscous damping ratios for rocking frame systems are typically no more than 5%. Some reinforced concrete systems that have used relatively weak connections between elements, achieved mainly by welding, bolting and dry packing, can be considered as a branch of jointed systems. They are in the limited ductility category shown in Fig. 9.

The first jointed system comprises walls designed for limited ductility response. In one limited ductility jointed wall design, the connection between the precast reinforced concrete wall panels is so that planes of significantly reduced stiffness and strength exist at the interface between adjacent precast concrete wall panels. Such construction has been extensively used in New Zealand in tilt-up construction generally of one to three storey apartment, office and industrial buildings. Generally tilt-up wall panels are secured to the adjacent elements using jointed connections comprising various combinations of concrete inserts, bolted or welded steel plates or angle brackets, and lapped reinforcement splices within cast-in-place joining strips. A tilt-up construction is generally designed for elastic or limited ductile response. In another limited ductility jointed wall design the reinforcing bars which pass through the wall-to-foundation connection are designed to yield and provide energy dissipation. A major design consideration in this system is the effect that sliding shear can have on the response. Sliding shear leads to pinching and can result in large permanent lateral deformations. Sliding shear is minimized in this system when the gravity load exceeds the ultimate tensile force of the reinforcing bars passing through the connection. In this particular case a self-centering response, similar to the response of hybrid wall systems described below, is obtained.

The second jointed system comprises hybrid walls. In hybrid walls energy dissipation devices (e.g. mild-steel reinforcement, u-shaped plated coupling devices, etc.) and unbonded prestressing tendons are combined to obtain a self-centering mechanism that eliminates residual displacements following an earthquake. This results in a centered-oriented hysteretic response, with equivalent viscous damping ratios of up to 20% [Restrepo (2002)].

The third jointed system comprises rocking walls. In rocking walls the non-linear response results from the opening of a gap at the wall-to-foundation interface. The response of rocking walls is essentially non-linear elastic; these systems also have the self-centering characteristics of hybrid systems but lack energy dissipation capacity.

3 International standards

This document is a state of the art on the response and mechanical behavior of connection systems for concrete structures that is based on international standards, guidelines and recommendations on the subject, particularly for the case of prefabricated structures.

The main advantages of incorporating precast reinforced and precast concrete in construction are the significant increase in the speed of construction, the high quality of precast concrete units and the improved durability, as well as their versatility, their multipurpose potential and less formwork and labor required on-site.

By contrast, the main disadvantages are that economical and effective means need to be developed for joining precast concrete elements together to resist seismic actions. The construction techniques for the joints between precast concrete elements may be unfamiliar and need to be conducted with high quality controls. Relatively small tolerances may need to be worked within, and enhanced craneage may be required to lift heavy precast concrete units.

3.1 Codes, guidelines, recommendations and specifications

In light of the aforementioned observations, a brief review of the prevailing specifications for the systems under investigation will be given in the following, in order to create a background for the upcoming discussion of experimental and numerical investigations. Definitions will be provided for wall and connection systems, according to current US and European seismic rules.

3.1.1 Definition of a wall system according to Eurocode 2

The Eurocode 2 (par. 9.6) defines wall a reinforced concrete element with a length to thickness ratio of 4 or more and in which the reinforcement is taken into account in the strength analysis. The amount and proper detailing of reinforcement may be derived from a strut-and-tie model.

The vertical reinforcement area should lie within $A_{s,vmin}$ and $A_{s,vmax}$: the value of $A_{s,vmin}$ for use in a Country may be found in its National Annex and the recommended value is $0.002\ A_c$; the value of $A_{s,vmax}$ for use in a Country may be found in its National Annex and the recommended value is $0.04\ A_c$ outside lap locations unless it can be shown that the concrete integrity is not affected and that the full strength is achieved at the ultimate limit state (ULS). This limit may be doubled at laps.

The horizontal reinforcement running parallel to the faces of the wall (and to the free edges) should be provided at each surface. It should not be less than $A_{s,hmin}$. The value of $A_{s,hmin}$ for use in a Country may be found in its National Annex and the recommended value is either 25% of the vertical reinforcement or $0.001\ A_c$, whichever is greater. The spacing between two adjacent horizontal bars should not be greater than 400 mm.

The transverse reinforcement in any part of a wall where the total area of the vertical reinforcement in the two faces exceeds $0.02\ A_c$, transverse reinforcement in the form of links should be provided in accordance with the requirements for columns. The large dimension referred to in 9.5.3 (4) (i) need not be taken greater than 4 times the thickness of the wall. Where the main reinforcement is placed nearest to the wall faces, transverse reinforcement should also be provided in the form of links with at least of $4/m^2$ of wall area. The transverse reinforcement need not be provided where welded wire mesh and bars of diameter $\varphi \leq 16$ mm are used with concrete cover larger than 2φ.

3.1.2 Classification of precast structures and connection systems according to Eurocode 8

In the context of European rules, prefabricated structures are regulated in Part 1 Chapter 5.11. In this chapter the code gives a classification of the possible structural types:

- frame systems;

- wall systems;

- dual systems (mixed precast frames and precast or monolithic walls);

- wall panel structures (cross wall structures);

- cell structures (precast monolithic room cell systems).

The code suggests to identify the different roles of the structural elements when modeling precast structures as one of the following:

- those resisting only gravity loads, e.g. hinged columns around a reinforced concrete core;

- those resisting both gravity and seismic loads, e.g. frames or walls;

- those providing adequate connection between structural elements, e.g. floor or roof.

Three types of connection are identified in relation to the dissipation capacity of the structure:

- connections located well outside critical regions, not affecting the energy dissipation capacity of the structure;

- connections located within critical regions but adequately over-designed with respect to the rest of the structure, so that in the seismic design situation they remain elastic while inelastic response occurs in other critical regions;

- connections located within critical regions with substantial ductility.
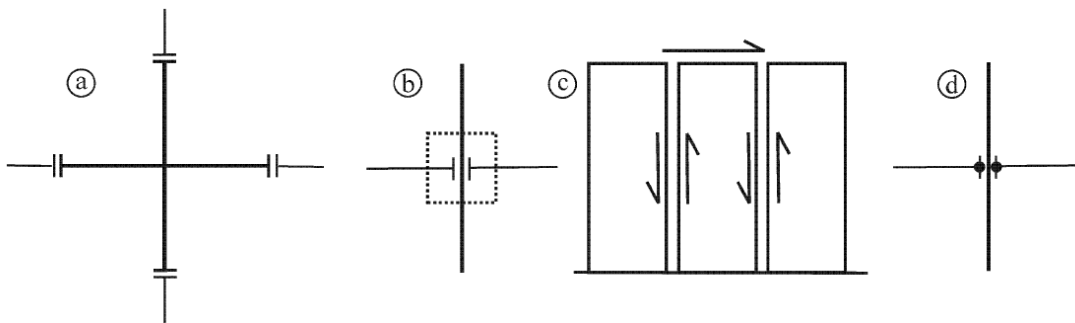
Fig.7: a) connection located outside critical regions; b) overdesignedconnection with plastic hinges shifted outside the connection; c) ductile shearconnections of large panels located withincritical regions (e.g. at ground floor);and d) ductile continuityconnections located within critical regions of frames

In relation to the local resistance of the elements, the cyclic deformation in the post-elastic field can lead to a decay in the resistance of the connection itself, degradation that must be properly taken into account by reducing the connection resistance evaluated in a monotonic fashion. In general, this degradation is more than offset by the partial safety factors adopted materials. In addition to plastic rotations in elements, prefabricated structures are able to dissipate energy through more complex mechanisms in the joints that the rule defines "plastic shear mechanisms", but on condition that they are checked on the following two conditions: i) the forces dissipating should not degrade much during the earthquake; ii) should be discarded carefully the possible instability.

With regard to the three types of connection mentioned before, it can be assumed that the connection is outside the critical zone provided that this is at a distance from the end of the same at least equal to the maximum dimension in plan of the cross section. It also must be designed to absorb a shear resistance equal to that obtained by the project with the hierarchy of strength increased by 10% in ductility class average and 20% in high ductility class to take into account work hardening of the steel, and for a bending stress equal to the time obtained from analysis incremented as for cutting. If the link is located in the critical region, this can be considered oversized if designed to absorb bending stress equal to the moment of resistance of the current section increased by 20% in ductility class average and 35% in high ductility class and respects the hierarchy of resistance with regard to the shear resistance. If the connection is to represent the dissipative element, it must meet the criteria of flexibility provided in the rule, and such evidence is obtained by means of cyclic tests in the plastic range; the connection must have the same characteristics of ductility of a monolithic connection in place in the same section.

3.1.3 Metal anchors for use in concrete – ETAG

The Guideline for European Technical Approval (ETA) of "Metal anchors for use in concrete" sets out the basis for assessing anchors to be used in cracked and non-cracked concrete or in non cracked concrete only and consists of:

- – Part 1 Anchors in general;

- – Part 2 Torque-controlled expansion anchors;

- – Part 3 Undercut anchors;

- – Part 4 Deformation-controlled expansion anchors;

- – Part 5 Bonded anchors;

- – Part 6 Anchors multiple use for non-structural applications.

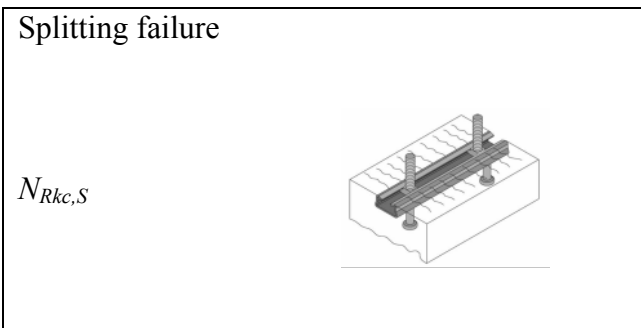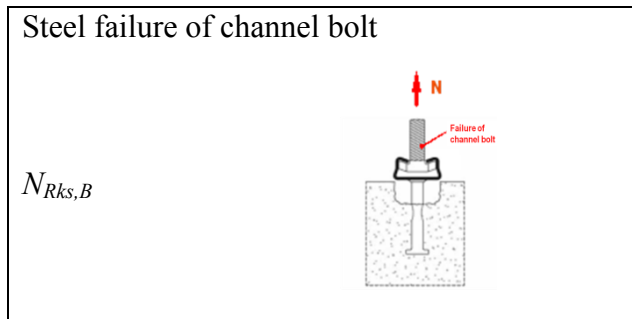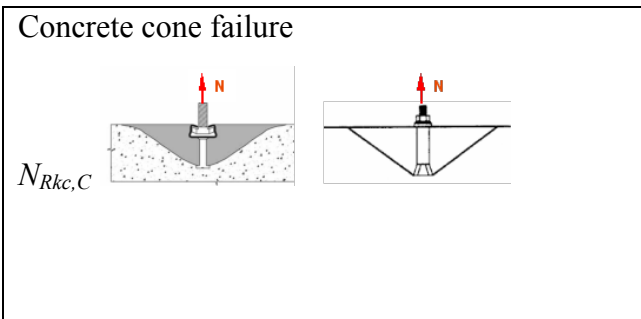The document also includes three annexes which contain:

• Appendix A: Details of tests;

• Appendix B: Tests for admissible service conditions – Detailed information;

• Appendix C: Design methods for anchorages;

• Appendix E: Assessment of metal anchors subjected to seismic action (April 2013).

There are 13 different failure mechanisms that account for the shear stress and the traction on the concrete side and on the side steel. For each mechanism is provided a calculation model, as well as for the verification of the combined stresses composed shear-traction.

Resistance of the connection to TENSION LOADS

CONCRETE failure	STEEL failure

Concrete cone failure

$N_{Rkc,C}$

Steel failure of channel bolt

$N_{Rks,B}$

Splitting failure

$N_{Rkc,S}$

Steel failure of anchors

$N_{Rks,P}$

Pullout failure

$N_{Rkc,P}$

Failure due to the flexure of the channel

$N_{Rks,C}$

Blow – out failure

$N_{Rkc,B}$

Local flexure of the channel
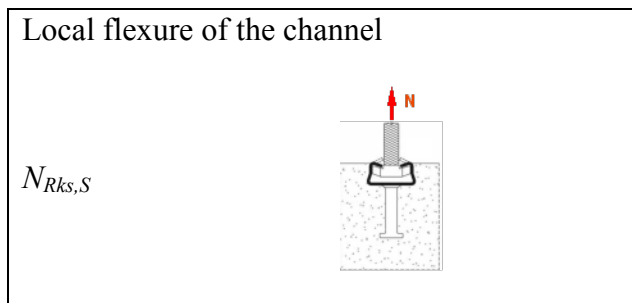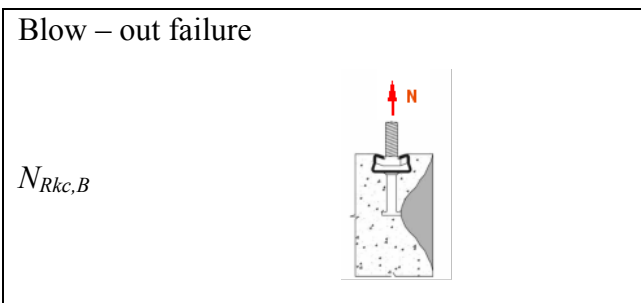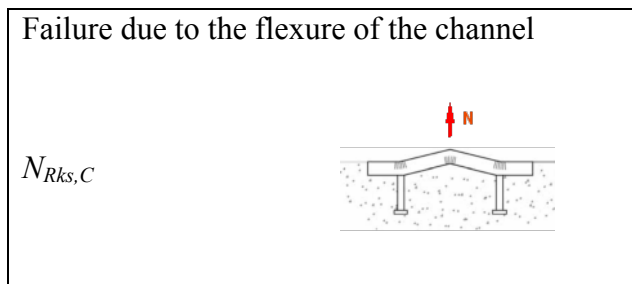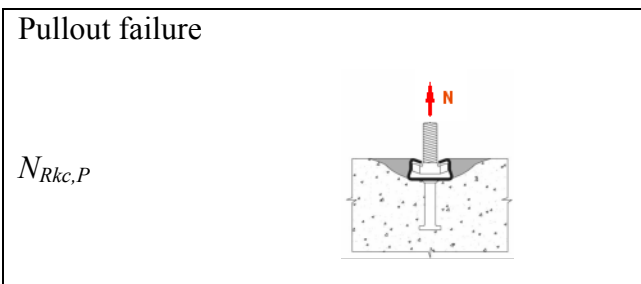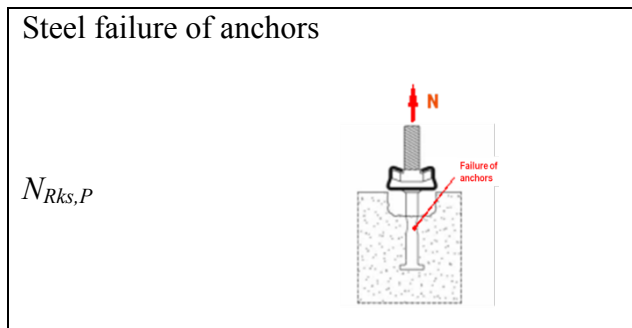
$N_{Rks,S}$

Resistance → $N_{Rd} = min\{N_{Rkc,C}; N_{Rkc,S}; N_{Rkc,P}; N_{Rkc,B}; N_{Rks,B}; N_{Rks,P}; N_{Rks,C}; N_{Rks,S}\}/\gamma_M$

Fig. 8: Failure mechanisms in case of connection between the structural elements subject to traction action

Resistance of the connection to SHEAR LOADS

CONCRETE failure	STEEL failure

Concrete edge failure $V_{Rkc,C}$	Shear failure of the bolt $V_{Rks,B}$

Pry-out failure failure $V_{Rkc,P}$	Shear failure of the channel $V_{Rks,C}$

	Shear failure of anchors $V_{Rks,P}$
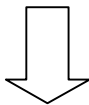
Resistance $\rightarrow V_{Rd} = min\{V_{Rkc,C}; V_{Rkc,P}; V_{Rks,B}; V_{Rks,C}; V_{Rks,P}\} / \gamma_M$

Fig.9: Failure mechanisms in case of connection between the structural elements subject to shear action

3.1.4   FEMA P-751: definition of a precast structure

Tilt-up concrete wall buildings in all seismic zones have long been designed using the precast wall panels as concrete shear walls for the seismic force-resisting system. Such designs usually have been performed using design force coefficients and strength limits as if the precast walls emulated the performance of cast-in-place reinforced concrete shear walls, which they usually do not. Tilt-up buildings assigned to Seismic Design Category C or higher should be designed and detailed as intermediate or special precast structural wall systems as defined in ACI 318.

In addition to the Provisions, the following documents are either referred to directly or are useful design aids for precast concrete construction:

- ACI 318 American Concrete Institute. 2008. Building Code Requirements for Structural Concrete.

- AISC 360 American Institute of Steel Construction. 2005. Specification for StructuralSteel Buildings.

- AISC Manual American Institute of Steel Construction. 2005. Manual of SteelConstruction, Thirteen Edition.

- Moustafa Moustafa, Saad E. 1981 and 1982. "Effectiveness of Shear-FrictionReinforcement in Shear Diaphragm Capacity of Hollow-Core Slabs."

- PCI Journal, Vol. 26, No. 1 (Jan.-Feb. 1981) and the discussion contained inPCI Journal, Vol. 27, No. 3 (May-June 1982).

- PCI Handbook Precast/Prestressed Concrete Institute. 2004. PCI Design Handbook, SixthEdition.

- PCI Details Precast/Prestressed Concrete Institute. 1988. Design and Typical Details ofConnections for Precast and Prestressed Concrete, Second Edition.

- SEAA Hollow Core Structural Engineers Association of Arizona, Central Chapter. Design andDetailing of Untopped Hollow-Core Slab Systems for Diaphragm Shear.

3.2   Scientific researches

In this Paragraph, a review of recent advanced on the topic covered by this report will be provided in order to point out the prevailing observations concerning the behavioral aspects of these systems. In particular, a wide set of scientific contributions will be examined and discussed to examined and explore even further the experimental response of these systems.

To start with, in a recent study of Pavese and Bournas published in 2011, the authors investigated experimentally the behaviour of prefabricated reinforced concrete sandwich panels (RCSPs) under simulated seismic loading through a large experimental campaign. The prevailing results obtained will be summarized in the following, after a brief description of the construction technology which characterized those members.

A reinforced concrete sandwich panel (RCSP) is composed of an Expanded Polystyrene (EPS) foam core with a prefabricated galvanised steel wire mesh reinforcement encased in two layers of sprayed concrete on both sides.

The steel wire mesh of reinforcement mounted on each face of the polystyrene foam is drawn with hot galvanisation and consists of 2.5 mm and 3.5 mm diameter horizontal and longitudinal reinforcement, respectively. The spacing was assumed to be 65 mm; as a result, this assumption gives a longitudinal reinforcement ratio of 0.42%, which is more than the minimum longitudinal reinforcement of 0.2% that is prescribed in the Eurocode.

An example of the technology studied by Pavese and Bournas is given in Figure 10.
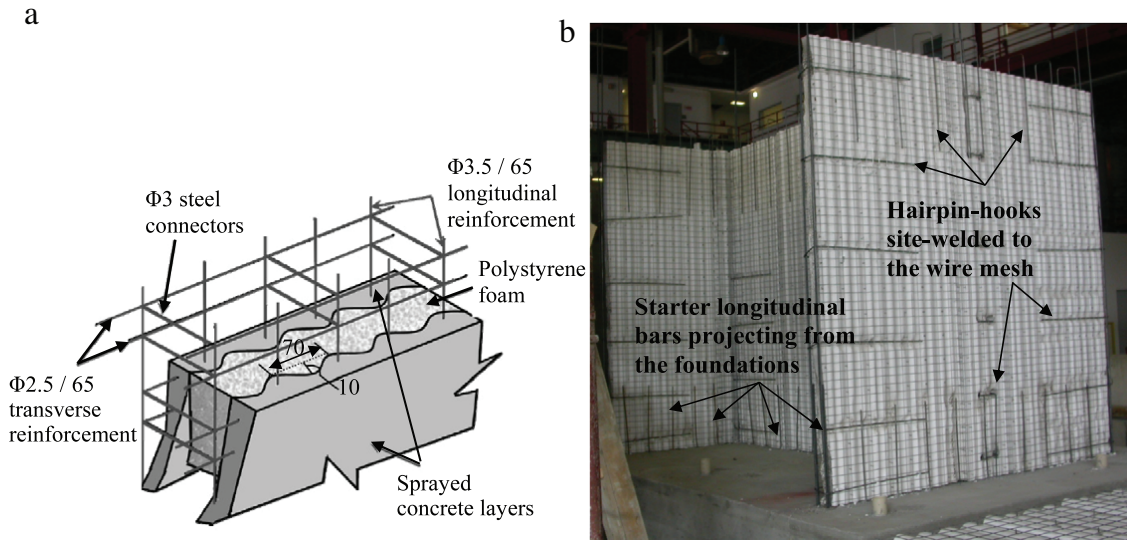
Fig.10: (a) Detail of a typical prefabricated RCSP. (b) Starter longitudinal bars connecting vertical panels with foundations and slabs.

The connection between the two concrete layers through the core of the wall panel is secured with 3 mm diameter steel connectors welded to the front and back wire meshes through the polystyrene. These connectors (~80/m^2) could be straight or inclined depending on the manufacturing plan. The uniform connection between the parts of the sandwich panel is also favoured by the surfaces of the polystyrene which have been initially corrugated. The panels considered in this study have depth and length of corrugation equal to 10mmand 70 mm, respectively.

Typical characteristics of low-rise buildings constructed with this construction system comprise 1-5 stories with 3 m height and typical span of the walls 3-5 m. The wall thickness ranges from 150 mm to 200 mm depending on the thickness of the EPS foam, while the density of the sandwich panel may be varying between 0.9 and 1.1 t/m^3. The fundamental period of vibration for a characteristic 3-storey building of this type is low, and in general does not exceed 0.2s, if full fixity at the base is assumed. The wall structure has small natural periods (in the elastic range), may often lengthened substantially if soil-structure interaction is properly accounted for.

Tests were carried out on single full-scale panels with or without openings, simulating the behaviour of lateral resisting cantilevers and fixed-end walls.
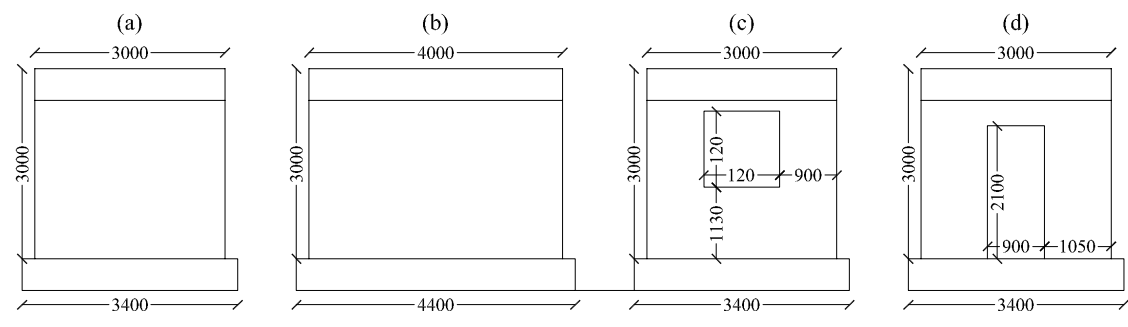
Fig.11: Geometry of panels: (a) P3S_150, P3S_300, P3D_150 and P3D_300. (b) P4S_150 and P4S_300. (c) P3S_150_W and P3S_300_W. (d) P3S_150_D and P3S_300_D. (Dimensions in mm.)

The second part of the experimental campaign comprises the test of a 2-storey full-scale H-shaped structure which was subjected to horizontal cyclic loading applied in the plane of the web under

constant vertical load. The H-shaped structure, which was constructed by six horizontal wall panels (three in each floor)and two 0.2 m thick RC slabs, is 3.50-by-2.75 m in plan; it has two 2.75 m tall stories
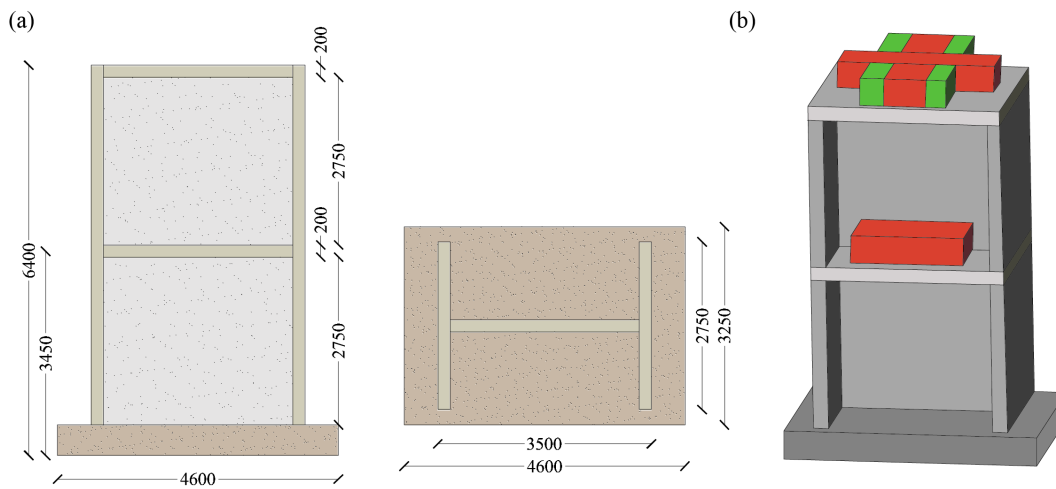
Fig.12: (a) Geometry of the 2-storey H-shaped structure. (Dimensions in mm.) (b) Isometric view of the H-shaped structure
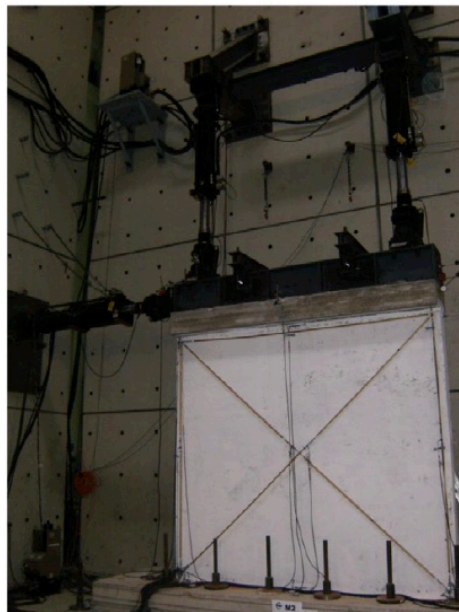

Fig.13: Photograph of the test setup of the panels tested with fixed ends

The performance and failure mode of all panels tested revealed strong coupling between flexure and shear due to the squat-type geometry of the panels.

The prefabricated walls of the structural system investigated herein seem to meet all the requirements of Eurocode 8 for walls to be designed as "large lightly reinforced walls".
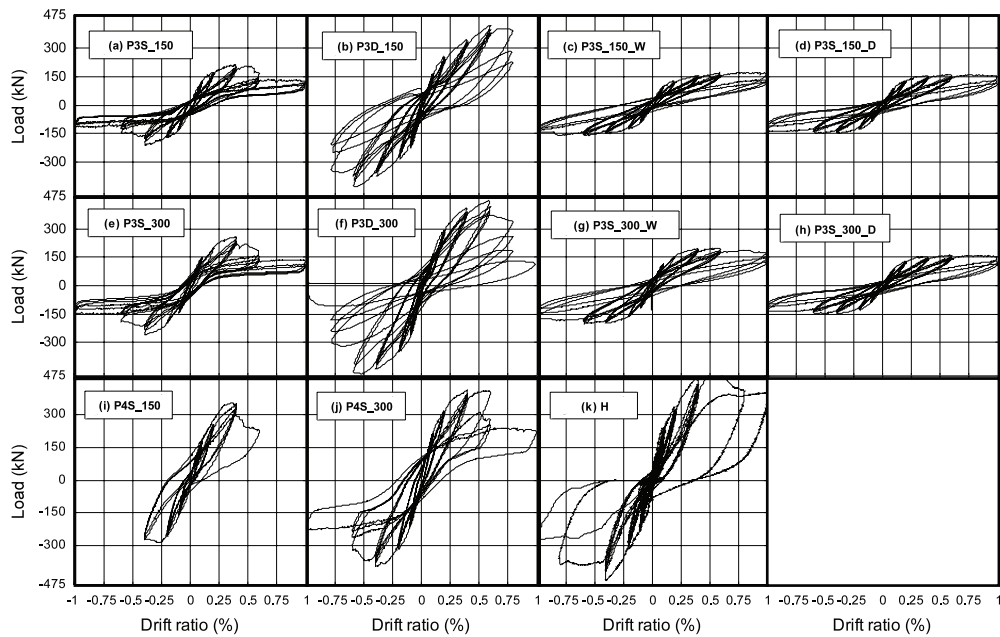
Fig.14: Load versus drift ratio curves for all specimens tested.

The walls without openings tested as cantilevers (single bending setup), developed significant bidirectional tensile and shear cracks but finally failed due to concrete crushing and bar buckling at the base of their corners. Bar buckling at wall end sections could be prevented by providing adequate confinement to these sections, which could be achieved with the creation of well-detailed concealed columns. The response of the walls tested with fixed ends (double bending configuration) was primarily controlled by shear mechanisms. However brittle failure owing to diagonal tension was controlled due to the well-detailed steel reinforcement.

The response of panels with openings was initially controlled by shear cracking which was not accompanied by lateral strength degradation due the good detailing of steel reinforcement, which prevented sudden shear failure.

The response of the H-shaped structure was mainly governed by shear cracking on the web and by flexural yielding of the flanges.

The increase of the walls' length (from 3 to 4 m) resulted in an increase of walls' shear resistance in the order of 50% regardless of the level of axial load; whereas the deformation capacity at failure was practically unaffected.

The strength of the walls with windows and doors decreased on the average (for both levels of axial load) by 28% and 48%,respectively. Their damping capacity was affected to a lesser extent by the presence of openings, with corresponding average decreases equal to 13% and 17%, respectively. On the contrary, the presence of openings in the prefabricated walls resulted insubstantial increases of the deformation capacity in the order of80%.

In the study of Palermo et al. (2014), the experimental results of a series of shaking table tests performed on a full-scale 3-storey building composed of thin reinforced concrete sandwich walls are presented, as will be discussed hereafter.

R/C slender walls have been the objective of numerous extensive research works, starting from the '60s, and nowadays their seismic behavior is fairly well understood since most code provisions give detailed guidelines to the practitioners. On the contrary, less research effort has been devoted to R/C

squat walls, despite they showed valuable strength resources (limited damages) during large earthquakes (e.g. Montenegro and Chile).

Sandwich R/C walls are characterized by basic characteristics – like thickness, reinforcement ratios, construction details – which are far from those of traditional R/C walls and they may exhibit a quite complex behavior due to the interaction between the R/C elements and the connections. Therefore experimental tests are required to provide a reliable assessment of their behavior.

The basic elements of the studied structural system are polystyrene modular panels acting as support for the concrete casting. The single modular panel has a fixed length of 1120 mm and a variable height equal to the building inter-storey height (Fig. 1). It is composed of a single corrugated polystyrene sheet (with thickness between 60 and 160 mm in order to accomplish different thermal and acoustic requirements) inserted between two grids of electro-welded steel wire mesh. The wire meshes are connected by metallicties (having a diameter of 3 mm and typically placed in quantity of 40-50 per m^2). At the edges of the modular panel, the wire meshes are overlapped of about 100 mm in order to guarantee the adequate anchorage. The steel mesh is typically characterized by 2.5 mm diameter and it is 50 mm spaced along both the vertical and horizontal directions.

The modular panels are assembled in situ in order to obtain the so-called support walls of the desired dimensions. Additional reinforcements are added: (i) around the openings (windows/doors) and (ii) at the edges of the support walls, in order to provide the necessary over-strength in highly stressed zones. Once the support walls are set in place, two shotcrete layers of typically 40 mm thickness are sprayed to obtain the R/C wall. The amount of the base reinforcement provided by the wire mesh (i.e. Ø2.5/50 mm x 50 mm) together with the typical total thickness of the two concrete layers (40 + 40 mm) leads to a reinforcement ratio equal to 0.00245 (without any additional bars).

The connections between walls and foundations are realized through anchor rods (1 + 1Ø8/30 cm, anchorage length equal to60 cm).

(a)   (b)
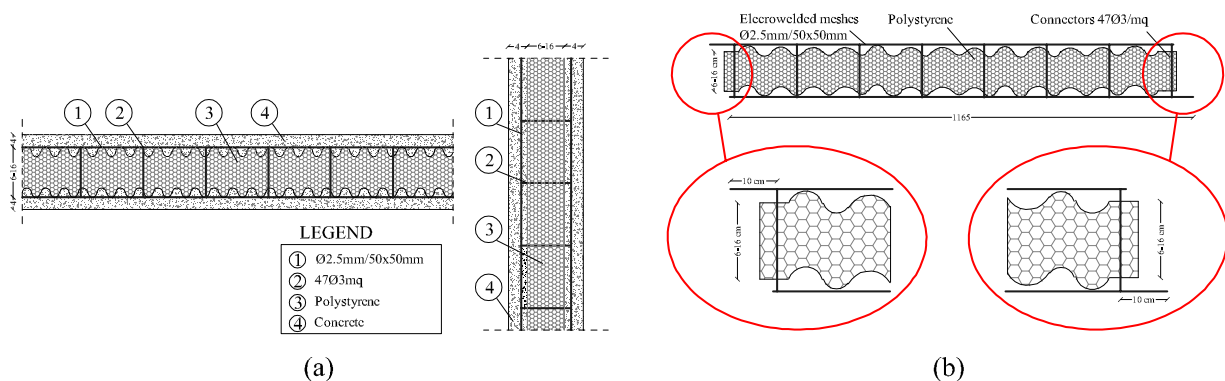
Fig.15: (a) The modular panel; (b) details of the edge.

A full-scale 3-storey building was chosen as the prototype building. The building dimensions in plan are equal to 4.10 m x_ 5.50 m. The building height is equal to 8.25 m, with equal inter-storey heights of 2.75 m.
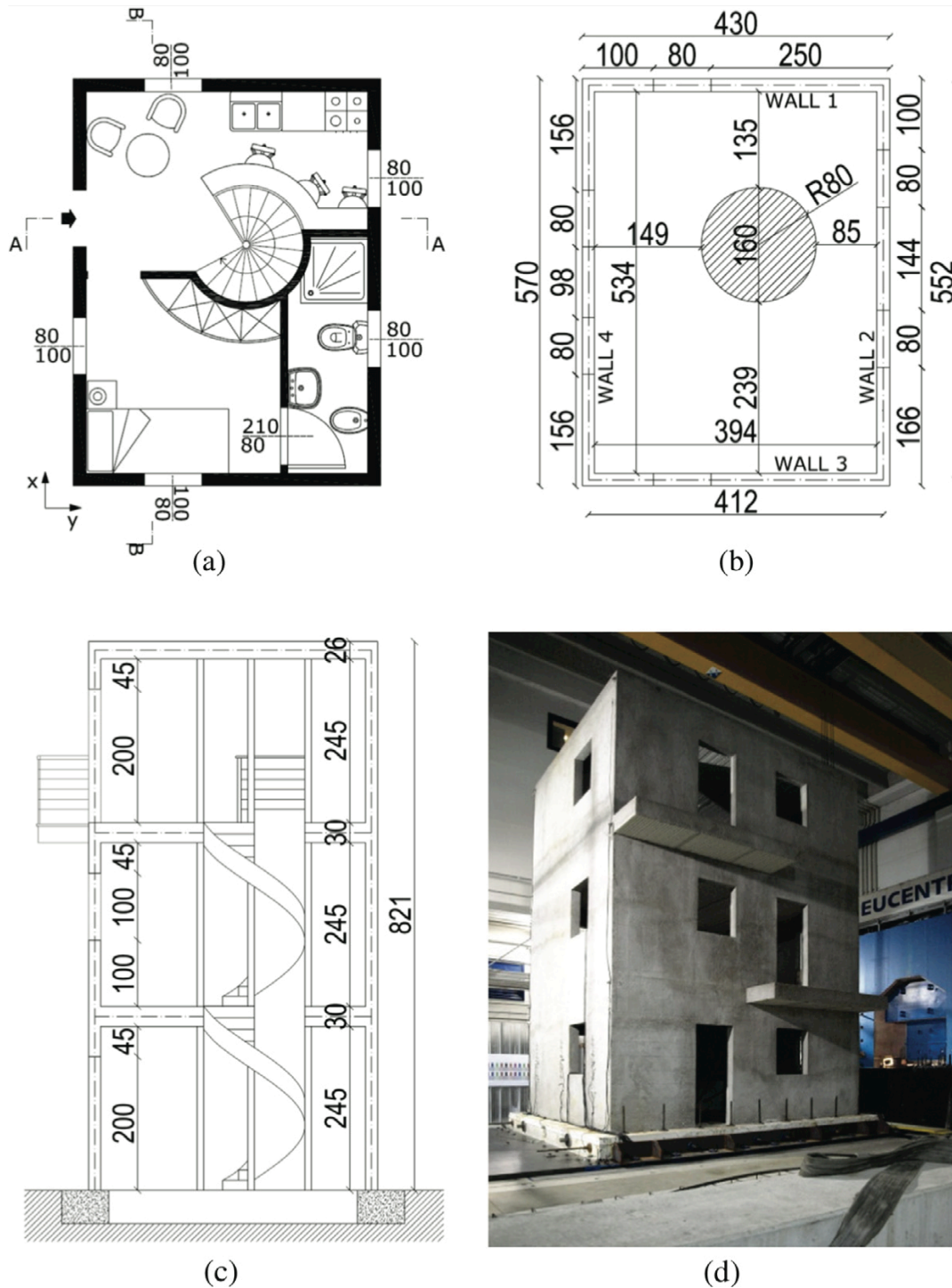
Fig.16: (a) First floor architectural plan; (b) first floor structural plan and exterior walls nomenclature; (c) section A‑A; (d) the prototype building.

The materials adopted for the design phase may be summarized as follows:

– Shotcrete having strength properties similar to those of C35/30 concrete (according to the Italian building code) for the walls. In detail, the specific material is referred to as "RR32"

– C25/30 concrete for the additional R/C elements.

– Smooth galvanized steel with low carbon content classified as "C7D" (according to UNI EN 10016-2) for the wire mesh.

- B450C corrugated steel (according to the Italian building code) for the additional reinforcement.

Figure 17 presents the details of typical reinforcement arrangement provided at the corners of the openings.
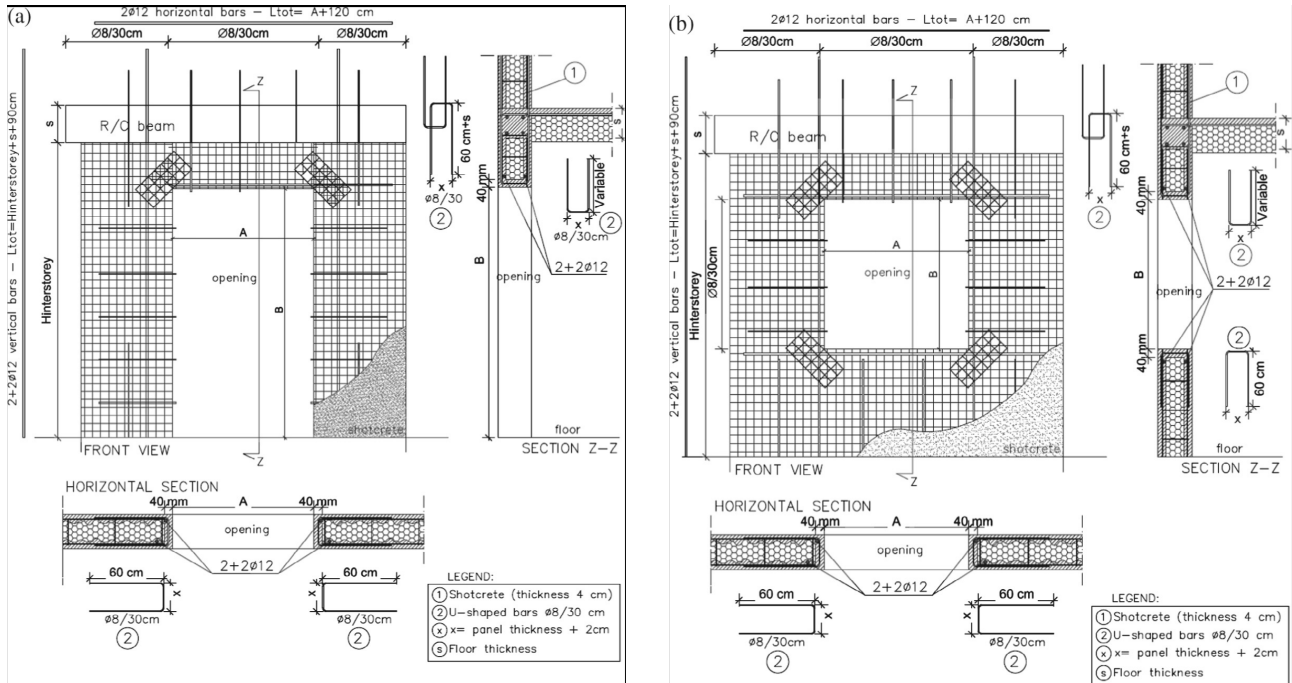
Fig.17: Details of the added reinforcement around the openings: (a) door; (b) window

No visible cracks were observed after the first four seismic tests (i.e. up to 1.0g PGA). The first visible cracks appeared during WN6(i.e. the white noise test performed after ST4, characterized by PGA values up to 0.5g) and were mostly concentrated around the openings.

The major findings obtained from the test results were that the prototype building was able to sustain increasing levels of the seismic input up to 1.2g PGA without visible damages and exhibited a dynamic response in terms of fundamental frequency that can be obtained by a linear elastic FE model in which the concrete is assumed in partially cracked conditions (i.e. an equivalent elastic modulus equal to approximately one half of the uncracked one is used).

The prototype building exhibited "partially-unexpected overstrengths" which did not allow to observe the expected sequence of mechanisms of failure, whose predictions were obtained neglecting the concrete tensile strength (the assumption is based on the results of previous pseudo-static cyclic tests). The theoretical shear strength at first cracking of the tested panels, which is consistently higher than the ultimate shear strength (due to the low reinforcement ratios and the negligible concrete contribution in tension after cracking), should be a possible explanation of the "partially-unexpected overstrengths" showed by the prototype building during the most severe shakings.

In the study of Psycharis and Mouzakis (2012) the authors evaluate the shear resistance of pinned connections of precast members to monotonic and cyclic loading. This case is the most common solution in Southern Europe and elsewhere for single-storey or low-rise precast buildings, and is the subject of the experimental research that the authors have carried out. The experiments were performed at the Laboratory for Earthquake Engineering of the National Technical University of

Athens, Greece in the framework of the European FP7 project, SAFECAST. Precast beam and column elements connected with dowels were tested under monotonic and cyclic, pure shear loading and the research was focused on several design aspects, as the shear ductility capacity of the connections and the effect of various parameters on their strength. The parameters examined include the diameter D of the dowels, their number, their distances d and d_n from the edges in the longitudinal and the transverse direction of the beam respectively, and the strength of the grout of their ducts. Improvements in the design were also proposed and tested experimentally.

The primary objective of this experimental research was to investigate the effect of various design parameters on the resistance of pinned beam-to-column connections under pure shear monotonic and cyclic loading. The specimens represented a typical pinned connection of linear precast members and consisted of the end parts of the beam and the column that were connected by steel dowels. A schematic of the prototype is presented in Figure 18.
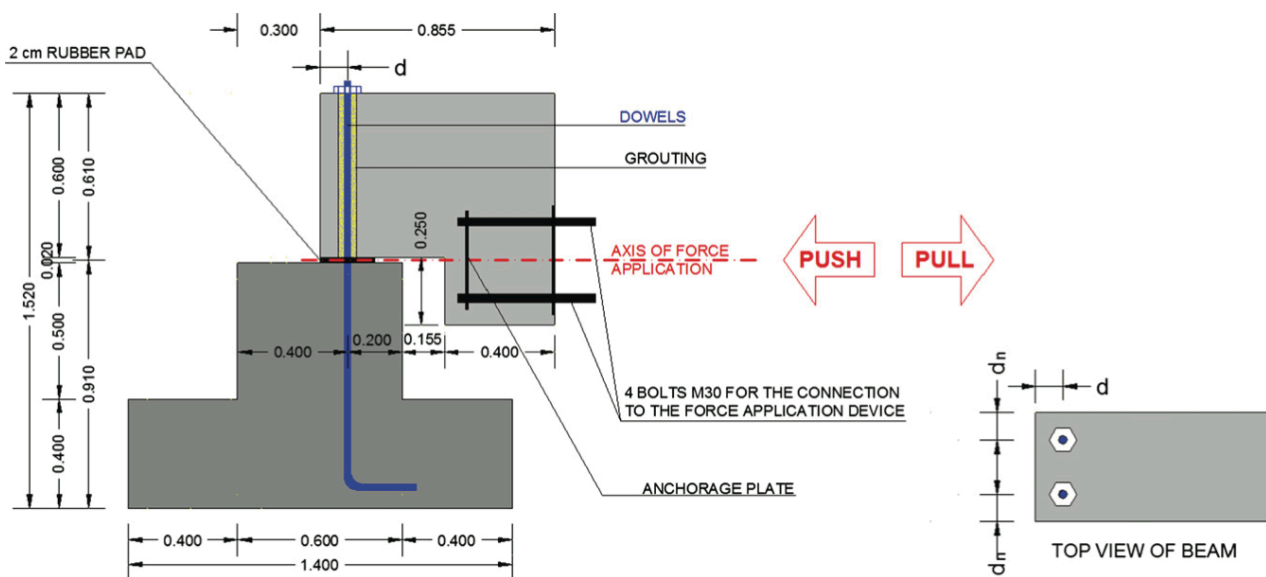
Fig.18: General layout of the specimens

The experimental setup is shown in the following figure (Figure 19).

(a)   (b)
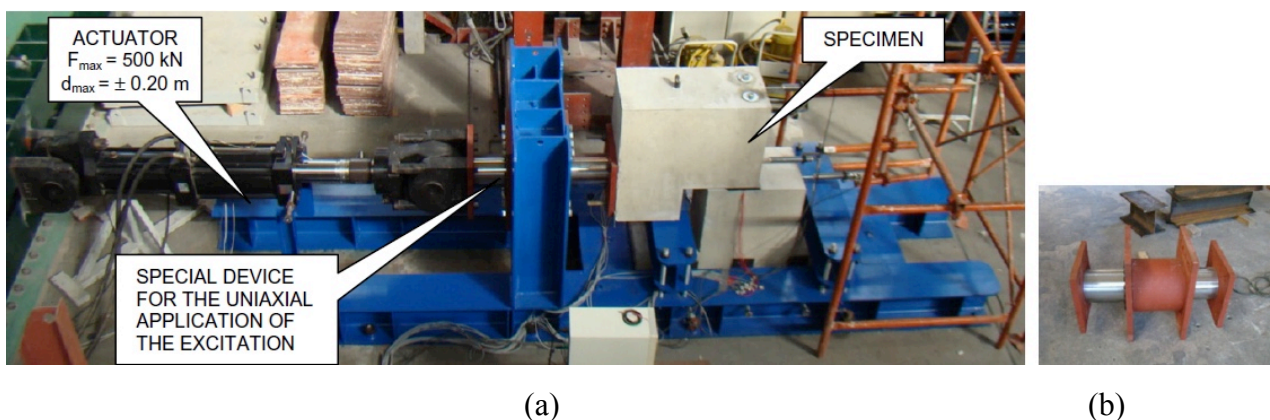
Fig. 19: (a) Experimental setup and (b) special device for the uniaxial application of the excitation.

Each specimen was subjected to monotonic or cyclic, displacement-controlled loading, applied to the rear end of the beam, while the column was securely fastened to the strong floor of the Laboratory. The driving force was applied exactly at the level of the joint, in order to achieve pure

shear conditions. To prevent any out-of-plane motion, a special device was used (Fig. 19b), which consisted of a piston and a sleeve connected to the strong floor and which allowed only uniaxial motion of the beam. No extra vertical load was applied to the joint.

The specimens were constituted by column elements were short and stiff in order to prevent any bending deformation during the tests. The cross sections of the column and beam elements were orthogonal with dimensions similar to the ones usually applied in precast single-storey buildings (physical scale). In particular, the cross section of the column was 0.60 m x 0.40 m and the cross section of the beam was 0.40 m x 0.60 m. All specimens were identical in dimensions.

For the proper sitting of the beams on the columns, elastomeric (neoprene) pads of about 20 mm thickness are typically used in practice.

The columns and the beams were constructed of high strength concrete (the mean value of the measured compression strength of the concrete of the specimens was 30-35 MPa) while the steel of the dowels and the reinforcement was of grade B500C.

For the assembly of the specimens, Ø65 waiting ducts were placed in the beams for the passage of the dowels during mounting. In most cases, jagged steel ducts were used. All the experiments, except two, were performed 24 h after grouting. The mean compression strength of the grout at that time was measured 23 MPa, considerably less than the strength of the concrete. The column elements were reinforced with 12Ø20 rebars andØ10/100 stirrups. The beam elements were reinforced with 3Ø18longitudinal bars at the top and the bottom sides and Ø10/100 stirrups. Horizontal hooks, fully anchored to the body of the beam, were also placed in front of the dowels, specifically: 5Ø12/50 at the lower 0.30 m of the section and 3Ø12/100 at the rest of the section.

A mechanism made of two steel plates and four high strength screws was embedded in the rear part of the beam (Fig. 18) for the fastening with the force application system.

The dowels were fully anchored according to the requirements of EC2.

The authors have focused the experimental investigation on the effect of various parameters like the diameter of the dowels. Dowels of three diameters were tested, namely: Ø32, Ø25 and Ø16 while in practice, dowels of Ø28and Ø32 are commonly used.

Most of the tests were performed on connections made of 2Ø25 dowels; in this case, the resulting strength of the joint was within the limits of the hydraulic actuator and the authors were able to bring the specimens to failure or close to it.

Other parameters investigated were the number of dowels, the distance d of the axis of the dowels from the beam edge in the loading direction (most experiments were performed on specimens with d = 0.10 m) and the strength of the grout that is placed in the dowels' ducts.

In total, 22 tests were performed as shown in table 1, which schematically summarizes the prevailing geometrical features of the connection systems tested, as well as the nature of loading that was assumed to test each specimen (i.e. monotonic push or pull and cyclic loads). In addition to that, the prevailing remarks concerning any experimental test carried out have been summarized in table 1 in order to allow one for a better comprehension of the experimental results discussed in the following.

Tab.1 Experimental data

Dowels	d (m)	d/D	d_n/D	Specimen-test	Type of test	Remarks
2Ø25	0.10	4.00	4.00	2D25-d10-PSH	Monotonic Push	
				2D25-d10-PLL	Monotonic Pull	
				2D25-d10-CY-1	Cyclic	Start in push direction
				2D25-d10-CY-2	Cyclic	Start in pull direction
				2D25-d10-CY-PL	Cyclic	With anchored steel plate
	0.15	6.00	4.00	2D25-d15-PLL	Monotonic Pull	
				2D25-d15-CY	Cyclic	Start in pull direction
	0.20	8.00	4.00	2D25-d20-PLL	Monotonic Pull	
				2D25-d20-CY	Cyclic	Start in pull direction
1Ø25	0.10	4.00	8.00	1D25-d10-PSH	Monotonic Push	
				1D25-d10-PLL	Monotonic Pull	
				1D25-d10-PSH-G	Monotonic Push	With high strength grout
				1D25-d10-CY	Cyclic	Start in pull direction
				1D25-d10-CY-F	Cyclic	With fibre reinf. concrete
2Ø16	0.10	6.25	6.25	2D16-d10-PSH	Monotonic Push	
				2D16-d10-PLL	Monotonic Pull	
				2D16-d10-CY-1	Cyclic	Start in push direction
				2D16-d10-CY-2	Cyclic	Start in pull direction
				2D16-d10-CY-G	Cyclic	With high strength grout
1Ø32	0.20	6.25	6.25	1D32-d20-PSH	Monotonic Push	
				1D32-d20-PLL	Monotonic Pull	
				1D32-d20-CY	Cyclic	Start in pull direction

The monotonic tests were executed with the driving force applied in the pull or in the push direction up to failure of the dowels or when the maximum capacity of the actuator was reached. The cyclic tests were displacement-controlled and were performed at a rate of 0.2 mm/s. The protocol shown in Fig. 20 was followed: three cycles were performed at each displacement level, which was increasing in steps of d_y.
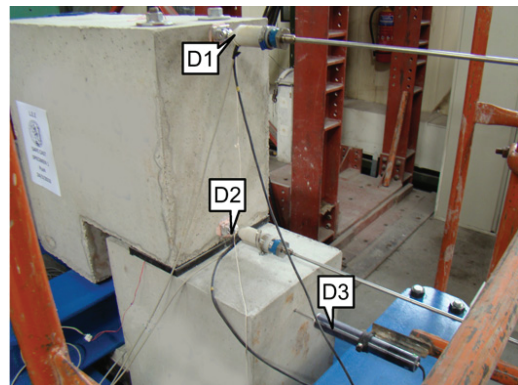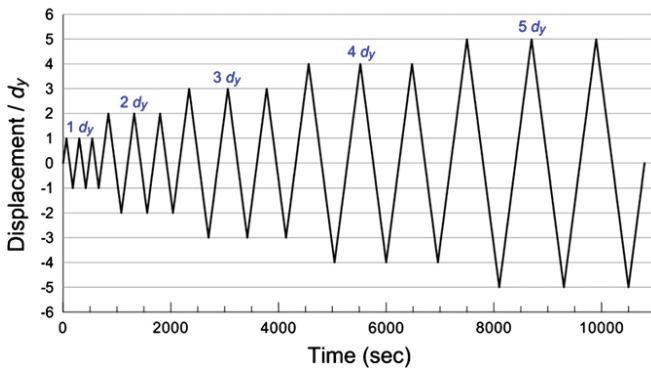
Fig. 20: (a) Loading protocol for most cyclic tests. In some tests, loading at displacement levels 0.5 dy and 1.5 dy were also applied; (b) Instrumentation setup.

The results for cyclic loading also show that significant values of shear ductility can be achieved by dry pinned joints, provided that the concrete cover of the dowels has sufficient thickness. Comparisons between the experimental results obtained for various design parameters show that secondary effects related to the number of the dowels can occur for large forces during monotonic loading, but are less important for cyclic response. An example of the experimental results obtained is shown in Figure 21.
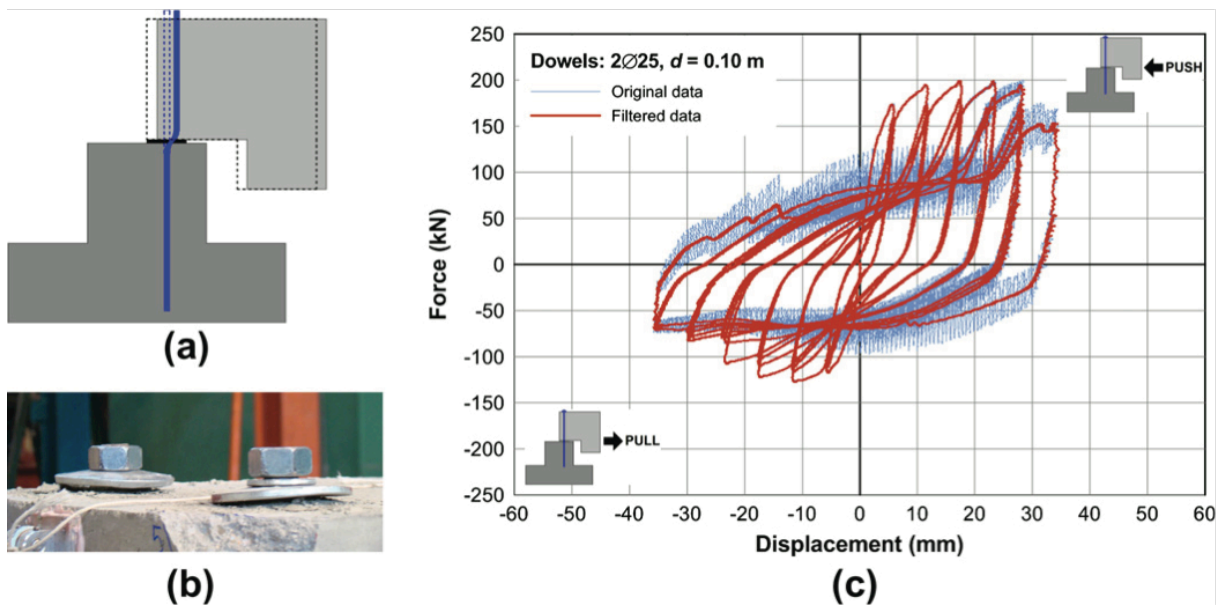
Fig. 21: (a) Deformation of dowels during testing; (b) upward displacement of dowels' bolts on top of the beam, observed during cyclic tests; (c) saw‑type force‑displacement diagrams for cyclic tests (thin blue line) and smoothed response after filtering (thick red line).

The main conclusions are that the thickness of the cover concrete of the dowels in the direction of the loading plays an important role to the response. For dowels placed close to the edges (small values of d/D), spalling of the cover concrete occurs during pulling, which reduces the resistance and leads to asymmetric response.

Another conclusion is that for monotonic loading in the push direction, the force‑displacement diagram shows an almost elastic branch up to yielding, followed by a post elastic branch with significant stiffness, which is attributed to the horizontal component of the axial force of the dowels, which increases with the shear displacement, since the inclination of the dowels in the area of the joint increases.

The resistance of the connection for cyclic response is less than one half the monotonic one, the cross section of the dowels is the main parameter that determines the resistance of the joint, the use of high strength grout increases the resistance of the connection, Significant values of shear ductility, around 4‑6, can be achieved by dry pinned connections and the failure of the dowels does not necessarily imply loss of resistance because broken dowels usually protrude inside the opposite element and resist the horizontal movement.

In another study of Psycharis and Mouzakis(2012) the authors present a research that concerns the experimental investigation of the seismic performance of single-storey frames with pinned beam column connections for the assessment of current design procedures.

The frames that the authors have examined were made of various types of columns: flexible and weak (under-reinforced), in which large rotations were induced at the joints; flexible and strong (over-reinforced), in which significant rotations and shear forces were induced at the joints; stiff and strong (over-reinforced), in which small rotations and large shear forces were induced at the joints; and flexible and normally reinforced designed according to Eurocodes 2 and 8. The base motions were applied in the plane of the frame and were piece-wise increasing up to the point that significant damage was observed, either at the beam-column connection or at the column's base.

The shaking table tests were performed on single-storey, one-bay frames made of precast columns and beams connected with dry pinned connections materialized by dowels. Due to limitations in the span length imposed by the shaking table dimensions (4.00m×4.00 m),only one half of each frame was modeled (Fig. 22a) . At the free end of the beam (right end in Fig. 22b), which corresponds to the mid-span in the prototype structure, appropriate boundary conditions were applied, specifically free rotation around the normal-to-the beam horizontal axis and free sliding in the longitudinal axis of the beam, while no vertical motion was allowed at this point. This was achieved by a special device that provided a sliding pinned support to the beam (Fig. 22c). This device was fixed on the shaking table through an independent stiff steel frame (Fig. 22b)
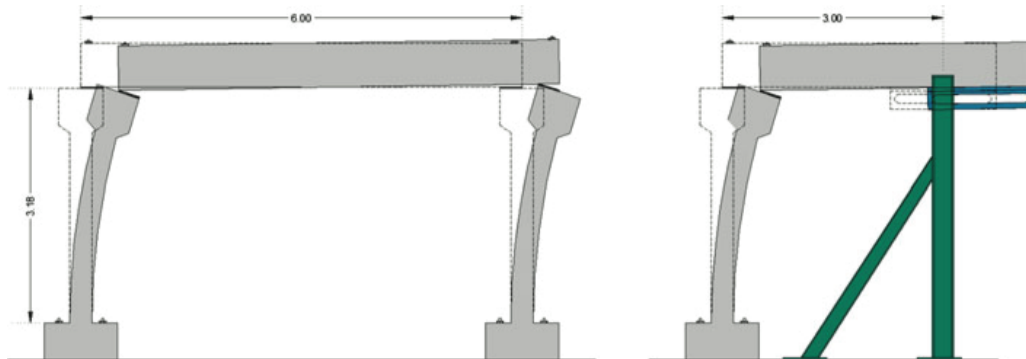
(a)

(b)
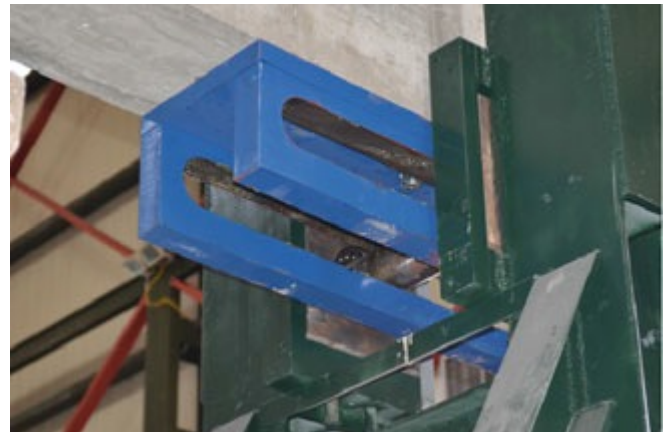
(c)

Fig. 22: (a) Prototype single-bay frame (left) and corresponding half-frame specimen (right) in deformed position (displacements and rotations are exaggerated); (b) experimental setup showing the half-frame specimen and the additional mass; (c) special device for achieving sliding pinned support at the free end of the beam

The dimensions of the cross section of the columns are shown in Table 2. The columns were fixed at their base.

In all specimens, the cross section of the beams was of dimensions 0.40m × 0.60 m. Away from the end areas, flanges were provided on the top side forming a T-shaped section, in order to facilitate the placement and the fastening of the extra mass that was added on top (Fig. 22b).

For the proper sitting of the beams on the columns elastomeric (neoprene) pads of 20mm thickness were used, as typically done in practice to prevent impact between the beam and the column due to the rotation at the joint during the seismic response.

Tab. 2 Specimens' description

Column type	Specimen	Dowels	Cover d (m)	Column dimensions[a]/ reinforcement[b]	Normal. axial force, ν[d]	Design parameters	
						$S \cdot a_g$ (g)[e]	q[f]
FW	ST-1	2Ø25	0.10	30× 40 / 8 Ø14	0.032	0.40	3.50
	ST-2						
SS	ST-4	2Ø25	0.10	60× 40 / 14 Ø20	0.018	0.50	1.00
	ST-5						
FS	ST-3	2Ø25	0.10	30× 40 / 24 Ø25[c]	0.031	0.50	1.00
	ST-6				0.032		
	ST-7	2Ø25	0.20	30× 40 / 24 Ø25[c]	0.048	0.50	1.00
	ST-8	1Ø25	0.10	30× 40 / 24 Ø25[c]	0.048	0.50	1.00
FN	ST-9	2Ø25	0.10	30× 40 / 12 Ø20	0.032	0.16	3.50

In the shaking table experiments, Ø25 dowels were used in all specimens, thus d/D was equal to 4.0 for the specimens with d = 0.10 m. Therefore, asymmetric behaviour was expected according to the results of the static tests; however, the behaviour during the dynamic tests was less asymmetric than expected.

For the assembly of the specimens, Ø65 waiting ducts made of jagged steel were placed in the beams for the passage of the dowels during mounting. The ducts were grouted after assemblage with non-shrinking concrete and the dowels were bolted at their top. All the experiments were performed 24 hours after grouting, when the strength of the grout in compression was about 20MPa.

The beams and the columns of the specimens were designed according to Eurocode 2 and Eurocode 8 (CEN 2004) for ground type B, importance factor $\gamma_I = 1.0$ and 5% damping.

Various values of the peak ground acceleration S_{ag} and the behaviour factor q were used for the design of the columns (see Table 2) in order to produce columns of different strength as explained in the next section. The analyses were performed considering the beam-to-column connections as pinned and the columns fixed at their base.

The design of precast frame structures with pinned connections is performed assuming that the beam-column joints are located away from critical regions where plastic hinges can develop. Such hinges are allowed at the base of the columns only, while the joints are expected to behave elastically during the ground motion and are designed according to the capacity criterion.

The instrumentation setup is shown in Fig. 22. Accelerations were measured at the external masses, at the top of the beam and at the top of the column. Absolute displacements in the horizontal direction were measured at the top of the column, while the relative displacement between beam and column (joint slip) and the change in their distance in the diagonal direction of the joint were also recorded.

(a)   **(b)**
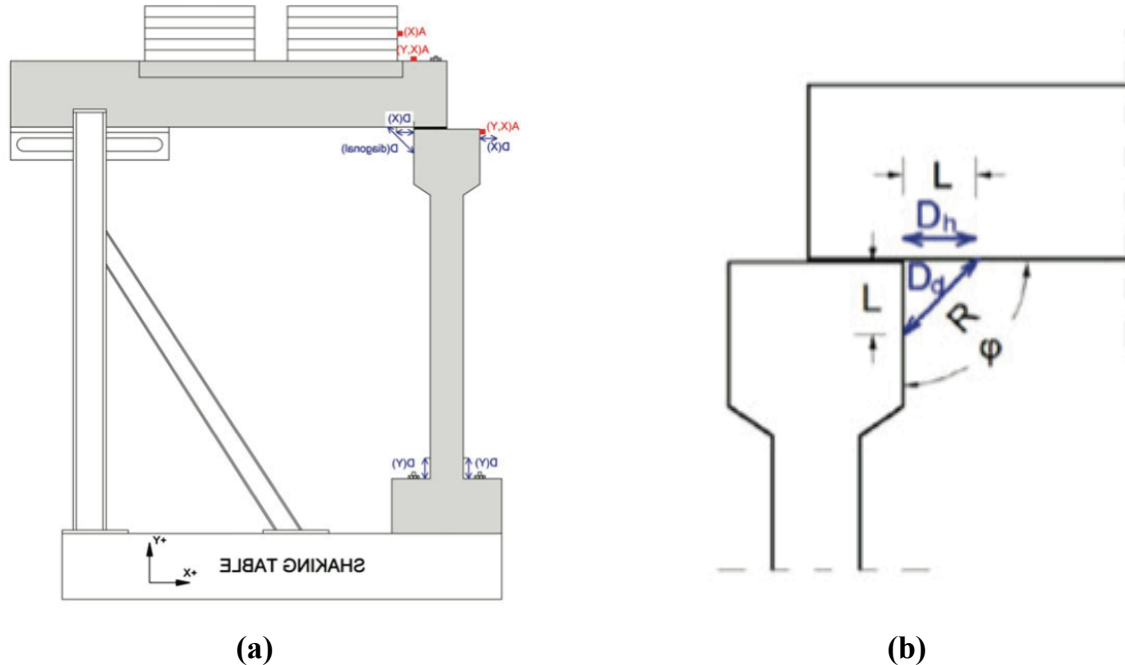
Fig. 23: Instrumentation setup: (a) accelerometers (denoted with "A") and displacement transducers (denoted with "D"). The directions of the motion of the shaking table are shown and the direction of recording of each instrument is given in parenthesis; (b) instruments used to measure the rotation of the beam-column joint

The rotation of the cross section at the base of the columns was recorded by two displacement transducers placed at a distance of 0.30 m from the top of the footing, measuring the vertical displacement at two opposite sides of the column. The rotation was calculated by dividing the difference of the two recordings by the width of the section.

The acceleration and the displacement of the shaking table were also recorded during each test. Additionally, strain gauges were used to measure the strains developed in the dowels at a depth of about 0.10 m from the top of the column; however, the induced strains at this depth were small.

The authors shows in the following plots the indicative diagrams of shear force versus joint slip for the beam-column connections. On these plots, the push and the pull directions are marked, as defined in Fig. 22b.

The theoretical shear resistance, as predicted by the following equations for C0 = 1.10 and γ_R = 1.00 given by a study of Psycharis and Mouzakis in 2012 part of a experimental investigation within the SAFECAST project for pure shear loading of specimens modelling the connection only:

$$R_d = \frac{C_0}{\gamma_R} \cdot n \cdot D^2 \cdot \sqrt{f_{cd} \cdot f_{yd}} \quad \text{for } d/D > 6.00$$

$$R_d = \frac{C_0}{\gamma_R} \cdot (0.25 d/D - 0.50) \cdot n \cdot D^2 \cdot \sqrt{f_{cd} \cdot f_{yd}} \quad \text{for } 4.00 \le d/D \le 6.00$$

where D is the diameter of the dowels, n is their number, d is the distance of the dowels' axis from the edge of the beam or the column (whichever is smaller) in the longitudinal direction of the beam, $f_{cd} = f_{ck}/\gamma_C$ is the design compression strength of the concrete, $f_{yd} = f_{yk}/\gamma_S$ is the design yield stress of the steel of the dowels, γ_R is a general safety factor and C_0 is a coefficient varying from 0.90 to 1.10 depending on the magnitude of the expected rotations: for large rotations (flexible columns), C_0 is suggested to be set equal to 0.90, while for small rotations (stiff columns) this coefficient can be increased up to a maximum value of 1.10 that corresponds to zero rotations.
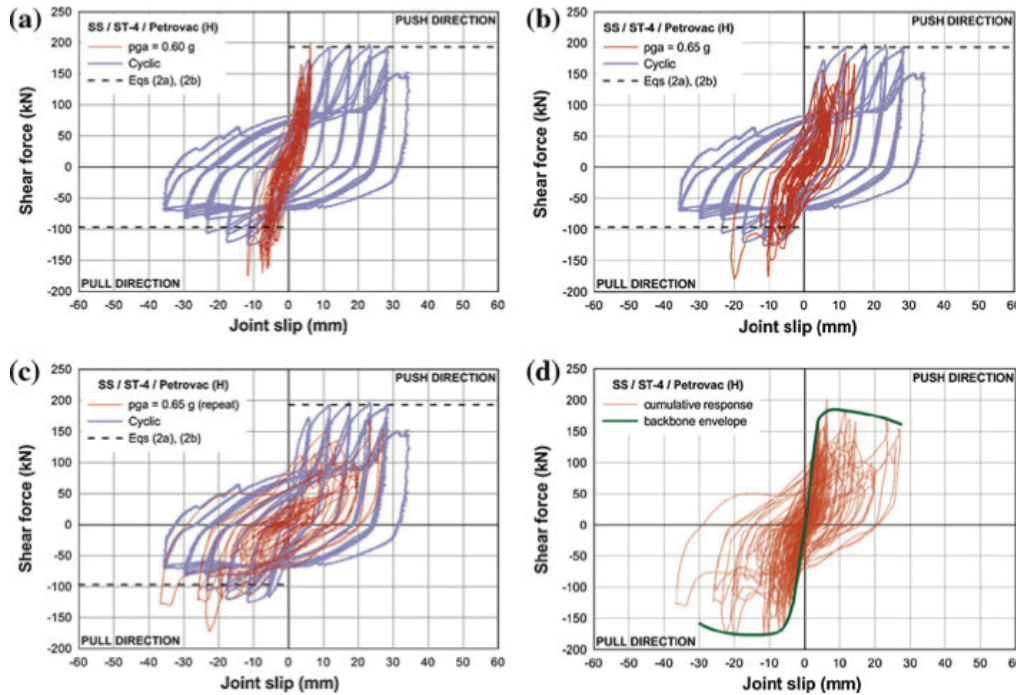
Fig. 24: a–c Shear force versus joint slip diagrams for ST-4 specimen (SS column) subjected to Petrovac earthquake in the horizontal direction for stepwise increasing PGA and comparison with the corresponding cyclic response (Psycharis and Mouzakis 2012); d backbone envelope of the cumulative response

Fig. 25: Damage to the connection of specimen ST-4 (SS column) subjected to Petrovac earthquake in the horizontal direction: (a) after test with PGA = 0.60g; (b) after test with PGA = 0.65g; (c) after repetition of base motion with PGA = 0.65g

The main conclusions the authors have proposed can be summarized as follows:

- The inelastic response of the connections under dynamic loads was, in general, compatible with the response for cyclic loading. Specifically, the shear resistance in the push direction was similar to the cyclic one, while in the pull direction, equal or larger strength was attained compared with that for cyclic loading.

- In cases in which damage occurred at the connections, the spalling of the concrete cover at the beams was significantly less than the one observed during cyclic tests for the same d/D ratio and the same level of joint slip. On the contrary, more pronounced damage was observed at the columns.

- For flexible columns, large rotations (i.e. more than 0.10 rad) occurred at the joints. In general, pinned connections can accommodate such large rotations without losing their strength. However, if damage has occurred at the connection due to large shear forces, large joint rotations may increase the damage.

- Pinned connections are designed for shear forces determined by the capacity design rule, thus, they are expected to behave elastically during earthquakes. However, if they are stressed beyond their elastic limit due to unexpected reasons, the experimental results have shown that they can bear significant post yielding displacements before they lose their strength, showing shear ductility capacity larger than 4.0.

- The empirical formulae previously presented, which were derived from the results obtained for cyclic loading, are also applicable to earthquake excitations and can be employed for the estimation of the shear resistance of pinned connections to be used in the capacity design rule. In case that large axial forces are expected to be induced to the dowels due to the base excitation in the out-of-plane direction or due to the load of the superstructure, the reduction factor proposed by Vintzeleou and Tassios (1987) can be used for the assessment of the shear resistance.

- Concerning the overall ductility of precast structures with pinned connections, in which plastic hinges are expected to develop at the base of the columns, it was verified that they possess satisfactory ductility capacity; thus behaviour factors similar to the ones used for cast-in situ structures can be used, as stated in EC8.

- If damage occurs at pinned connections, repetition of the earthquake motion might increase the damage considerably. Thus, if such connections are damaged during an earthquake, they must be repaired in order to be able to sustain successfully aftershocks and future earthquakes.

- The vertical component of the earthquake does not seem to be important.

In the study of B.F. Allan et al. (2012) the authors presents the results of tests on bolted connection of precast panels as a consequence of the failures after the Canterbury earthquake sequence. The failure modes most commonly occurring in bolted connections include panel-to-roof, panel-to-column and panel-to-panel (vertical joint) connections. The failure mechanisms were attributed to insufficient edge distance to the bolts, insufficient bolt anchorage, and insufficient tensile capacity to resist the large out-of-plane forces acting on the panels during the earthquake events.

The authors also present a review of the seismic performance of connections currently used in constructions consisting of precast concrete panels. This review was undertaken by classifying connections currently used in the New Zealand concrete construction industry and identifying failure modes that occurred in the recent Canterbury earthquakes, where a number of buildings that incorporated precast concrete panels exhibited unexpected and undesirable failures.

The authors affirm that Earthquakes generate both in-plane and out-of-plane loading on precast concrete panels, and following the Canterbury earthquakes it was concluded that precast panels had generally performed well when resisting in-plane loads, with only a few panels showing some diagonal cracking (Henry and Ingham 2011). Out-of-plane loading on panels had caused horizontal cracks across the middle of some panels and caused cracking around some connections (Henry and Ingham 2011). There were a number of examples in the 22 February 2011 Christchurch earthquake of failures that occurred in precast concrete panels at panel-to-panel connections, as pointed out by Henry and Ingham (2011). While these failures did not result in the complete collapse of the precast panels, many panels required extensive repair.

Damage to precast panel connection was investigated for 26 case study buildings to identify the sources of failure. Out of the 26 case-study buildings investigated, 54% failed due to connection failure (see Figure 26a). These connection failures were sub-divided into four main groups (see Figure 26b): failure due to pounding and compression from adjacent buildings; failure due to cast-in reinforcing connections (such as drossbach connections); failure due to bolted connections; and failure due to poor construction (such as nuts welded directly to the bolt which prevented movement). A significant amount of the connection failures (i.e. 63%) were observed to take place in bolted connections, being them either cast-in anchors or mechanical anchors, with the majority of these bolted connection failures being due to pull-out of the anchor from the concrete (see Figure 26c). In a particular case study, pull-out of the anchor occurred as a result of stripping of the thread or necking of the bolts. Out-of-plane movement and insufficient edge distance were also identified as common failures in bolted connections (see Figure 26c).

The authors made a review also of the procedures for testing concrete anchors. Restrepo et al. (1996) undertook research on precast concrete panels and their connections. Commonly used connections were catalogued and classified, and cast-in-place and welded embedded steel connections were tested. Their research project is the most comprehensive testing to have been undertaken in New Zealand to date. Eligehausen et al. (2011) undertook testing of single anchors to establish if high loading rates were required when analyzing the behaviour of concrete anchors subjected to seismic loading conditions. The four anchor types investigated were adhesive anchors, torque-controlled adhesive anchors, sleeve-type expansion anchors, and bolt-type expansion anchors. Test specimens were reinforced concrete slabs constructed using normal-strength concrete, with reinforcement rebars symmetrically placed at the top and bottom of the slab in order to allow for a uniform crack width throughout the member. Of interest to this project was the testing of the anchors in tension, with four general failure modes that were recognized as potentially occurring when concrete anchors are subjected to tensile loading: pullout or pull-through; concrete breakout; splitting; and steel failure.

(a)

(b)

(c)
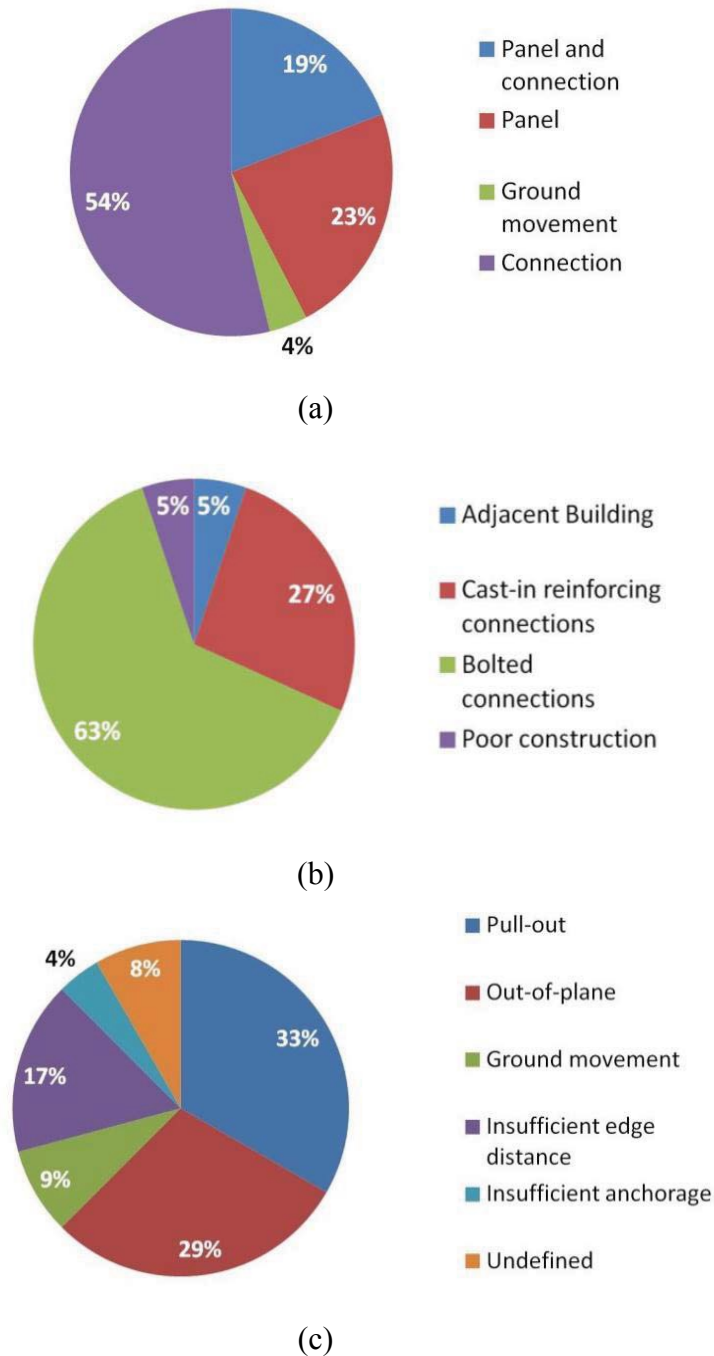
Fig. 26: Quantitative review of panel failure modes

The authors tested two types of anchor bolts commonly used in New Zealand for precast concrete connections, aiming to replicate damage observed in the Canterbury earthquakes.

Four different types of connection were tested (see Table 3). In particular, the anchors were loaded in tension to determine their strength when subjected to out-of-plane actions.

There were two stages for what concerns the experimental testing protocol: Stage One consisted of anchors installed with unlimited edge distance, while Stage Two consisted of anchors installed with varying edge distances that were each equal to or less than 150 mm.

Tab. 3 Tested connection types

Bolt Type	Bolt Size	Number of Monotonic Tests	Number of Cyclic Tests
Cast-in Type A Threaded Insert (Length = 95 mm)	M20	1	3
Cast-in Type B Threaded Insert (Length = 120 mm)	M20	1	3
Single mechanical anchor	M16	1	3
Group of four mechanical anchors	M16	1	3

The specimens were designed to simulate precast concrete panels used in current building practice, assuming a configuration of panel reinforcement (see next Figure) replicating the details used in an earlier experimental study that was performed to investigate precast concrete components joined together to form structural walls.

(a)
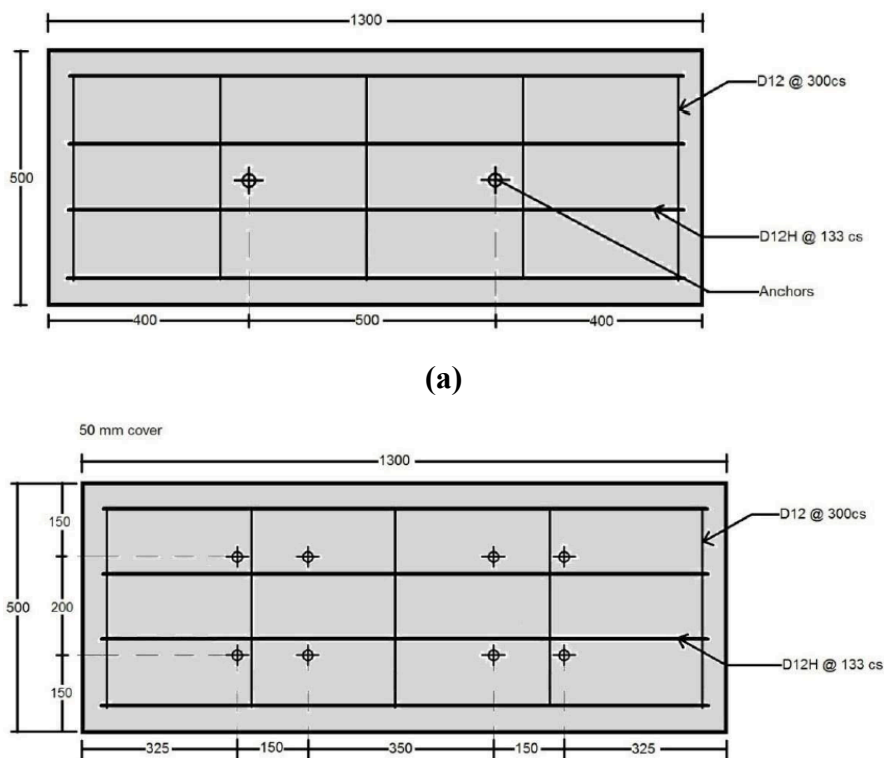
Fig. 27: Panel test specimen: (a) Test panel for individual anchors; (b) Test panel for anchor groups

The panels were constructed in an Auckland precast concrete factory (see Figure 28), and transported to the laboratory once adequately cured. The panels were then secured to the strong floor using two 100x150 RHS, with a string-pot transducer that was used to measure the withdrawal displacement of either the mechanical anchor or the threaded rod of a cast-in anchor, as shown in Figure 29.

(a)	(b)

Fig. 28: Panel manufacture at precast yard: (a) Before concrete placement (b) After concrete placement

(a)	(b)
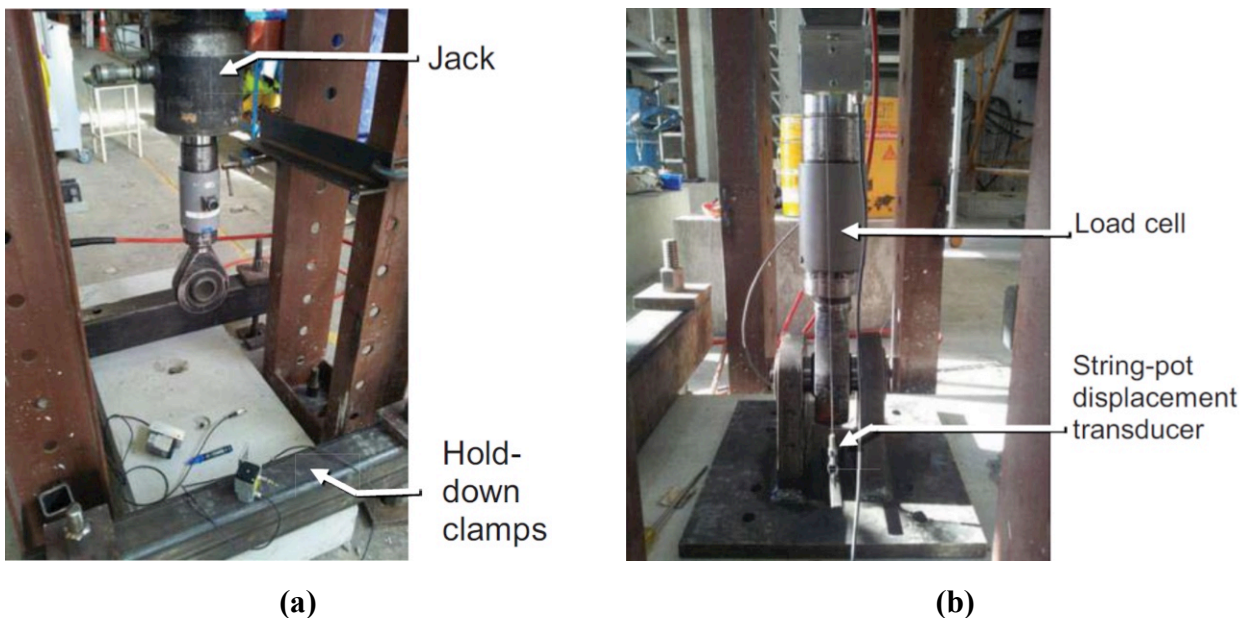
Fig. 29: Test setup-attachment of the jack and plate to the anchors being tested

Four tests were carried out for each type of connection. For the first test of each connection system, the load was applied monotonically, until failure, in order to determine the ultimate resistance of the connection. For what concerns the last three tests, the connection was loaded cyclically to simulate the loading reversals (loading-unloading) experienced during a seismic event.
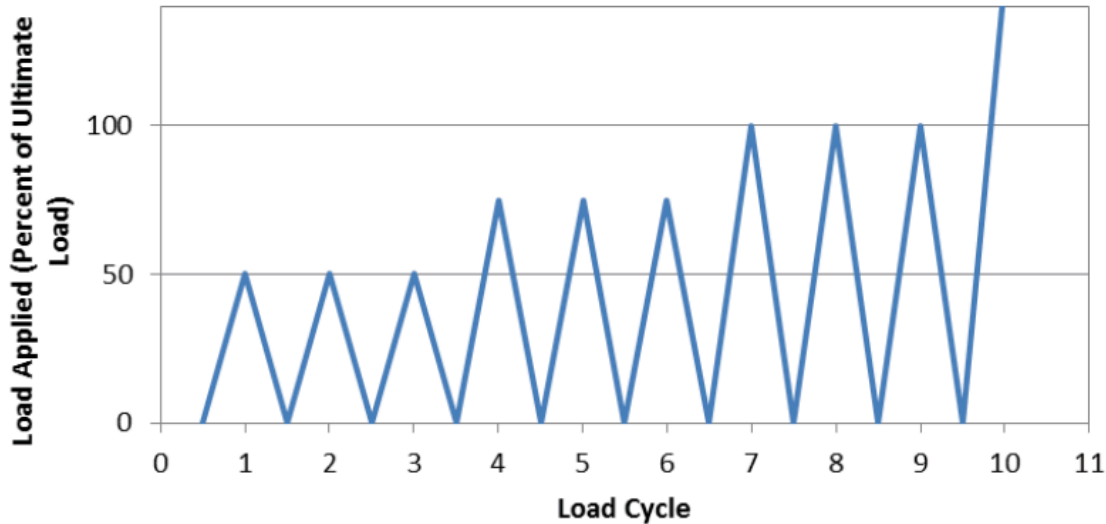
Fig. 30: Loading sequence for cyclic tests

Figure 31 shows the concrete panel after testing of the mechanical anchors. The failure mechanism observed in this test presents a cone of cracked concrete, and the damage was much more localised when compared with the cracking of cast in Type A and Type B inserts.

Fig. 31: Localized cracking after monotonic (left) and cyclic loading (right)

As a conclusion, the authors have found that the loads at which cast-in anchors and mechanical anchors fail exceed their respective design capacities when installed correctly; the failure of bolted connections during the Canterbury earthquakes were associated with the anchors being subjected to a force of a magnitude significantly greater than their intended design one (thus resulting in pull-out failures) and also potentially due to insufficient edge distance.

In the study of K. M. McMullin et al. (2014) the authors presents the main test program for the Pathways NEESR-SG project that concerns the experimental testing of full-scale façade systems. San Jose State University has conducted research exploring the seismic behavior of building façade systems, paying particular attention to the response of precast concrete cladding systems.

Six experimental test specimens composed of precast concrete cladding panels were built up and two of them were provided to have punch-out windows. Two different types of specimen have been designed: a so-called architectural specimen and a so-called engineering specimen; the architectural specimen is the exact copy of an actual cladding system, including full-scale panels, actual cladding connections, grouted joints and punch-out windows.

The two panel geometries that were tested are shown in Figure 32. One represents the Ground Level of the prototype building (where the column covers are significantly taller) and the other represents the Typical Level. The column covers of Ground Level specimen are commonly taller for two main reasons: there is no spandrel beam at the sidewalk level and the first floor of an office building is often significantly taller than the typical story height for architectural reasons.

(a)

(b)

(c)
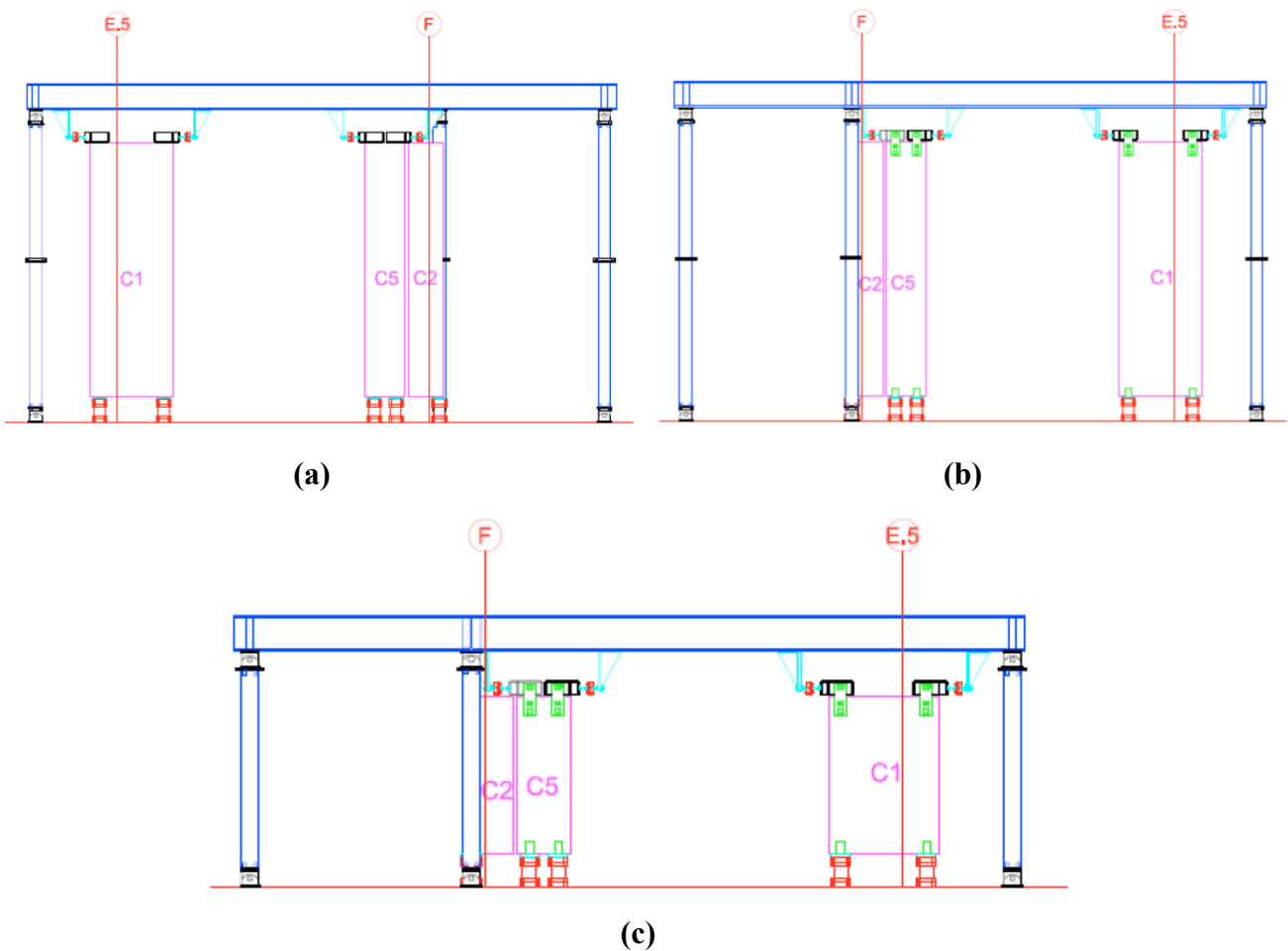
Fig. 32: Panel sizes: (a) Exterior Elevation of Ground Level Test Specimen; (b) Interior Elevation View of the Ground Level Specimen; (c) Interior View of Typical Level Test Specimen

A second variable of the experimental investigation is the loading protocol; two loading protocols were used as defined in Table 4. Both loading protocols used a displacement control. To allow for future implementation of performance based design, four tests used the ATC-58 loading protocol, that consisted of cyclic loading with increasing displacement amplitudes.

Tab. 4 Loading protocols

	Remarks
ATC-58	Cyclic displacement-controlled loading with incremental increases in amplitude. Peak drift of 5%.
Displacement Time History	Selection of a critical ground motion for the SAC 9-story LA Building frame. Applied at incremental increases of severity to achieve failure of the façade system.
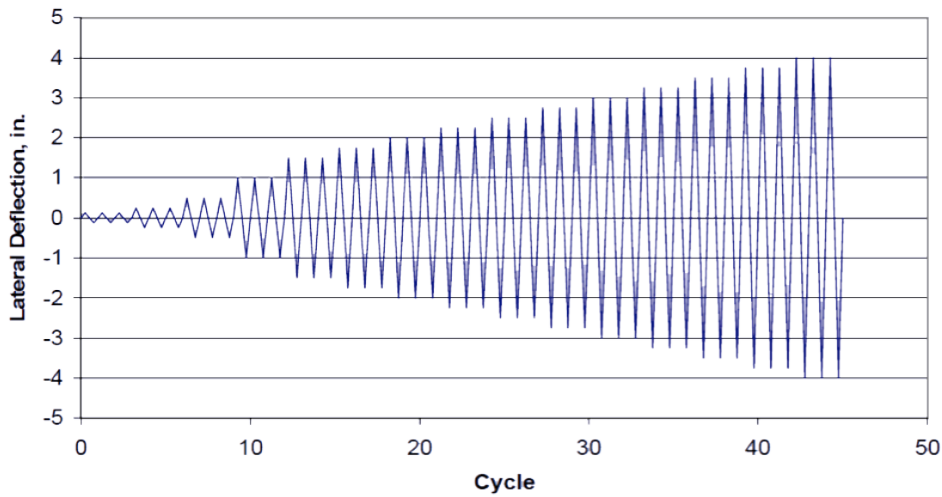
Fig. 33: Test 1 loading protocol

The frames and the specimen for static tests have been properly assembled in the Reaction Frame of the nees@berkeley equipment site, as shown in the schematic of Figure 34.
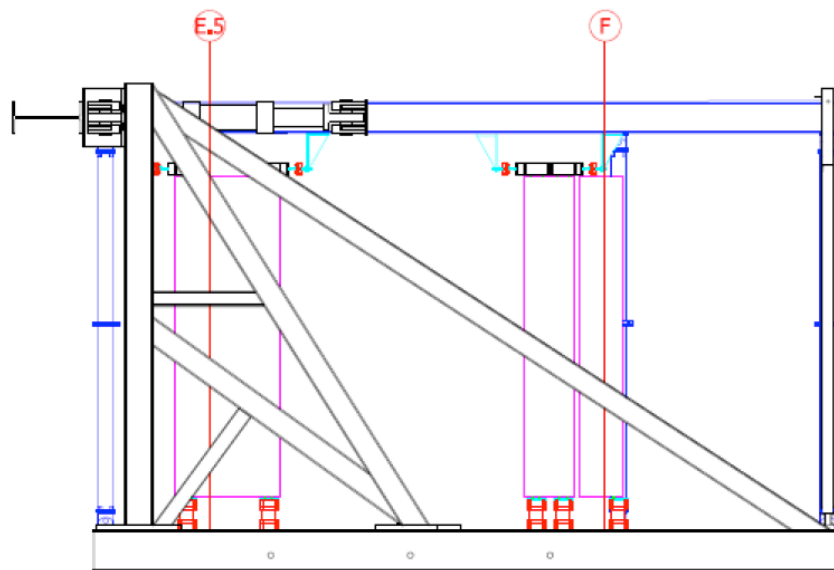
Fig. 34: Exterior Elevation of Ground Level Test Specimen installed in Reaction Frame

In the past years, significant work has been done to design and test prototypes representative of real-life panels, in terms of geometric features and reinforcement arrangements in close agreement with detailing and schemes commonly assumed in current U.S. building practice. Prior work had resulted in the identification of panel geometry, panel connection and punch-out window layout. Additional work had suggested suitable reinforcement requirements.

The size and complexity of the research project have required industry-level expertise to deal with the production of the majority of the single components used for the assemblies that were tested (Figure 35). Of primary concern for this purpose was the reproduction of accurate precast concrete panels that would possibly represent common commercial solutions for the American market. The size and weight of the precast panels are also conducive to the industry in order to allow for large-scale batch mixing of concrete, repetitive use of forms, and consistent material testing.

Fig. 35: Panels cast and detailed by industry

The steel connections that link concrete panels together were expected to provide the inelastic deformation during testing. To ensure that the steel used in the connections of different specimens was consistent, the connection plates were fabricated to meet common building practice.

The Pathways Project at UC Berkeley has completed static loading of six full-scale experiments under simulated displacement-controlled seismic loading. The advantage of static testing was that systems can be loaded to near-collapse levels of displacement in order to evaluate how the system perform under extreme overloading. The E-Defense testing and the UC San Diego testing were both single full-scale, complete-structure specimens which were loaded using shake table facilities that are able to reproduce the actual ground motion recorded during past earthquakes. The advantage of

shake table testing was that the true acceleration and dynamic environment can be developed in a three-dimensional space.

All three test programs had similar features. Test Specimen 4 of Pathways Project was tested at the nees@berkeley lab facility (Figure 36a). A total of three members has been used to compose the prototype. In particular, the specimen is an assembly consisting of a single precast concrete panel in combination with an L-shaped system that is connected to another single panel in order to represent the corner bay of the typical floor of a building.

The precast concrete specimens used for the TIPS Project were tested at the E-Defense lab facility (Figure 36b). The panels were designed in the U.S. and cast in Japan. The steel connections were designed and fabricated in the U.S., according to common U.S. building design practice.

The precast concrete specimens used for the NEES Structural/Nonstructural test specimen (Figure 36c). Full bay panels are installed on the top two floors of the building, on all four elevations. All panels were designed and fabricated by a Californian precast fabrication company.

(a)

(b)
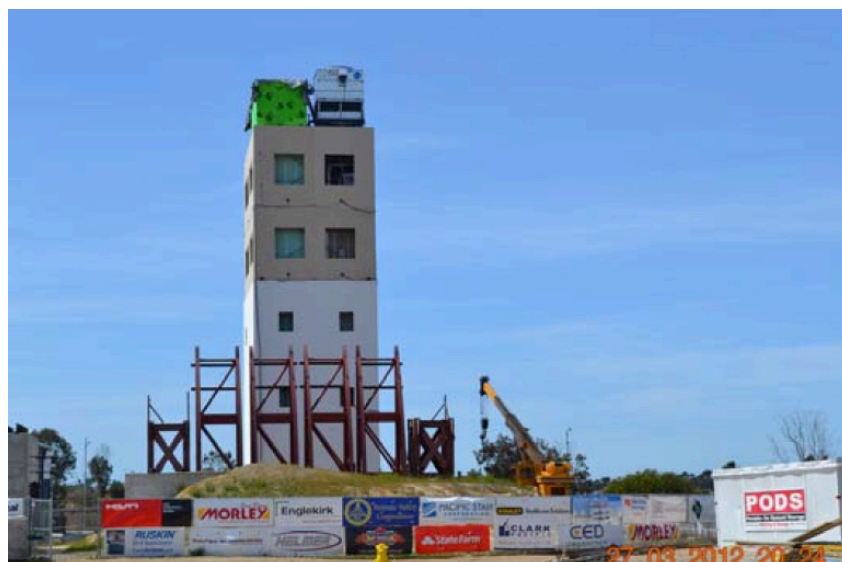
(c)

Fig. 36: Tests specimens: (a) Test Specimen of Pathways Project; (b) Precast concrete specimens for the TIPS Project; (c) Precast concrete specimens for the NEES Structural/Nonstructural test specimen

Due to peculiar aspects of each test program, each specimen had different peculiar characteristics, particularly for what concerns the detailing of the steel connections that were used to link the panels

to the structural frame. The Pathways project had primary focus on claddings and hence most of the design characteristics of the tests were controlled by them. Using the SAC 9-story LA Building as a preliminary schematic, a cladding system using spandrel panels and supported column covers was tested. The test program consisted of six individual tests with each test containing three panels. The E-Defense (TIPS) project used an existing steel frame structure and included two panels on a frame that would be shaken in three directions. The UC San Diego (Structural/Non-structural) project used a specific concrete frame that was completely enclosed by concrete facade on the top two floors and was shaken in a single longitudinal direction.

The primary findings that the authors have obtained from the experimental results have been that well designed and fabricated precast panel systems perform very well during seismic loading. The only significant damage observed in the tests has been obtained as a result of lateral displacements that visibly exceeded the design displacements. Various panels have been loaded in both static and dynamic fashion and the damage observed at displacements smaller than the design displacements have been minimal. All cladding systems represent modern design features by American fabricators in seismic zones. Damage was observed during the static tests when displacements exceeding the design ones were applied. The next figures show some common damage patterns observed during the tests. The most common damage mode observed for demands higher than capacity has been the cracking of the concrete panels due to flexure, particularly in the flat half width panel. This damage has coincided with cracking and loosening of the steel embeds in the interior face of the panels, particularly at the base of the panels. The slotted connection at the top of the panel were made with the nut on the slotted rod being placed finger tight. No wrench was used to tighten or install this nut. The threads of the bolt were then sealed to prevent loosening of the nut. With this finger-tight nut, the slotted connections performed as intended, with minimal resistance to movement. This was observed in both the horizontal slotted connections of the Pathways project and the vertically slotted connections of the E-Defense project.
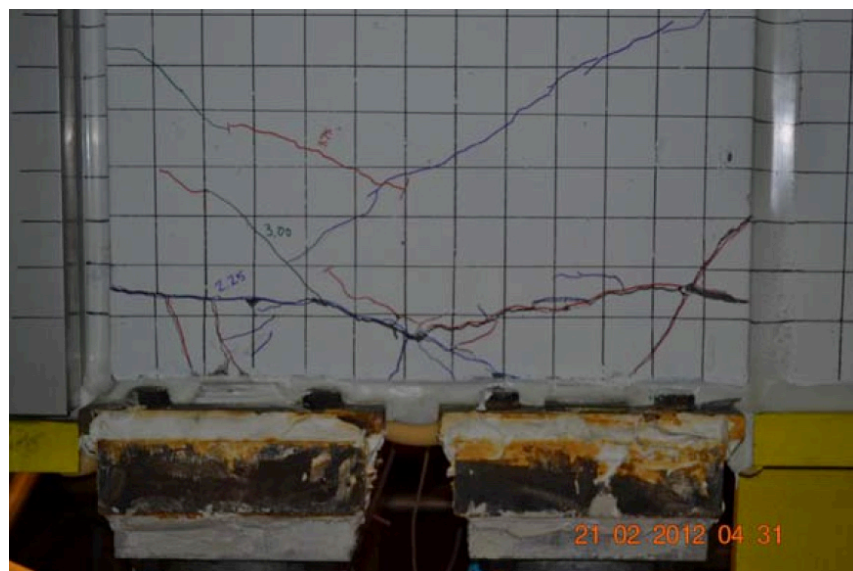
Fig. 37: Cracking of the exterior face of the panel occurred once the design displacement was exceeded.

The following figure shows the severe damage that occurred in correspondence to the steel plates that support the weight of the panel on its interior face. The connection at the base of a panel is a large steel plate that has been cast into the concrete and welded to the smaller plate used to connect

the system and the structural frame. Seismic loading has resulted in severe cracking of the concrete, potentially causing the embed to fail or make the panel collapse.

Fig. 38: Bottom connection: damage occurred at the welded steel plates

The slotted connections at the top of the panels, which allow the floor of the building for moving horizontally while the panel below remains essentially in place, performed well. At displacements much larger than the design ones, the coil rod has traveled the full length of the slot, thus causing the steel plate to rotate and applying horizontal shear to the panel (Figure 39a). The rotation of the plate resulting in the fracture of coil rod is shown in Figure 39b: this rotation can lead to severe damage such as fracture of a coil rod. The fracture of the coil rod results in a potential collapse of the panel, implying high risk of potential life threatening dangers (Figure 39b).

(a)   (b)

Fig. 39: Horizontal slot top slotted connection: (a) translation of the coil rod; (b) Rotation of the slotted connection plate connections with the fracture of coil rod at slotted connection

The experimental response is shown in the following figures to present the sensitivity of the slotted connections to cyclic reversals. The connection have slid very smoothly over the length of the slot and then have resisted significant force once the slot length is exceeded: the red graph correspond to the concrete panels alone, while the yellow graph correspond to a panel that includes windows and sealant.

Lateral force and lateral deflection -
specimen 1 and 3
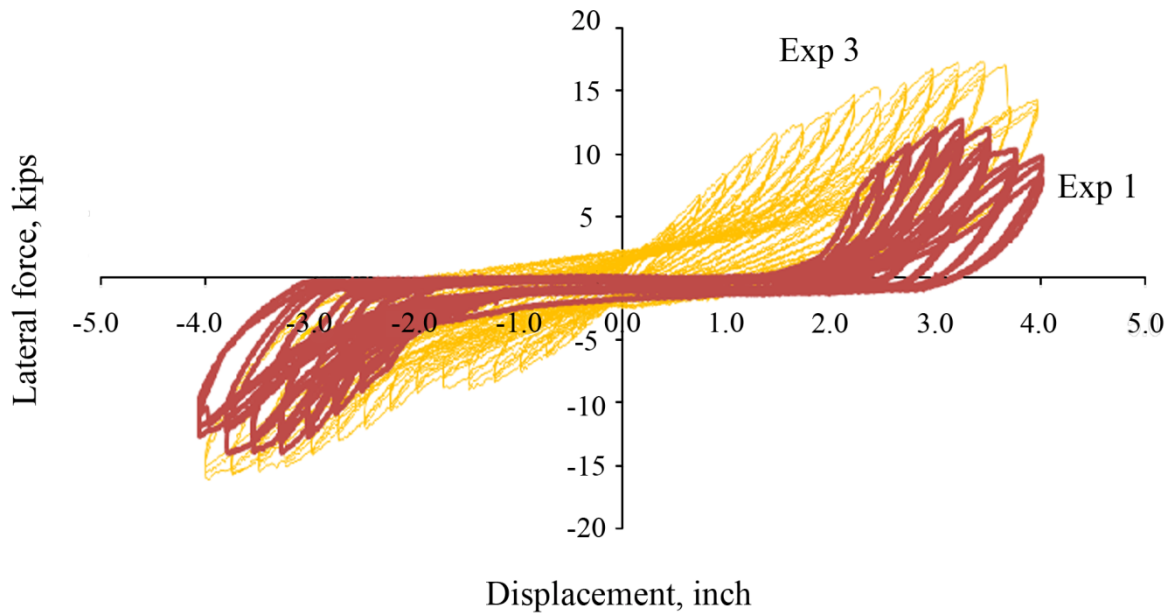
Fig. 40: Lateral force and lateral deflection – Specimen 1 and 3

In the next figure is shown the resistance, in terms of lateral force – displacement, of a single slotted connection of a full-width panel specimen.

Slotted connection at top of flat column
cover panel - specimen 3 - Feb 22, 2012
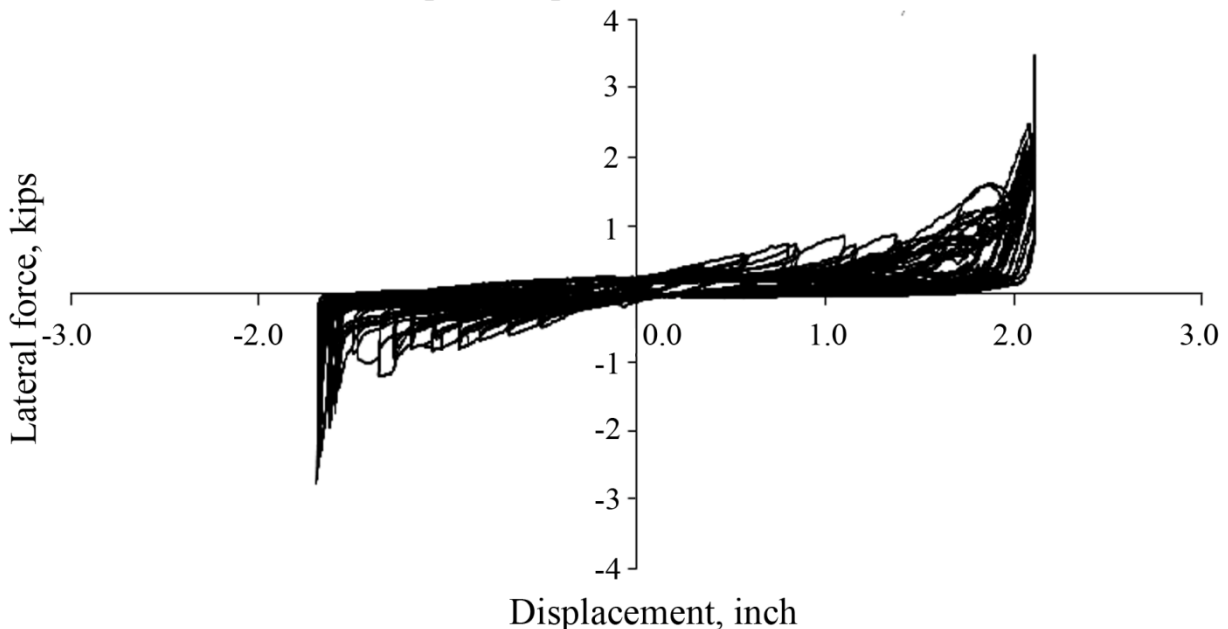
Fig. 41: Slotted connection resistance

Using the results of the full-scale tests, the authors were then focused on the response of the connection systems themselves in order study the effects that the cyclic lateral load produced on the coil rod connections. The full scale experiments have shown that a correct detailing of these connections may imply a significant potential to use their ductility capacity, thus reducing the size

of the seismic joint, being the system able to use flexural yielding mechanisms. Hence a series of tests used various levels of displacement to identify a limit state corresponding to fracture of the connections.

The following test setup was used to apply lateral force to the coil rod by extending and retracting the actuator.
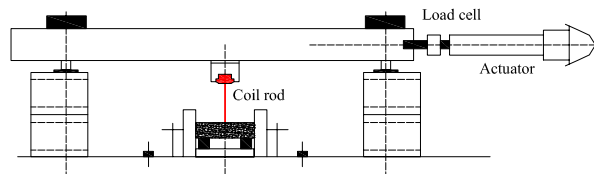
Fig. 42: Test setup

Consistently, the fracture occurs at a region of concentrated yielding at one end of the rod. While a fracture of the rod would result in the potential collapse of the panel and is thus unacceptable, predicting the fracture limit state would allow the precast producer to make suitable decisions about the proper detailing of connections.

The main conclusion found by the authors was that precast concrete facade systems designed for seismic loads perform very well when they displace up to the level that was imposed during the design process. In addition, when they displaced significantly beyond the design displacement, the prevailing form of damage observed was cracking of the concrete, both due to flexural response of the panel and to the behavior of the connection embeds.

The damage mechanism of the panels seems to be closely related to the size of the seismic joint. Modern design procedures usually contain very large width of joints. Concern about the successful performance of older systems with narrow joints does not appear to be a concern.

Finally, the detailing of cladding connections to allow ductile yielding during major earthquakes has the potential to develop suitable performance of commercial buildings with narrower seismic joints.

In the study of Bora et al. (2007) the authors present a load-limiting foundation connection for precast, prestressed panels used as shear walls that is able to prevent the development of excessive uplift forces in the joint. This connection allows precast, prestressed concrete wall panels, such as hollow-core members, to act as shear walls when resisting seismic loads without relying on the ductility of the wall ductility or causing an anchorage failure in a thin concrete section of the wall panel (where a connector is located).

The main aim of the authors was to develop a tool for practitioners to use precast concrete members with thin cross sections, such as hollow-core panels, as shear wall systems.

Precast concrete walls have been used for seismic load resistance by designing them to emulate cast-in-place shear walls. This is typically accomplished using ductile vertical reinforcing coupled with splice sleeves or other devices to create continuity across horizontal wall joints because some codes prohibit the use of prestressing across joints to resist seismic load.

The resistance to overturning moment from lateral seismic loads appears as a vertical force couple at the wall corners as shown in Fig. 43. In such a system, the lever arm of the lateral force (the height of the wall in a single-story system) is often greater than the wall width. Thus, at one base connection, a large uplift force is created and at the other base corner, a compressive force is developed.
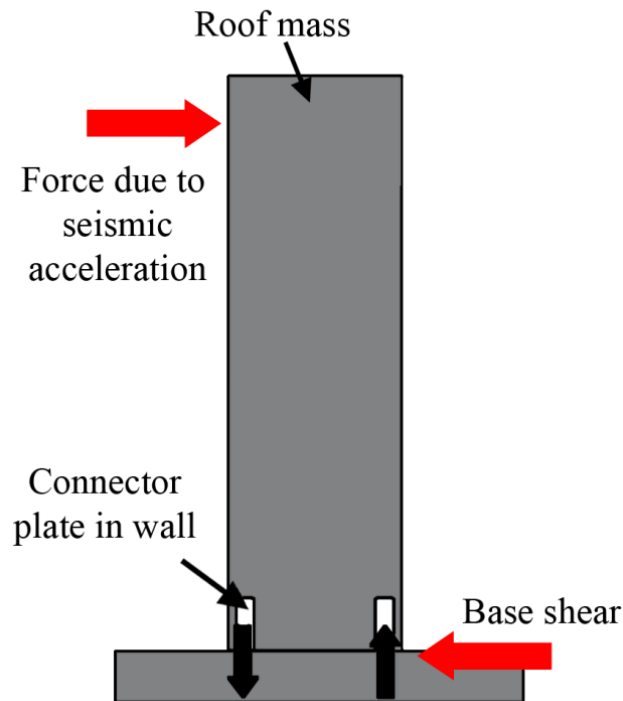
Fig. 43: Force couple and overturning moment

The force that the ground applies to the wall system and to the connection anchorage can be limited by the use of special connectors. The authors made an investigation of the seismic performance of a variety of connection details that shows that friction joints or slotted-bolted (SB) connections may provide an effective way for limiting the shear force applied to the wall system while dissipating substantial earthquake energy.

The authors studied the development of an SB connector system for thin-walled precast concrete panels that allows the panels to resist earthquake-induced lateral load as a shear wall and also as an exterior curtain wall. The paper focuses on describing the system components, key experimental tests, and a suggested design method.

If SB connectors can maintain an elastic-plastic response, as shown in Fig. 44, when subjected to a seismic loads, the force passing through a connection can be limited to avoid anchorage failure in thin-wall sections while providing energy dissipation.
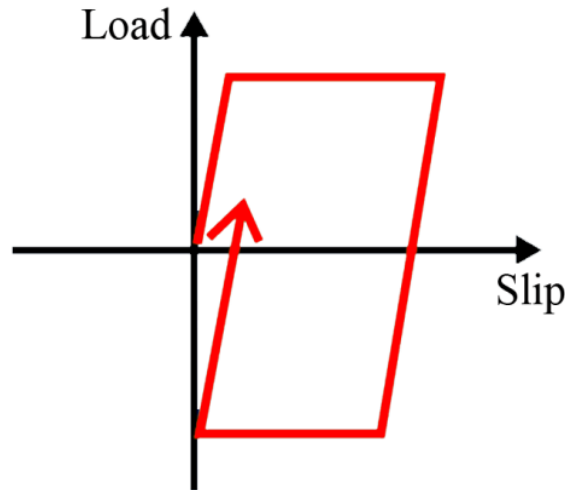
Fig. 44: Ideal load-slip plot

One method to reduce the force couple at the base of thin wall panels is to connect adjacent panels, forming a wide wall as in Fig. 45. The wider moment arm at the base of the panel reduces the vertical force components.
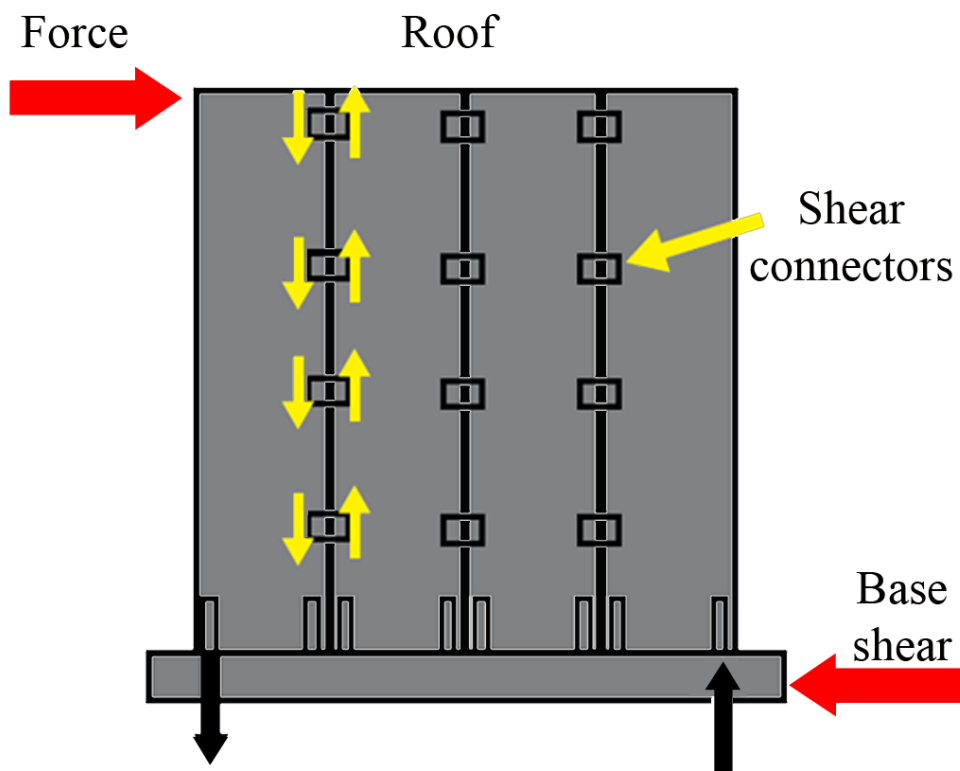
Fig. 45: Joining adjacent panels

Figure 46 shows a schematic of the wall system proposed by the authors. The system includes all components required to transfer lateral seismic load between a roof diaphragm and the foundation: the connection to a roof diaphragm (top connection), the wall itself, a compression/shear connection at the base, and a tensile connection at the base.
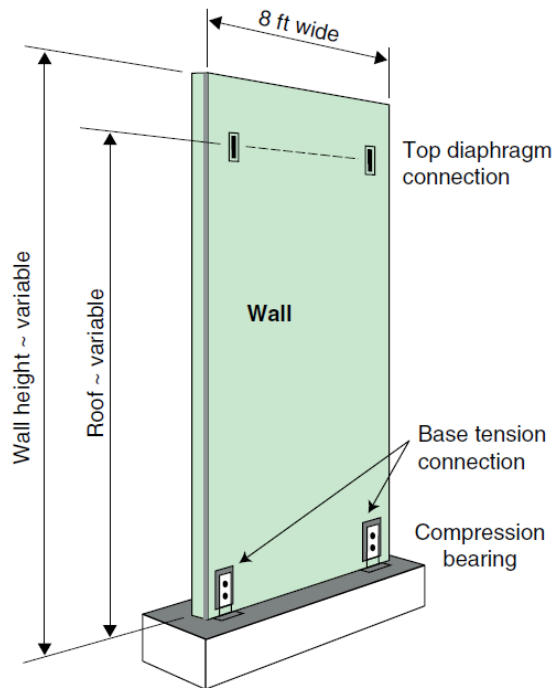
Fig. 46: Components of the proposed system(8ft = 2.44 m)

A typical top connection uses two commercially produced slotted connectors, such as Corewall or PSA-type inserts. A Corewall connection to a lightweight steel roof structure is shown in Fig. 47a, and added anchorage reinforcing to fix the insert to the concrete is shown in Fig. 47b.

(a)   **(b)**

Fig. 47: Top connection: (a) Corewall attachment to roof; (b) Anchorage of slotted insert

The wall is a standard U.S. hollow-core panel, 8 ft (2.4 m) wide and 8 in. (200 mm) thick, with the cross section shown in Fig. 48. In some instances, the panel may also include an insulation layer or wythe covered by a thin, protective concrete layer. Because these added elements do not contribute to the panel's lateral-load resistance, their presence is irrelevant in the performance of the shear wall and the authors have ignored its contribution.
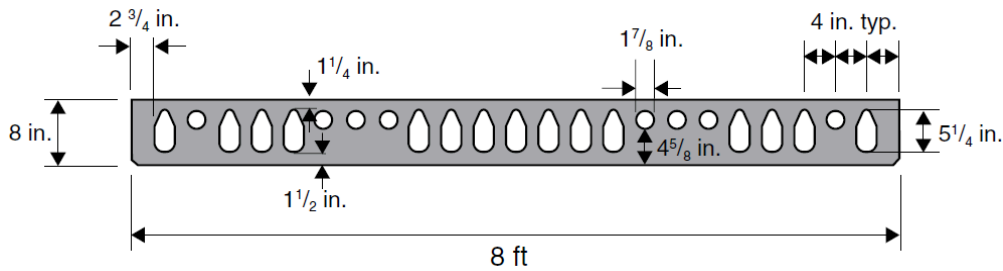
Fig. 48: Wall section. Note: 1 ft = 0.305 m; 1 in. = 25.4 mm.

Prestressing strands, not shown in the Figure, are added inside the panel as needed for out-of-plane resistance and handling of the wall panel.

With lateral loading, a tension-compression couple develops, as illustrated in Figure43.

A special SB connection is used to resist the tensile component of the coupling force developed at the base. In addition to the mechanism of the SB connection, an anchorage system is required within the wall. The SB connection system resisting in tension is shown assembled in Fig. 49a, and the individual components are shown in Fig. 49b.

The SB connection is intended to slip and dissipate energy through friction under cyclic loading.

(a)   **(b)**
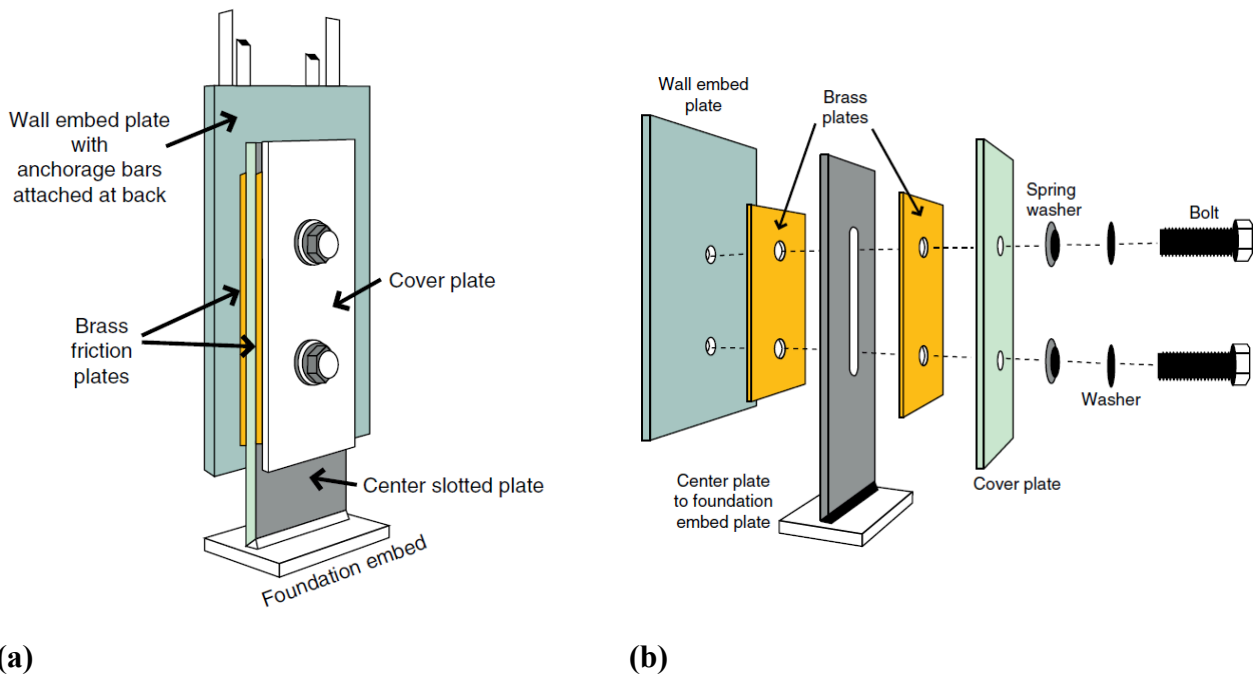
Fig. 49: Tension Base Connection: (a) Diagram of slotted-bolted connector; (b) Components of the slotted-bolted connector system

The goal of the proposed system might be expanded beyond just the aim of controlling forces applied to the thin sections of special precast concrete wall elements.

The SB connection may be designated as the key component to keep the size of loads transferred to the panel below the SB connection's elastic limit and may also be designed to dissipate energy introduced by seismic movement.

For the top connection, the capacity of a single connector was measured in three separate out-of-plane tensile tests. Two connectors were attached to a single loaded beam in measuring their

horizontal shear capacities to simulate the actual loading of a wall panel with two top inserts. Three identical tests were conducted. The failure occurred with a popout or spall of the concrete on the far side of the insert, as shown in Fig. 50, due to twisting of the insert in the concrete.

Fig. 50: Slotted connector shear test

The performance of the connector is shown in Fig. 51. Initial softening occurred at a load of 10 kip (44 kN) when cracks developed from the strands to the concrete surface. The connector appeared to yield and the capacity dropped slightly after the circular crack visible in Fig. 50 that occurred at 0.8 in. (20 mm).
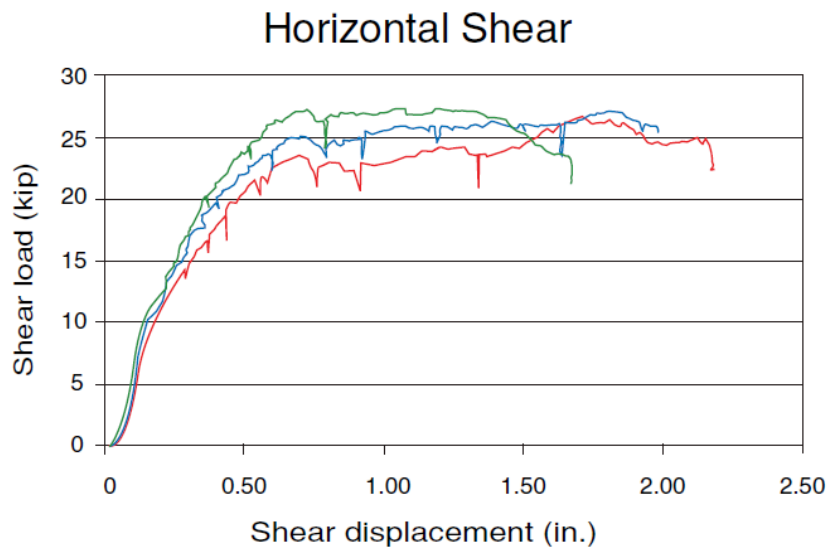
Fig. 51: Slotted-insert pullout test results. Note: 1 kip = 4.45 kN; 1 in. = 25.4 mm.

The prestressed wall panel is protected by the limited capacity of the SB base connection.

Without axial load, the cracking moment for a hollow-core panel can be directly calculated. If a lateral load was applied, as in Fig. 43, at a roof height of 34 ft (10.4 m) and the wall moment is limited to the cracking moment, the lateral capacity equals the cracking moment divided by the distance to the lateral force. A dilemma in defining the shear capacity of the wall comes from the two separate approaches in considering its behavior.

The authors pay particular attention at evaluating the performance of the SB connection because it is relied on controlling the peak seismic force applied to the wall.

Because the connection is expected to experience the effects of a minor earthquake before a major earthquake occurs, the cyclic testing started at low lateral force levels. Three cycles in tension were first applied at a level equal to 25% of the expected slip force (6.25 kip [27.8 kN]). They were followed by three more cycles at an amplitude of up to 50% of the expected slip force (12.5 kip [55.6 kN]). Then, the joint was tested at a series of larger tensile displacement levels of 0.28 in.[7 mm], 0.4, 0.7, 1.1, 1.6, 1.1, 0.7, and 0.4 in. (10, 18, 28, 41, 28, 18, and 10 mm) that would induce slip-yield displacement. Three cycles were repeated at each displacement level. Upon completion of those tests, the joint was finally subjected to three cycles at a peak tensile displacement of 2.5 in. (64 mm), or nearly 3% wall drift in an 8-ft-wide (2.4 m) panel. The two cyclic loading programs are shown in Fig. 52.

(a)   (b)
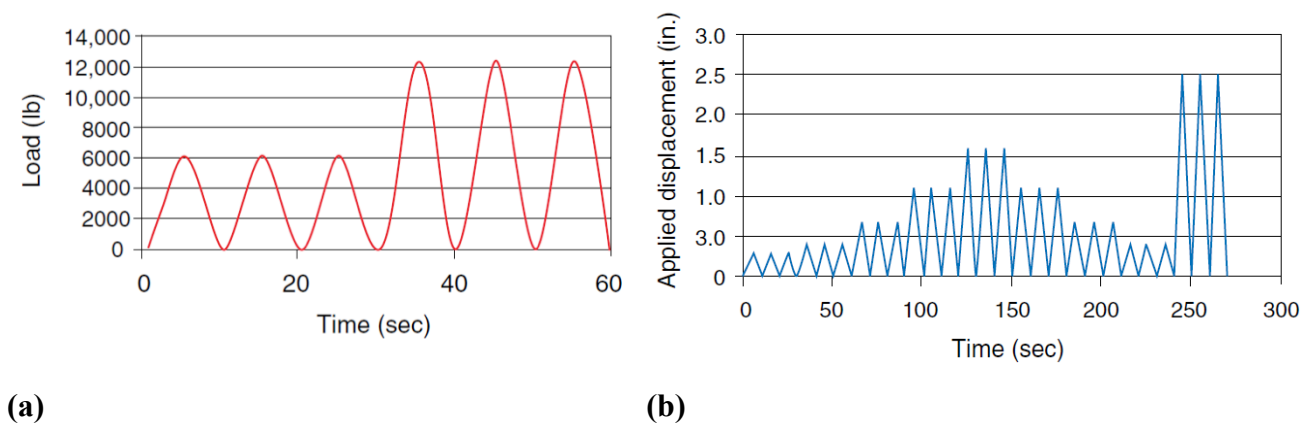
Fig. 52: Applied cycles: (a) Initial slotted-bolted connector applied load cycles. Note: 1000 lb = 4.45 kN; (b) Applied displacement cycles. Note: 1 in. = 25.4 mm.

By means of a series of experimental tests, the authors defined the capacities and behavior of a complete precast concrete hollow-core shear-wall system. Those quantities were coupled with a design procedure developed to ensure that the seismic forces introduced into the wall remained lower than the elastic capacities of the wall elements.

4 Residential precast building practice

Once the prevailing findings and trends of modern Standard and current research applications were presented, a detailed review of residential precast building practice will be provided considering the International market with particular emphasis on the Dutch scenario. In the upcoming discussion, a general overview of the main characteristics will be given, and specific aspects are referenced when needed to explain key points. Particular care will be paid to examine the wide variety of solutions pursued by different Dutch precast producers.

4.1 International practice

Panels are the most common members used in building construction, and may serve as structure or cladding or both. The use of such panels can result in a fast, simple construction process on site followed quickly by finishing trades. As structural-architectural panels, they provide a cost effective solution for building enclosures. Panels can be full or half-sandwich or hollow core constructions. Full-sandwich panels are popular because they provide two durable faces and allow a space between that is filled with insulation. The half-sandwich panels contain just one concrete face and therefore require additional insulation and finishing after erection. Hollow core panels can be used for walls, but are especially well suited to floors. The cores can be used for utility chases or sometimes as ducts for heating, ventilation, and air conditioning (HVAC).

Some companies have a broad range of experience of precast members and some have also studied the potential for panelised or volumetric precast in their designs for houses. The most popular use for precast concrete, however, is in components. This includes walls, beams, floors, columns, panels, lintels, stairs and cills. The benefits of such products for housing are well known. Items such as lintels and cills are mainly stock items, available in standard sizes, often concealed after first/second fix and very economical when procured in quantity.

In general, there are three broad categories of use for precast concrete, namely:

- Components;
- Panels (2D construction);
- Volumetric (3D construction).

The housing system subject of the research is a single-family detached home, also called a "single-detached dwelling" or "separate house" and is a free-standing residential building.

Load-bearing wall elements for instance can be used in either cross-wall or spine wall arrangements; for low-rise housing, the most likely option is cross-wall construction with party walls between dwellings acting as the key structural elements.

Based on considerations of buildability, economy and standardization of precast components, the structural concept developed consists of:

- Conventional foundations comprising footings, raft slab or piles and pile caps.
- Cast in-situ first storey, typically reinforced concrete beam and slab system.
- Precast concrete load bearing walls.

- Precast concrete non-load bearing façade panels.

- Precast concrete floor system, either:

- Precast concrete beams and precast slabs (reinforced concrete or prestressed solution) with a composite in-situ topping or Precast concrete walls with precast concrete slab system.
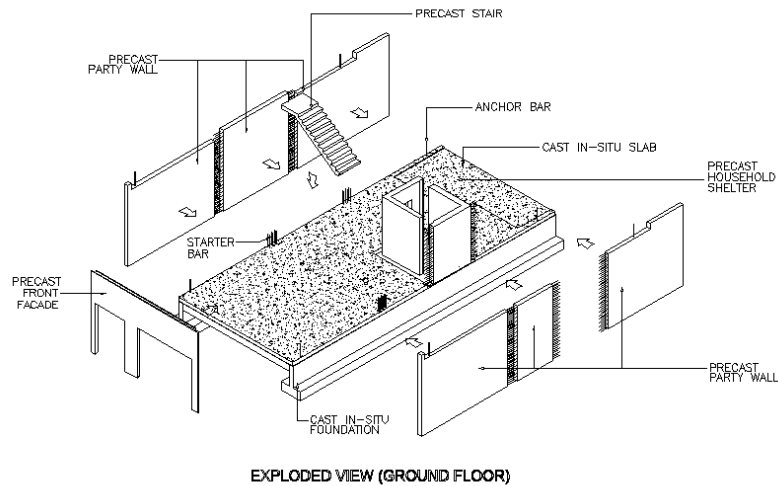
Fig.53: Precast prestressed slabs spanning between walls with composite in-situ topping for 1st storey
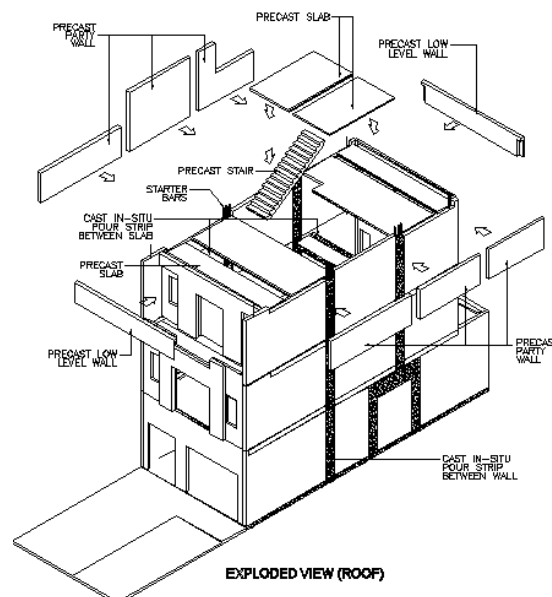
Fig.54: Precast prestressed slabs spanning between walls with composite in-situ topping for roof

The foundation loads for the precast structural system will be similar to those for conventional design. However, the arrangement of the foundations below the load bearing walls will be different from those normally adopted for a column and beam structural system. The desirable arrangement should provide a relatively uniform support along the entire length of the wall and minimize the eccentricity effects due to any possible misalignment of the walls relative to the foundations.

In the case of a footing foundation system, the recommended solution is a continuous strip footing below the load bearing walls.
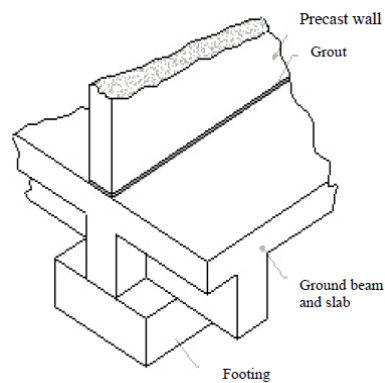
Fig.55: Footing below precast load bearing walls

Precast load bearing walls provide an economical solution when compared to the conventional column/beam/infill wall system. The primary advantages are the speed of construction and a partial or complete elimination of wet trades. Specification of precast components is determined usually by cost, speed and performance benefits and hence components that offer significant advantages will be able to compete against traditional materials.

With reference to structural and non-structural use of concrete in buildings, there are a number of key benefits that are inherently related to concrete as a material, wherever it is used. The advantages considered relevant to house building are fire resistance (for example, a 150mm thick concrete wall can provide over 90 minutes fire resistance), thermal performance and sound insulation.

Normal density concrete is able to contribute usefully to the thermal comfort conditions within a building (other solid construction materials can perform a similar function). Concrete's thermal capacity allows heat to be absorbed and stored in the building structure and either re-radiated or "purged" during cooler periods. Moreover, concrete can provide high level of internal temperature stability that is simply not attainable with lightweight construction.

Unlike steel or timber systems, concrete offers the possibility of housing that is intrinsically solid, with high acoustic performance.

Another key factor is the production in controlled environments such as precast concrete factories. In addition, the greater degree of control (and the lesser degree of risk) will result in a higher quality product compared to its on-site equivalent. The ability to work in a weather-independent and controllable environment means that strength, surface quality and consistency, and detailed design features in precast concrete components should be much easier to achieve. Indeed both the material and dimensional properties of the product should benefit from such a production environment.

In adopting the wall thickness, structural adequacy is not the sole consideration.

Other factors to be considered include:

- Connection details for supported beams and slabs;
- Sound transmission and fire rating;
- Joint details at panel-to-panel connections;

- Possible future embedded services, which could reduce the concrete area available.

For corner terrace and semi-detached units, the external side wall is required to be load bearing. In this case, the panel design will be influenced by factors such as:

- The extent of openings required for windows and doors;

- Available load paths for transmission of vertical loads;

- Horizontal joint details, which due to waterproofing considerations are likely to lead to eccentric load transfer;

- Connection details for supported beams and slabs;

- Joint details at panel-to-panel connections.

In some cases, plain concrete design may be applicable. However, it may usually be necessary to adopt reinforced concrete design with continuity of vertical bars in these load bearing walls. For these walls, the recommended thickness is 150mm (in Singapore).

In the case of the presence of precast non-load bearing façade panels, typically, the wall panels for the front and rear elevations are non-load bearing façade elements. Support of these panels is achieved by any of the following methods:

- The façade panel is connected to main load bearing walls and is designed to carry its own weight between supports.

- The façade panel is connected to the floor slab or beam, which is then designed to provide support to the wall.

Facade panel spans between walls

End connections to main load bearing walls support the facade panel
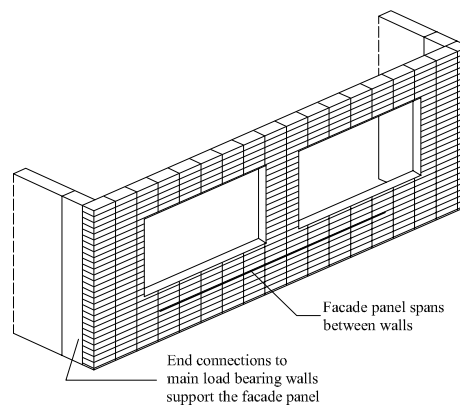
Fig.56: Facade panel supported by load bearing external walls

These panels will typically be designed for vertical loads due to self weight and an allowance for floor loads, if applicable, in addition to horizontal loads due to external wind pressures.

Façade panels will often require three-dimensional architectural features, such as hoods, sills and ledges.

The location of joints between the external wall panels should be selected based on a careful consideration of the following factors:

- Structural considerations;

- Aesthetics;

- Panel weight;

- Transport limitations;

- Internal crack control.

There are two main types of prefabricated panels: solid panels and flat slab sandwich panels.

Solid panels are uninsulated flat slab concrete panels of uniform thickness, typically 15 to 20 cm, which are cast on flat forming beds within controlled factory conditions. Non-load bearing conditions typically require no more than a 15 cm thickness, whereas load bearing conditions usually require 20 inches. Solid panels can be made in a wide variety of shapes and configurations.

Solid panels are typically used for special applications such as:

- Interior bearing walls and fire walls without the need for insulation.

- Institutional buildings requiring unique, deep thickness for security reasons, such as for instance correctional and other high-security applications.

- Residential and commercial applications where the owner and designer seek to insulate walls separately and apply specialty interior finishes.

Solid panels are typically used as interior partition walls and can be either load or non-load bearing. These panels can weigh from 3.5 kN/m^2 to 4.5 kN/m^2.

Flat slab sandwich panel are available in both composite and non-composite panels. The flat slab insulated sandwich panel has two layers of concrete with rigid insulations. Cast in a form on a flat bed, these panels can be made in a wide variety of shapes and configurations.

| (a) | (b) | (c) | (d) |
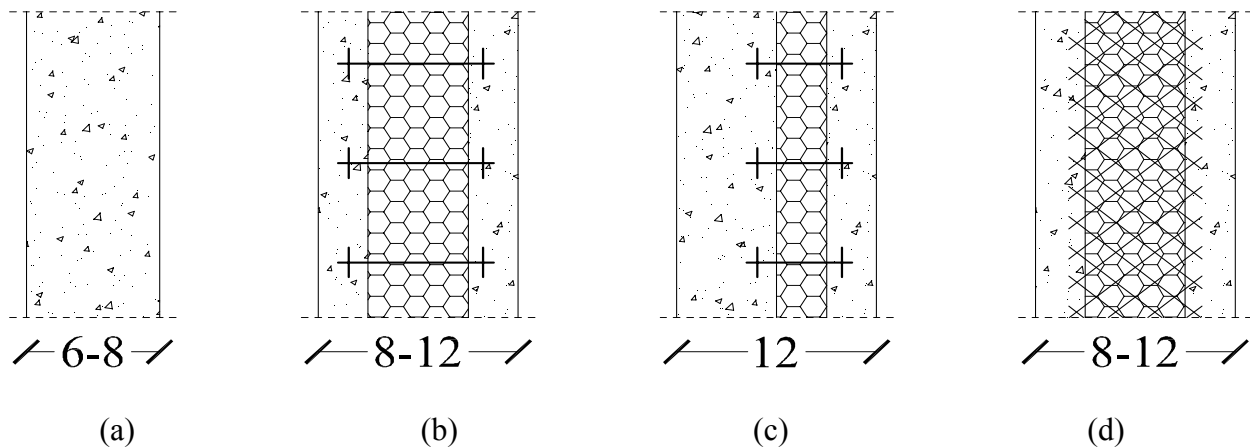
Fig.57: Typologies of wall panels: (a) solid panels; (b) non-composite/non-load bearing panels; (c) non-composite/load bearing panels; (d) composite/load and non-load bearing panels

Sandwich panels are concrete wall panels that have two layers of concrete separated by a layer of rigid insulation. They can be broken down even further into composite and non-composite sandwich wall panels.

Composite panels are fabricated so that the two layers of concrete, with rigid insulation in-between, act together as a single unit to resist the applied loads by providing a shear transfer mechanism between the concrete wythes.

Non-composite panels are fabricated with two concrete wythes acting independent of each other, with rigid insulation in-between them, typically with a nonstructural exterior wythe and a thicker structural interior wythe.

Wythe connectors are used to tie two concrete wythes together. They penetrate the rigid insulation and they are embedded in each concrete wythe. There is a wide range of connector sizes, shapes and materials based on the structural requirements of the wall panel.

Insulation used in concrete wall panels is of the cellular (rigid) type because it provides material properties that are most compatible with concrete. Cellular insulation comes in two main types: thermoplastic and thermosetting.

4.2 Dutch practice

In the Netherlands there are social and technical factors influencing the specification of materials in housing. As a result of the greater experience with precast concrete, there have been significant advancements in materials and production, which have contributed to the greater use of precast for building elements such as external and internal walls, and even roof panels. Such is the volume of production of these various precast elements, that it has been economically viable to build factories dedicated solely to the production of 2D and 3D precast concrete, as well as simpler components like walls, panels, floor slabs and lintels and stairs.

The tradition of brickwork and masonry construction in the Netherlands offer stiff competition for precast concrete in the housing market. Precast commands 10% of the total housing market and is steadily increasing its market share. This success is due to being able to offer a significant 30% cost saving by using standardized components, flexible manufacturing processes, industrialised building techniques and "streamlined contracting" (Glass, 2000).

The basis of Dutch law on building work is the Housing Act. The Building Decree (Bouwbesluit) which came into effect in October 1992 contains nationally uniform technical legislation. The main points are:

a) it covers the essential requirements of safety, health, usefulness and energy economy;

b) requirements are formulated as far as possible as performance requirements and by reference to Standards;

c) relevant certificates of conformity and Technical Approvals may act as proof of meeting the requirements of the Building Decree;

d) municipalities cannot impose separate technical requirements and the planning legislation is separately controlled.

The Building Decree is published as 14 independent Chapters covering the technical regulations for construction work and the state of existing construction works. It contains a collection of performance requirements, by which building plans can be tested using measurements or calculations and indicates, through a test value, whether the requirements have been complied with. The builder can decide how to construct and which materials to use providing the performance requirements are met. The Decree refers to Dutch Standards (NEN's) concerning buildings and civil engineering works (Category 'A' Standards). Provision has been made in the Building Decree for

Dutch Standards (NEN's) to be replaced by harmonized European Standards (NENEN's) as these become available.

With reference to the mechanical resistance and structural stability, Standard NEN 6702 refers to the ultimate limit state of the structure. Compliance relating to the ultimate limit state is referred to in accordance with the relevant parts of specific Standards for the type of construction, e.g. NEN 6720 and NEN 6790 for brick or concrete materials. There are specific requirements in respect of collapse in a fire situation whereby the limit state shall not be exceeded within specified time periods.

Requirements for fire resistance, surface spread of flame and means of escape are set out in tabular form and appear to be broadly similar to UK requirements.

There are also requirements for the limitation of sound transmission between adjoining dwellings and for the external walls of the dwelling. Detailed requirements are set out in NEN 5077.

For what concerns energy economy and heat retention, as well as for the requirements related to dwellings and residential buildings, the external walls in habitable rooms, toilets and bathrooms must have a thermal resistance of 2.5 m^2K/W determined in accordance with NEN1068 (equivalent to a U value of 0.4 W/m^2K). A maximum total area of 25% of a dwelling or residential building can consist of windows, doors and their frames, providing this area has a thermal resistance of at least 0.11 m^2K/W (equivalent to a U value of 9.0 W/m^2K), and an area of 4% which does not need to comply with any thermal insulation requirement. These requirements do not apply if the dwelling or residential building has a thermal insulation index of at least 14 as defined in NEN 1068. The external and internal walls, floor and ceiling of a "staying area" (similar to a habitable room in UK regulations) must not have a greater air permeability flow rate (as referred to in NEN 2686) than 0.2 m^2/s.

The main producers of prefabricated buildings in the Netherlands are reported as follows.

CRH Structural is an international group which produces and distributes building materials (such as cement, aggregates and ready-mixed concrete), as well as precast concrete products for the construction sector (such as precast concrete floors, walls and building structures).

CRH Structural with its various partner companies for Netherlands works for both construction and prefabrication in residential and commercial construction and offer solutions for projects such as offices, garages, basements, commercial buildings and apartments.

The CRH group includes several companies that provide different products: Alvon walls and solid walls, Dycore flooring solutions, Heembeton walls and façades, Calduran limestone products and Stalius steel frame solutions. These companies provide the design solution and procedure, as well as the material transportation and the construction/erection of buildings.

A brief overview of the prevailing products, with their specific features in terms of geometry and material properties, will be given in the following.

Fig.58: CRH Structural wall panels
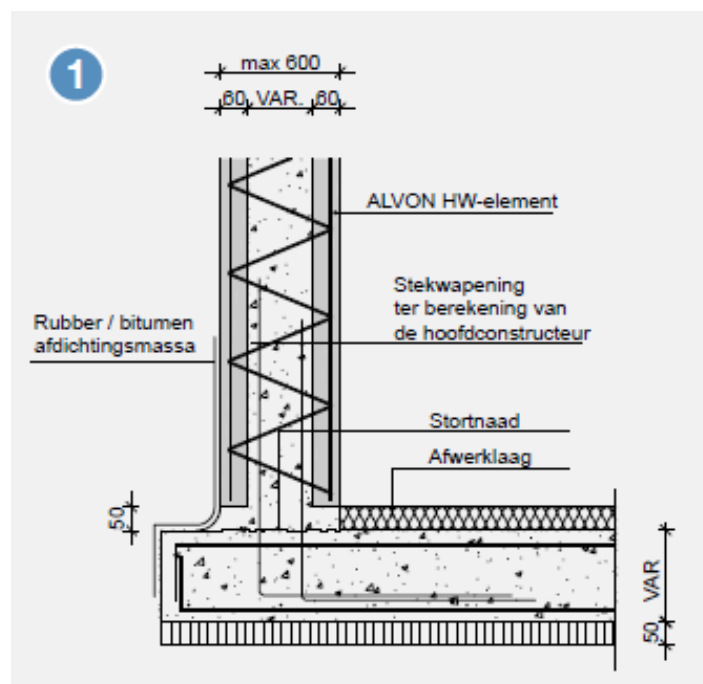
Fig.59: CRH Structural wall-foundation connection

The number-one precast concrete frame producer in the Netherlands is Heembeton. Part of the CRH Group, Heembeton is a market leader in the construction of prefabricated housing in the Netherlands.

The company provide a prefabricated housing framework and a comprehensive custom-made solution for constructing both the framework of a building and elements that can be used as façade elements or as gable panel walls.

Fig.61: Heembeton elements
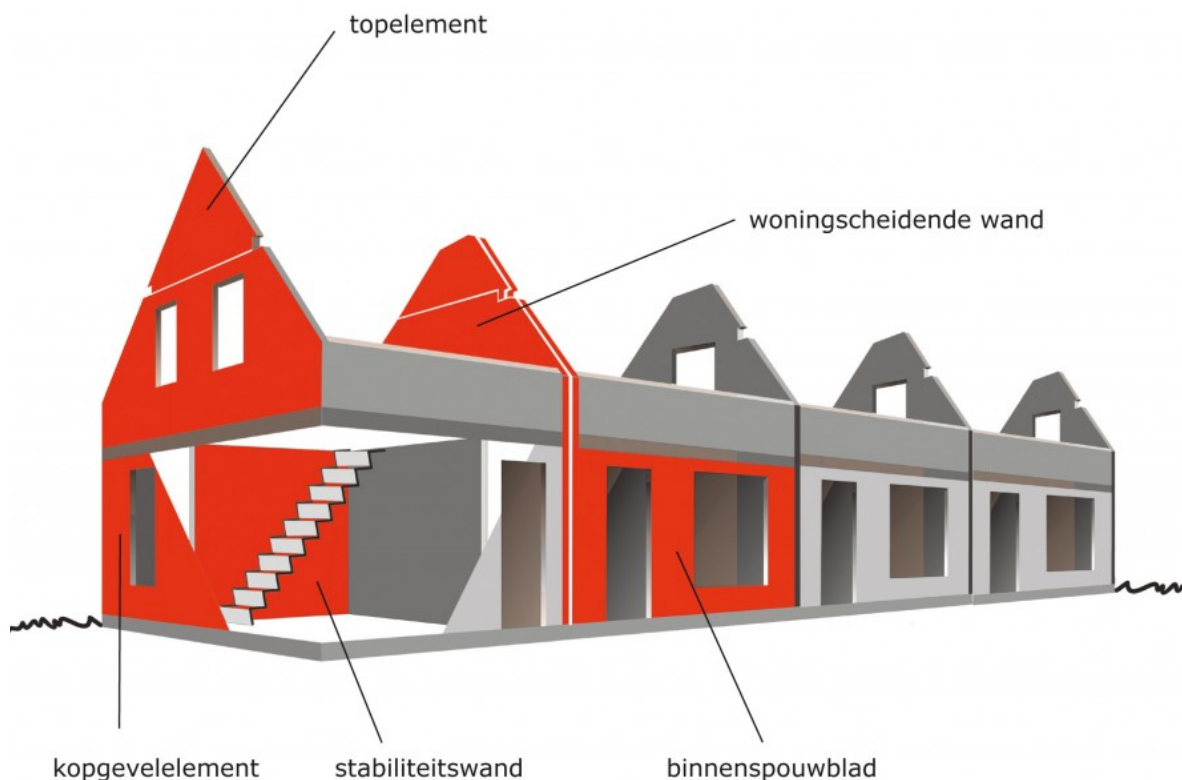
Fig.62: Heembeton costruction system

As previously mentioned, Heembeton produces façade elements, floor elements and wall elements. Some examples of typical precast members that are associated with this group will be provided in the following figures in order to present solutions representative of the market.

Fig.63: Heembeton construction phases

In the construction system the connection between the elements is provided by welded joints (conform to NEN-EN 287-1) and anchors, but also important are the cup joints and the connections with the foundations. During the construction phase of the building, to carry the horizontal load given by the wind action, temporary props are placed for the stability of the structure, until all the connections between the elements are realized.

Fig.64: CRH Structural wall panels with openings
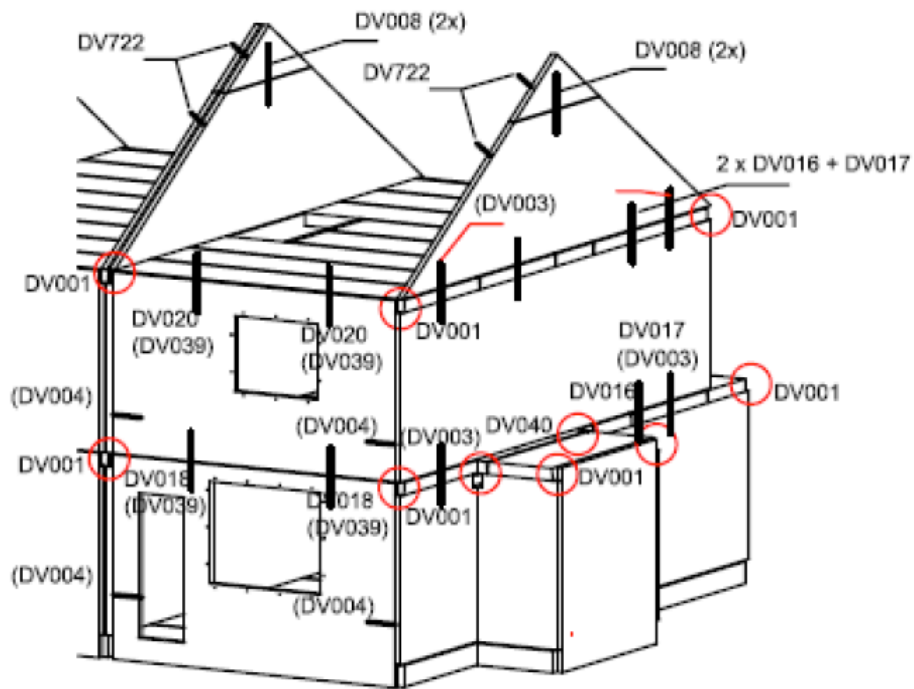
Fig.65: Heembeton connections and anchorages
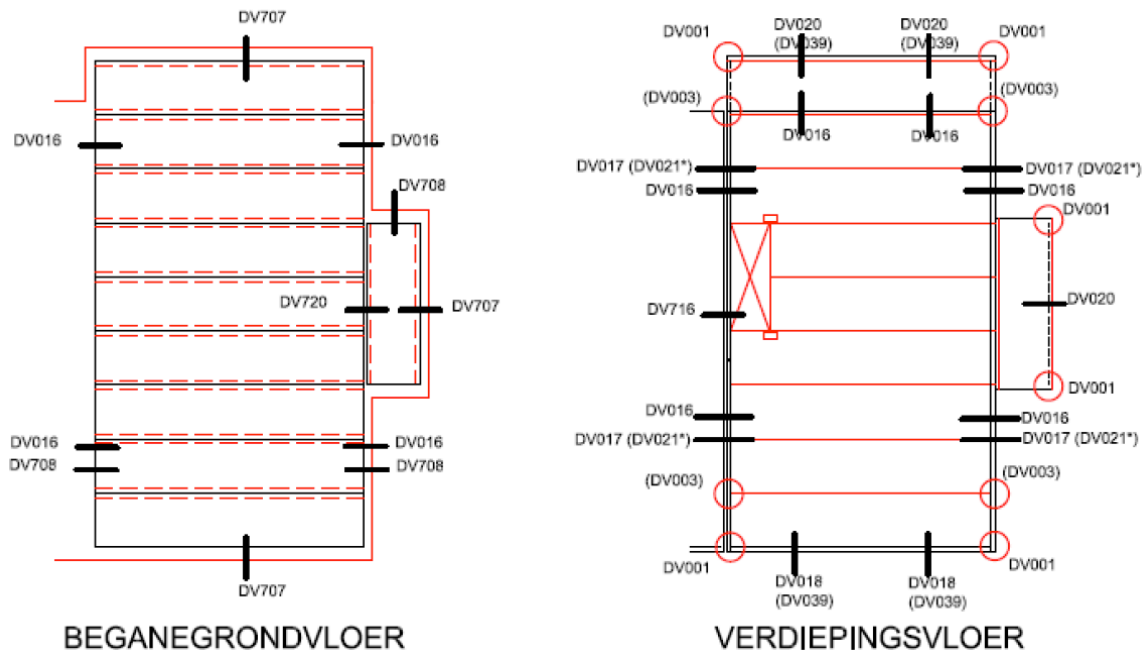
Fig.66: Heembeton connections and anchorages: ground floor (left); storey floor (right)

The material specifications and the dimensions of a standard façade element may be summarized as follows. These members typically present maximum length and height of up to approximately 10 m and 3.75 m, respectively. These products are 90, 100 or 120 mm thick elements and their weight per unit volume is roughly 2.400 kg/m^3. Concrete class C35/45 is commonly used to prefabricate them, making these members able to carry loads up to 1.5 N/mm^2.
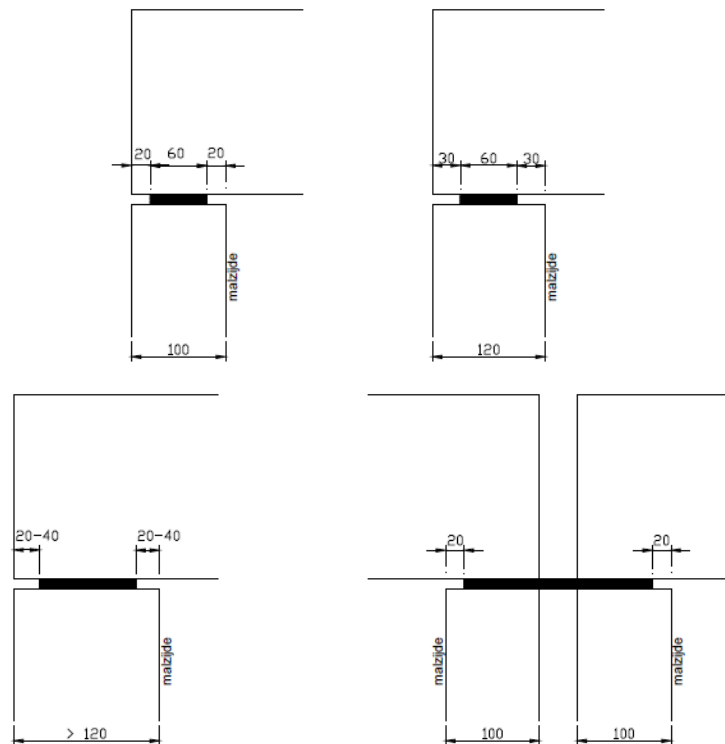
Fig.67: Heembeton dimensions of bearings
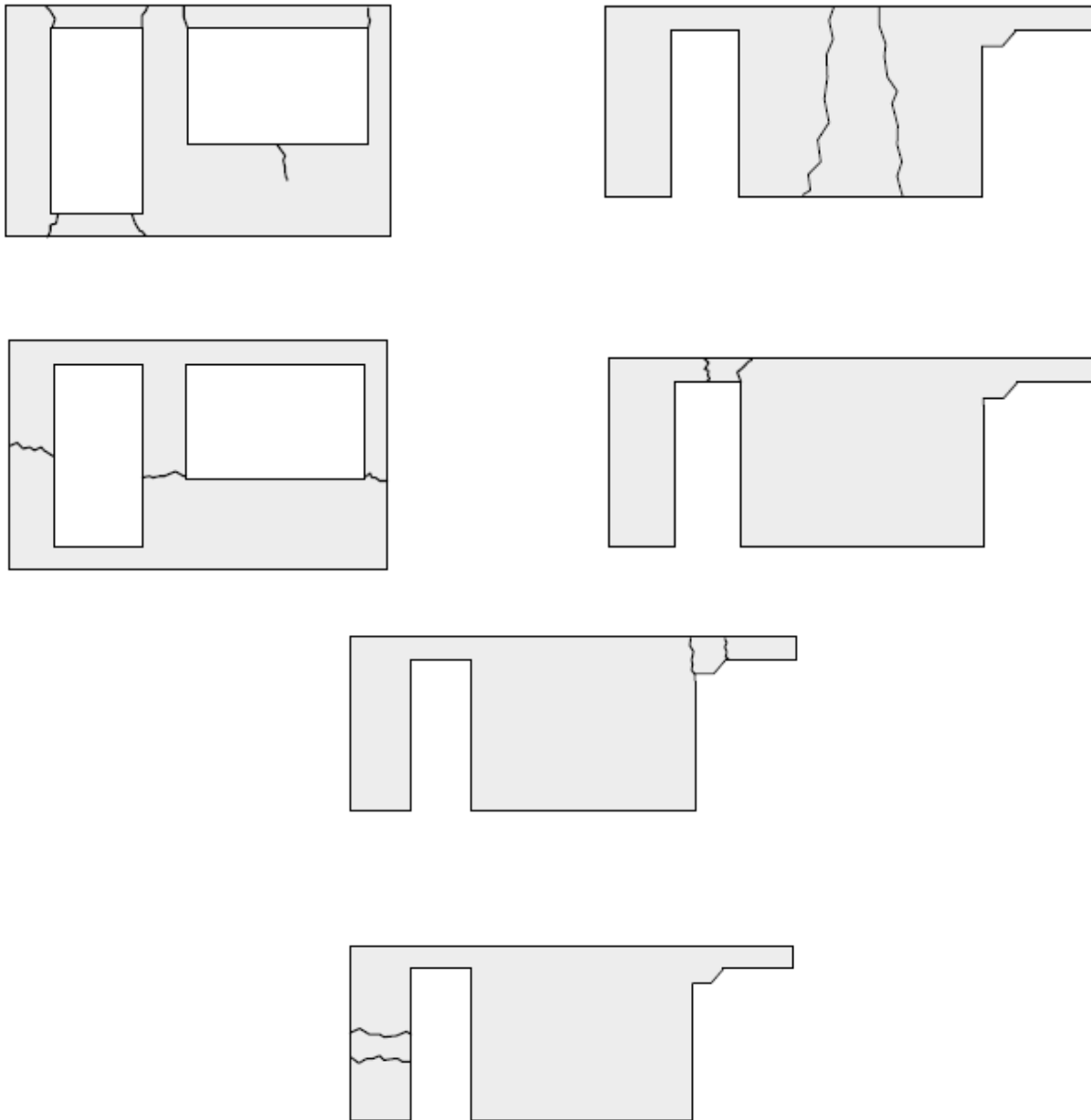
Fig.68: Heembeton façade elements: typologies with possible cracking

Within CRH Structural, Dycore produces precast concrete floor systems for ground and middle floors, from small to very large spans, which may be used for residential and commercial buildings and constructions in general.

Depending on the support structure of the building, the floor system can be selected from various types. In presence of columns there are different possible solutions such as hollow core slab with steel beams and precast concrete beams or a wide slab floor element with steel or concrete beams. A wide plate floor has the advantage that the reinforcement is provided in two directions. In this case the floor has two principal orthogonal directions, and simple cantilevers can be made in the surrounding part of the floor.

Fig.69: Dycore logo

Fig.70: Dycore's floors

K260-5

tot ca. 12 m 379 kg/m² incl. voegvulling

R1200
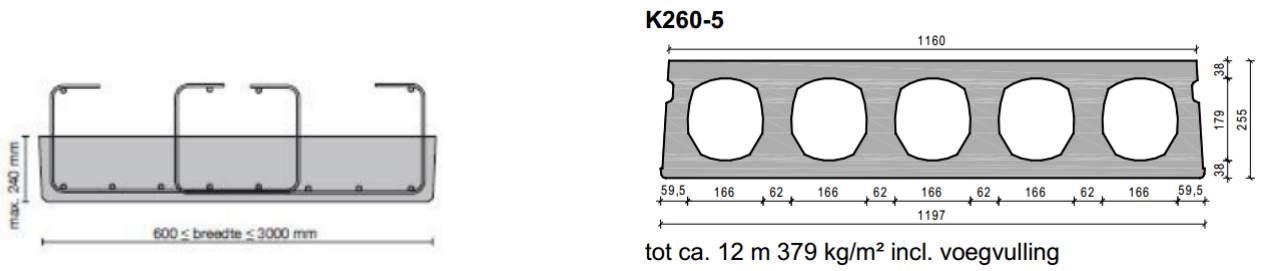
Fig.71: Dycore's types of floors
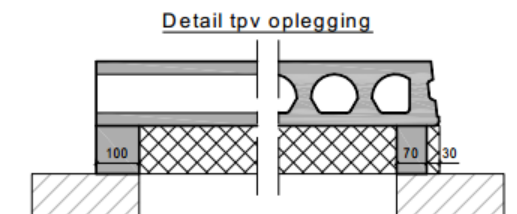
Fig. 72: Dycore – detail of typical supports

The material specifications and the technical characteristics may be categorized in two main classes according to product type (i.e. reinforced and pre-tensioned concrete wide plate floor). For what concerns the specifications of a reinforced concrete wide plate floor, these elements have a length ranging from 0.8 m to 10 m and a standard width of 3 m; they are usually 50, 60, 70 or 80 mm thick members, presenting a mass per unit area of 125, 150, 175 or 200 kg/m^2. By contrast, a prestressed concrete wide plate floor may be longer than the previous solution, since its length is conventionally in the range 0.8-12 m. Even in this case a standard width of 3 m is used for this floor typology. In addition to that, typical prestressed concrete wide plate floors are 80 or 100 mm thick members with a mass per unit area of 200 or 250 kg/m^2. The reinforced concrete slabs must have at least C28/35 concrete class, while the pre-tensioned floor standard concrete have strengths that correspond to concrete class C45/55. Pre-stressed strands quality FEP 1860 are used.
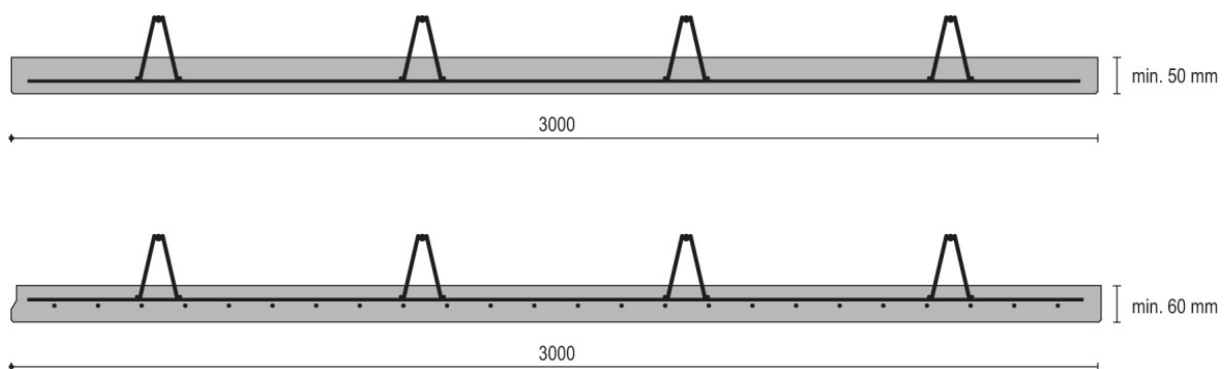
Fig.73: Example of Dycore floor

Another precast producer is Alvon which was founded in 1921 and is a leader in innovation and in efficiency of prefabricated building systems. Since January 2011 Alvon and Heembeton are trademarks of CRH Structural Concrete BV. Alvon works in close cooperation with Heembeton, Dycore System Flooring, Limestone and Calduran that are part of the same trademark.

Fig.74: Alvon logo

Examples of a typical construction system is provided in Figure 75, while Figure 76 presents the details of load bearing walls commonly used by this manufacturer.

Fig.75: Alvon construction system

The construction system proposed by Alvon consists of three different typologies of structural elements: two types of load bearing walls consisting of a cavity wall system and a solid wall system and one floor system. As previously mentioned, an example of each of them is given in Figure 76.

| (a) | (b) |
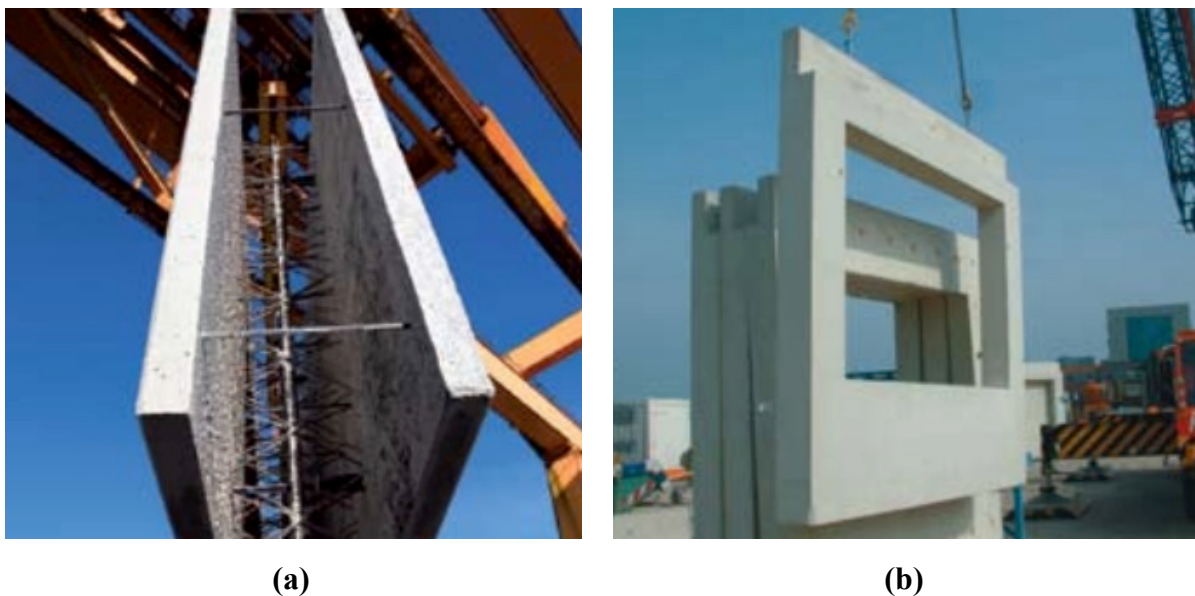
Fig.76: Alvon load bearing walls: (a) cavity wall; (b) solid wall

The Alvon cavity wall element consists of two precast panels that are connected to each other by means of a series of steel trusses. The steel truss ensure that the precast panels remain parallel on a certain distance from each other. In these precast panels a reinforcement is present. The steel truss ensure that the concrete panels that form cavity, during the filling of the cavity, are able to absorb the pressure of the concrete when grouting is carried out. After the cavity between the precast panels is filled with grouted concrete, the whole cross-section can be considered as monolithic. The shear stress is absorbed by the roughened inner sides of the panels that behave in combination with the diagonals of steel truss.

This solution can be used for commercial buildings, car parks, houses, dwellings and townhouses, apartment building, low-rise buildings, high-rise buildings or basements.

A further example of this precast solution is provided in Figure 77, where additional schematics are reported.

| (a) | (b) |

Fig.77: Alvon load bearing cavity walls

Similarly, Figure 78 shows an example of the solution commonly used to set in place and connect two exterior corner walls. Figure 79 presents a detail of a typical wall-foundation connection.

Fig.78: Alvon angle between two walls

Fig.79: Alvon wall-foundation connection

The prevailing material specifications are summarized hereafter. Portland cement CEM I 52.5 R, with a concrete strength corresponding at least to concrete class C28 / 35, is typically used for these members. They have a concrete cover in the range 15-50 mm and dimension of up to 3 x 8.9 m. The thickness of each panel ranges from 5 cm to 20 cm, while the thickness of the wall is in the range 20-60 cm. Construction tolerance are usually provided in accordance with NEN 2889. Steel FeB500 is used to reinforce this type of wall. Solid walls are mainly used in the construction of apartments, commercial buildings and offices. Solid walls are produced in steel molds with a flexible steel frame which enable virtually any shape and size. There is the possibility to add some integrating reinforcement. The advantages of solid walls are the fast assembly and a low cost of construction on site. A smooth surface is obtained and the erection of the panel is not dependent on the weather.
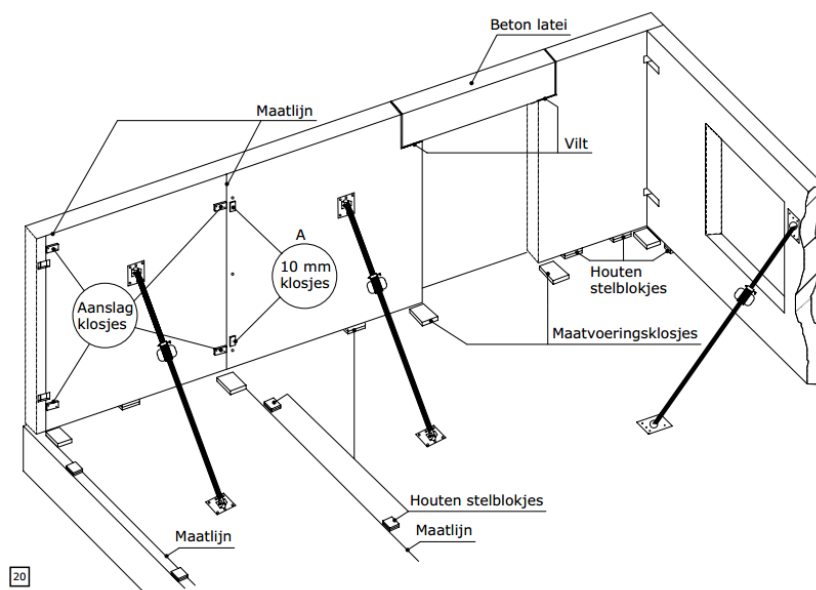
Fig.80: Alvon installation preparations

Fig.81: Alvon joint between two wall panel to be grouted with concrete
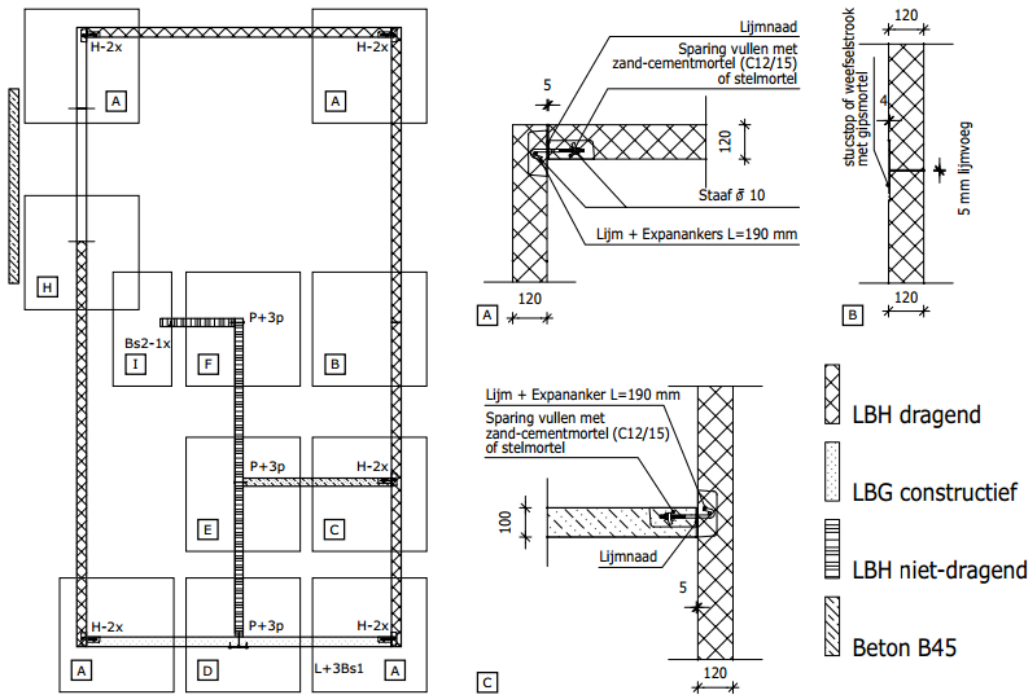
Fig.82: Alvon construction system: example of a floor plan

The typical thickness of the wall is in the range 70-300 mm and the maximum element weight is 11 tons. Portland cement CEM I 52.5R with conventional concrete strengths corresponding to concrete class C35/45 is assumed for this wall type. NEN 2889 is considered to determine tolerances.
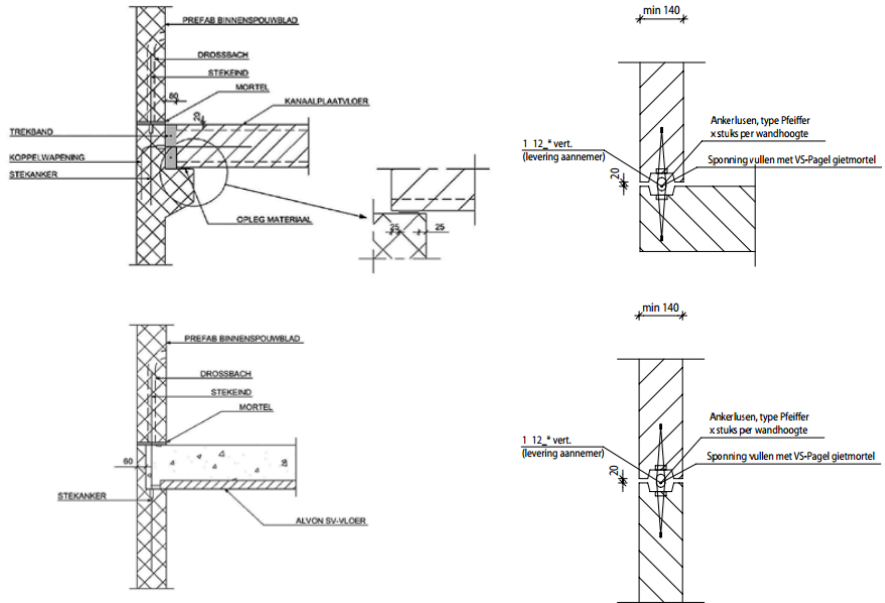
Fig.83: Alvon walls

Alvon also produces floor elements and long span slabs. In particular, the flooring system consists of a prestressed, self-supporting element that is assumed to realize a monolithic floor. An additional reinforcement consisting of steel FeB500 is arranged at the ends of each element. C35/45 concrete class is assumed (i.e. Portland cement CEM I 52.5 R). A standard width of 3 m is common for these products, the maximum length and weight of which is equal to 13 m and 10000 kg, respectively. As before, tolerances are computed in accordance with NEN 2889. The thickness of the slab is usually 200 mm and the concrete cover should be at least 20 mm.
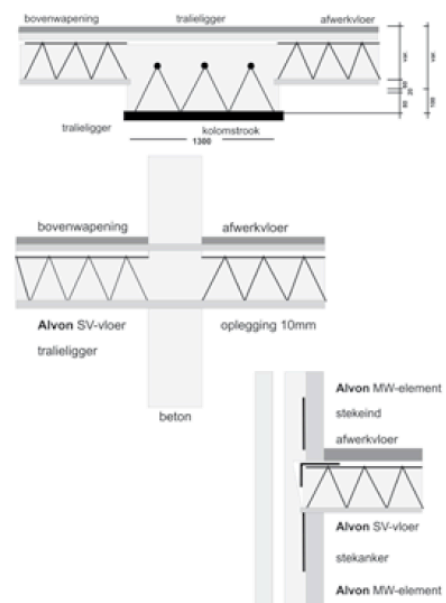
Fig.84: Alvon floor elements

Calduran Kalkzandsteen is a well-known supplier of sand-lime products in the Netherlands.

Fig.85: Calduran logo

For over a hundred years, it produced limestone and since 2004 the company exist under the name Calduran Kalkzandsteen. There are two production locations in the Netherlands: Hoogersmilde and Harderwijk. Harderwijk is also where the head office is located. From these locations the company supply limestone in many formats for construction in the Netherlands and parts of Germany and Belgium. The use of calcareous sandstone materials is very common in Netherlands and also in Germany. In fact, roughly two out of three houses are built with this particular technology.

Sand-lime stone products currently have a very wide utilization, both in the construction of housing and in renovation projects. The company produce bearing and non-load bearing walls for housing, apartments, schools, offices, commercial buildings, public buildings and agricultural construction.

Sand-lime products are available in different sizes and levels of strength. In general, the available formats are stones, blocks and elements. In terms of strength, sand-lime products are classified as CS12, CS16, CS20 or CS36. The CS36 quality is used for elements employed in the construction of medium/tall buildings (Hoogbouwelement®) which must be characterized by a greater resistance to compression and by a much higher density.
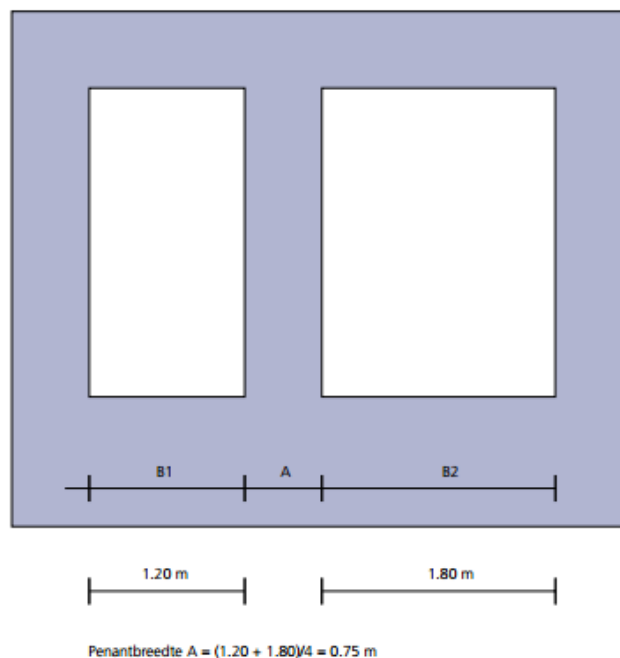
Fig.86: Calduran typical wall system. Detail of the openings

In Figure 87, some examples of the construction system usually adopted by Calduran are reported.

Fig.87: Calduran construction system

This type of elements is suitable for both load bearing and non-load bearing walls in residential and commercial construction.

Below are shown the resistances of the material according to the thickness of the wall, as well as a set of specifications concerning this type of system.

Tabel 7 elementen						
Wanddikte in mm	Type	Afmetingen (LxBxH) mm	Gewicht per stuk in kg	Druksterkte N/mm²	Aantal per m² (incl. voeg)	Lijmmortelverbruik in kg/m² excl. mors-verlies
67	E 67/538	997x67x538	67	12	1,85	0,9
	E 67/648	997x67x648	80	12	1,54	0,9
100	E100/538	997x100x538	99	12/20	1,85	1,4
	E100/648	997x100x648	119	12/20	1,54	1,3
120	E120/538	997x120x538	119	12/20	1,85	1,8
	E120/648	997x120x648	143	12/20	1,54	1,6
150	E150/538	997x150x538	148	12/20	1,85	2,3
	E150/648	997x150x648	179	12/20	1,54	2,0
214	E214/538	997x214x538	212	12/20	1,85	3,4
	E214/648	997x214x648	255	12/20	1,54	3,0
240	E240/538	997x240x538	255	12/20	1,85	3,8
	E240/648	997x240x648	238	12/20	1,54	3,4
300	E300/538	997x300x538	297	12/20	1,85	4,8
	E300/648	997x300x648	358	12/20	1,54	4,2

Fig.88: Calduran materials

5 Selection of the case studies and numerical modeling

The main aim of this research work is to define the collapse mechanism of the connection system of concrete walls, estimating both ductility and energy dissipation capacity, evaluating the seismic performance, feasibility and effectiveness of the representative connectors. An experimental activity will be carried out in order to include tests on different specimen typologies of precast panels and connectors.

The precast panels under investigation were extracted from a prototype that was design emulating a typical configuration of a Dutch single-family house. Figure 89 shows the typical dimensions of precast panels which are currently used in Dutch building practice. The prevailing steps concerning the design process of the building will be given in the upcoming discussion.

The reference standards used for the design of the structure are the Eurocodes, in particular:

- BS EN 1990 principles for structural design.

- BS EN 1991-1-1 Part 1-1: General actions – Densities, self-weight, imposed loads for buildings.

- BS EN 1991-1-4 Part 1-4: General actions – Wind actions.

- BS EN 1992-1-1 Design of concrete structures – General rules and rules for buildings.

These standards are consistently and concomitantly used the Dutch National Annex (NB).
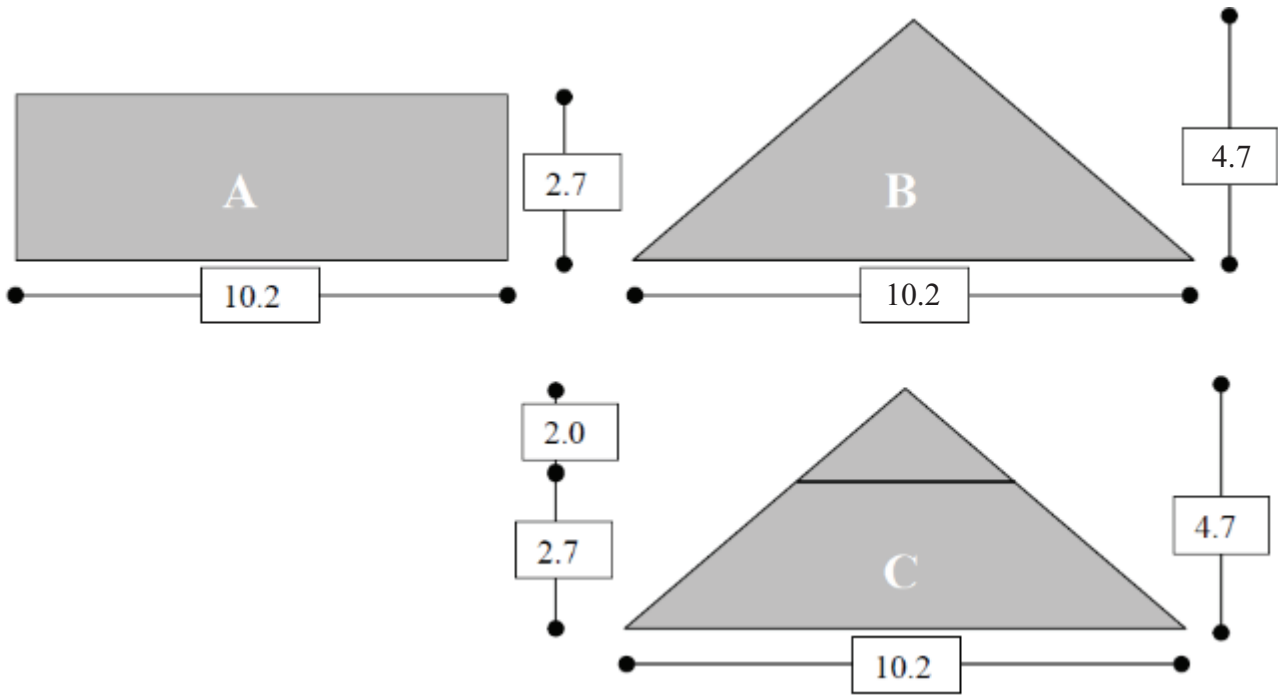
Fig.89: Typical dimensions of precast Dutch panels

The concrete class used herein is the C35/45.

The wind load and load combination factors used to determine the total horizontal force acting on the building are those given by the Dutch national Annex NEN-EN 1990(NB) of the Eurocode:

Gevolgklasse CC1 - volgens tabel NB.4 - A1.2(B) en NB.5 van NEN-EN1990

CC	Blijvende en tijdelijke ontwerpsituaties	Blijvende belastingen		Overheersende veranderlijke belasting	Veranderlijke belastingen gelijktijdig met overheersende	
		ongunstig	gunstig		Belangrijkste (indien aanwezig)	Andere
1	(vlg. 6.10a)	1.20 $G_{k,j,sup}$	0.90 $G_{k,j,inf}$		1.35 $\psi_{0,1} Q_{k,1}$	1.35 $\psi_{0,i} Q_{k,i}$ (i > 1)
	(vlg. 6.10b)	1.10 $G_{k,j,sup}$	0.90 $G_{k,j,inf}$	1.35 $Q_{k,1}$		1.35 $\psi_{0,i} Q_{k,i}$ (i > 1)

Relevante waarden volgens tabel A1.1 van NEN-EN1990 (NB)

Belasting	ψ_0	ψ_1	ψ_2
Windbelasting	0	0.2	0

Fig.90: Load combination factors

For a building height less than 10 m, the value of the wind action was obtained according to the Holland wind action map that is reported below.

Onbebouwd, hoogte ≤ 10 m:

windgebied	$q_p(z)$ kN/m² [kN/m²]	verhouding tov windgebied I
I	1.02	1.00
II	0.85	0.83
III	0.70	0.69

Fig.91: Wind load values

The panels which will be object of the experimental tests have been extracted from a building case study whose dimension were assumed according to the size of standard panels. The building that was design is a two-storey house plus a hip roof. The total height of the building is approximately 10 m, and the plan dimension are 10.2 x 13.2 m.

In Figure 92, 93 and 94, a series of schematics presenting elevation and plan views of the case-study building prototypes under investigation in the present report are provided to identify a typical structural scheme, as well as the prevailing geometric characteristics of the specimens extracted.

Fig.92: Building case study: west and south elevation

FLOOR PLAN
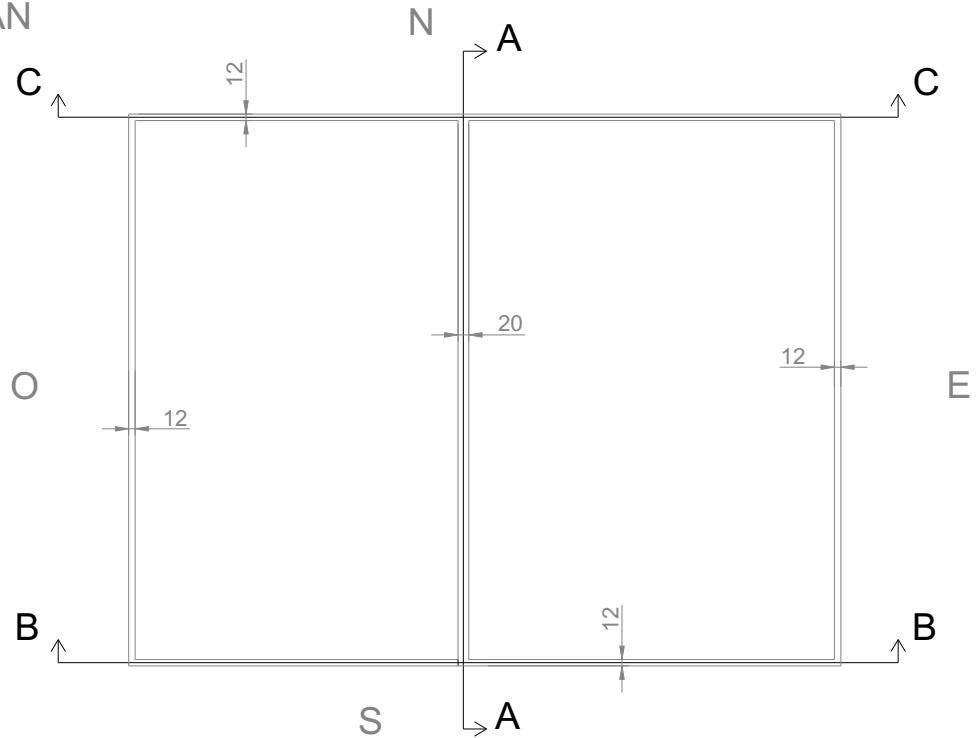
Fig.93: Building case study: floor plan

sez C-C
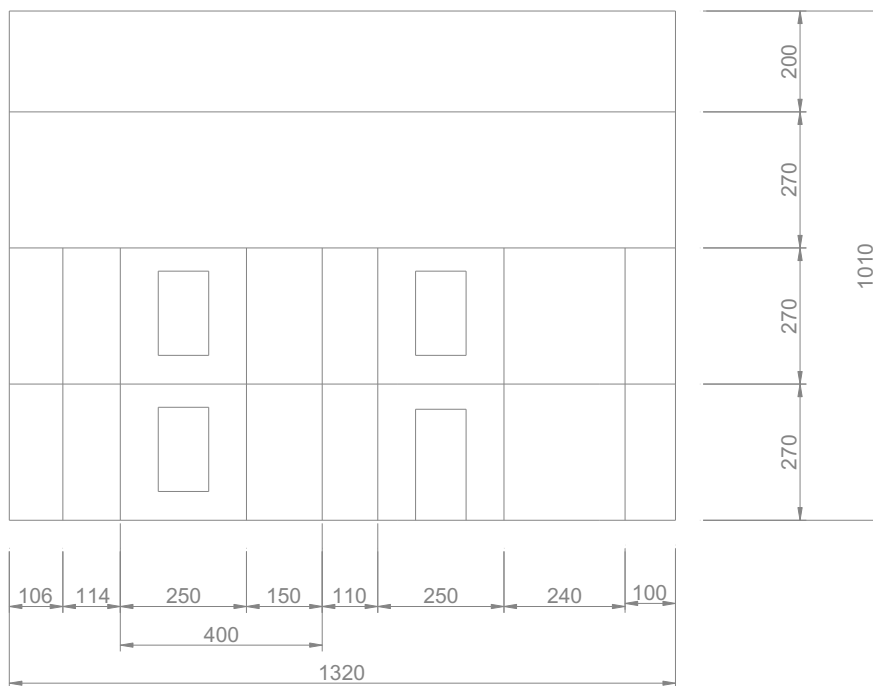
Fig.94: Building case study: side view

The project involved a preliminary design phase where the number of tests to be performed, and the choice of the geometry of the panels to be tested and axial loads imposed were chosen; the design of the reinforcement and the selection of the concrete was made in accordance with EC8.

The experimental test to be carried out are twelve. In particular, eight in-plane tests on full-scale panels and four tests on L-shaped specimens to assess the reponse of connections between panels. Therefore, the geometry of the panels has been selected and the levels of axial load to be applied on each panel has been determined in accordance with numerical assumptions representative of Dutch building practice for this structural typology. Each specimen of the eight in-plane tests consists of two panels connected together by means of special steel connectors. The global dimensions of the specimens are: 4 m in length and 3 m in height. In the case of full panels, each panel is 2 m long, while in the case of the presence of an opening, the panel with the window or the door is 2.5 m long while the other panel is 1.5 m long for a total length of 4 m.
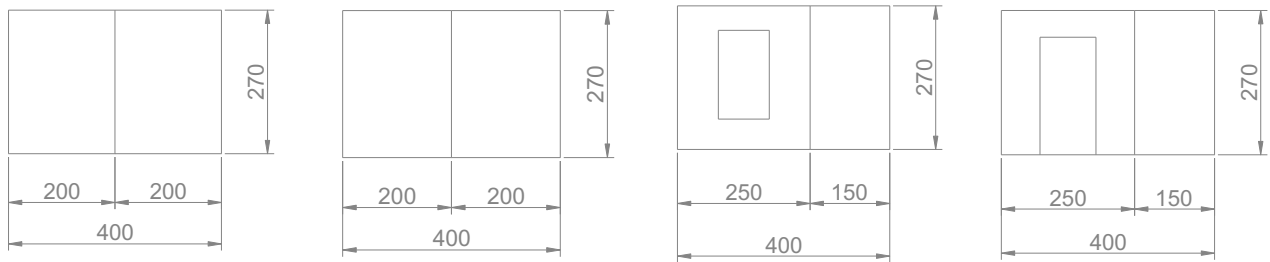
(a)   **(b)**   **(c)**   **(d)**

Fig.95: Case studies: geometry

The design of the reinforcement and the section of the concrete was made with reference to the EC8. The reinforcement is the minimum for large lightly reinforced walls. In the case of the panels where there are protruding bars, these bars where design only for wind forces. Some examples of the reinforcement arrangement assumed are provided in Figure 96, 97 and 98.

(a)
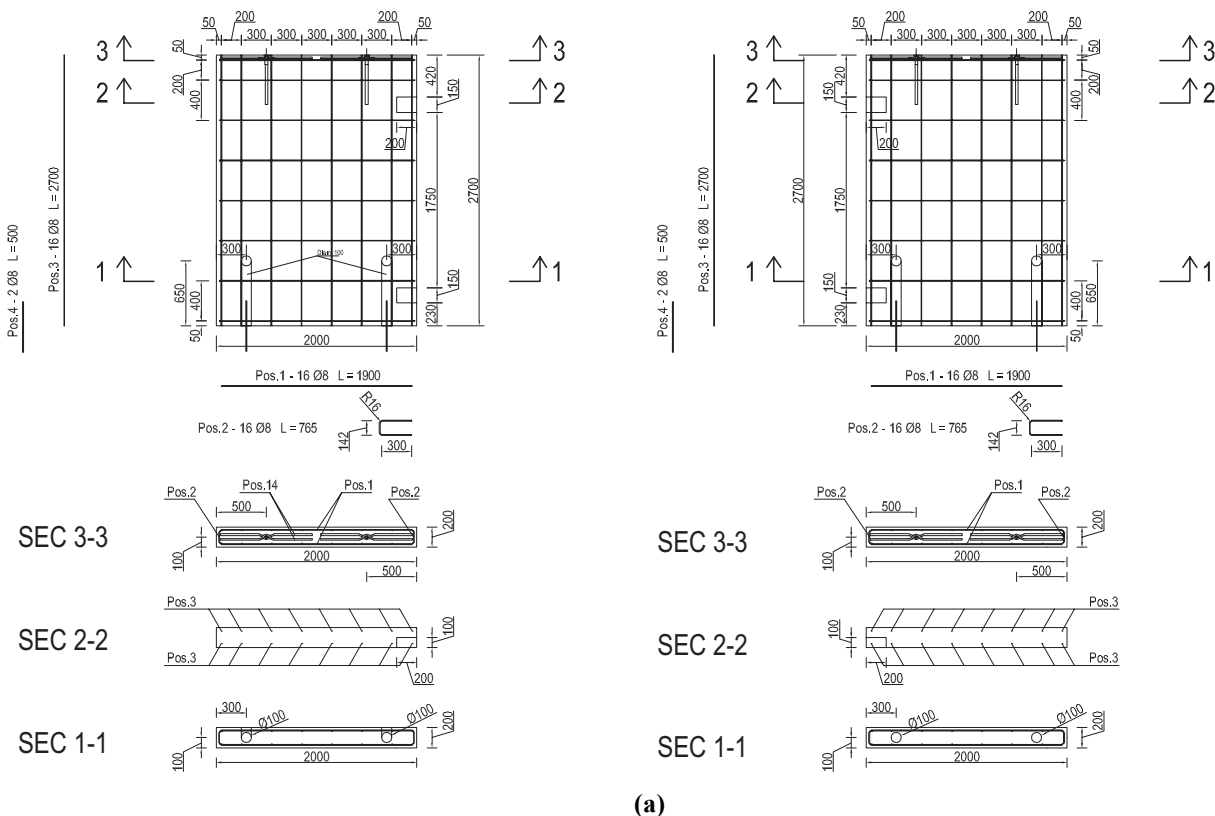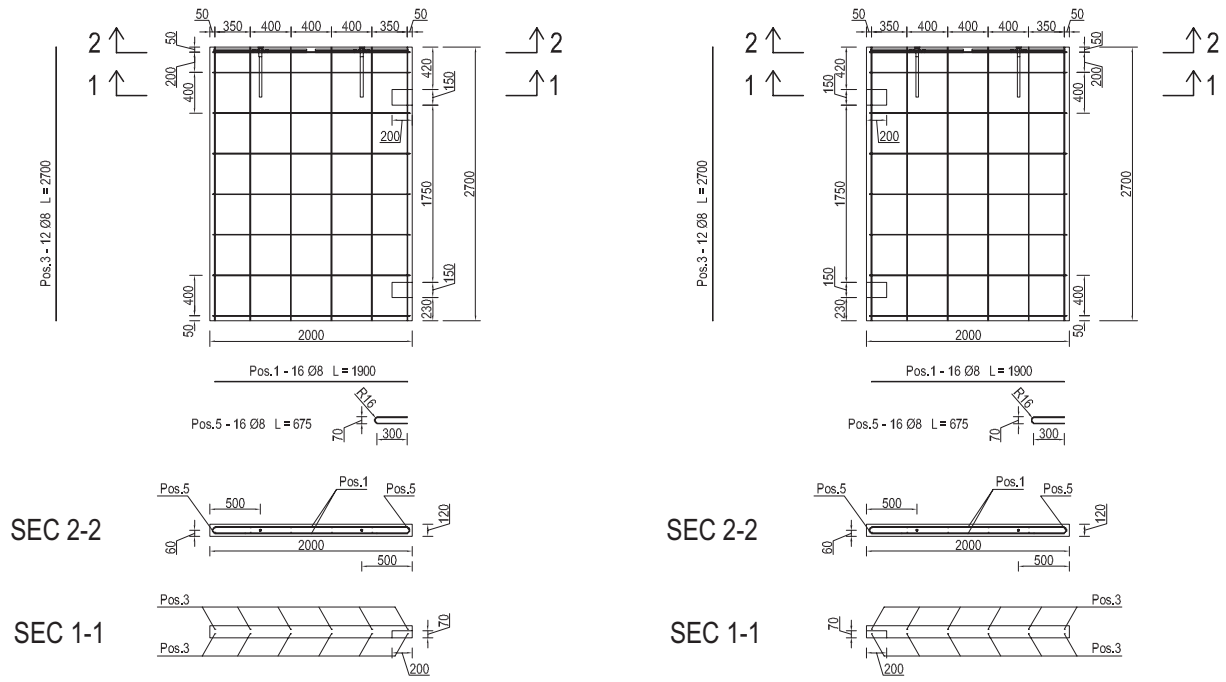
Fig.96: Case studies reinforcement: (a) panels with protruding bars; (b) panels without protruding bars
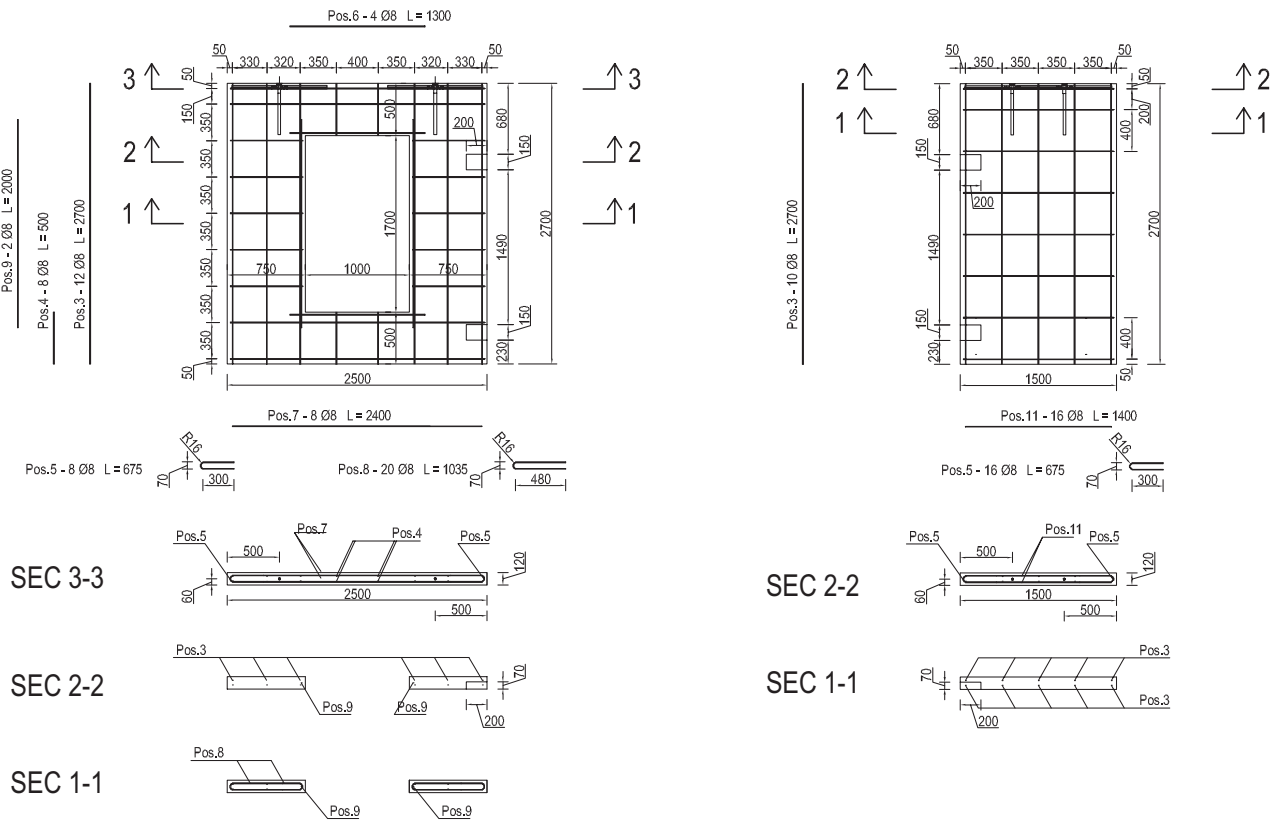
Fig.97: Case studies: panel with window

Fig.98: Case studies: panel with door

In order to make a prediction of the experimental tests, a series of numerical finite element analysis was conducted with reference to the case studies previously designed. The setup of the test were reproduced numerically by finite element modeling with three-dimensional (brick) elements, as regards the concrete elements, while the reinforcing bars and steel connectors have been modeled by one-dimensional (line/embedded) elements, embedded in continuity into the layers of concrete. The interaction between the concrete elements of the panels and the foundation has been reproduced by two-dimensional interface elements using a non-linear constitutive law that is based on a well-known bond-slip model.

The non-linear constitutive law assumed for the elements of concrete, is the "total strain crack" – type "fixed" – in order to consider directly the transfer of shear stresses during the entire loading history. This law allows one to capture properly the evolution of the cracks in the concrete elements and is based on the three-dimensional extension of the well-known "Modified Compression Field Theory". Its calibration is based on the definition of an uniaxial law in order to represent the tensile and the compressive behavior of concrete. In particular, for the traction has been assumed the Hordijk law, while for the compression the Thorenfeldt law.

As regards the numerical finite element modeling in particular have been verified the embedded bars between adjacent panels.

Fig.99: Modeling steel connectors with embedded bars

It was made the selection of the type of friction between panels: bond-slip or contact. With general-contact elements there were problems of convergence, therefore it has been used the bond-slip elements.
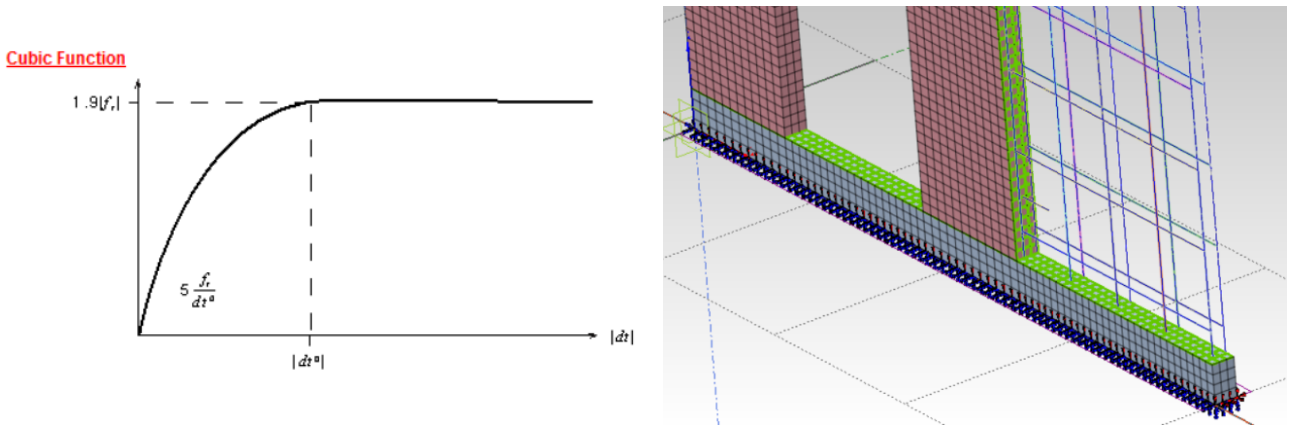
Fig.100: Modeling with general contact elements

Afterwards an analysis of the panels in simple support on the foundation was performed.

Once constructed the numerical model for each case study, a pushover analysis was performed. Below are the curves obtained for each panel in terms of base shear and top displacement.

(a)

(b)
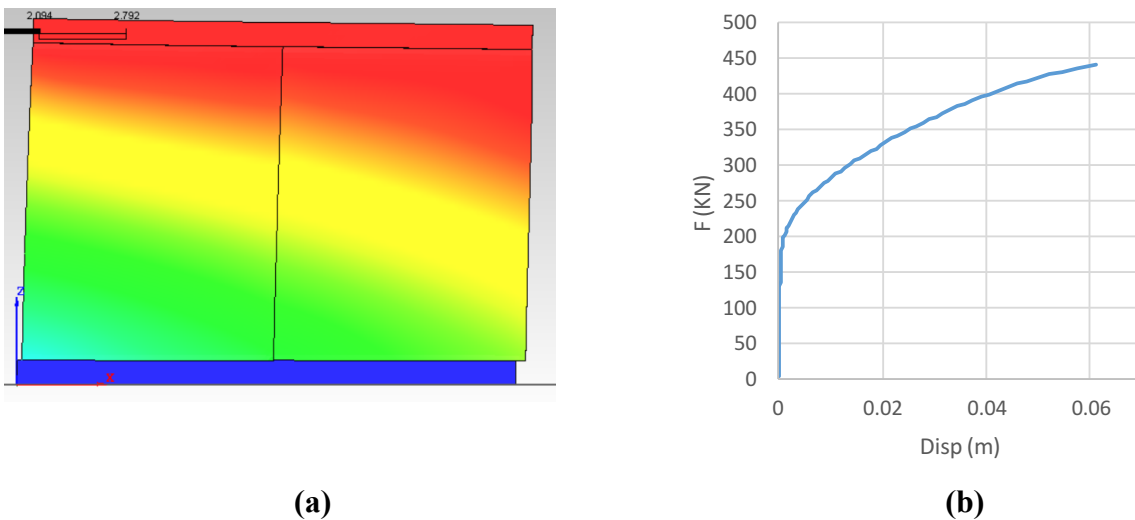
Fig.101: Results of analysis: (a) stress output of panel with protruding bars; (b) pushover curve of panel with protruding bars
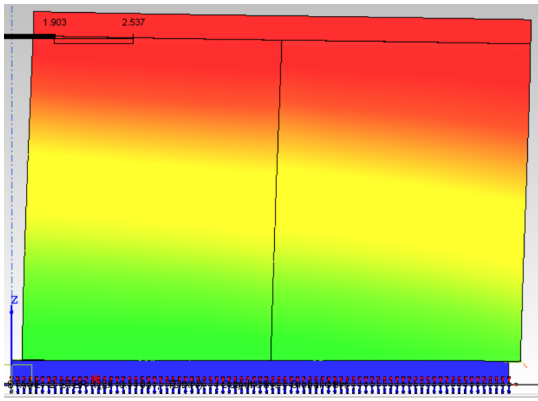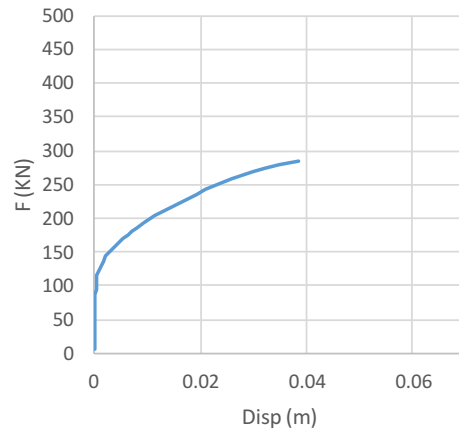
(a)   (b)

Fig.102: Results of analysis: (a) stress output of panel without protruding bars; (b) pushover curve of panel without protruding bars
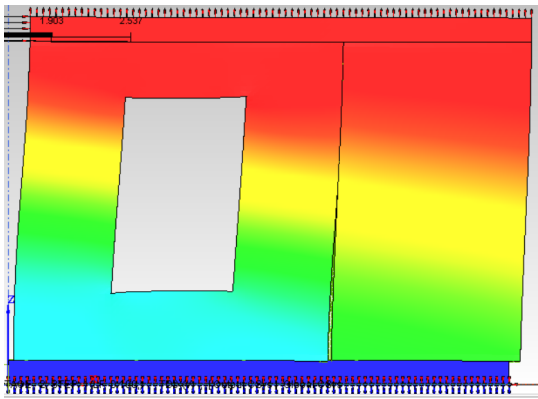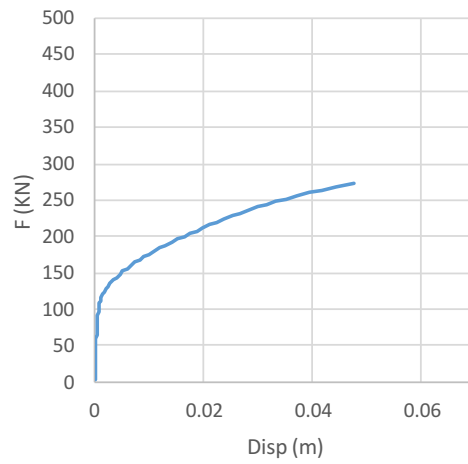
(a)   (b)

Fig.103: Results of analysis: (a) stress output of panel without protruding bars with window; (b) pushover curve of panel without protruding bars with window
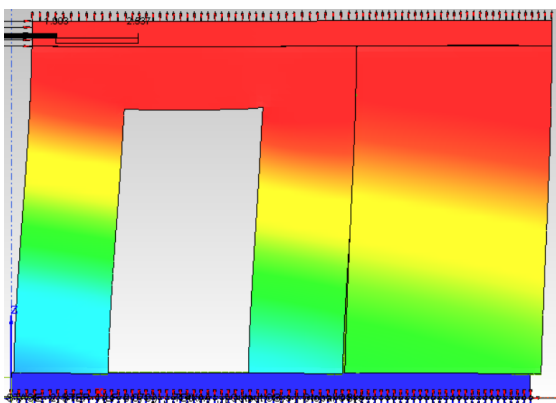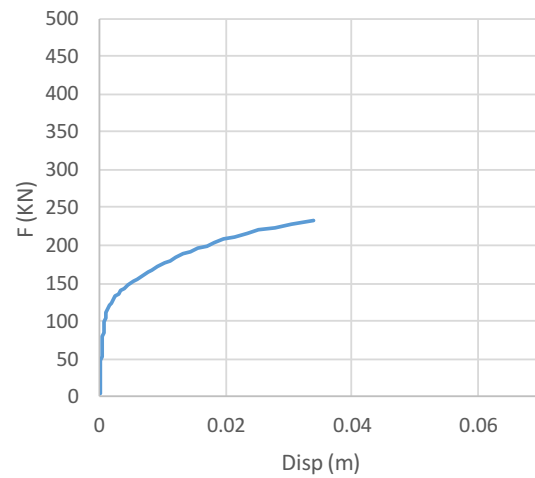
(a)   (b)

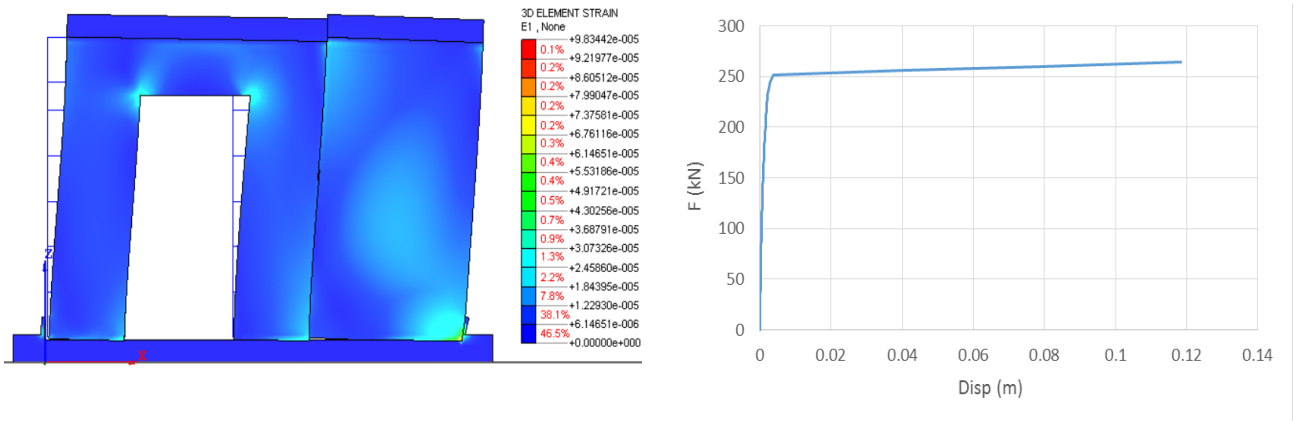**Fig.104: Results of analysis: (a) stress output of panel without protruding bars with door; (b) pushover curve of panel without protruding bars with door**

The results obtained by numerical modeling have shown how the panels slide undamaged as a result of the application of a lateral load. The curves thus obtained were interrupted at the point where indefinite sliding occurs, i.e. the load for which the panel starts to slide on the foundation. An example of this mechanism has been presented in Figure 105.

Fig.105: Panel sliding

Subsequently, it was made the choice to design some brackets that simulate the presence of other contiguous units in order to prevent the sliding of the panel relatively to the foundation, thus causing the panel to damage. These brackets have been included in the model at the base of the panel by directly modeling them by means of nonlinear solid elements.

Fig.106: Design of steel plates

An example of the response of these members in terms of stress is given in Figure 107.

Fig.107: Steel plates stresses

The stresses found by comparing the values obtained theoretically with values obtained in Midas FEA are in good agreement. The design of the brackets was made with and without ribs.

Therefore, a further series of FE models have been performed in order to simulate their behavior and provide information to define the experimental set up adopted.

In the following plots, the series of force-displacement capacity curves predicted will be provided, in combination with the stress/strain levels observed at ultimate conditions.

In this case the corbel at the top of the panels has been assumed to be continuous and overdesigned to enforce its linear elastic response.

(a)

(b)
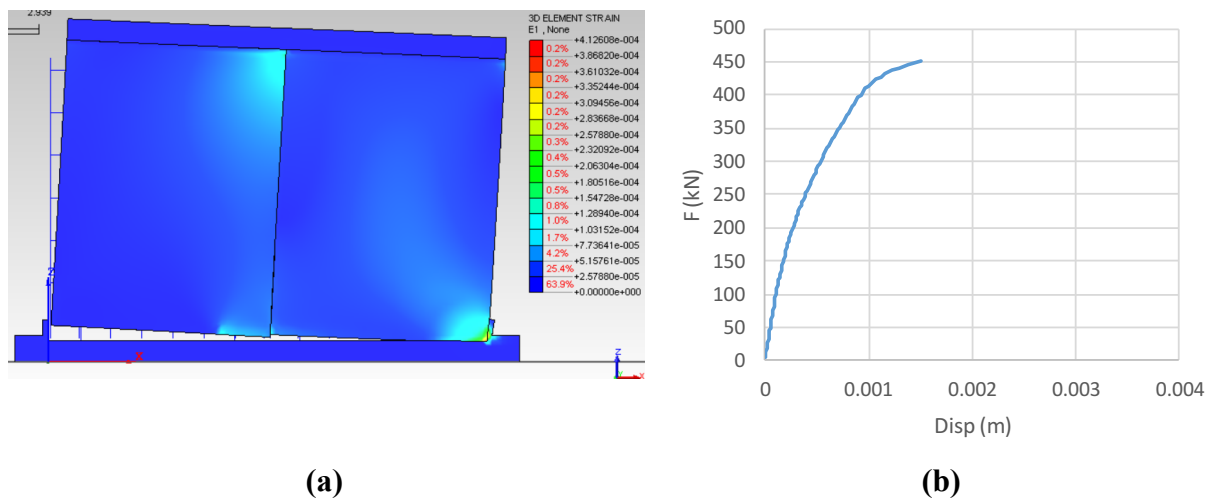
Fig.108: Panel without sliding; (a) stress output of panel with protruding bars; (b) pushover curve of panel with protruding bars
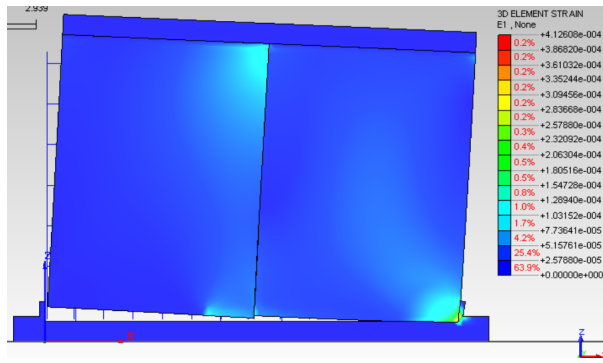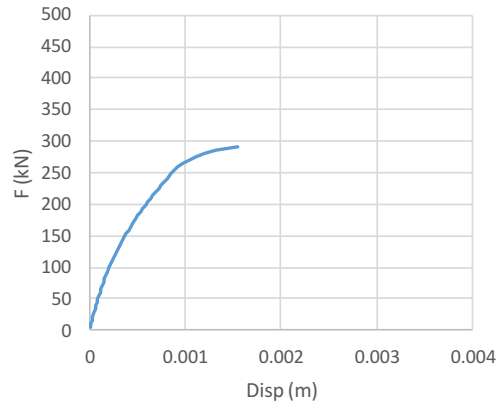
(a)   **(b)**

Fig.109: Panel without sliding; (a) stress output of panel without protruding bars; (b) pushover curve of panel without protruding bars
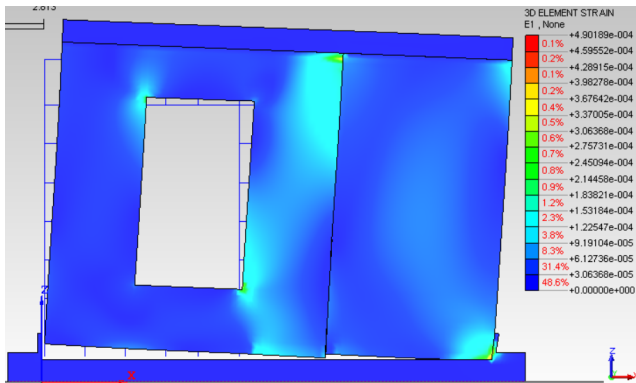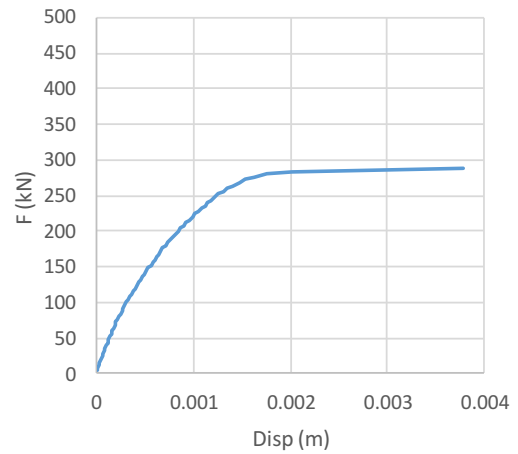
(a)   **(b)**

Fig.110: Panel without sliding; (a) stress output of panel without protruding bars with window; (b) pushover curve of panel without protruding bars with window
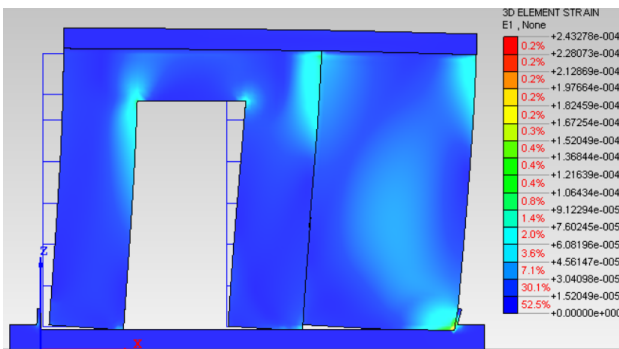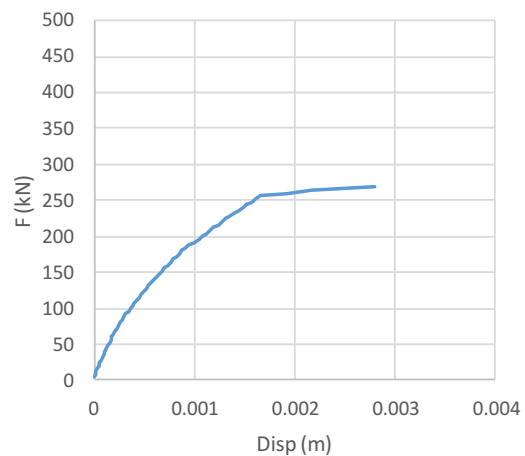
(a)   **(b)**

Fig.111: Panel without sliding; (a) stress output of panel without protruding bars with door; (b) pushover curve of panel without protruding bars with door

The continuous rigid beam in the top of the panels limits the rate of the stresses of horizontal connecting bars ($\sigma \approx 5$ MPa).
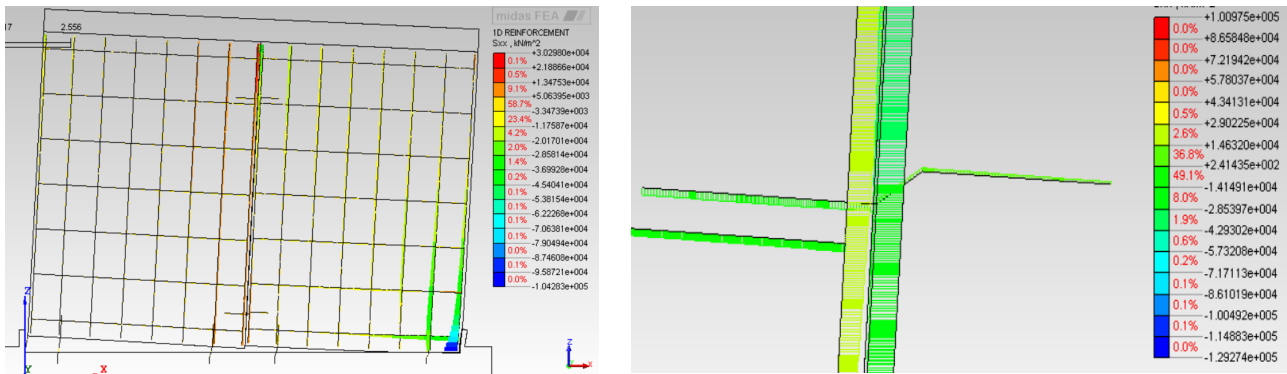
Fig.112: Panel without sliding; horizontal connecting bars stresses

For this reason it was decided to divide the top beam in the point of continuity of the panels, with the insertion layer of Teflon with 2% of friction and applying to the top beam a prestressing force of 300 kN. Subsequently it has been modeled the top beam divided into two parts at the joint between the two panels. Since the top beam during the experimental test will be compressed by an external system, it were made three different modeling in order to verify the effectiveness of the simulation procedure in comparison with the set up of the test: the first one consists of a prestressed tendon, the second one is based on the application of an external compressive force of 300 kN at the end faces of the top beam and the third one considers this compressive force to be uniformly distributed along the corbel (i.e. directly on the nodes of the mesh). At the middle of the top beam, a layer of Teflon has been introduced. The results will be reported in the following.

(a)   **(b)**
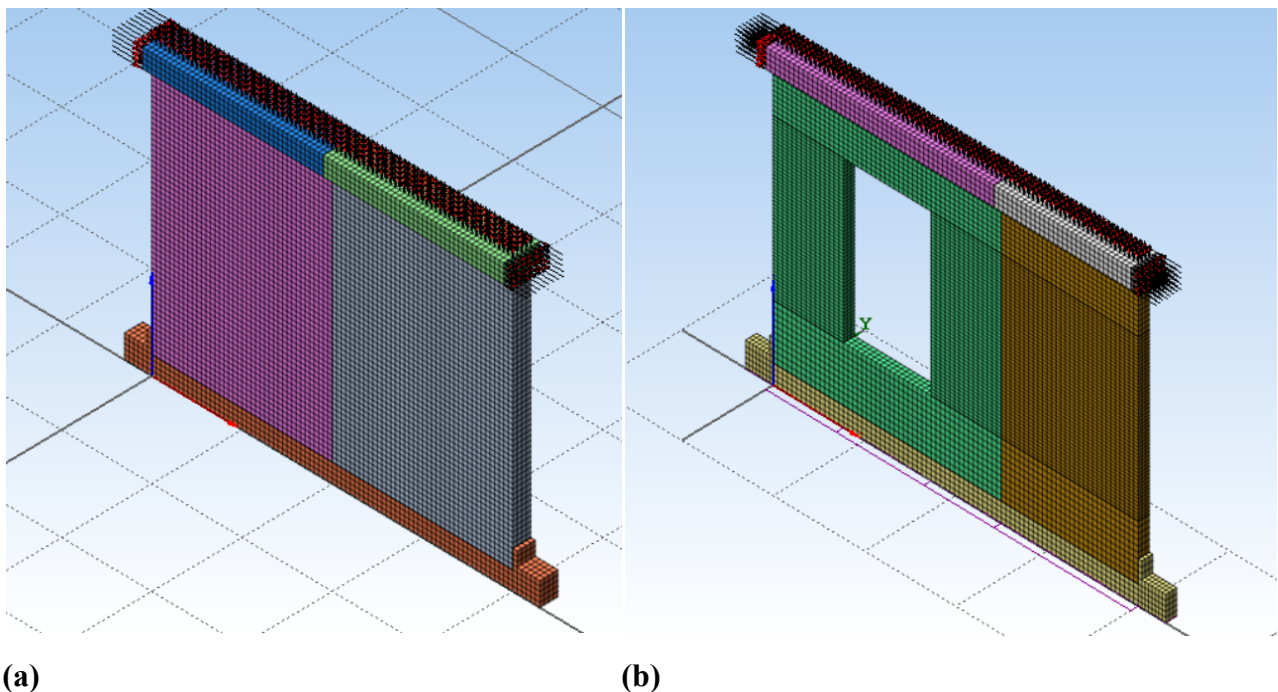
Fig.113: Panel with top beam divided; (a) full panel; (b) panel with window
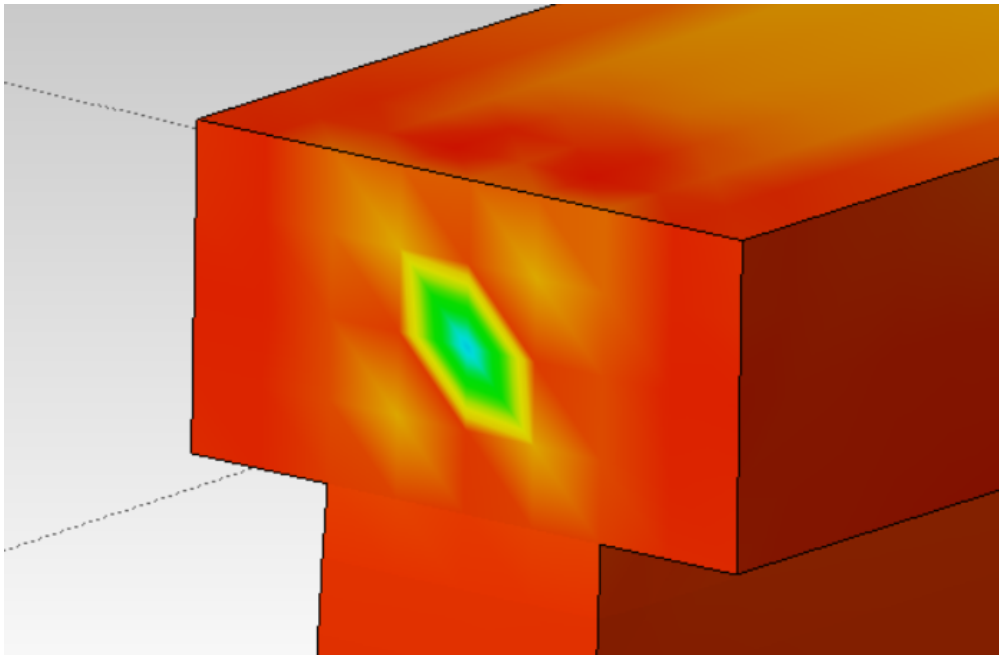
Fig.114: Model with prestressed tendon

(a)   **(b)**
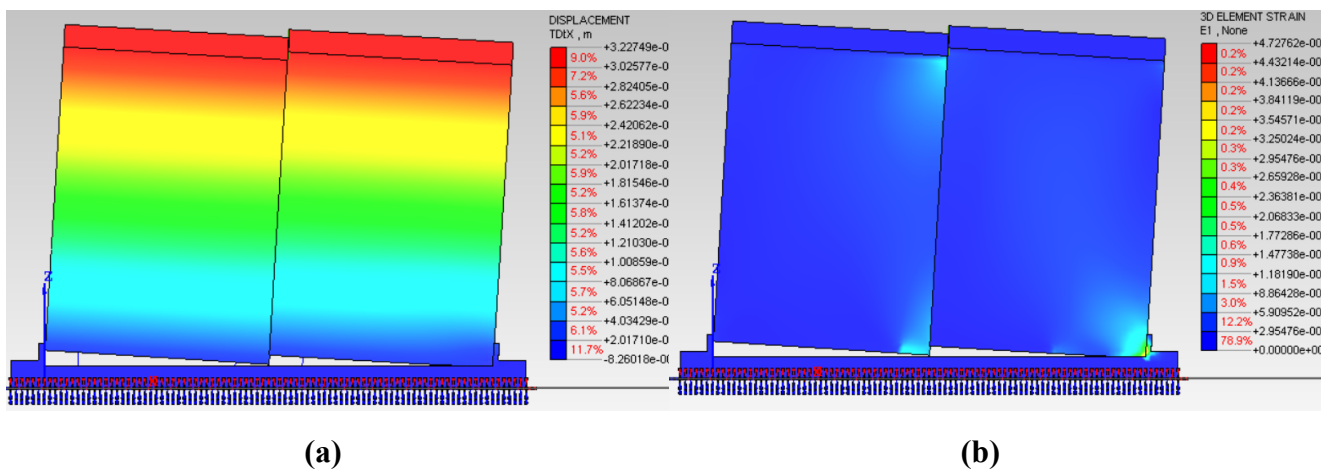
Fig.115: Model with prestressed tendon: (a) displacement; (b) 3D element strain
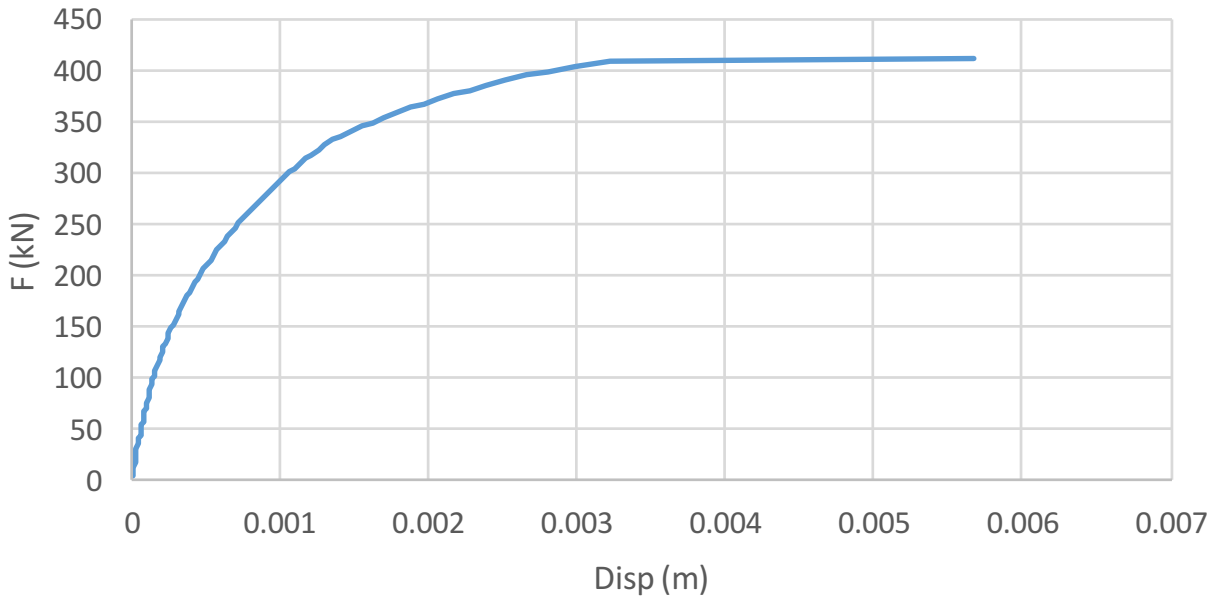
Fig.116: Pushover curve: model with prestressed tendon
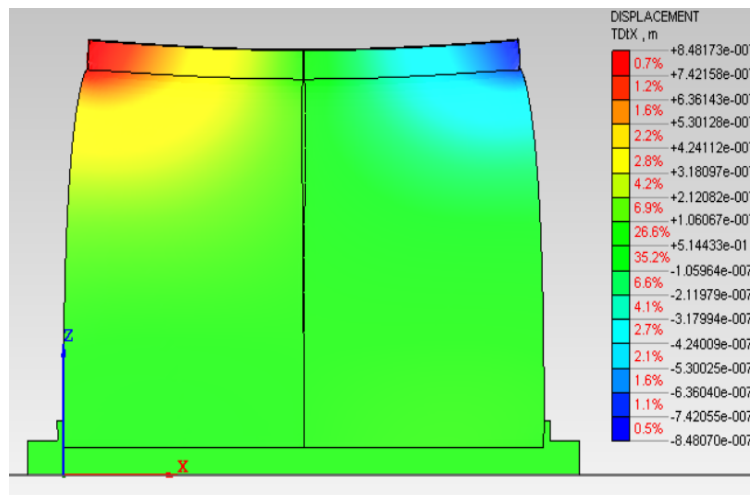
Fig.117: Model with external compression forces

| (a) | (b) |
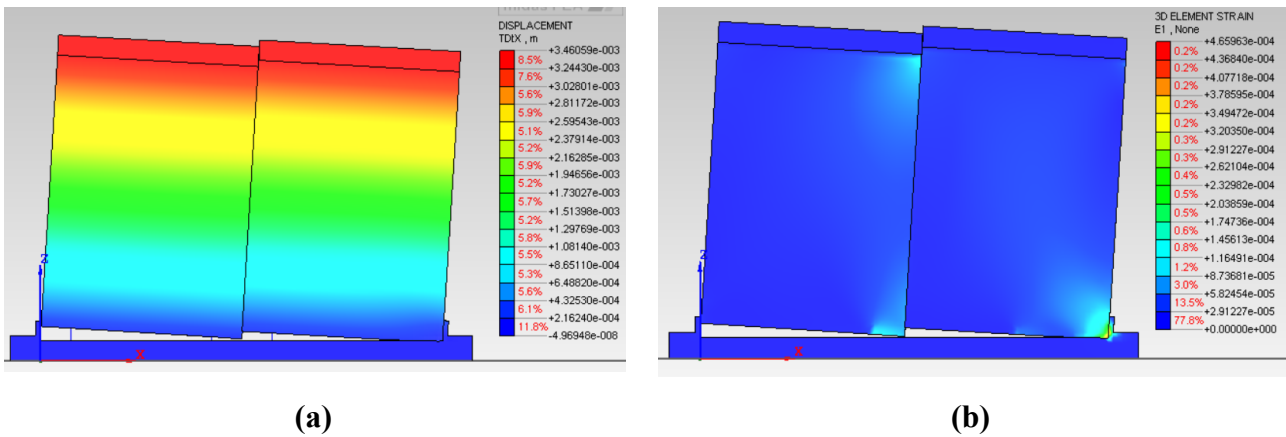
Fig.118: Model with external compression forces: (a) displacement; (b) 3D element strain
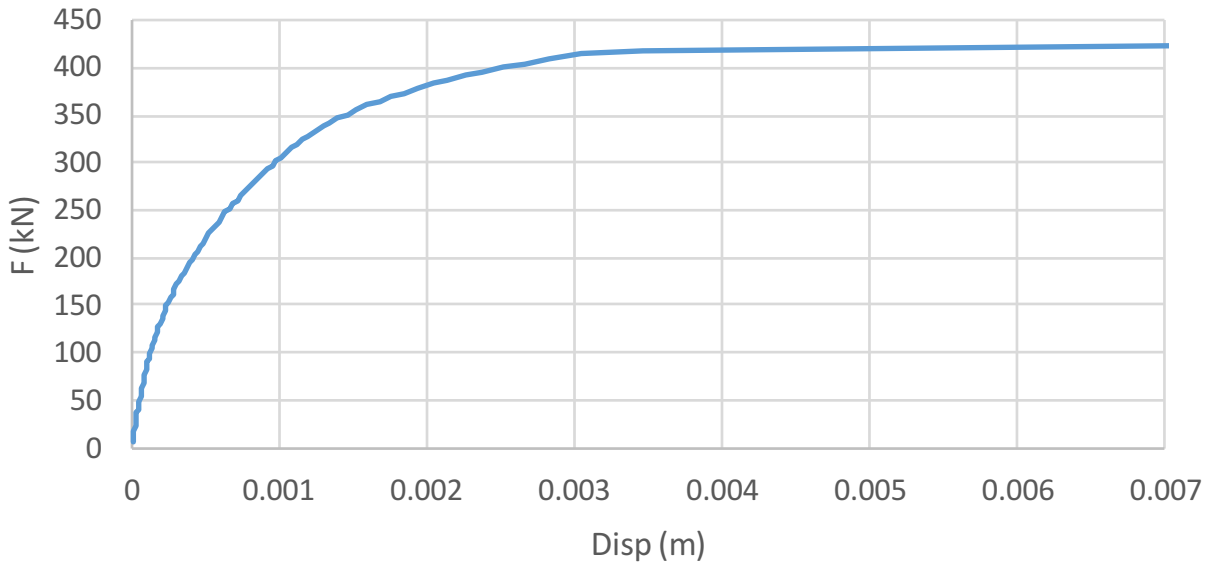
Fig.119: Pushover curve: model with external forces
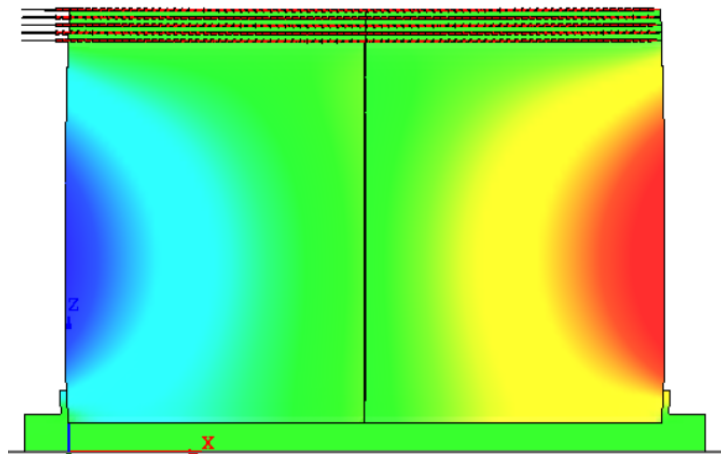
Fig.120: Model with distributed forces

(a)   (b)
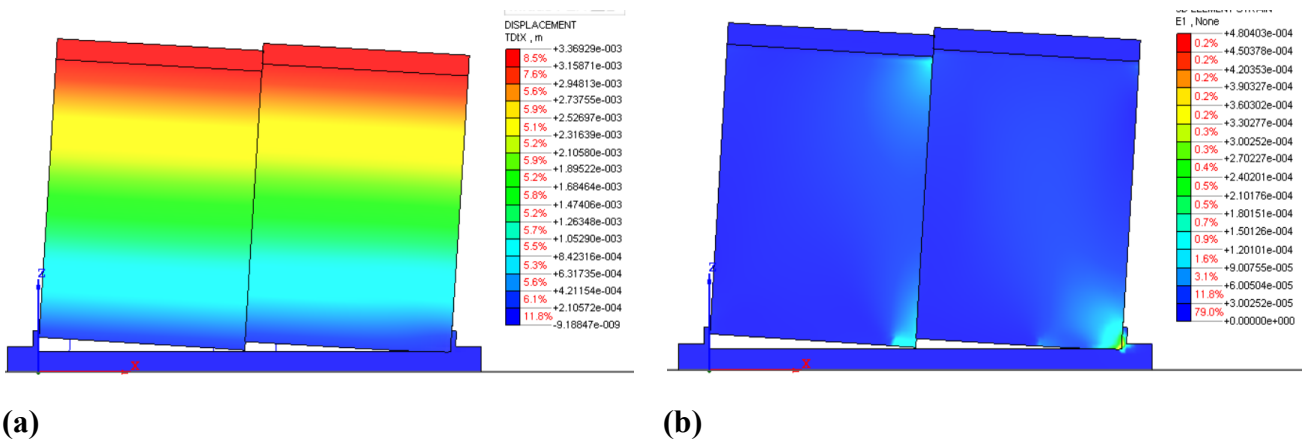
Fig.121: Model with distributed forces: (a) displacement; (b) 3D element strain
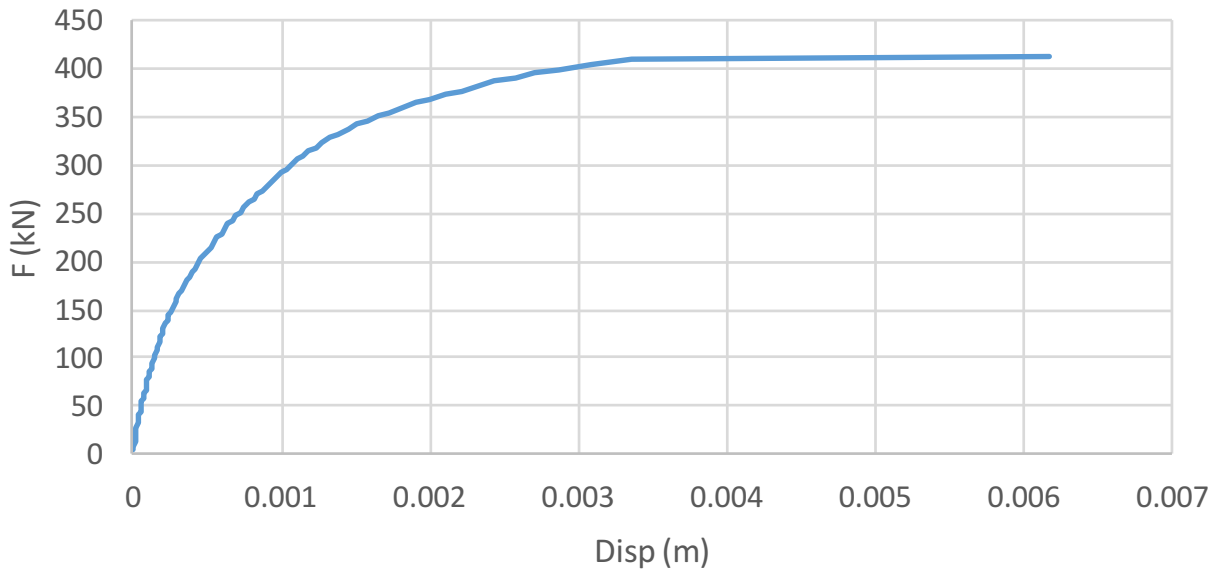
Fig.122: Pushover curve: model with distributed forces

It is noted that the results of three different modeling are equivalent in terms of strength and displacement. Moreover the subdivision of the top beam leads to a drop of resistance of 22% and an increase in the maximum displacement.
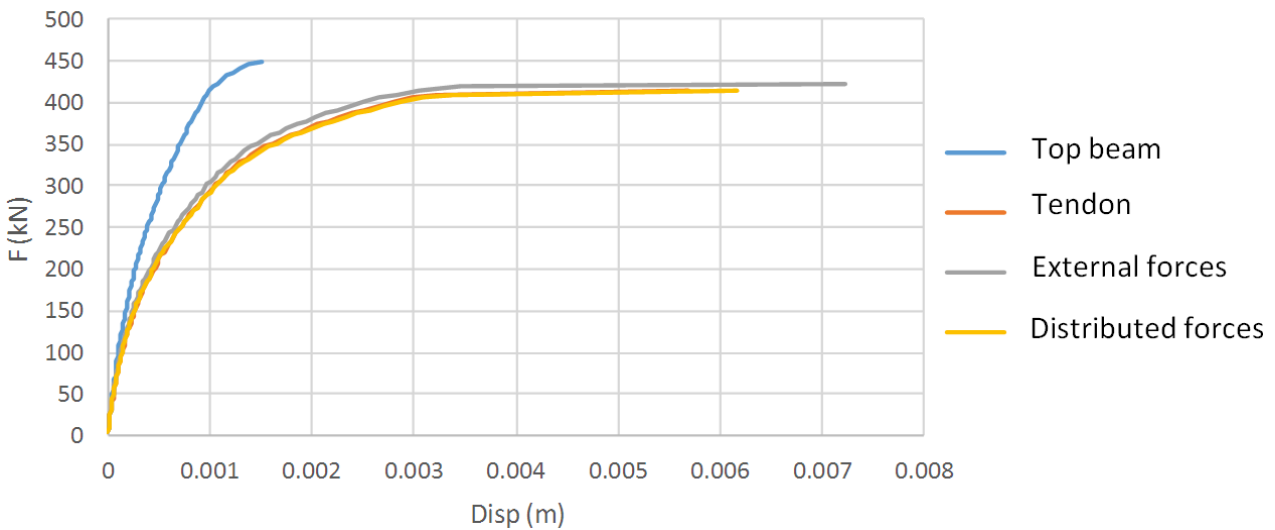
Fig.123: Pushover curve: model with distributed forces

Once the three different procedures used to apply the external load and to simulate the actual test set up were proven to be equivalent and effective, one of them has been assumed to carry out the set of simulations shown in the following. As before, the series of force-displacement capacity curves that were obtained will be given, as well as the strain pattern at ultimate conditions.

The following figures illustrate the strain output and the pushover curves of the new models with top beam divided and the tendon loading approach. Peak values of strain are shown for any system studied.
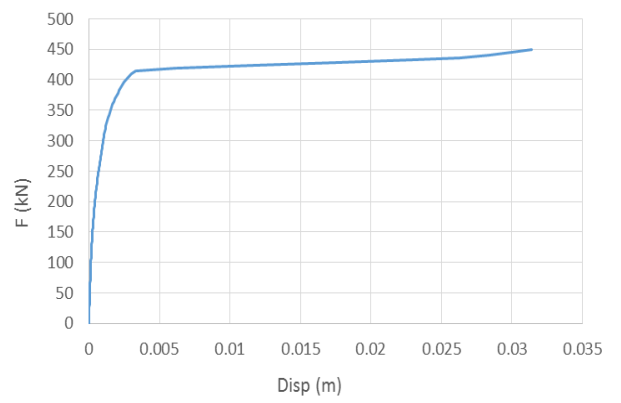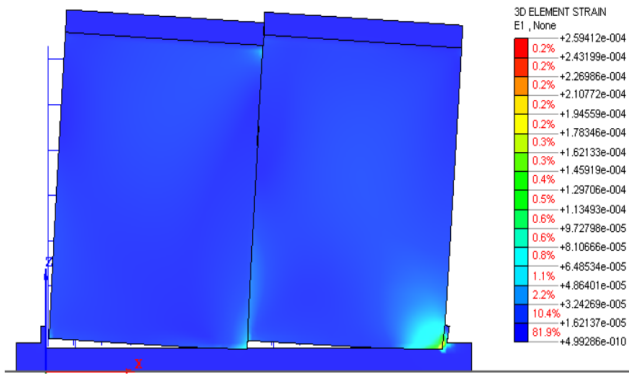
Fig.124: Panel with top beam divided; (a) strain output of panel with protruding bars; (b) pushover curve of panel with protruding bars
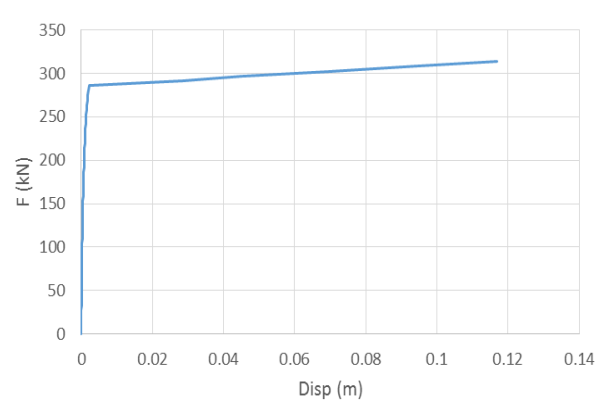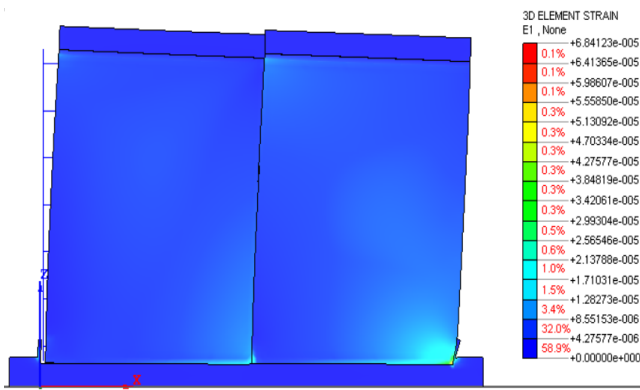
Fig.125: Panel with top beam divided; (a) strain output of panel without protruding bars; (b) pushover curve of panel without protruding bars
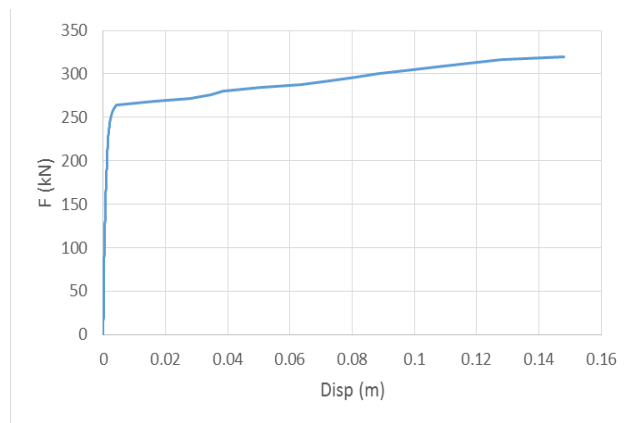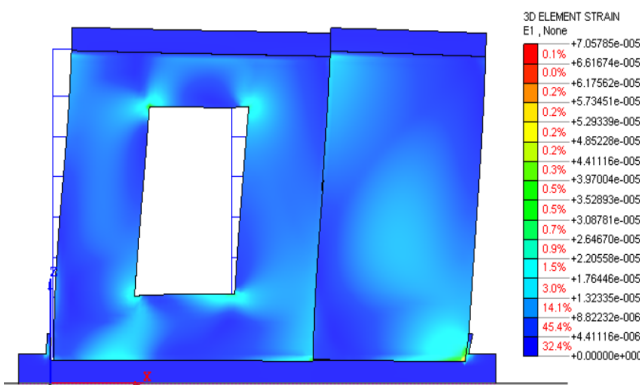
Fig.126: Panel with top beam divided; (a) strain output of panel without protruding bars with window; (b) pushover curve of panel without protruding bars with door

Fig.127: Panel with top beam divided; (a) strain output of panel without protruding bars with window; (b) pushover curve of panel without protruding bars with door

The following figures illustrate the evolution of the strain output predicted during the pushover analysis. It can be seen that initially the panel was hindered to move by the brackets, therefore it started to rocking. When the maximum was progressively reached on the pushover curve, the entire panel lifted up, concentrating the entire deformation at the connection between bracket and corner.
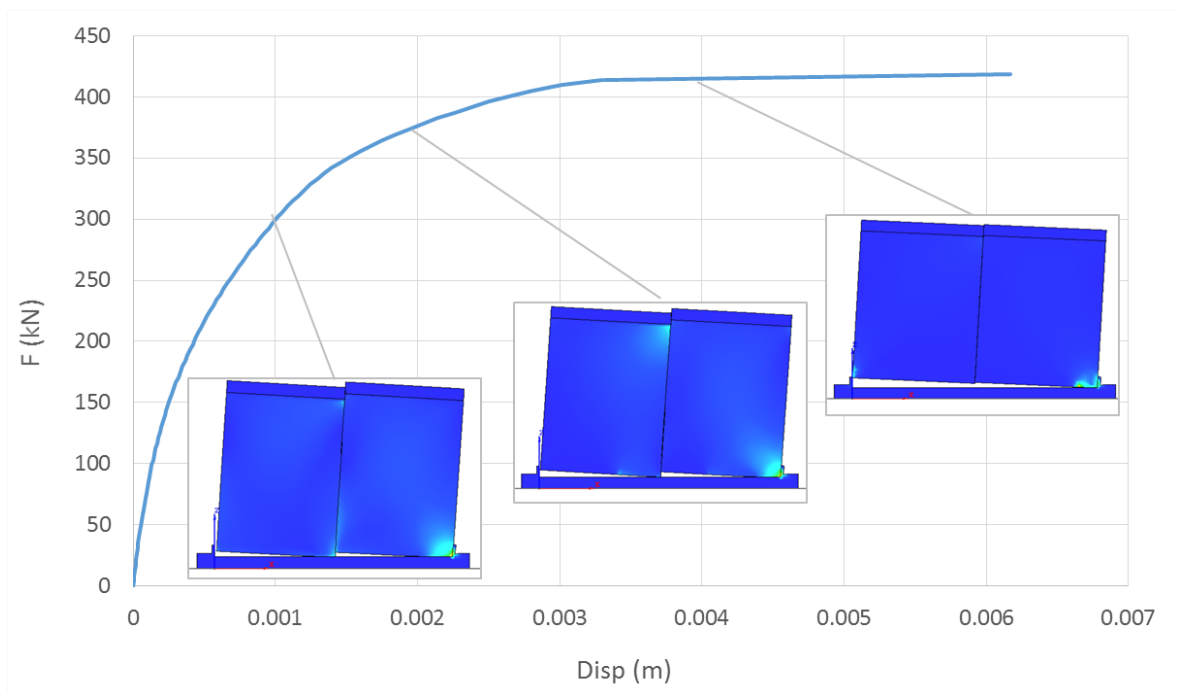
Fig.128: Strain output evolution on pushover curve, panel with protruding bars
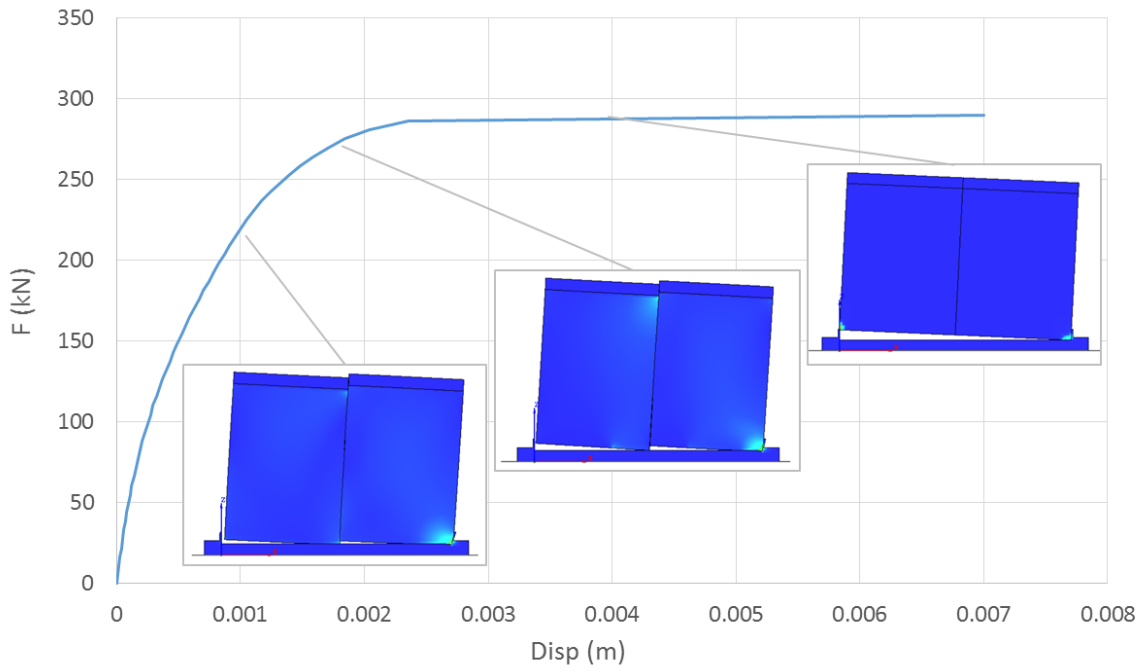
Fig.129: Strain output evolution on pushover curve, panel without protruding bars
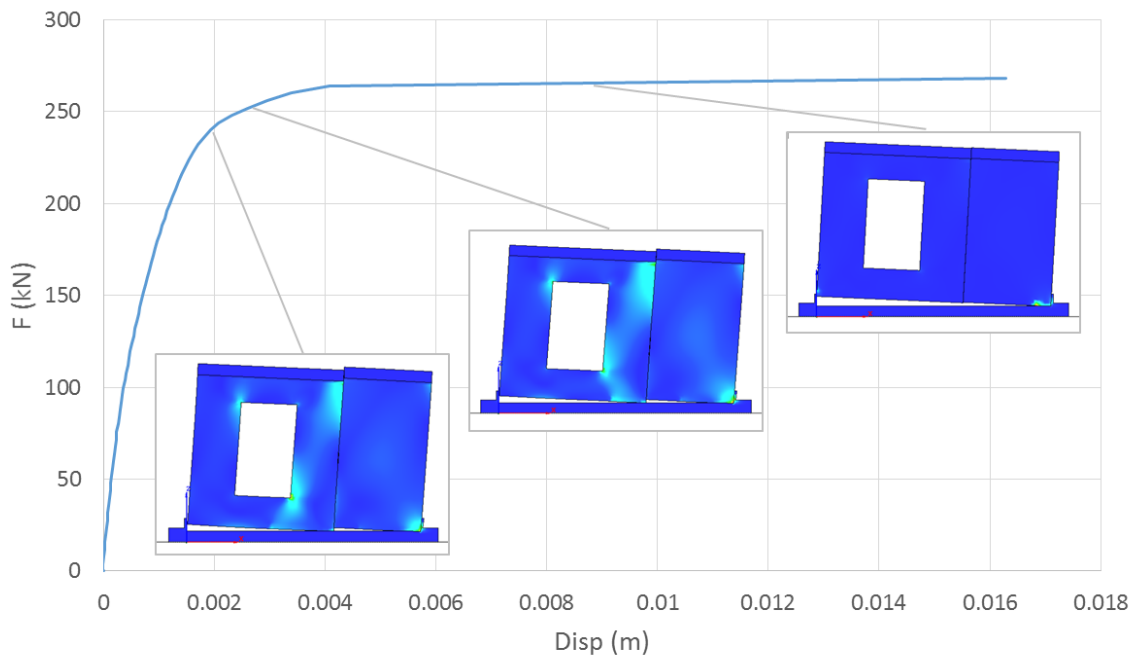
Fig.130: Strain output evolution on pushover curve, panel without protruding bars with window
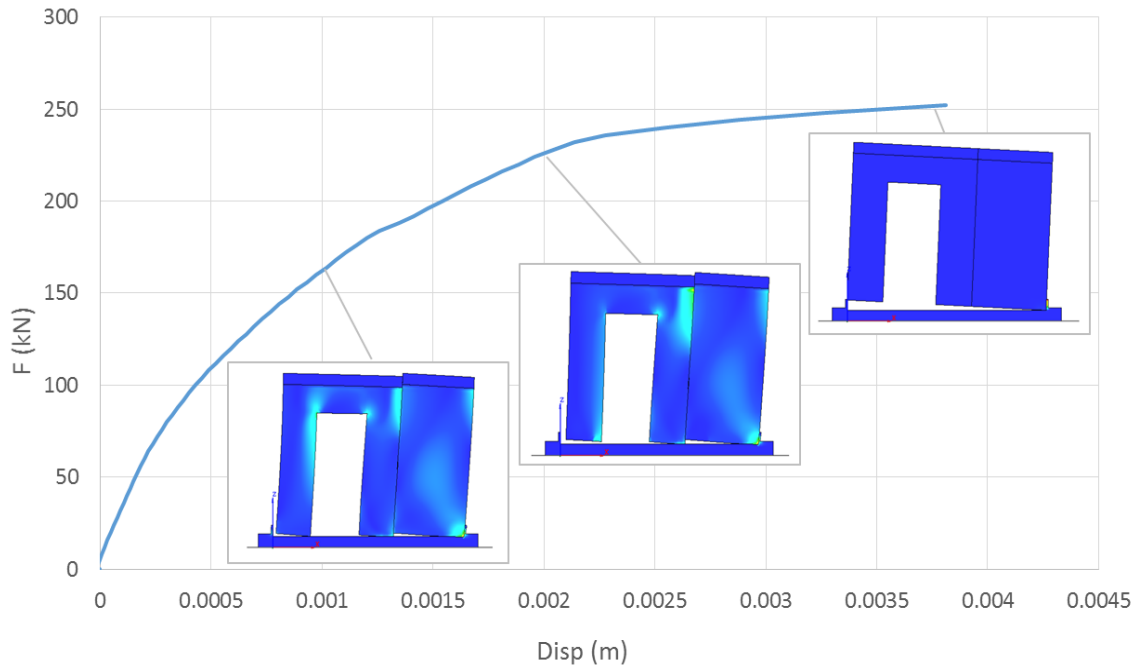
Fig.131: Strain output evolution on pushover curve, panel with protruding bars with door

6 Experimental investigation of precast panels and connections

This report is mainly focused on the experimental and numerical response of wall-to-wall and wall-to-foundation connection systems that are used in precast terraced houses typical of Dutch building practice. To this aim, the research described in the following examines and investigates the seismic behavior of lightly reinforced concrete bearing sandwich panels, using experimental and numerical investigations. An accurate and time-saving mechanical FE model was prepared to simulate the experimental response of this structural system. Their performance and failure modes were studied experimentally in order to have an extensive background for FE analysis. In detail, the calibration of the equivalent mechanical model proposed was conducted by means of a series of pseudo-static cyclic tests performed on single full-scale prototypes with or without openings, assuming them to have a cantilevered static scheme. Four additional tests on precast assemblies were carried out to explicitly investigate the response of wall-to-wall out-of-plane connection systems, thus providing specific information for their numerical modeling. After validation, this numerical procedure was proposed to assess the capacity of terraced buildings built with this particular construction technology, thus estimating base shear-roof displacement curves on the basis of conventional pushover analyses.

6.1 Introduction and framework of the research

The use of precast concrete in wall and framing systems is widespread in many European and non-European countries, particularly for what concerns single-story or low-rise residential and industrial buildings. Rapid and economical construction, high allowance for quality controls, and less labor required on-site have led the prefabrication of RC elements to become an established technique worldwide in the past fifty years.

While the majority of Italian and European industrial facilities consist of reinforced precast concrete frames comprising continuous monolithic columns and pin-ended beams characterized by high flexibility and low resistance of beam-to-column and panel-to-structure connections, a wider set of solutions may be used for residential structures, depending on design target, building practice and seismicity of the area under investigation. Despite the vast variety of feasible structural schemes and solutions, the seismic response of all of them greatly depends on the behavior of the connection system, and the key role played by proper design and detailing of the joints is well established in the literature [FIB, (2003); FIB (2008); Englekirk (1982); Englekirk (1990); Englekirk (2003); Magliulo et al. (2008); Belleri et al. (2015); Brunesi et al. (2015)]. In the last decades, extensive research was undertaken to test traditional structural layouts and connections in quasi-static, pseudodynamic, and dynamic fashion [Rodríguez and Blandón (2005); Fischinger et al. (2009); Belleri and Riva (2012); Psycharis and Mouzakis (2012a); Psycharis and Mouzakis (2012b); Bournas et al. (2013a); Brunesi et al. (2015)].

Despite significant progress in research, the majority of actual structures have shown inadequate seismic performance [Iverson and Hawkins (1994); Muguruma et al. (1995); Sezen and Whittaker (2006); Adalier and Aydingun (2001); Ghosh and Cleland (2012)] when connections were insufficiently detailed and recent major earthquakes in Italy (May 20 and 29, 2012, Emilia seismic sequences) resulted in a similar scenario [Magliulo et al. (2013); Bournas et al. (2013b); Liberatore et al. (2013); Belleri et al. (2015)]. To point out the prevailing seismic vulnerabilities of precast

systems and necessarily of its connections, a comprehensive experimental investigation of precast full-scale single panels and assemblies representative of past and current Dutch building practice for residential structures was carried out at Eucentre laboratory. Results from pseudo-static cyclic tests will be given in this report and discussed in detail as they will serve as a calibration of numerical beam-based modeling approaches that were prepared to reproduce the seismic response of entire structural prototypes rather than structural subassemblies.

First, the report will be focused on the experimental response of full-scale single panels, extensively describing geometries, mechanical properties and reinforcement arrangements of the specimens under investigation, as well as test setup and cyclic loading protocol. Then, a series of asymmetric push-pull tests of precast connection systems will be presented, exploring the performance of "ad hoc" precast assemblies that were constructed and tested to quantify flexural and shear capacities of dowels representative of those used in the Dutch context. After data collection, the prevailing experimental observations will be synthesized to provide systematic guidelines for accurate and time-saving modeling and analysis of such systems. Mechanical fiber-based FE idealizations will be prepared to reproduce the experimental responses of the aforementioned structural systems and components, explicitly including their complex contribution in a phenomenological sense. After validation in compliance with experimental data, the modeling approach prepared for seismic response assessment will be extended to a reference case-study prototype, consisting of multiple-units terraced building. A wide set of pushover analyses will be presented to determine the capacity of this structure in comparison with previous simulations in which the behavior of wall-to-wall and wall-to-foundation connections was preliminary modeled in a simplified and conservative manner.

6.2 Cyclic tests of full-scale single precast panels

Precast load bearing walls provide a cost-effective solution when compared to conventional cast in-situ column/beam/infill wall systems. The primary advantages are the speed of construction and a partial or complete elimination of wet trades. The prevailing specifications for precast components are usually determined by cost, speed and performance benefits and, hence, components that offer significant advantages will be able to compete against traditional materials.

As previously mentioned, one of the main aim of this research is to define the collapse mechanisms and flexural/shear capacity of connection systems that are used in precast concrete walls, estimating resistance, ductility and energy dissipation in order to characterize seismic performance, feasibility and effectiveness of the representative connectors. To this aim, an experimental activity was carried out in order to determine the sensitivity of the response to axial load and geometry, in terms of both wall thickness and presence of openings. Therefore different specimens were constructed and tested using the same type of connectors for different typologies of precast panels, as discussed later on in more details. In particular, the prevailing assumptions concerning test setup and procedure, as well as a brief description of specimens, materials and reinforcement layouts, will be summarized in the following. In addition, the rationale behind the definition of the experimental investigation is given.

The different types of precast panels under investigation were extracted from a prototype that was designed emulating a typical structural configuration of a Dutch single-family terraced house. Figure 132 shows the typical dimensions of precast panels which are currently used in Dutch

building practice, while the main steps related to the design process of this building will be provided in the upcoming discussion.

The reference standards used for the design of this structure and its components are the Eurocodes. In particular, the following codes and guidelines may be referenced:

- BS EN 1990 principles for structural design.
- BS EN 1991-1-1 Part 1-1: General actions – Densities, self-weight, imposed loads for buildings.
- BS EN 1991-1-4 Part 1-4: General actions – Wind actions.
- BS EN 1992-1-1 Design of concrete structures – General rules and rules for buildings.

These standards are consistently and concomitantly used the Dutch National Annex (NB).
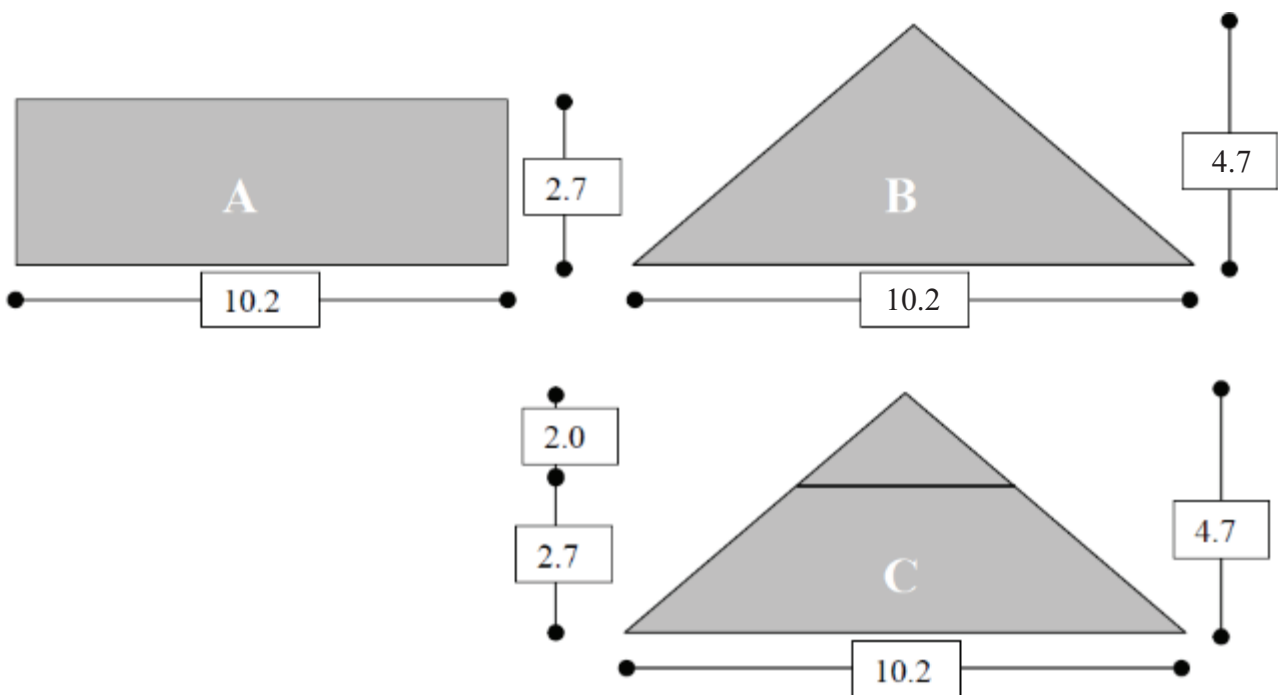
Figure 132: Maximum dimensions of precast Dutch panels

The concrete class used herein is C35/45.Further and more specific details concerning design and actual mechanical properties of concrete will be discussed in the following paragraphs.

The wind load and load combination factors used to determine the total horizontal force acting on the building are those given by the Dutch national Annex NEN-EN 1990(NB) of the Eurocodes, as reported in Figure 133 and Figure 134.

Gevolgklasse CC1 - volgens tabel NB.4 - A1.2(B) en NB.5 van NEN-EN1990

CC	Blijvende en tijdelijke ontwerpsituaties	Blijvende belastingen		Overheersende veranderlijke belasting	Veranderlijke belastingen gelijktijdig met overheersende	
		ongunstig	gunstig		Belangrijkste (indien aanwezig)	Andere
1	(vlg. 6.10a)	$1.20\ G_{k,j,sup}$	$0.90\ G_{k,j,inf}$		$1.35\ \psi_{0,1}\ Q_{k,1}$	$1.35\ \psi_{0,i}\ Q_{k,i}$ (i > 1)
	(vlg. 6.10b)	$1.10\ G_{k,j,sup}$	$0.90\ G_{k,j,inf}$	$1.35\ Q_{k,1}$		$1.35\ \psi_{0,i}\ Q_{k,i}$ (i > 1)

Relevante waarden volgens tabel A1.1 van NEN-EN1990 (NB)

Belasting	ψ_0	ψ_1	ψ_2
Windbelasting	0	0.2	0

Figure 133: Factors for loading combinations

For a building height less than 10 m, the value of the wind action was obtained according to the Holland wind action map that is reported below.

Onbebouwd, hoogte ≤ 10 m:

windgebied	$q_p(z)$ kN/m² [kN/m²]	verhouding tov windgebied I
I	1.02	1.00
II	0.85	0.83
III	0.70	0.69

Figure 134: Classification of wind load and values assumed for design

The panels, which will be object of the experimental tests, have been extracted from a building case study whose dimension were assumed according to the size of standard panels. The building that was design is a two-storey house plus a hip roof. The total height of the building is approximately 10 m, and the plan dimension are 10.2 x 13.2 m.

In Figure 135, Figure 136 and Figure 137, a series of schematics presenting elevation and plan views of the case-study building prototype under consideration in this report are provided to identify a typical structural scheme, as well as the prevailing geometric characteristics of the specimens extracted.

Figure 135: Case-study building: elevation views – West and South directions
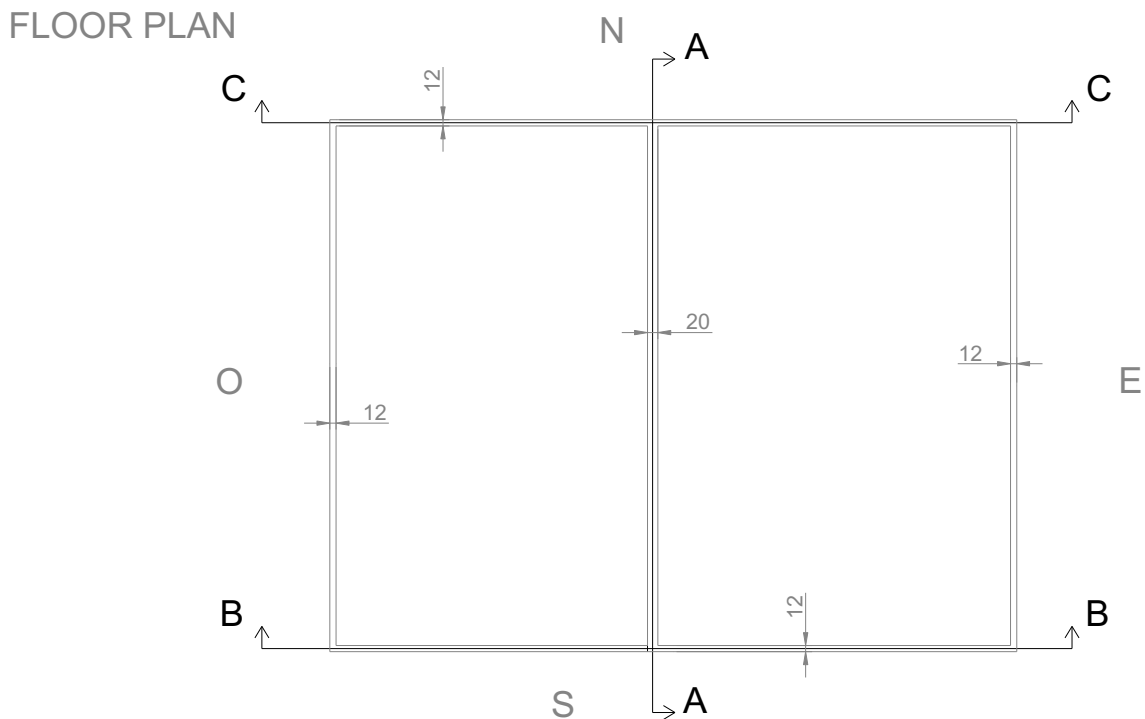
Figure 136: Case-study building: plan view
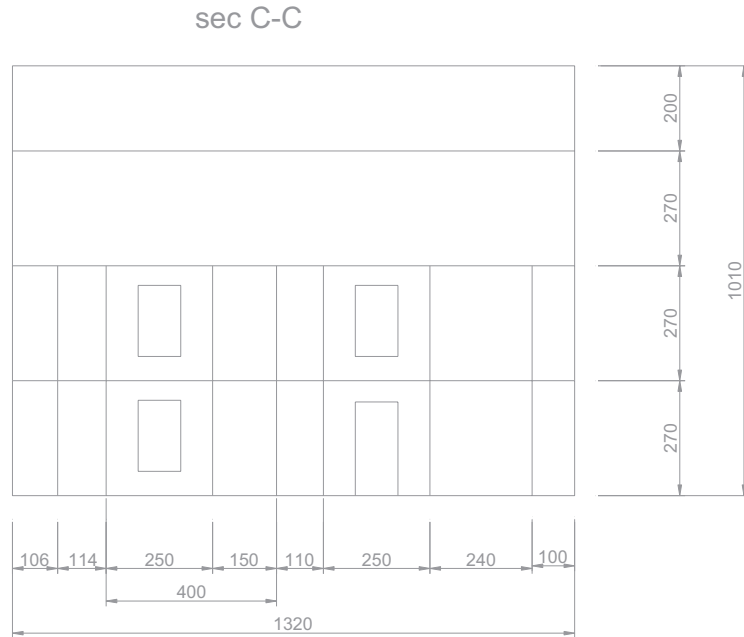
Figure 137: Case-study building: schematic of side view

The structural layouts considered will be more systematically described in the upcoming sections, while Figure 138, Figure 139, Figure 140 and Figure 141 preliminary sketch geometries and reinforcement arrangements that were selected. The tests carried out are 12. In detail, 8 in-plane tests on full-scale panels and 4 tests on L-shaped specimens to specifically assess the response of connections between panels were planned. Therefore, the geometry of the panels has been selected and the levels of axial load to be applied on each panel has been determined in accordance with numerical assumptions representative of Dutch building practice for this structural typology. Each specimen of the 8 in-plane tests consists of two panels connected together by means of special steel connectors. The global dimensions of the specimens are 4 m in length and 3 m in height. In the case of full panels, each panel is 2 m long, while in the case of the presence of an opening, the panel with the window or the door is 2.5 m long while the other panel is 1.5 m long for a constant total length of panels assembly equal to 4 m.

(a) (b) (c) (d)
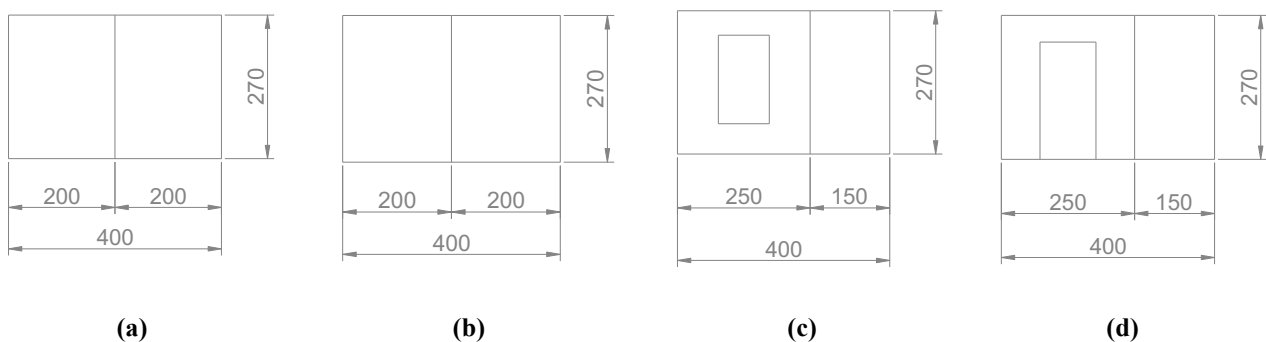
Figure 138: Precast panel prototypes: sketch of geometries considered during tests

The design of reinforcement and concrete sections was carried out according to EC8. As discussed later on, the amount of reinforcement provided is the minimum for large lightly reinforced walls. In the case of the panels where there are protruding bars, these bars were designed for wind loads only. Examples of reinforcement arrangement are provided in Figure 139, Figure 140 and Figure 141.
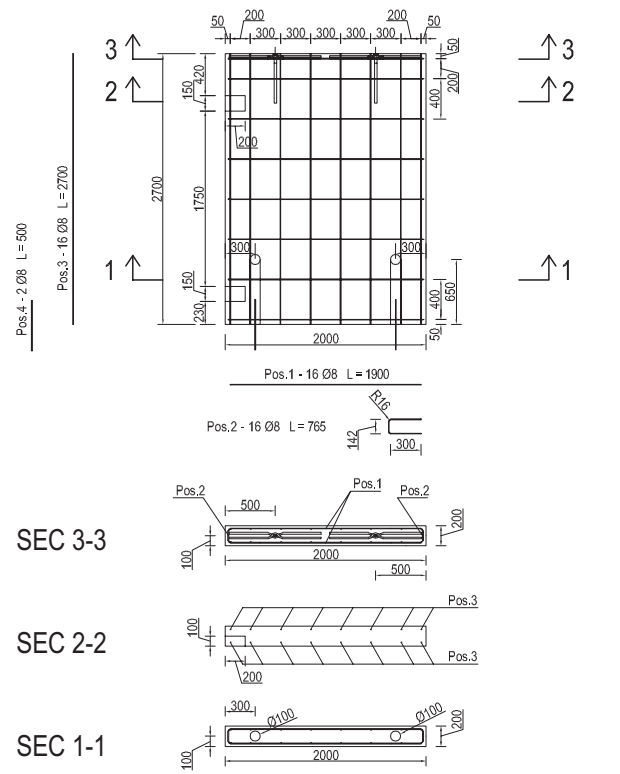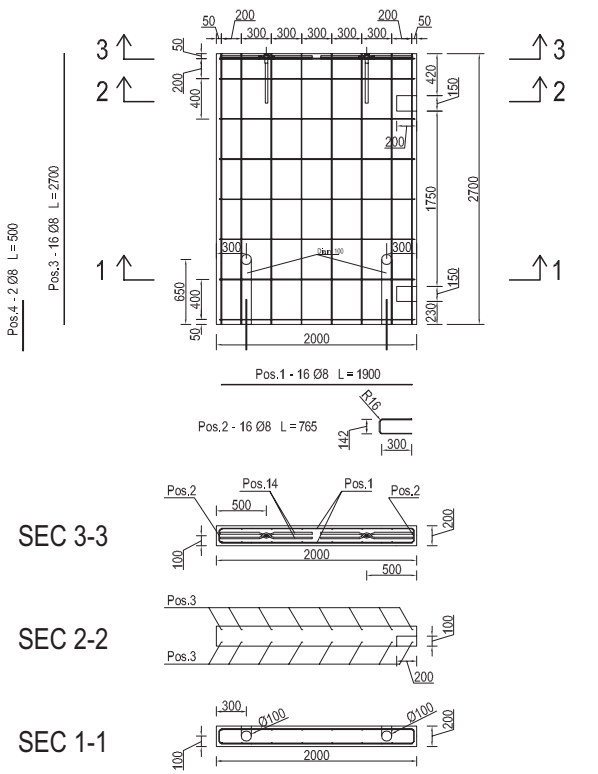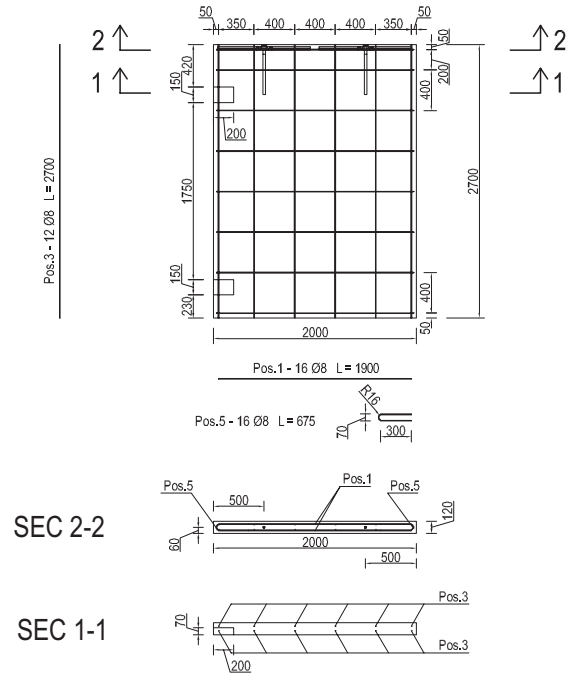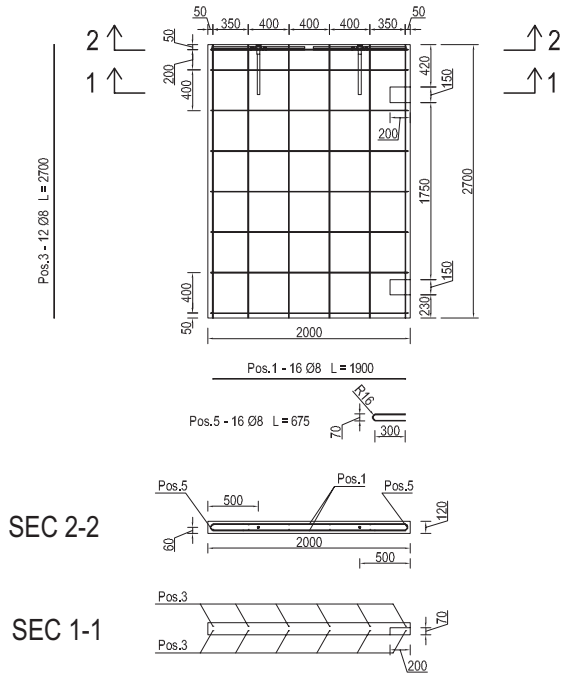
Figure 139: Reinforcement layout: (a) panels with starter-bars; (b) panels without starters
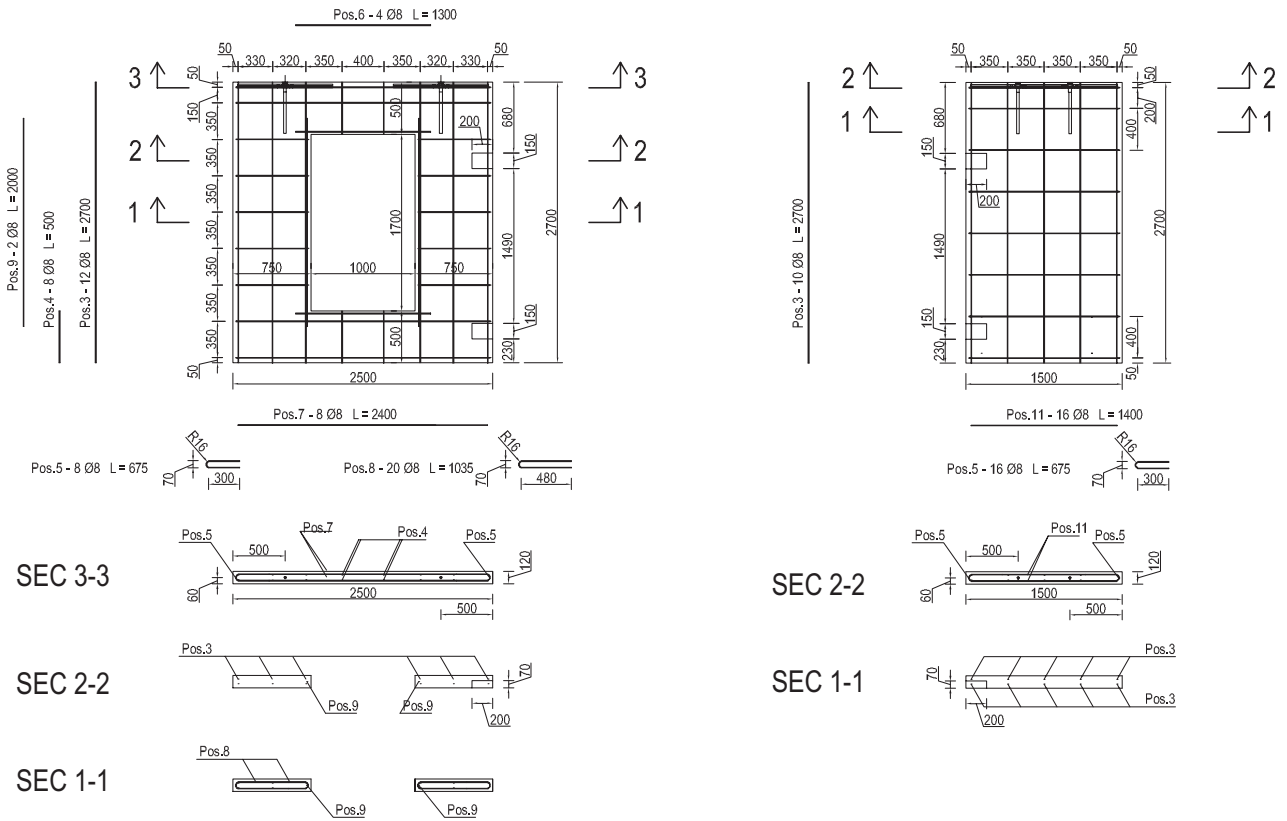
Figure 140: Example of a case-study prototype with openings– window
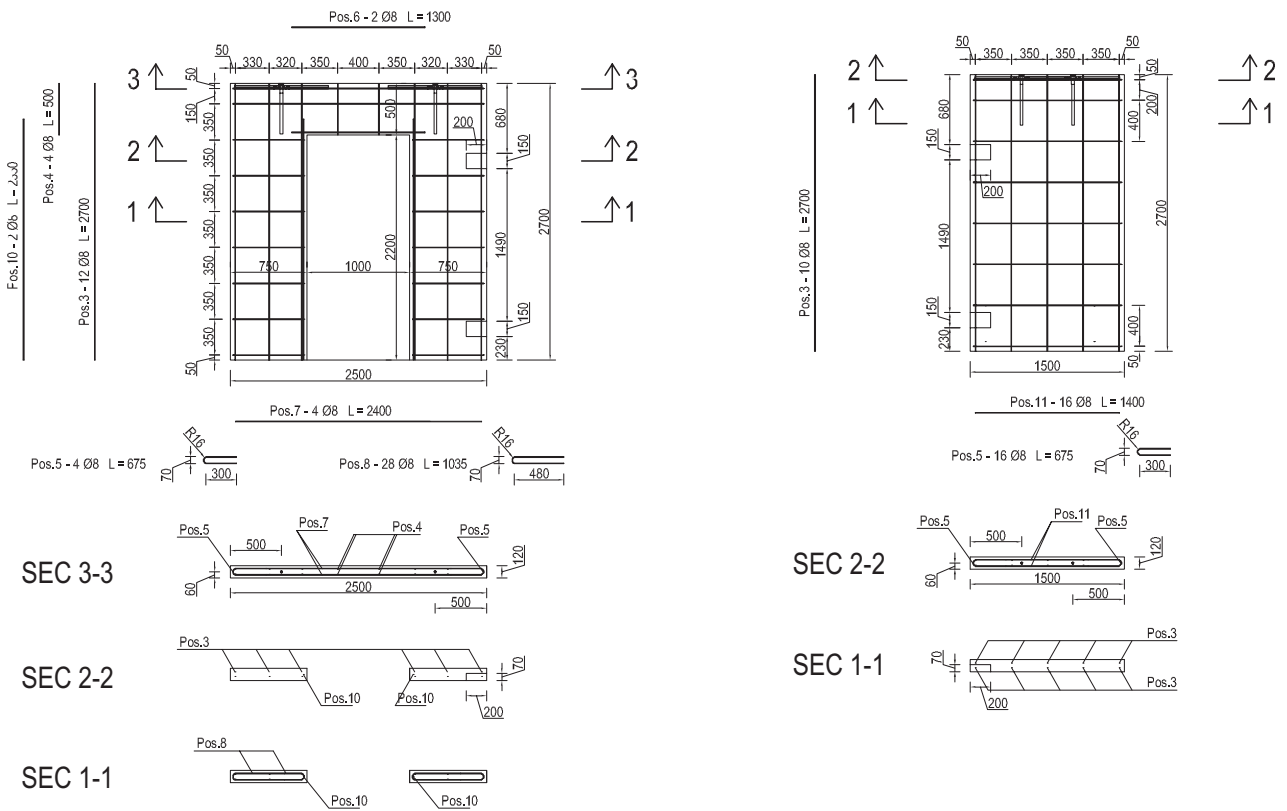
Figure 141: Example of a case-study prototype with openings – door

Once the rationale behind the design method assumed to identify and prepare a set of representative structural configurations for experimental tests, a more specific categorization/description of case-study specimens will be provided in the following. Therefore, details concerning test setup and procedure, as well as a brief description of specimens, materials and reinforcement layouts, will be summarized in the upcoming paragraphs.

6.2.1 Classification and description of case-study specimens

As previously mentioned, 8 prototypes with or without openings (i.e. doors or windows) were tested and their main characteristics are summarized in Table 5. In particular, 20 cm and 12 cm thick walls were tested under cyclic in-plane flexure with constant axial load. As specified in Table 5, different values in the range 200 kN-800 kN were assumed according to specimen thickness. In general, two different axial loads were considered for each structural configuration in order to provide upper and lower bounds for capacity estimates. Odd specimen tag identifies the minimum axial load level (i.e. N_{min}), while even test ID correspond to the maximum (i.e. N_{max}). In detail, 300 kN and 800 kN were selected for 20 cm thick specimens, while 200 kN and 500 kN were imposed for 12 cm thick solid walls. The walls with openings, regardless the door or window configuration, experienced 140 kN and 360 kN.

Table 5: test characteristics and specimen nomenclature

Specimen	Opening	Thickness	Axial load	Re-bars?
SP 01	w/o	20 cm	300 kN	2Ø8
SP 02	w/o	20 cm	800 kN	2Ø8
SP 03	w/o	12 cm	200 kN	w/o
SP 04	w/o	12 cm	500 kN	w/o
SP 05	Window	12 cm	140 kN	w/o
SP 06	Window	12 cm	360 kN	w/o
SP 07	Door	12 cm	140 kN	w/o
SP 08	Door	12 cm	360 kN	w/o

In addition, starter re-bars were considered or omitted in the tests depending on wall thickness, in accordance with Dutch building practice. In particular, 2Ø8 protruding re-bars were provided at the corners of 20 cm thick specimens.

Further details and schemes regarding each specimen will be given in the following. In particular, Figure 142, Figure 143, Figure 144, Figure 145, Figure 146, Figure 147, Figure 148 and Figure 149 show the characteristics of Specimen 01, 02, 03, 04, 05, 06, 07 and 08, respectively.

Furthermore, the reinforcement layout obtained for each specimen according the criteria specified in Paragraph 6.2 are provided hereafter. In Figure 150, the longitudinal and transverse reinforcement arrangements provided in Specimen 01 and 02, while Figure 151 presents schematics of those used in Specimen 03 and 04. Figure 152 and Figure 153 show the configuration of the reinforcement of panels with doors and windows respectively. The longitudinal reinforcement consists of Ø8 bars 30 cm spaced; the same bar diameter with 40 cm spacing was used as transverse

reinforcement. In addition to this standard reinforcement configuration, 2 Ø8 50 cm long starter bars were provided at the corners of Specimen 01 and 02. By contrast this type of detailing was omitted in the other panels. Furthermore, additional Ø8 bars were provided at the corner of the opening, for specimens presenting doors or windows. In these cases, the spacing of the longitudinal reinforcement was slightly adjusted to comply with the updated geometries. This resulted in an almost negligible difference in terms of volumetric reinforcement ratio. More specific details can be found in Figure 150, Figure 151, Figure 152 and Figure 153.

As mentioned in Section 6.2, concrete class C35/45 was used for all specimens under consideration, while steel type B450C was used both for the longitudinal and the transverse reinforcement. A series of tensile and compressive characterization tests were conducted and their main results are collected and reported in Table 6, Table 7 and Table 8. A measure of concrete compressive strength at different concrete ageing was provided comparing the values summarized in Table 7 and Table 8.
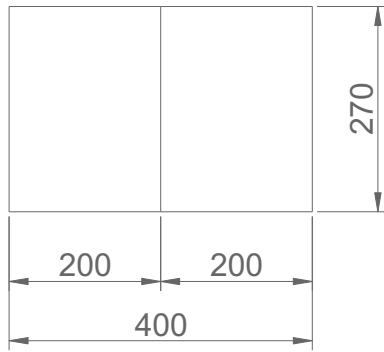
	SPECIMEN 01
	20 cm thick panel without openings
	N_{min} = 150 kN + 150 kN = 300 kN
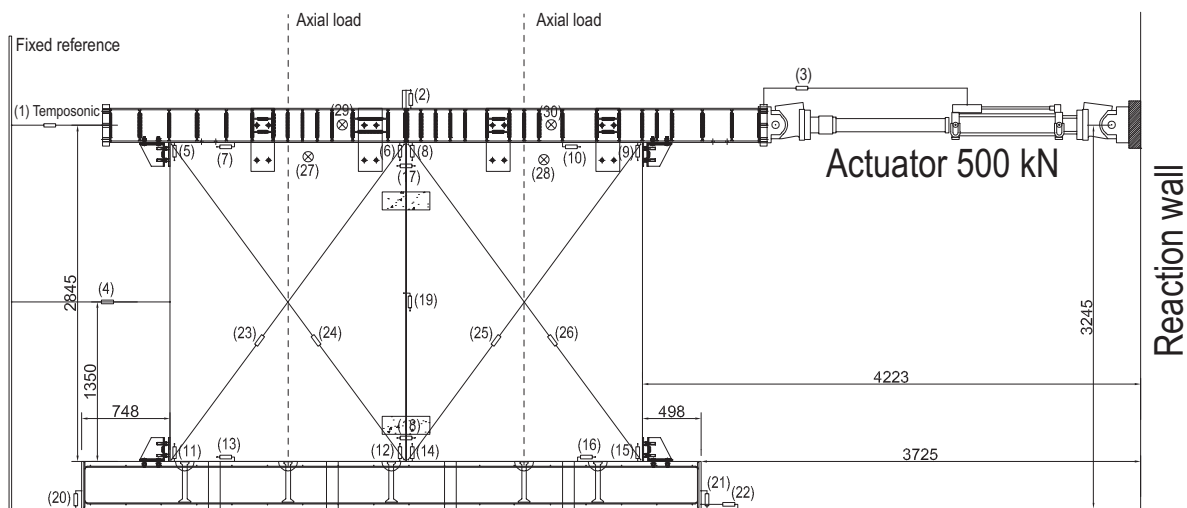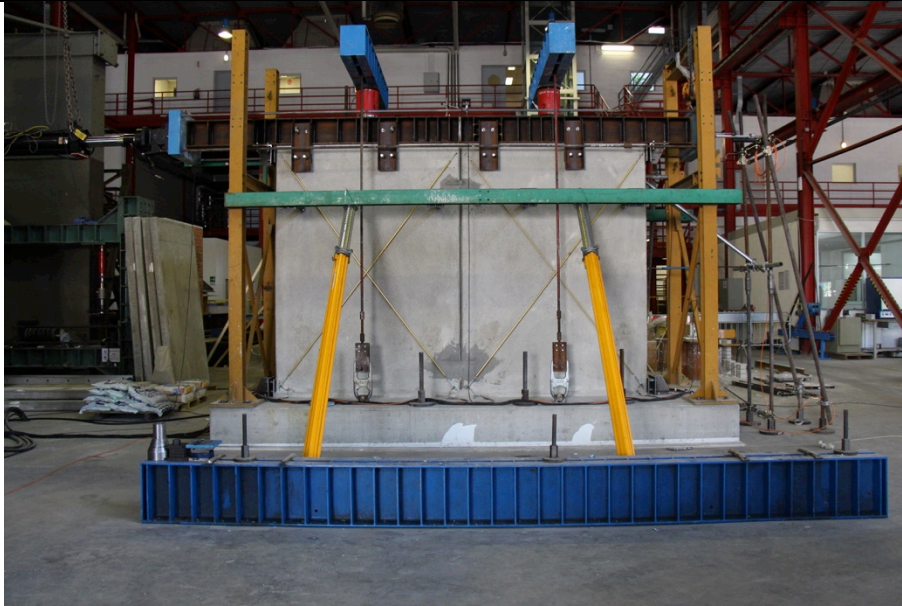
Figure 142: Specimen 01 – geometrical characteristics
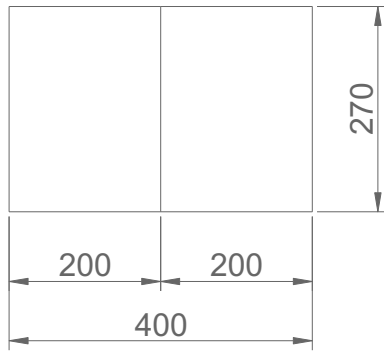
SPECIMEN 02

20 cm thick panel without openings

$N_{max} = 400kN + 400kN = 800$ kN
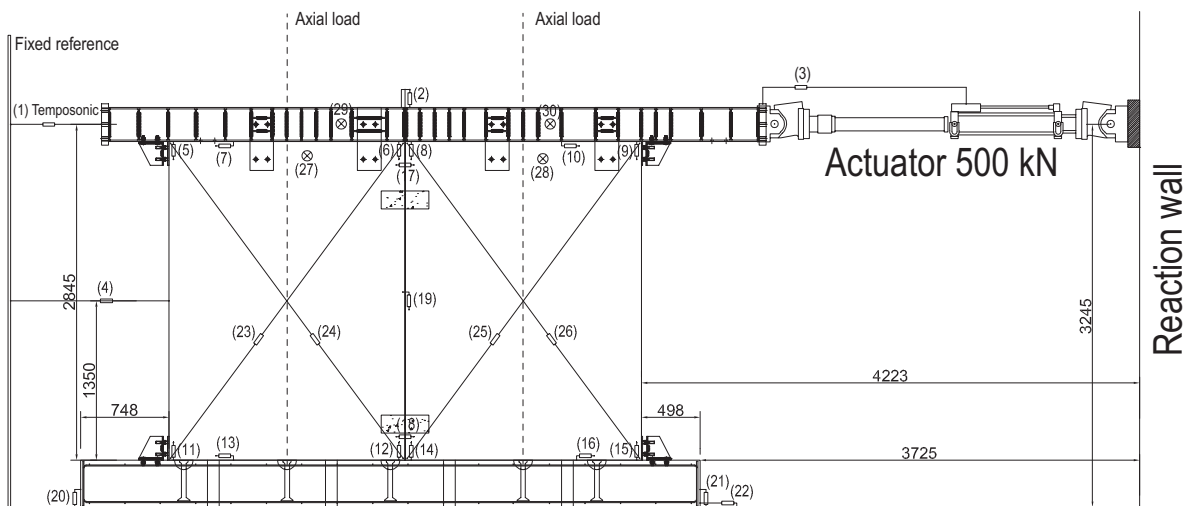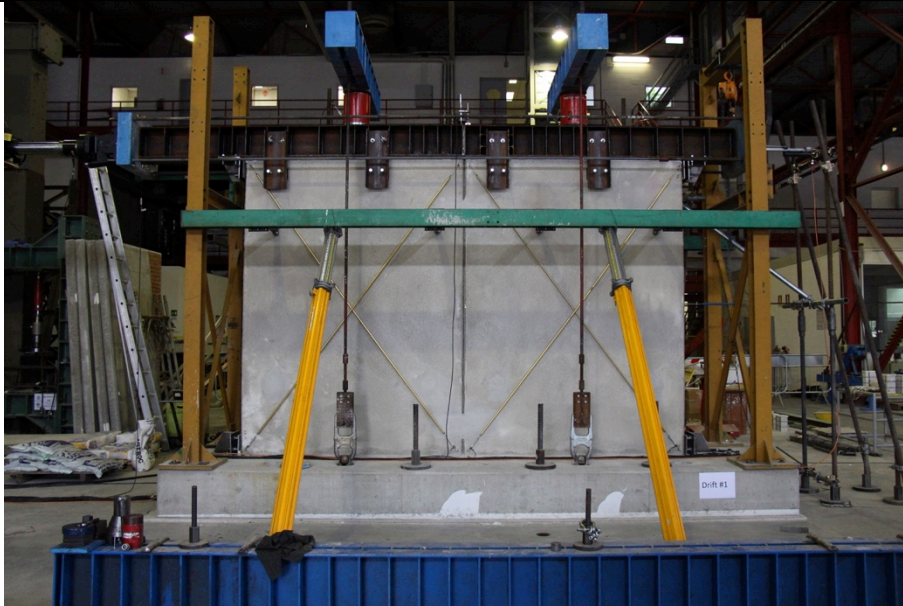
Figure 143: Specimen 02 – geometrical characteristics
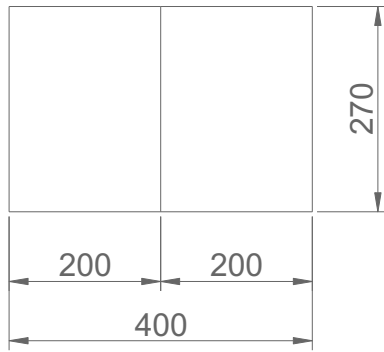
SPECIMEN 03

12 cm thick panel without openings

N_{min} = 100 kN + 100 kN = 200 kN
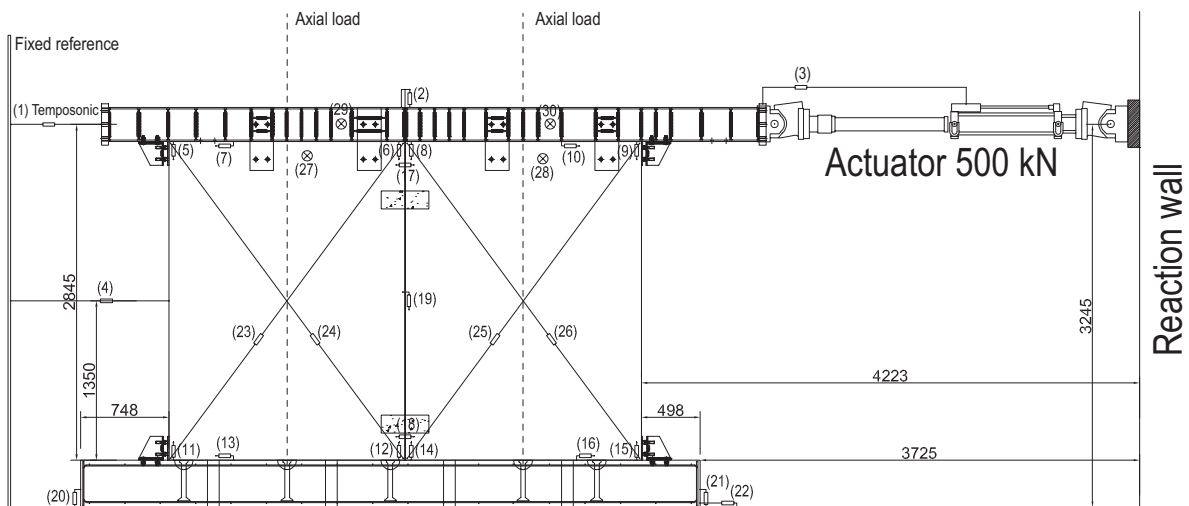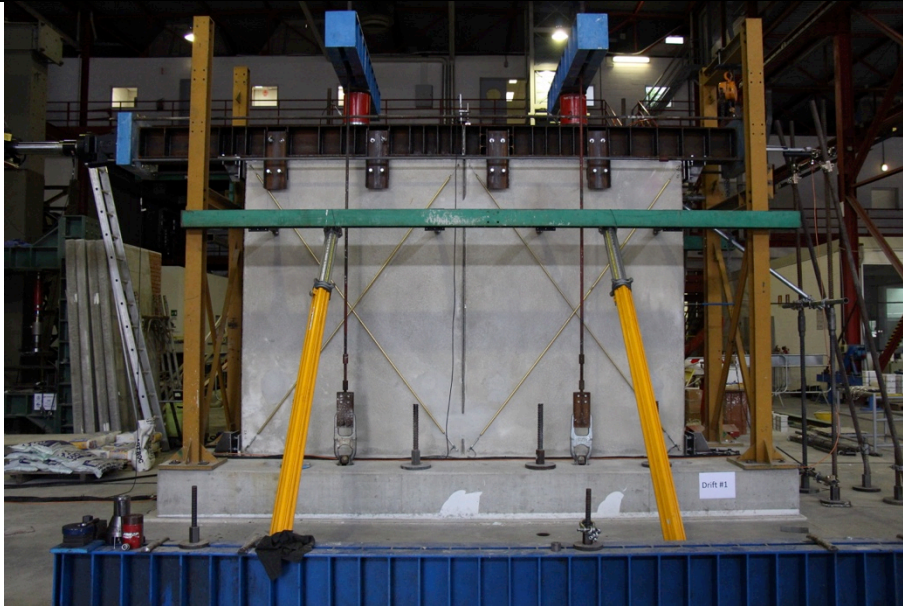
Figure 144: Specimen 03 – geometrical characteristics
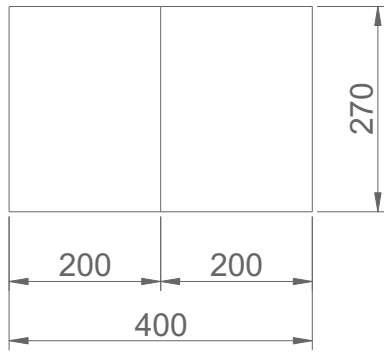
SPECIMEN 04

12 cm thick panel without openings

N_{max} = 250 kN + 250 kN = 500 kN
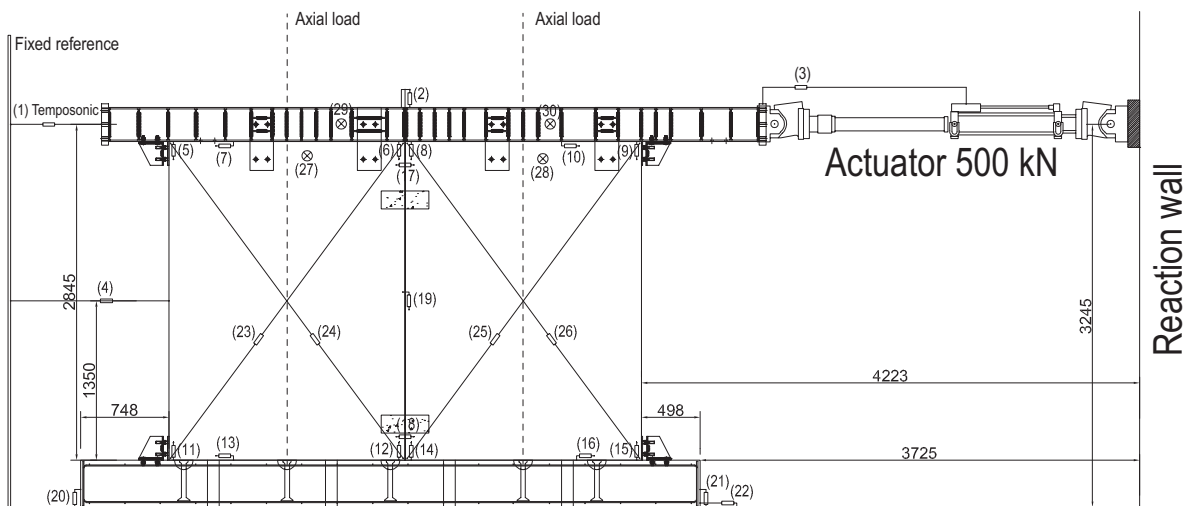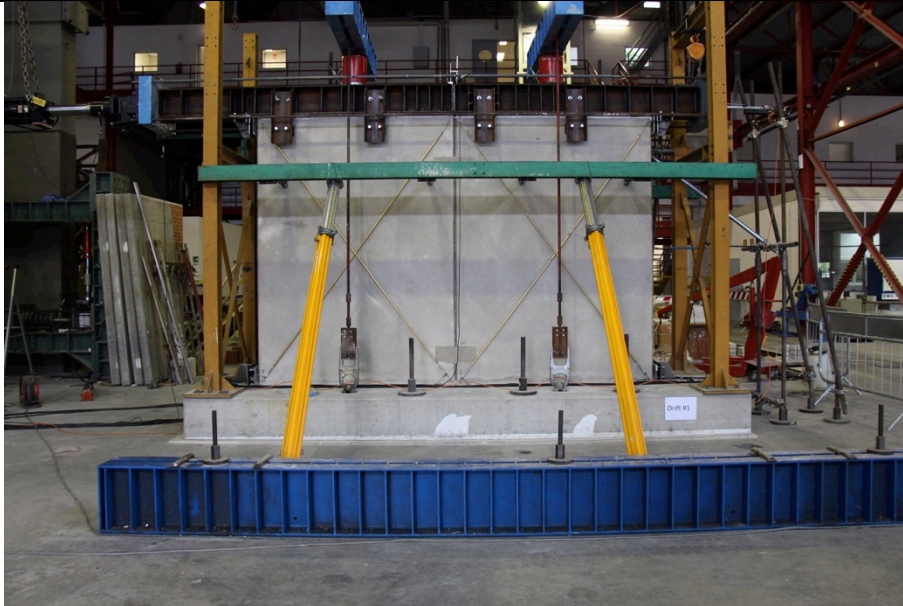
Figure 145: Specimen 04 – geometrical characteristics
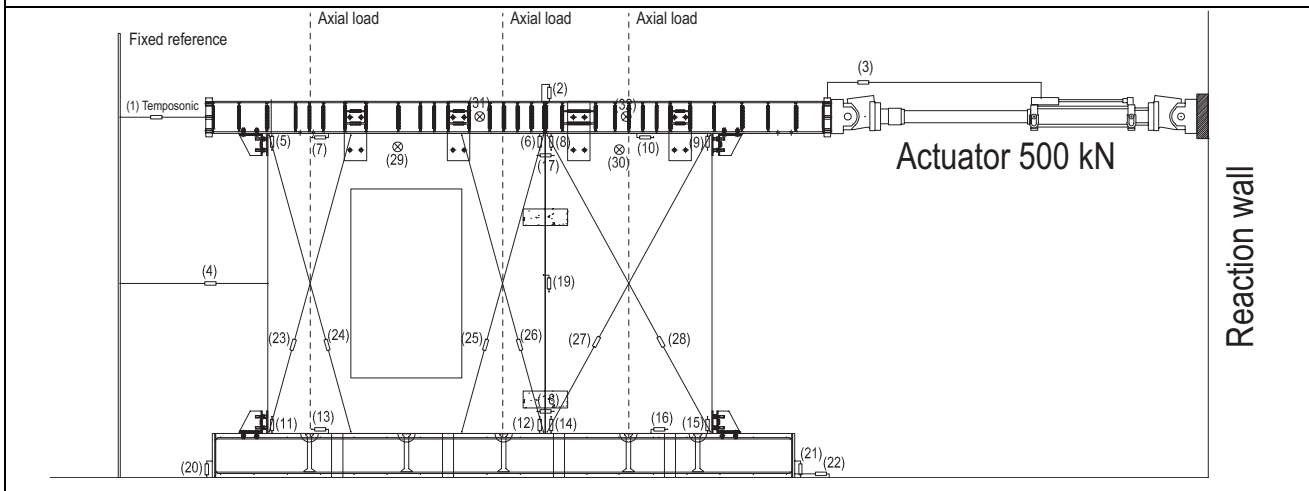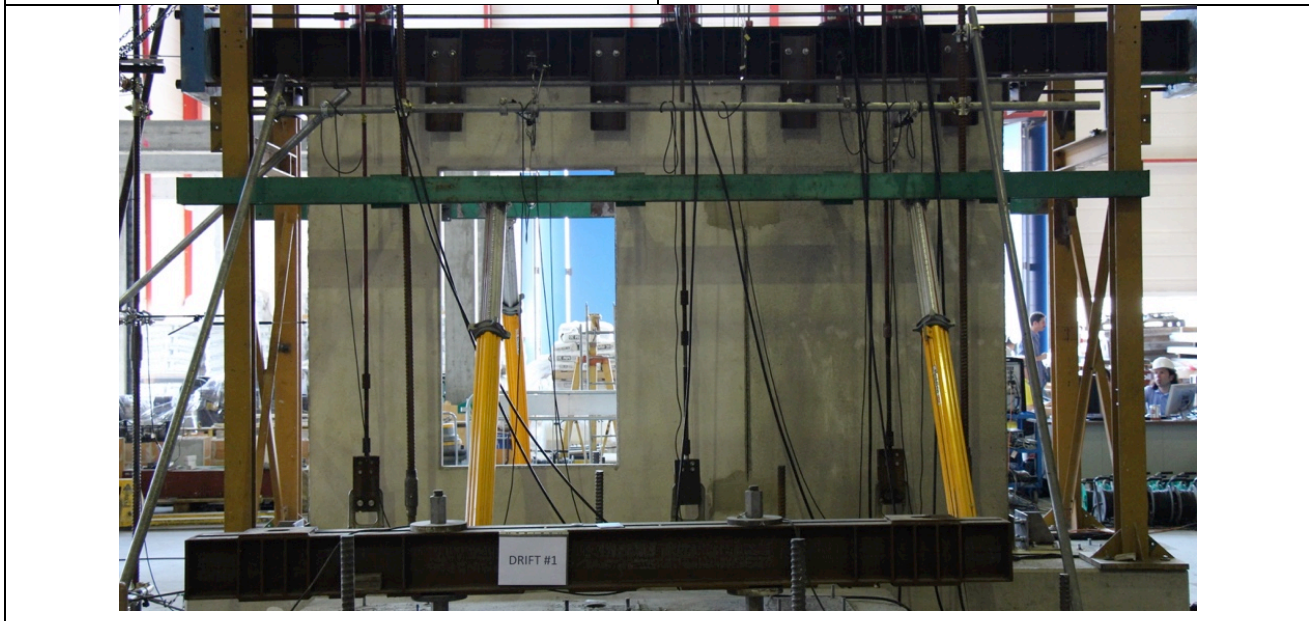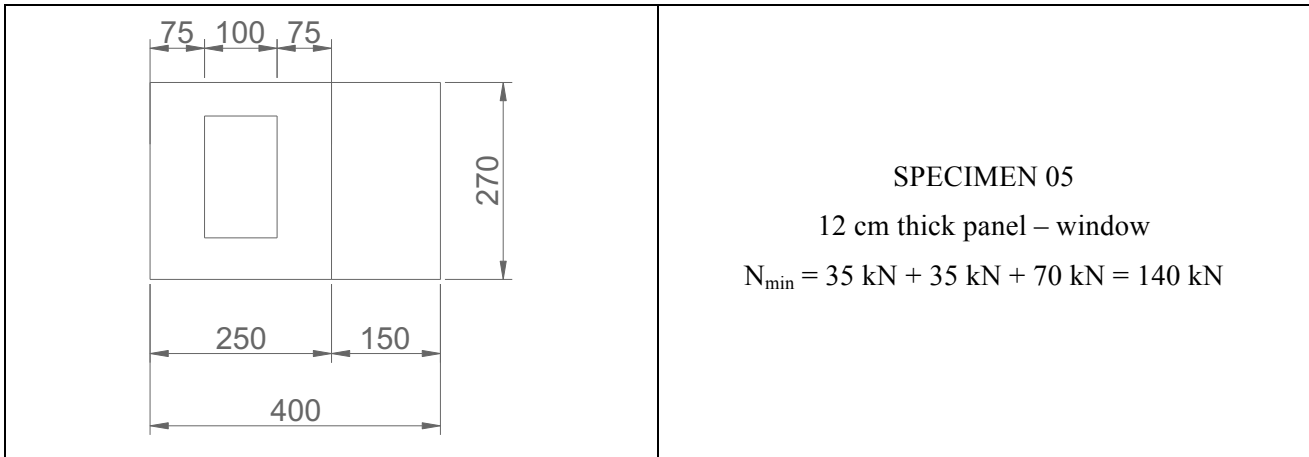
Figure 146: Specimen 05 – geometrical characteristics
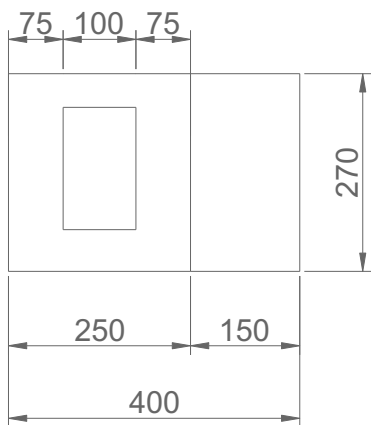
SPECIMEN 06

12 cm thick panel –window

N_{max} = 90 kN + 90 kN + 180 kN = 360 kN
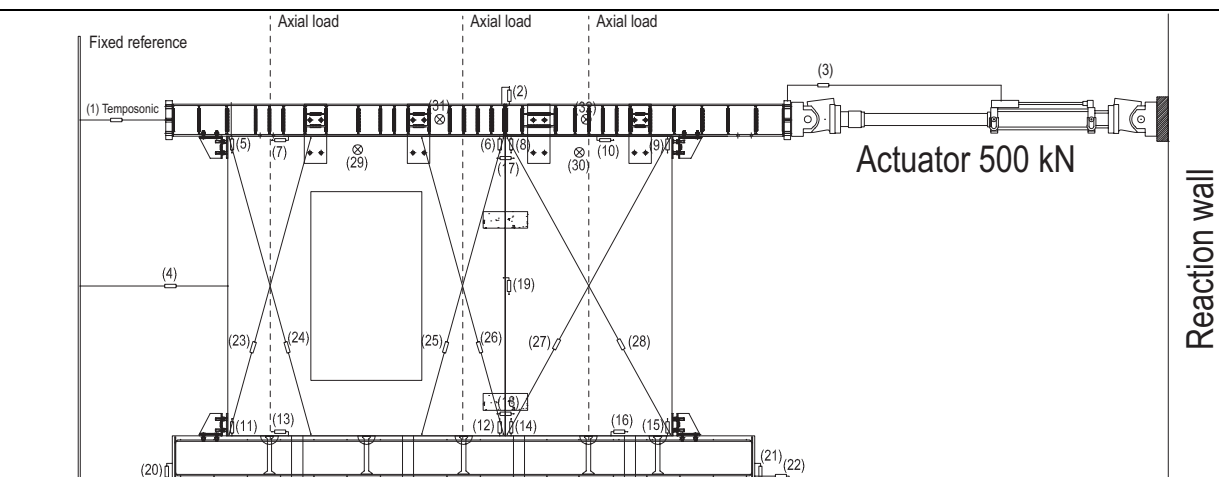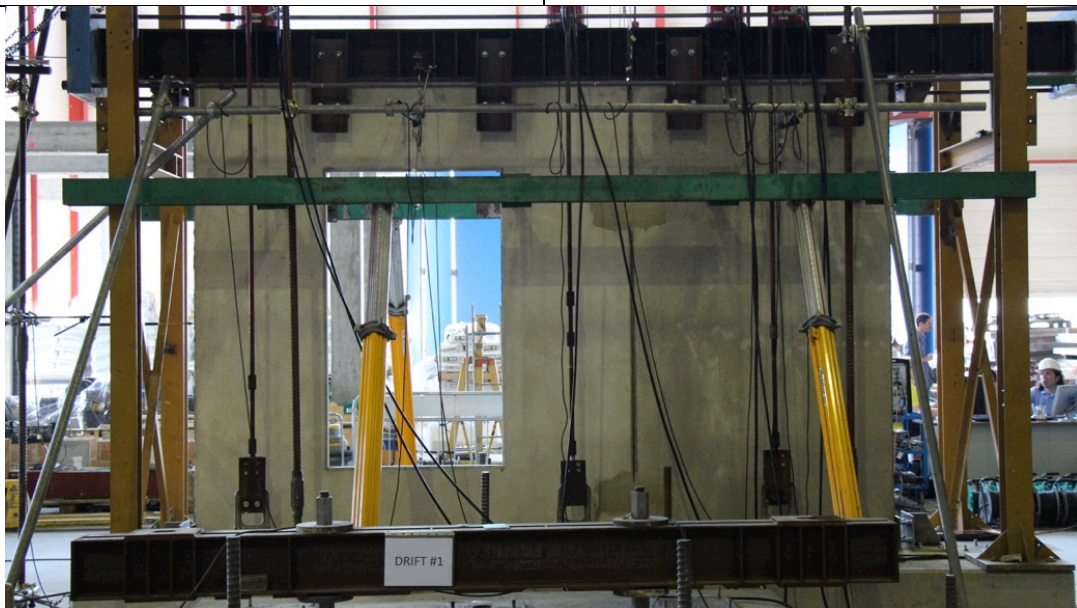
Figure 147: Specimen 06 – geometrical characteristics
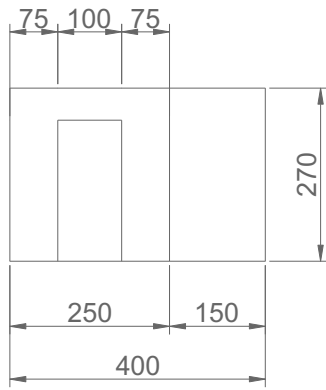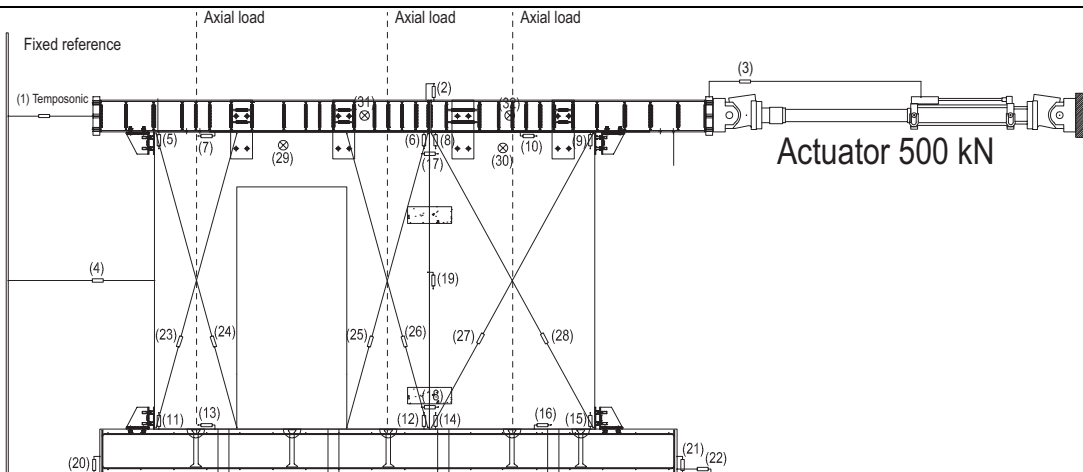
Figure 148: Specimen 07 – geometrical characteristics

75	100	75	
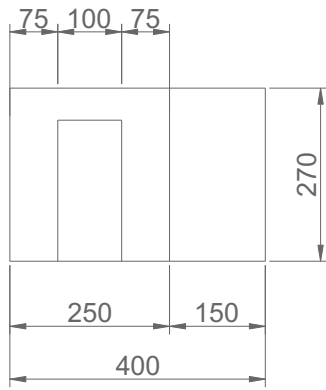
SPECIMEN 08

12 cm thick panel – door

N_{max} = 90 kN + 90 kN + 180 kN= 360 kN
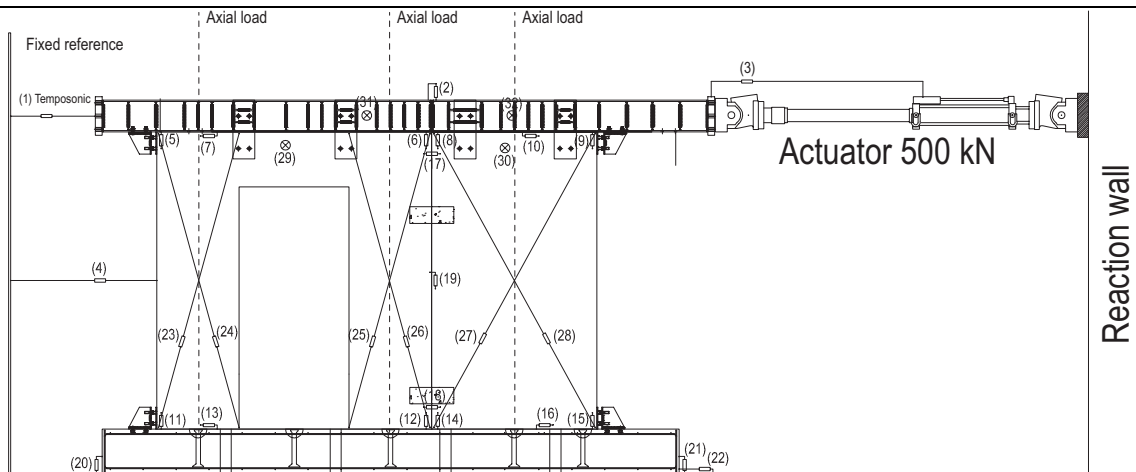
Figure 149: Specimen 08 – geometrical characteristics
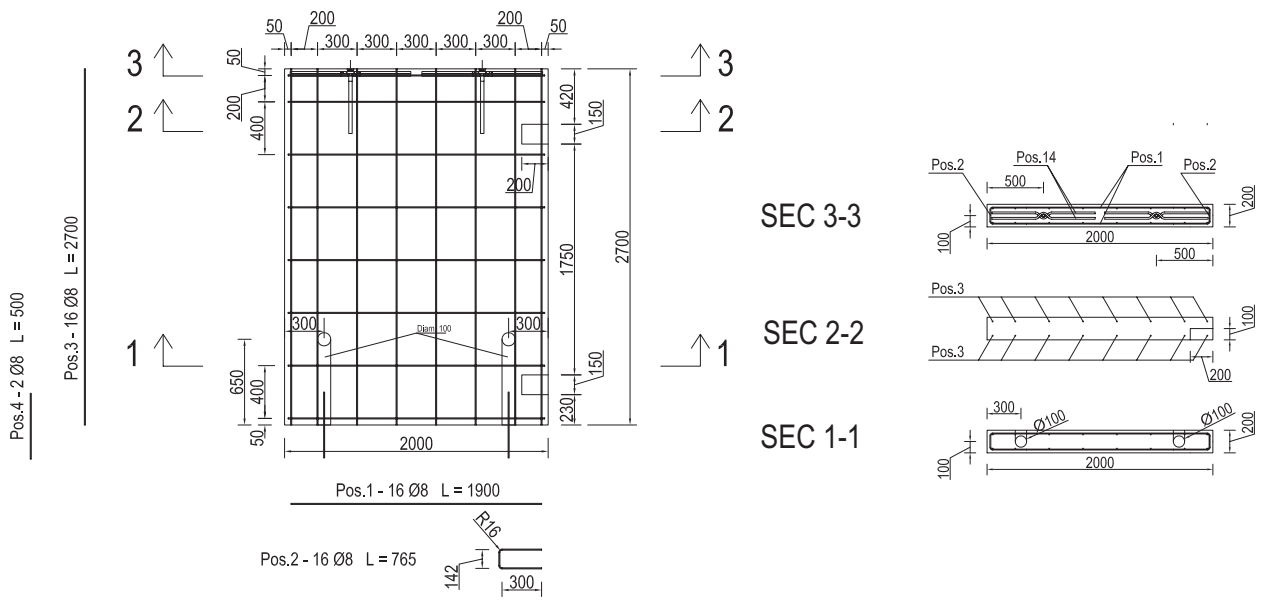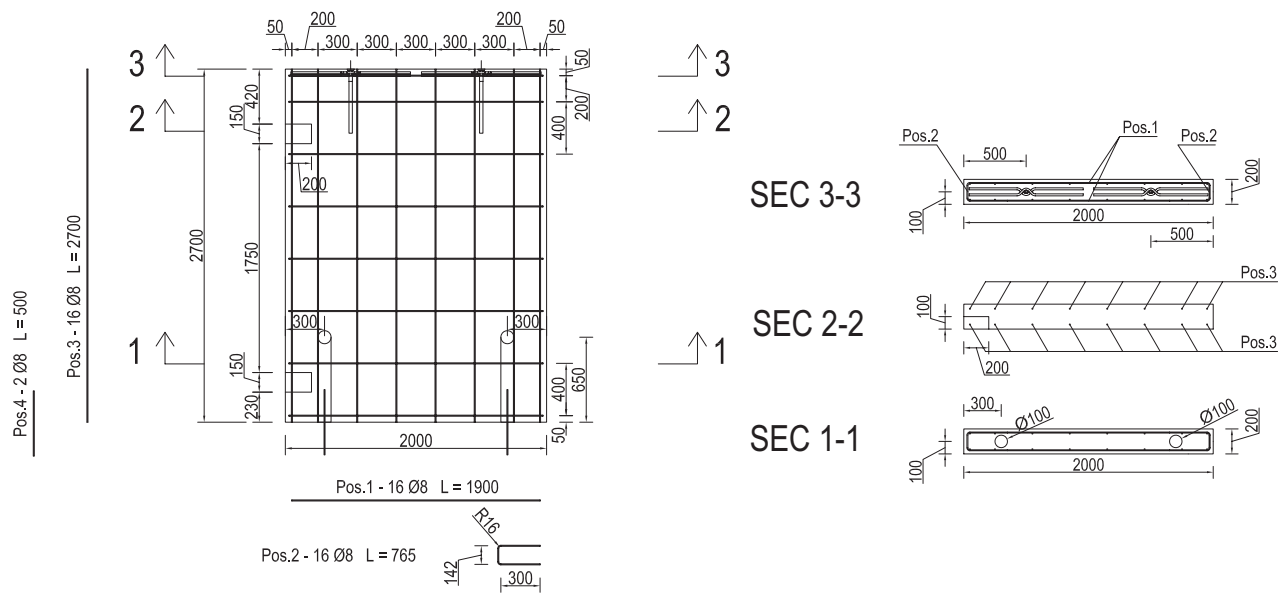
Figure 150: Reinforcement layout – Specimen 01 and 02.

Note: (a) right and (b) left side panels
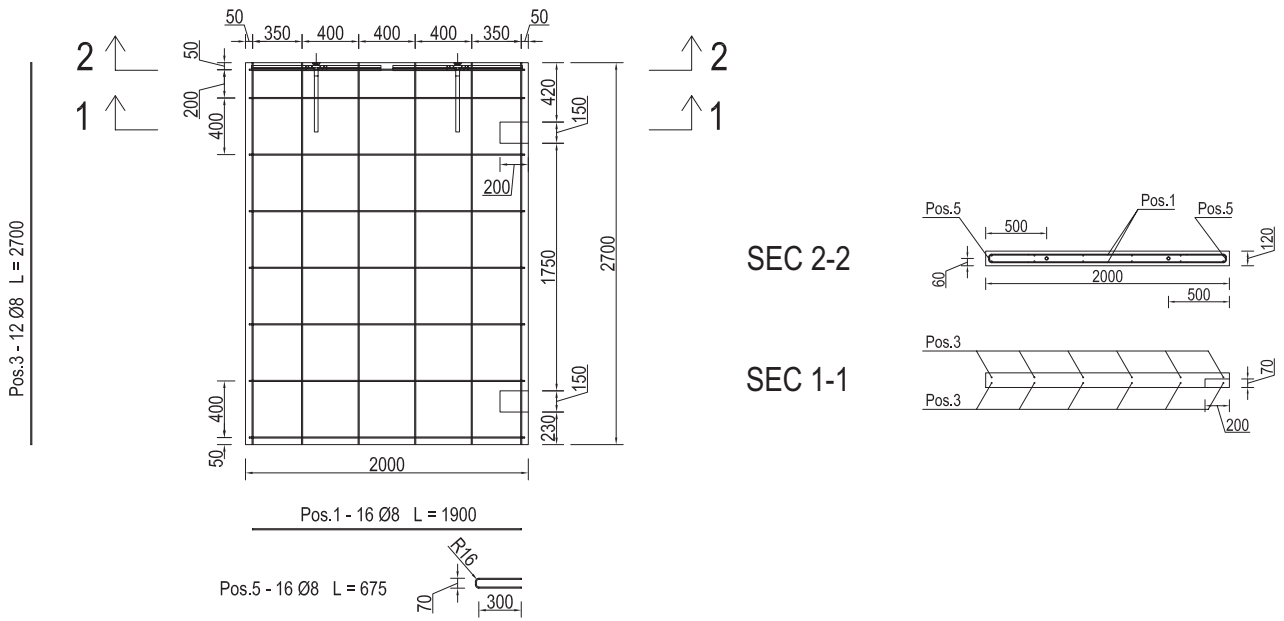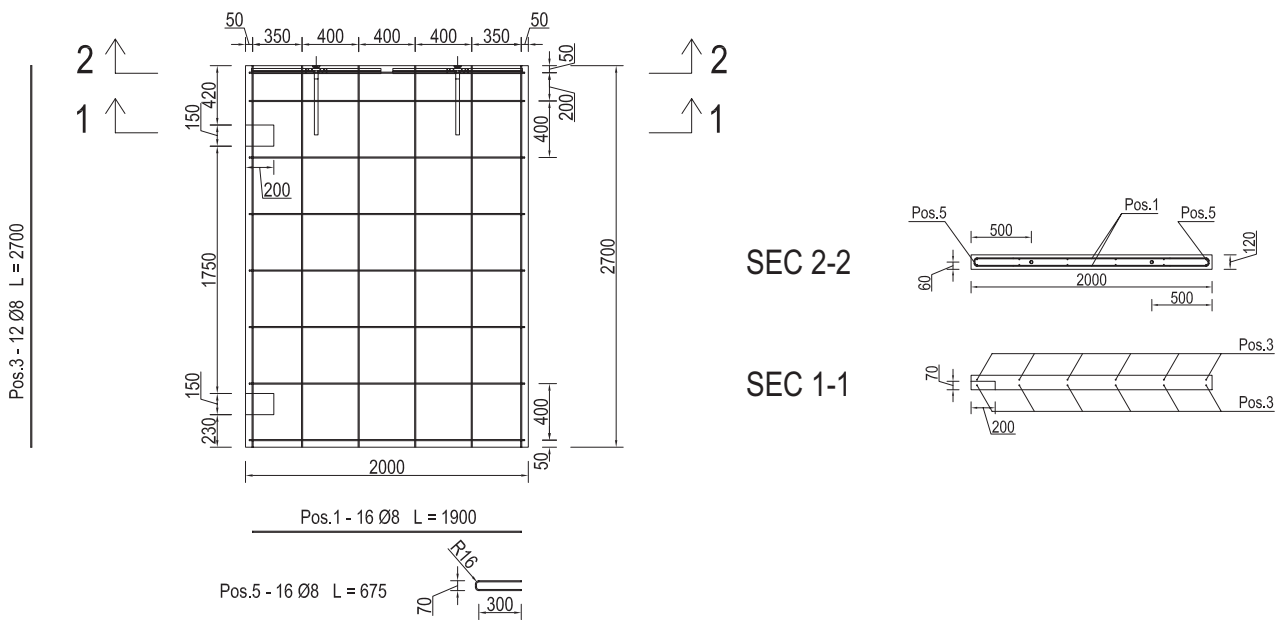
Figure 151: Reinforcement layout – Specimen 03 and 04

Note: (a) right and (b) left side panels
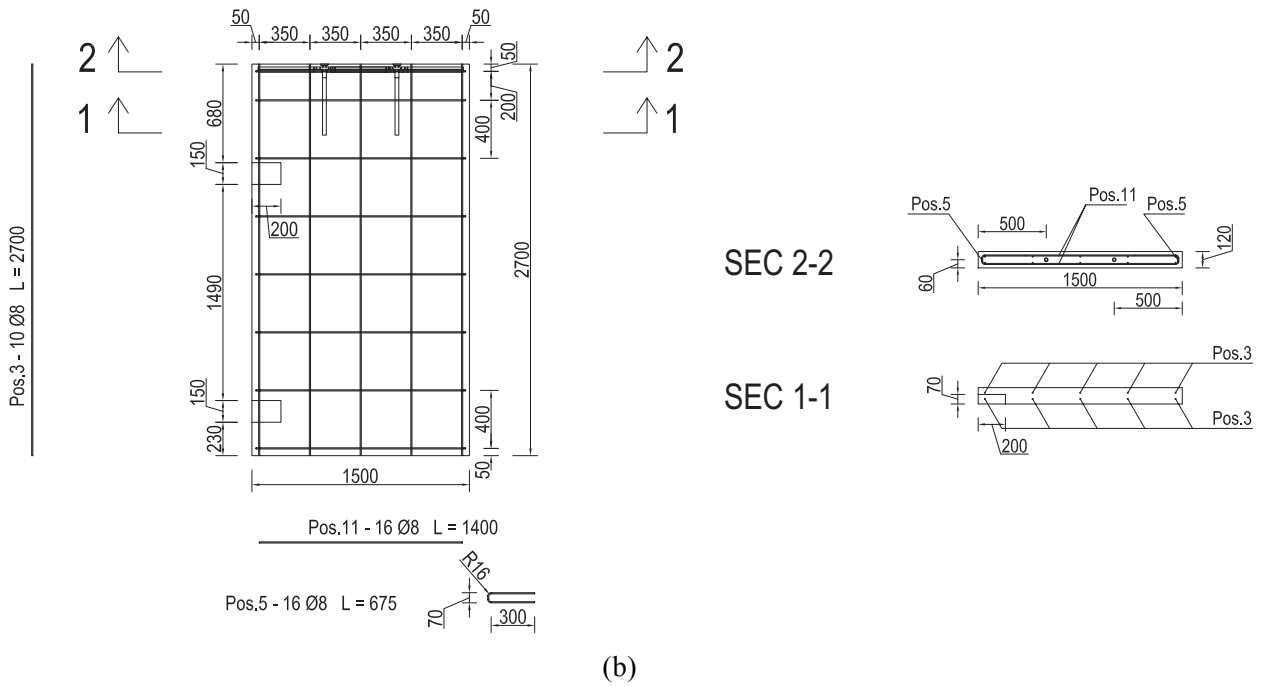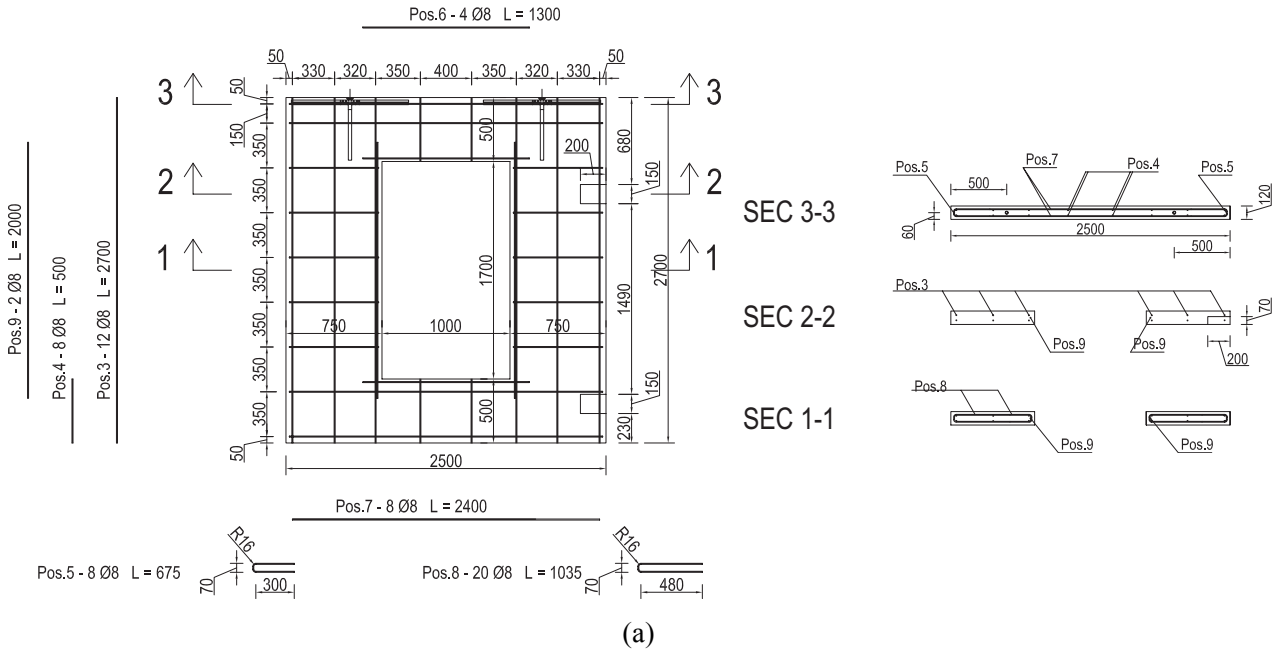
Figure 152: Reinforcement layout – Specimen 05 and 06

Note: (a) right and (b) left side panels
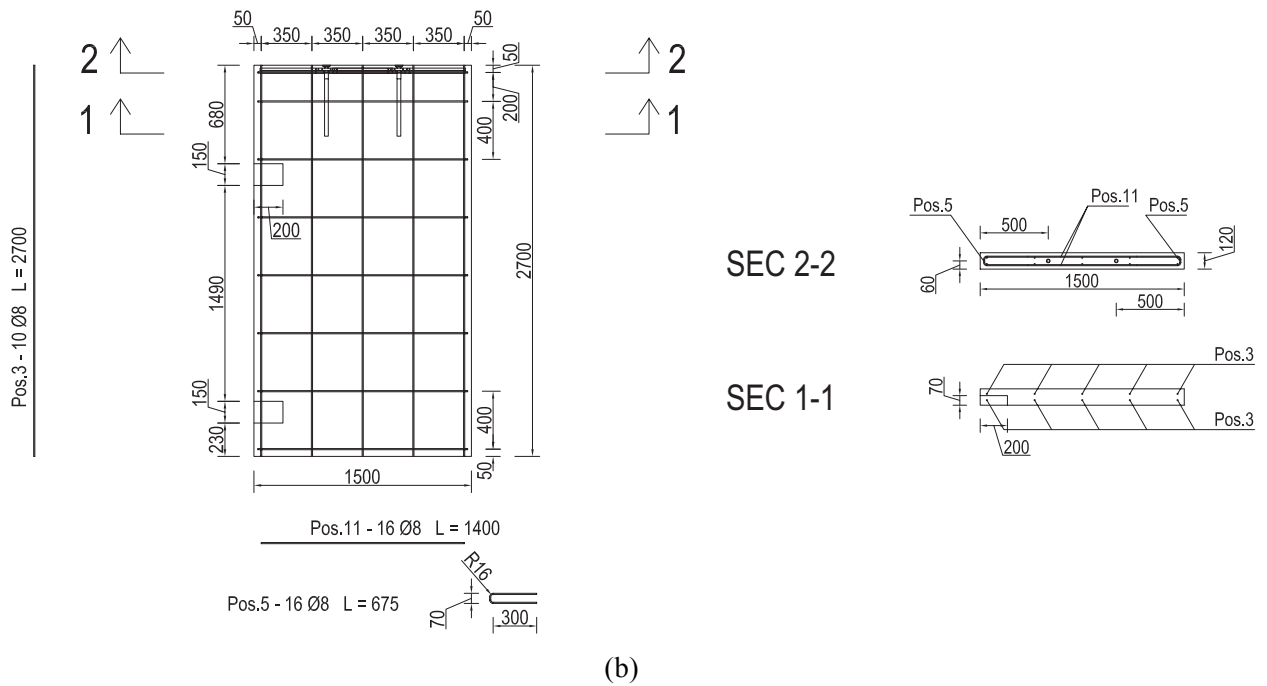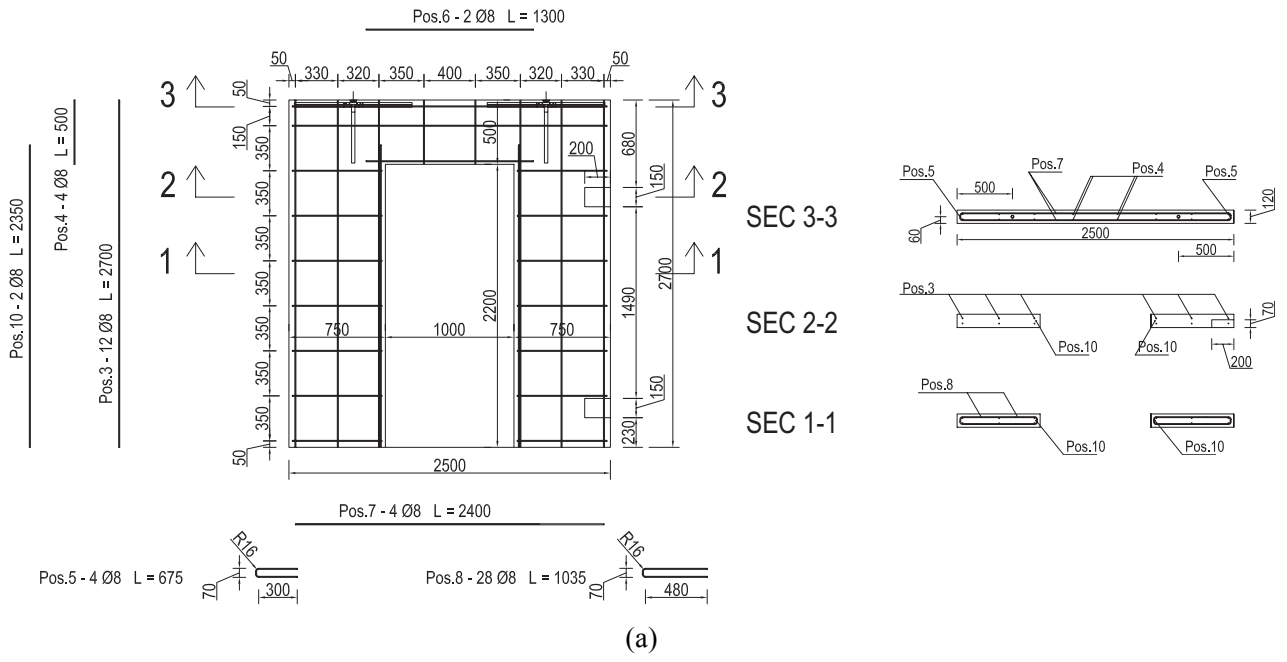
Figure 153: Reinforcement layout – Specimen 07 and 08

Note: (a) right and (b) left side panels

Table 6: characterization tests – Tensile tests of steel reinforcement (UNI EN ISO 15630-1)

N.	Diameter (mm)	Length (mm)	Area (mm²)	Mass per unit length (kg/m)	TENSILE TEST Yielding f_y (N/mm²)	Ultimate f_t (N/mm²)	Ratio f_t/f_y	Elong. A_{gt} (%)
1	8	500	49.63	0.390	565	637	1.13	6.4
2	8	500	49.81	0.391	559	634	1.13	6.8
3	8	500	49.73	0.390	564	635	1.13	8.2

Table 7: characterization tests – Compressive tests of concrete cubes at 7 days (UNI EN ISO 15630-1)

N.	Size (mm) L	B	H	Mass kg	Mass/Vol. kg/m³	Load kN	Resistance f_c N/mm²	Type of failure	Val.	Fail. kg
1	150.0	150.0	150.0	8.100	2,400	1,030	45.78	S	105	105000

Table 8: characterization tests – Compressive tests of concrete cubes at 28 days (UNI EN 12390-3-4-7)

N.	Size (mm) L	B	H	Mass kg	Mass/Vol. kg/m³	Load kN	Resistance f_c N/mm²	Type of failure	Val.	Fail. kg
1	150.0	150.0	150.0	8.100	2,400	1,207	53.63	S	123	123000
2									0	0
3	150.0	150.0	150.0	8.050	2,385	1,305	57.99	S	133	133000
4	150.0	150.0	150.0	8.040	2,382	1,167	51.88	S	119	119000
5	150.0	150.0	150.0	8.000	2,370	1,187	52.76	S	121	121000
6	150.0	150.0	150.0	7.990	2,367	1,109	49.27	S	113	113000
7	150.0	150.0	150.0	7.870	2,332	991	44.04	S	101	101000
8	150.0	150.0	150.0	7.920	2,347	922	40.98	S	94	94000
9	150.0	150.0	150.0	7.930	2,350	1,138	50.58	S	116	116000
10	150.0	150.0	150.0	7.940	2,353	961	42.73	S	98	98000
11	150.0	150.0	150.0	7.960	2,359	1,148	51.01	S	117	117000
12	150.0	150.0	150.0	7.850	2,326	1,089	48.40	S	111	111000

Further schematics concerning the foundation and the beam at the top of the panels may be found in Figure 154 and Figure 155, while Figure 156 and Figure 157 provides details related to the steel anchors and the L-shaped profiles placed at the base of the walls.
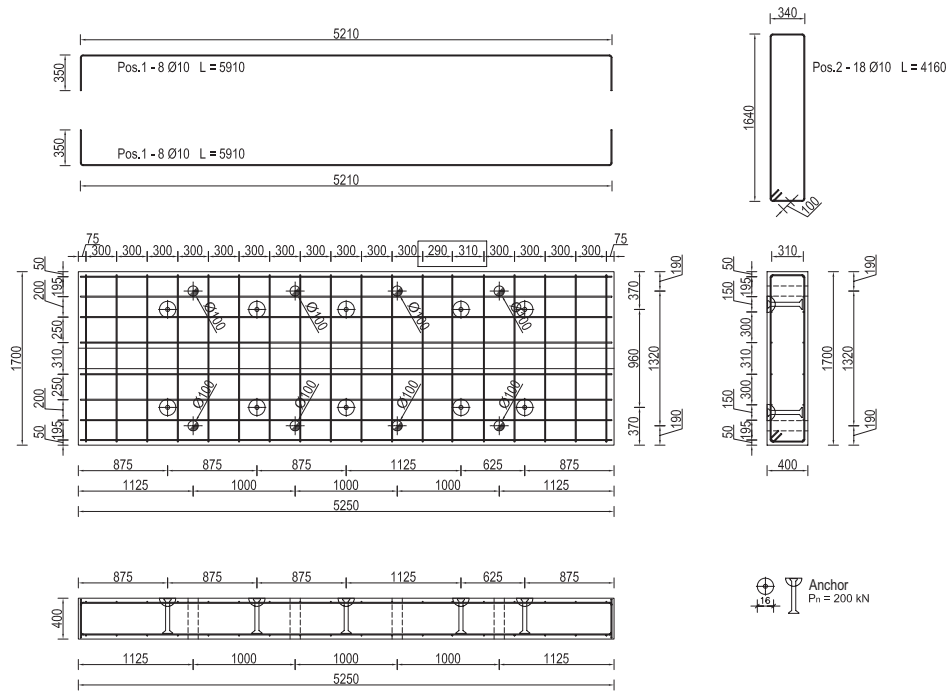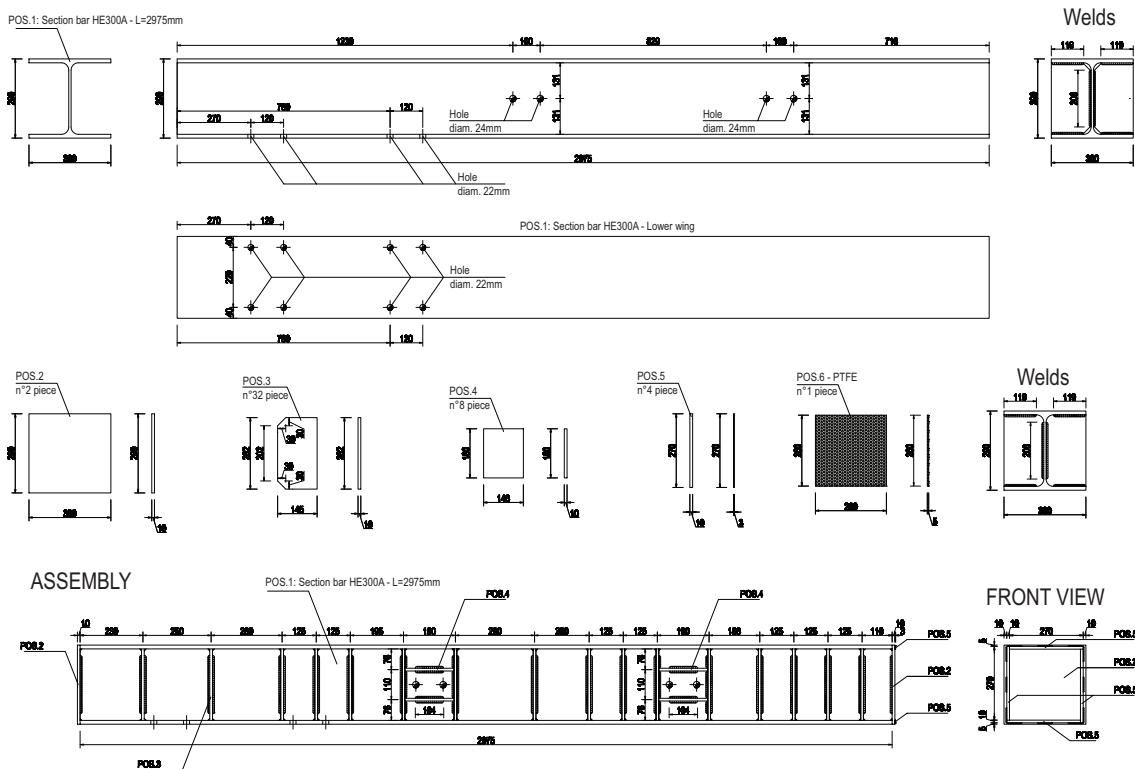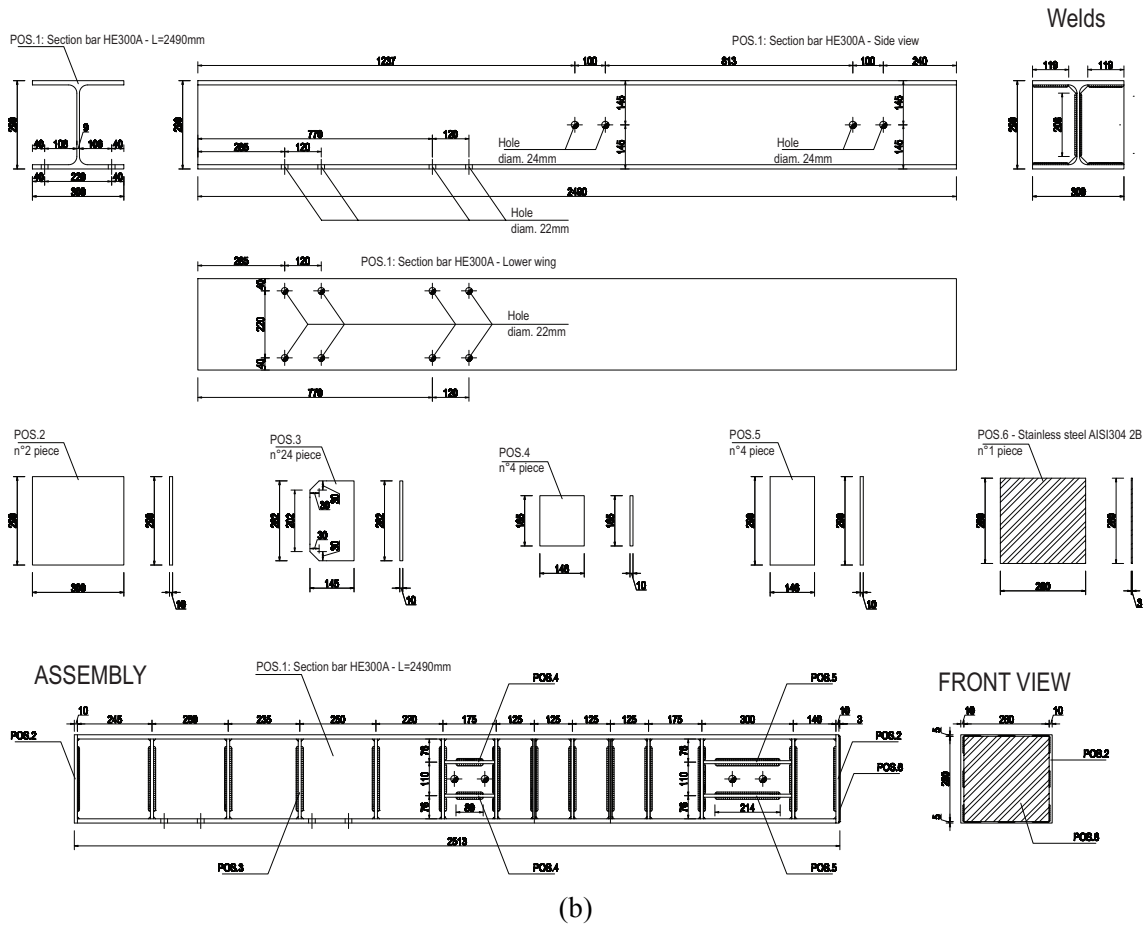
Figure 154: Concrete foundation

(a)

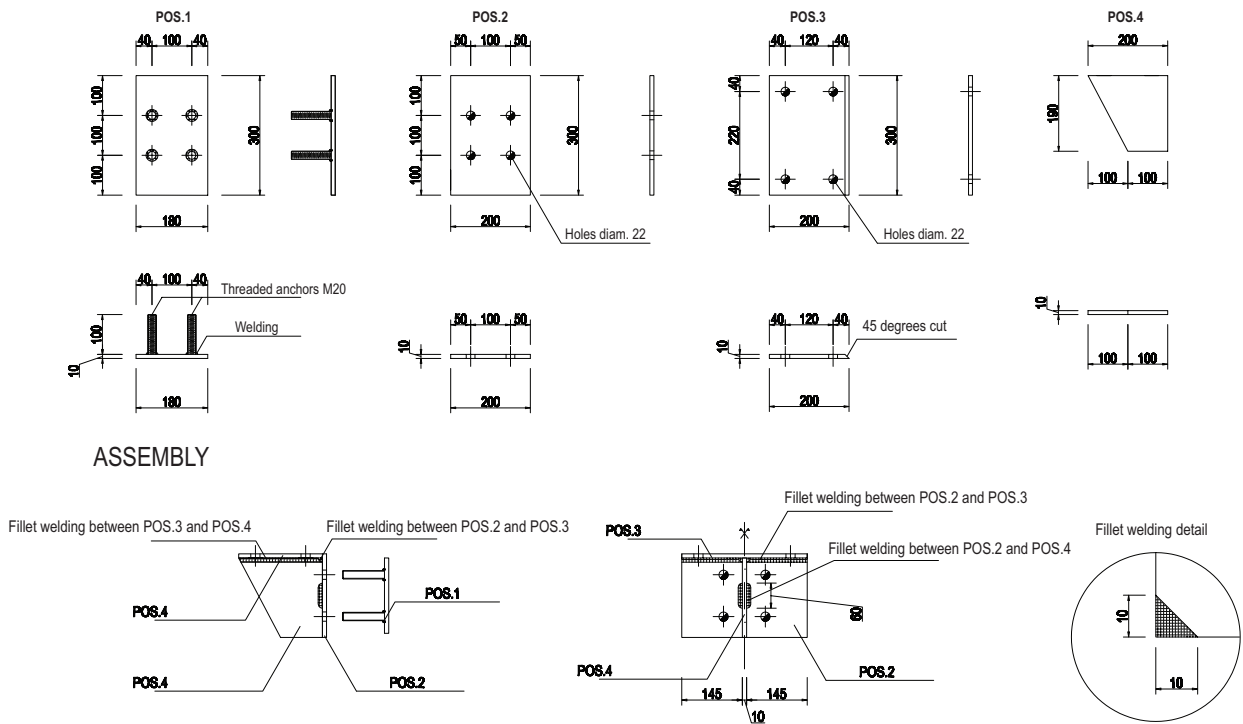**Figure 155: Steel beams – Loading of the specimens**

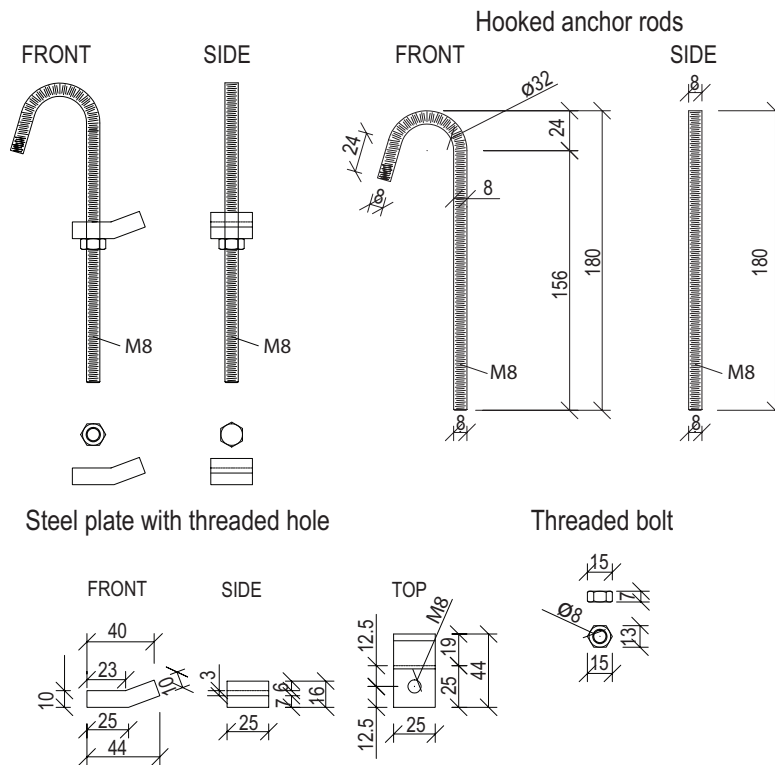**Figure 156: Sliding restrainers**

Figure 157: Panel to panel anchors

In particular, threaded M8 anchors made of steel grade 8.8 were placed in correspondence to edges of the panels to prepare the top and bottom anchoring zone. In order to prevent any type of sliding mechanism, L-shaped steel profile was placed at each of the external corners of the panel assembly. Clearly, both foundation and top beams were designed to remain elastic during the whole testing campaign.

6.2.2 Test setup and loading protocol

The 8 full-scale panels were pseudo-statically tested under cyclic in-plane flexure with a constant axial load level, assuming only a single bending configuration. A MTS actuator imposed a horizontal displacement to the top of the panels. The loading history involved series of 3 cycles with increasing amplitude using a displacement control strategy. Only the first two series of cycles were applied in force control. As an example, the experimental loading protocol planned for the Specimen 02 is reported in Figure 158 and Table 9. Hydraulic jacks, acting on the top steel beam and connected to the concrete foundation at the base of the panels, applied the constant vertical load.
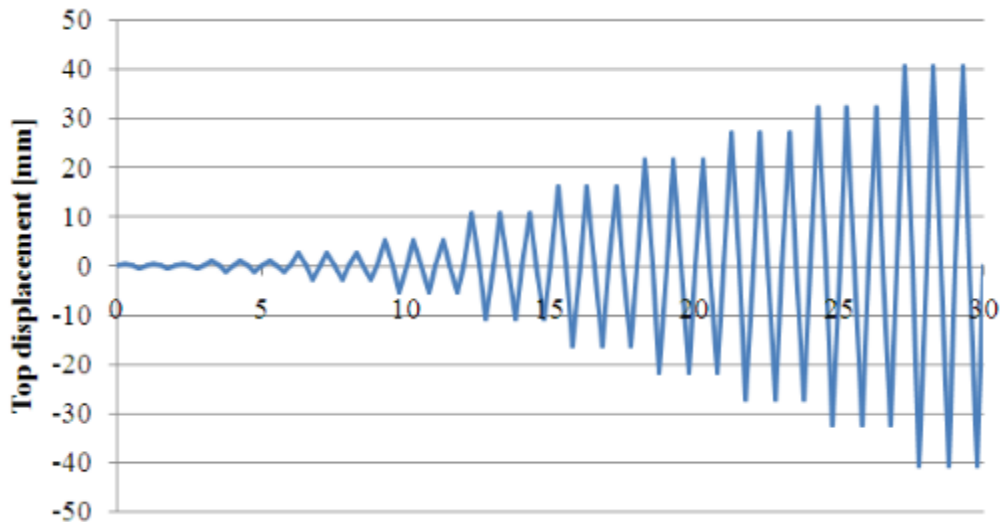
Figure 158: Experimental loading protocol

Table 9: experimental loading protocol – force and displacement control mode

Test #	Test Name	Label	Main DoF	Control Type	MAX Ampl.	MIN Ampl.	Loading Speed	Load Shape	Axial Load	Cycles
				(Force or Displ.)	[kN] [mm]	[kN] [mm]	[kN/s] [mm/s]		[kN]	[#]
0	Axial Loading	AL	Vert	Force	0	-400	3.333	ramp	-	-
1	Drift #1	D1	Long	Force	50	-50	0.833	triang.	400	3
2	Drift #2	D2	Long	Force	100	-100	1.667	triang.	400	3
3	Drift #3	D3	Long	Displ.	2.7	-2.7	0.045	triang.	400	3
4	Drift #4	D4	Long	Displ.	5.4	-5.4	0.090	triang.	400	3
5	Drift #5	D5	Long	Displ.	10.8	-10.8	0.180	triang.	400	3
6	Drift #6	D6	Long	Displ.	16.2	-16.2	0.270	triang.	400	3
7	Drift #7	D7	Long	Displ.	21.6	-21.6	0.360	triang.	400	3
8	Drift #8	D8	Long	Displ.	27	-27	0.450	triang.	400	3
9	Drift #9	D9	Long	Displ.	32.4	-32.4	0.540	triang.	400	3
10	Drift #10	D10	Long	Displ.	40.5	-40.5	0.675	triang.	400	3

Figure 159, Figure 160 and Figure 161 show a schematic of test setup and instrumentation used for walls with and without openings. In particular, Figure 159 presents the setup used for Specimen 01, 02, 03 and 04, while Figure 160 and Figure 161 sketch those considered for walls presenting windows and doors, respectively. To define the experimental setup, particular care was paid to the beams placed at the top of the specimen in order to permit a proper application and distribution of the vertical and horizontal loads. In particular, a layer of a low friction material (i.e. teflon) was provided at the beam-to-beam interface in order to inhibit/reduce the frictional force transfer at the interface of those steel beams. This was done in order to simultaneously permit the horizontal load imposed by the actuator to be transferred and the motion in the vertical direction (i.e.

rocking/sliding of the panels) to be released. One of the main objective of this setup was to enable such a behavior/mechanism during cyclic reversals for each drift level imposed, even if it is worth noting that, in some cases, the two top beams were observed to come in contact at their edges for large levels of imposed horizontal drift. As a consequence, this undesirable mechanism may result in spurious resistance overestimates at the last cycles of the loading protocol, as discussed later on. A series of potentiometers were used to measure displacements at key locations throughout the specimen. In detail, the potentiometers were arranged to monitor displacements at different levels along the height of the panel, its flexural and shear deformations, base uplift and slippage in the concrete footing.
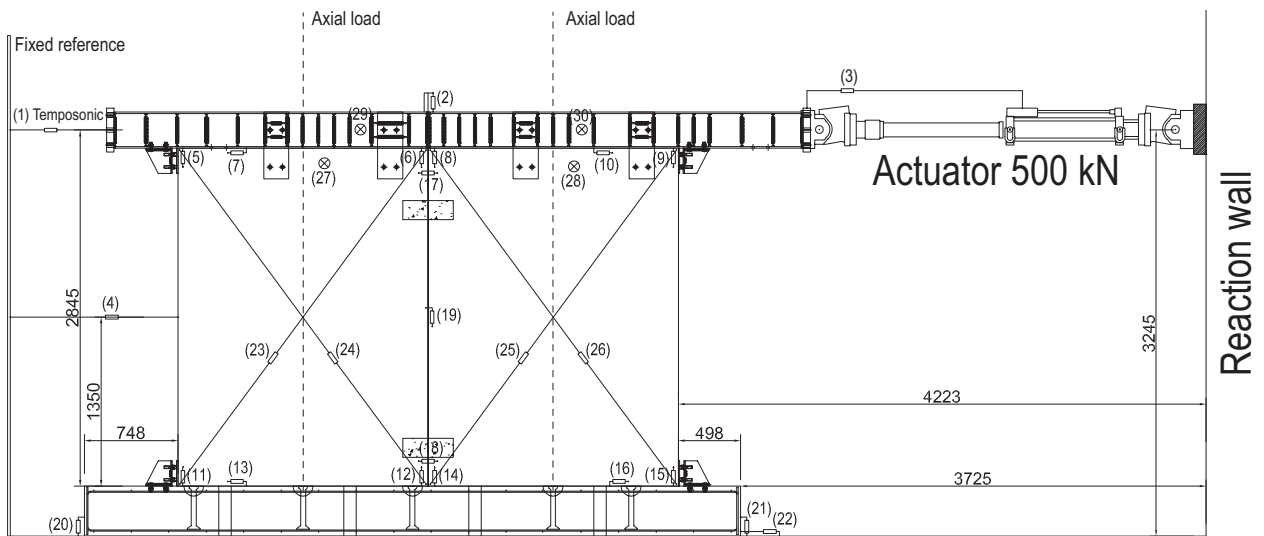
Figure 159: Experimental setup and instrumentation – Specimen 01, 02, 03 and 04
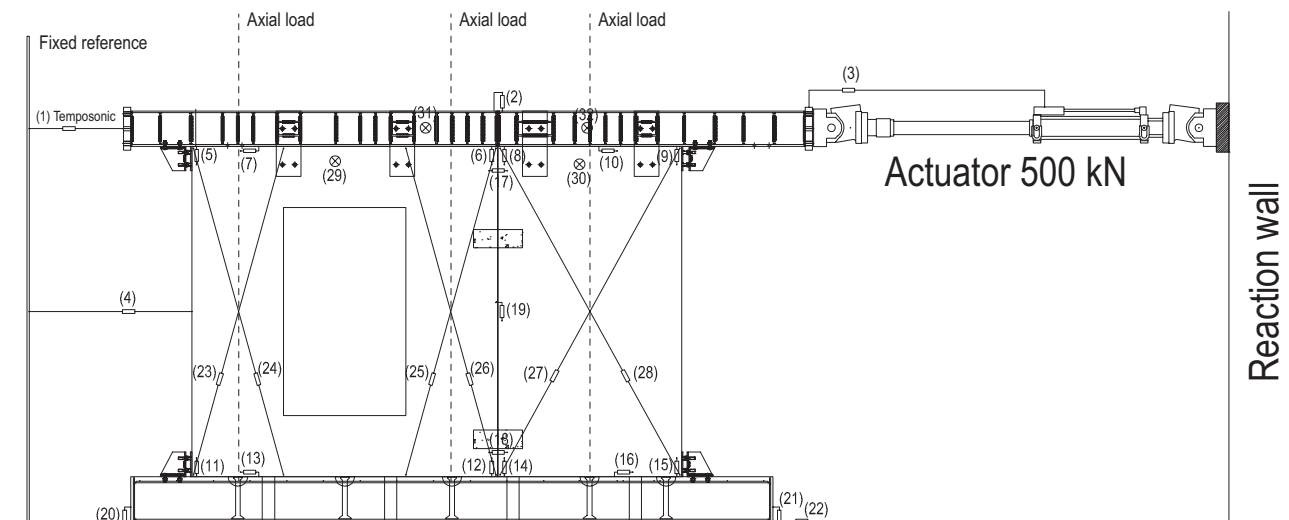
Figure 160: Experimental setup and instrumentation – Specimen 05 and 06
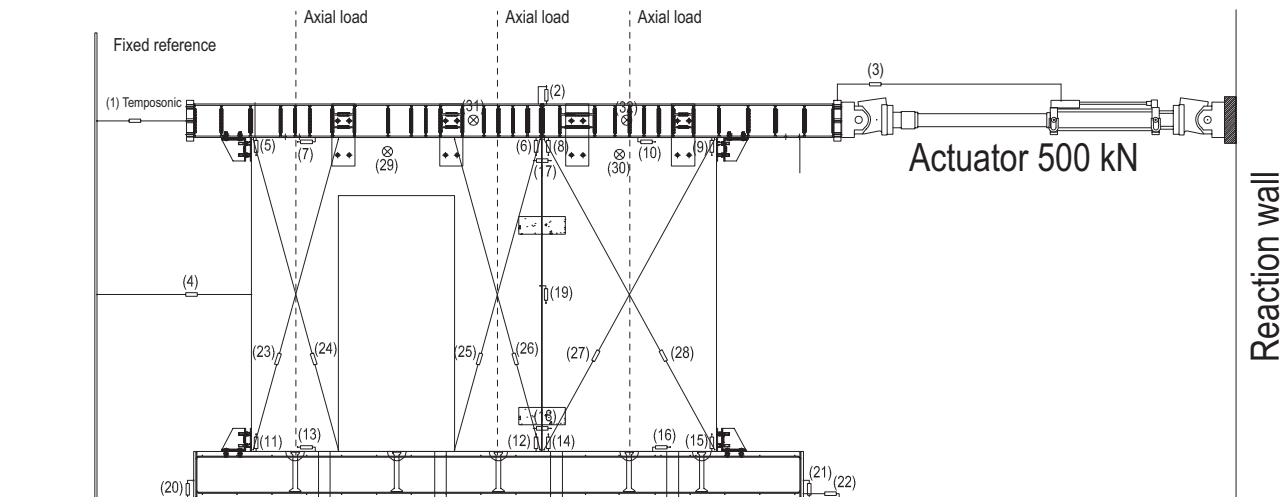
Figure 161: Experimental setup and instrumentation – Specimen 07 and 08

Once the main assumptions concerning the experimental investigation carried out were described in detail, the prevailing results obtained are collected and discussed in the following. The following paragraphs report the main results of the experimental investigation. In particular, the capacity curves, base shear-top displacement, obtained for each specimen will be given together with a series of photos presenting damage patterns. Additionally, the resisting mechanisms will be discussed.

6.2.3 Experimental results and observations

As previously mentioned, this section summarizes a detailed description of the main experimental results obtained by the 8 full-scale panel assemblies under investigation. In Figure 162 and Figure 165, the cyclic response obtained for the 20 cm thick wall specimen without openings under minimum and maximum axial load levels are shown. Similarly Figure 170 and Figure 175 present the capacity curves experimentally observed for the 12 cm thick wall assembly without any type of opening and tested under N_{min} and N_{max} respectively. In addition, the sensitivity of the seismic response to the presence of openings is addressed in Figure 182, Figure 189, Figure 196 and Figure 207. In detail, the base shear-top displacement curves obtained in case of the two specimens presenting a window (i.e. Specimen 05 and 06) are shown in Figure 182 and Figure 189, respectively. Furthermore, Figure 196 and Figure 207 show the response of Specimen 07 and 08, respectively.

To investigate the influence of the vertical load on the seismic behaviour, the capacity curves obtained for tests on panels with the same geometry but different vertical load levels are directly compared in Figure 216, Figure 217, Figure 218 and Figure 219. In particular, Figure 216 compares the behaviour of specimen 01 and 02, while a comparison between the responses of specimen 03 and 04 is provided in Figure 217. Furthermore, Figure 218 and Figure 219 highlight the sensitivity of seismic response to the axial load in case of panels presenting a window and a door, respectively.
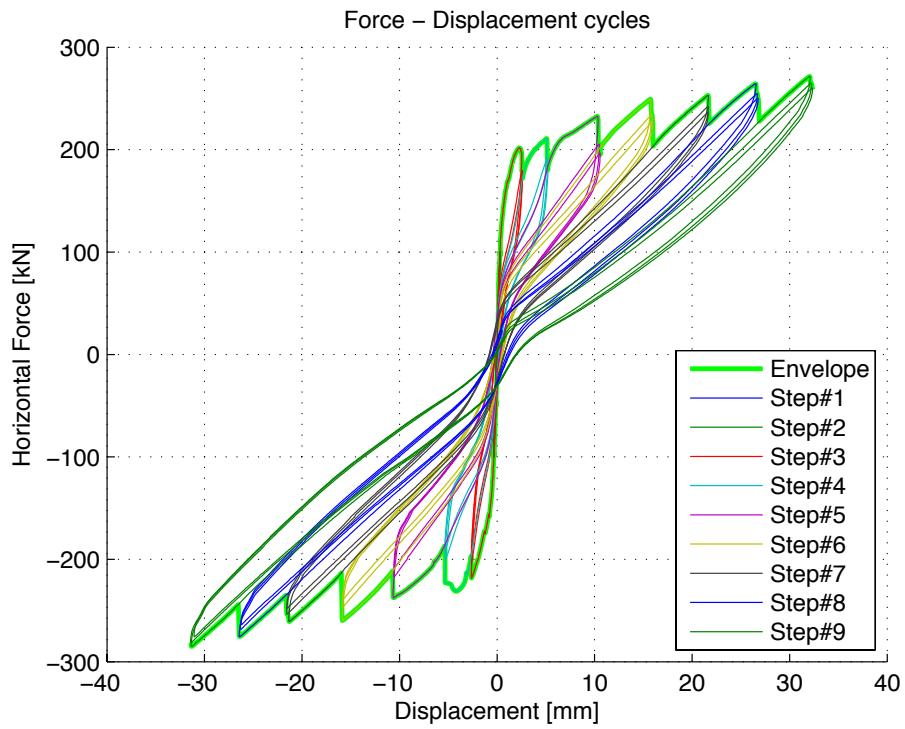
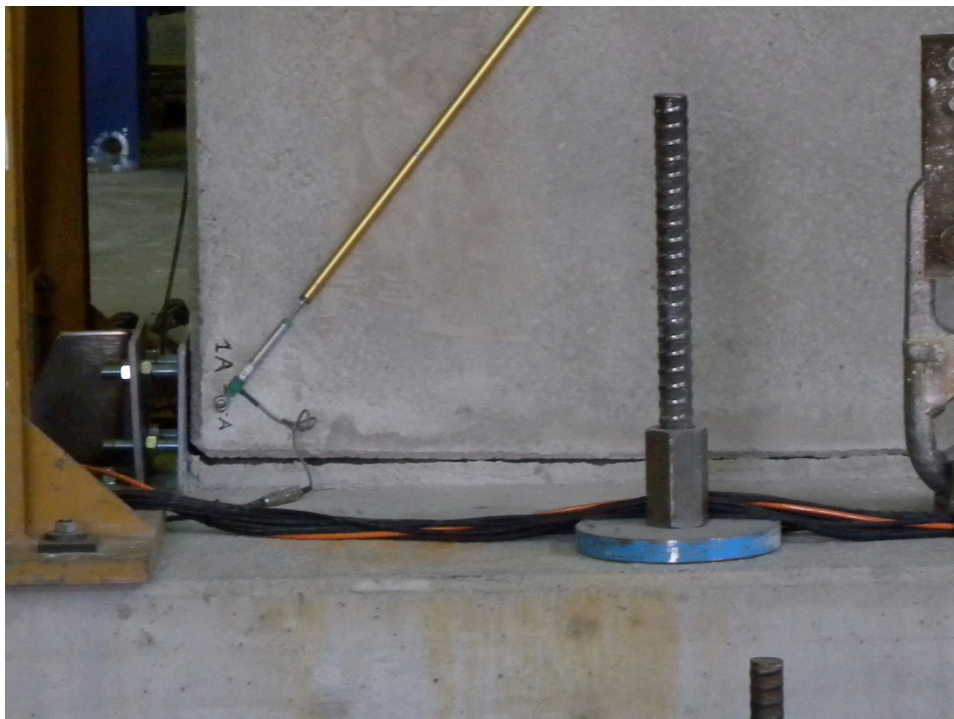**Figure 162: Specimen 01 – base shear vs. top displacement curves**

Figure 163: Crack induced by panel uplift and rocking mechanism – Specimen 01

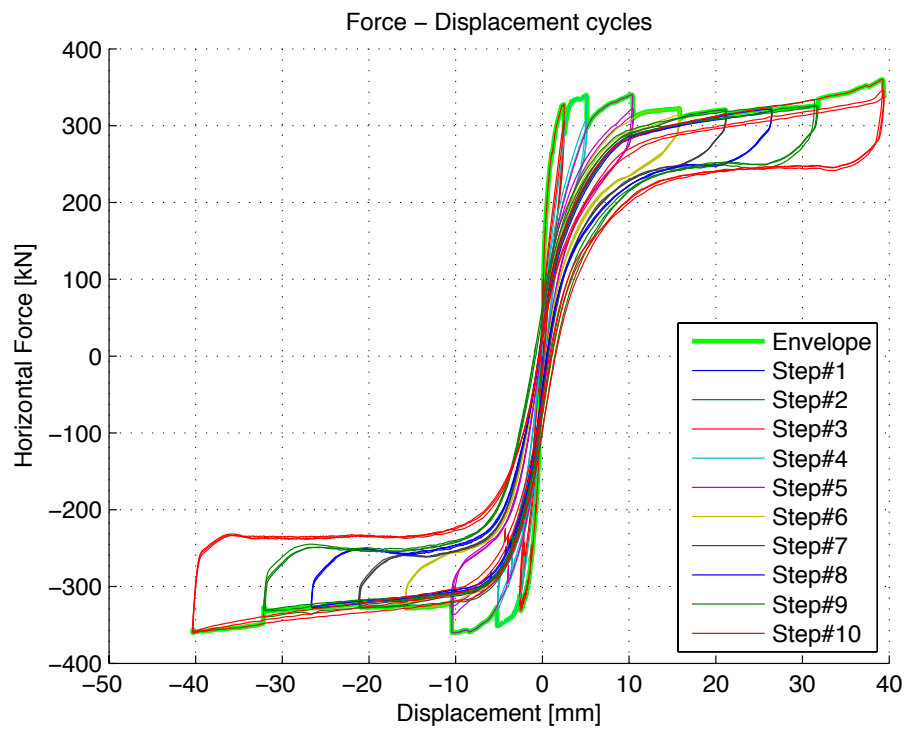**Figure 164: Damage pattern of the connection systems – Specimen 01**

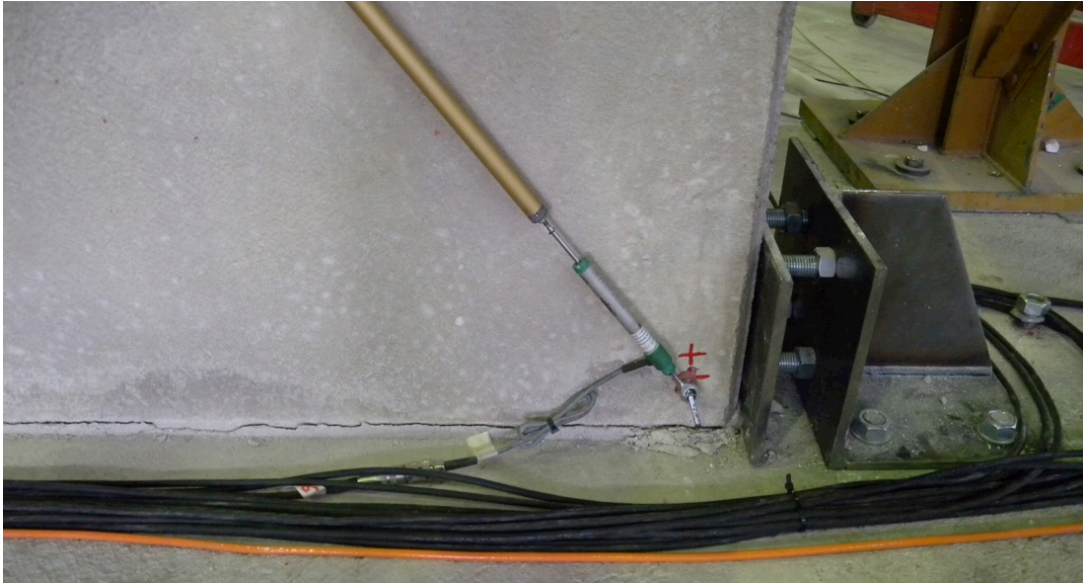**Figure 165: Specimen 02 – base shear vs. top displacement curves**

Figure 166: Crack induced by panel uplift and rocking at the base – Specimen 02

Figure 167: Damage mechanism of concrete and anchors in the connection – Specimen 02

Figure 168: Crack pattern at the base of the wall – Specimen 02
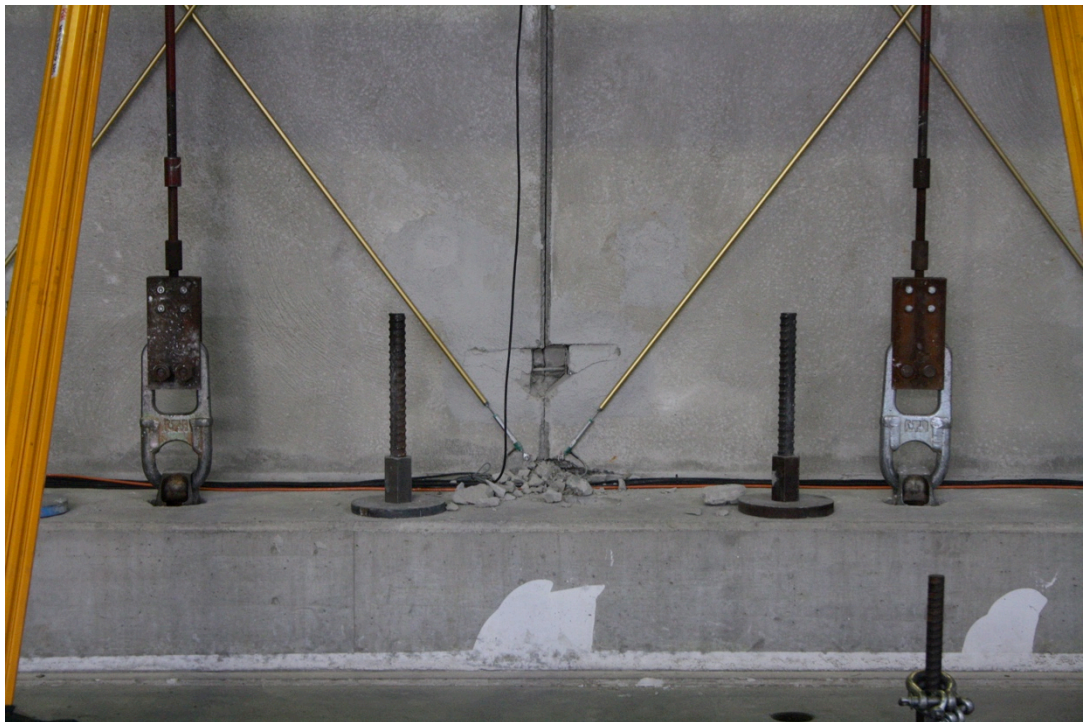
Figure 169: Damage mechanism of shear resistant connection at the bottom – Specimen 02
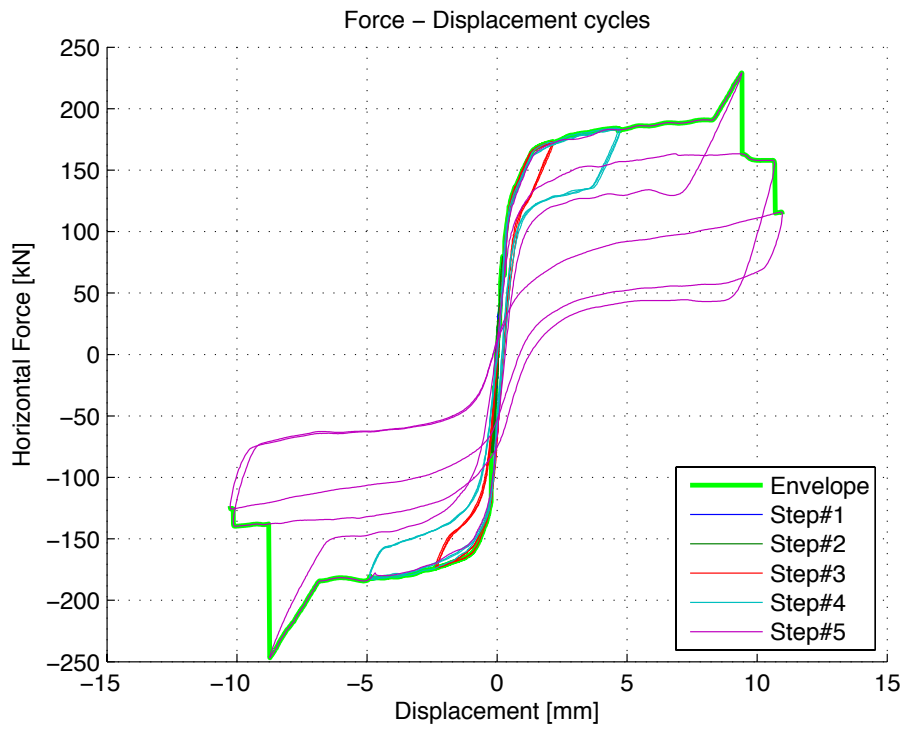
Figure 170: Specimen 03 – base shear vs. top displacement curves

Figure 171: Damage of mortar at the panel anchor location– Specimen 03

Figure 172: Rocking and base uplift at mid-panel assembly – Specimen 03

Figure 173: Crack at the corner of the panel due to rocking and base uplift– Specimen 03
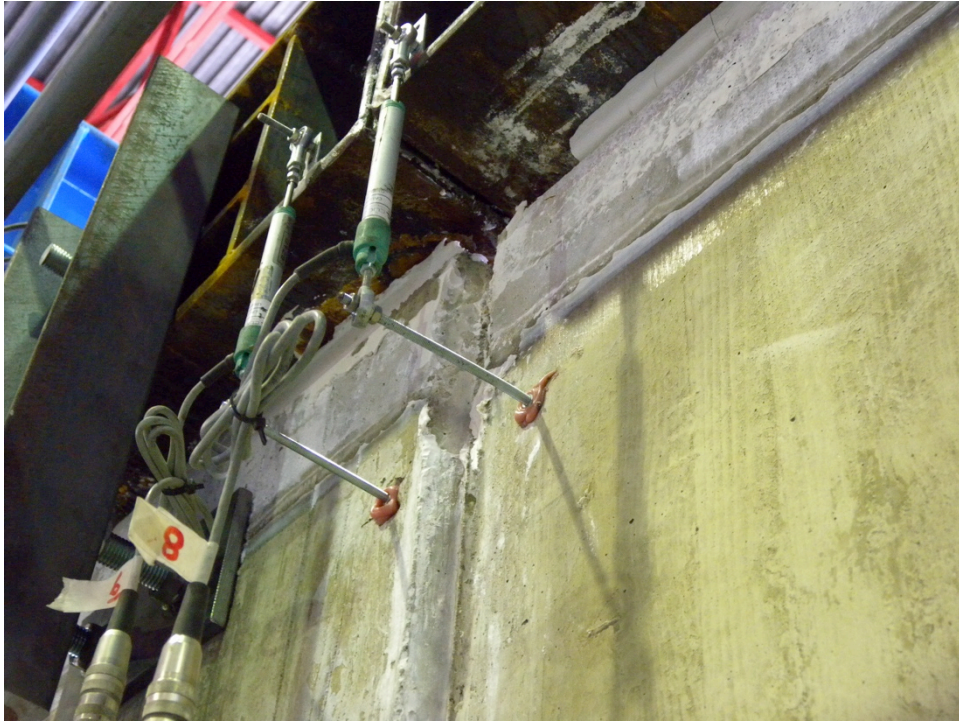
Figure 174: Out-of-plane misalignment between the two panels at the end of the test– Specimen 03
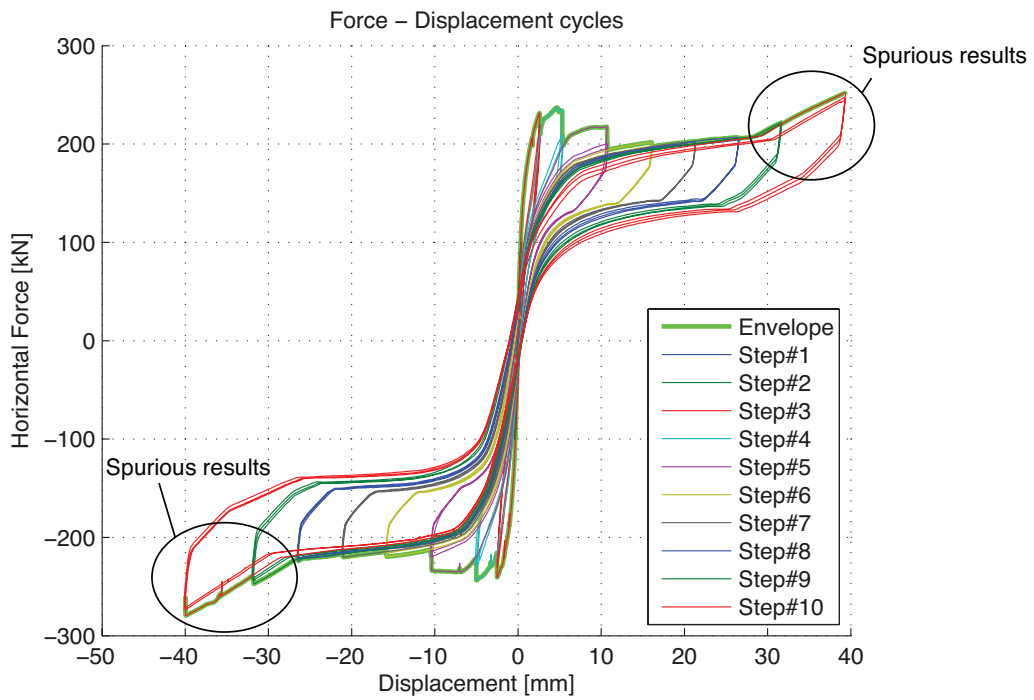
Figure 175: Specimen 04 – base shear vs. top displacement curves

po

Figure 176: Vertical displacement due to rocking mechanism of Specimen 04 – detail at the top of the assembly
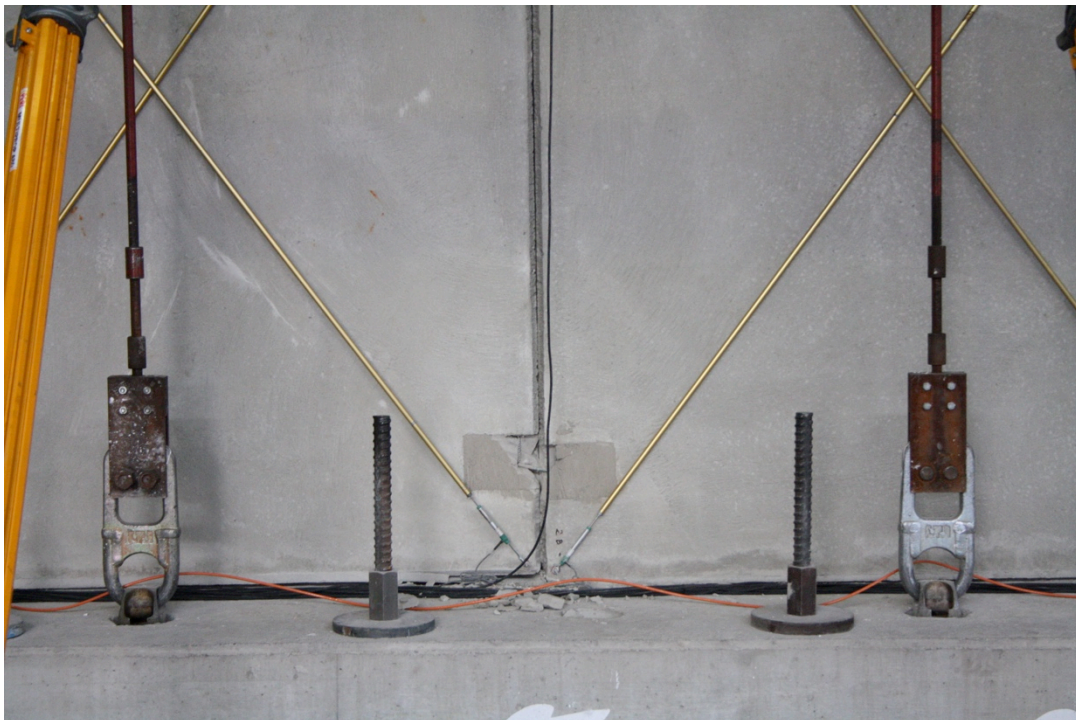
Figure 177: Vertical displacement due to rocking mechanism of Specimen 04 – detail at the bottom of the assembly

Figure 178: Rocking behaviour and base uplift at the corner of the panel – Specimen 04

Figure 179: Damage mode at the base steel anchor location – Specimen 04

Figure 180: Concrete spalling at the base of the wall – Specimen 04

Figure 181: Failure of the anchors – Specimen 04
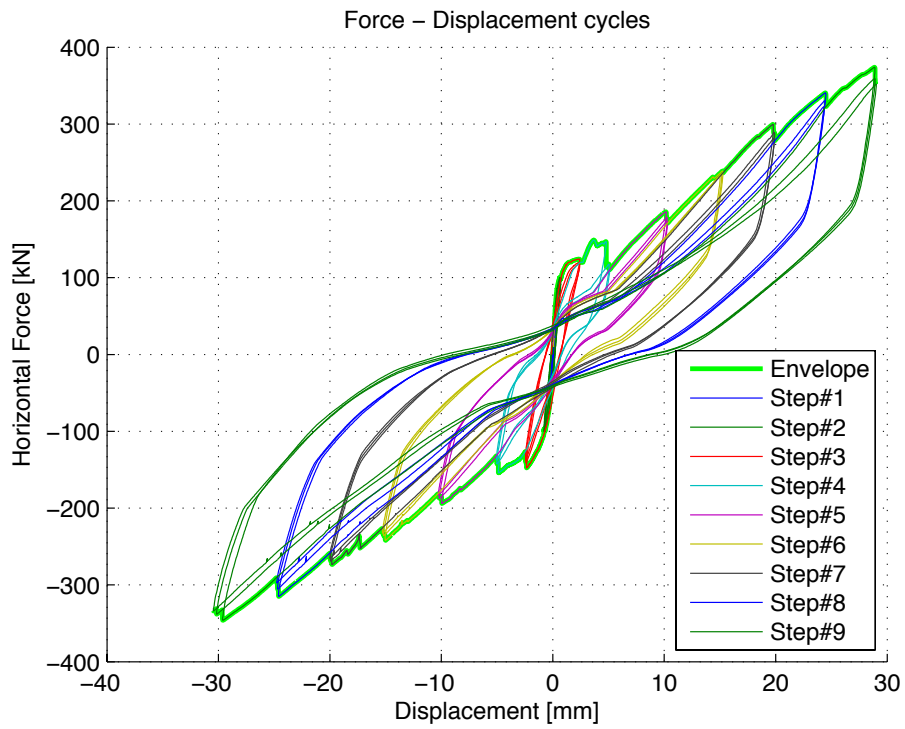
Figure 182: Specimen 05 – base shear vs. top displacement curves

Figure 183: Deformed shape at the end of the test – Specimen 05

Figure 184: Crack pattern at the corners of the window – Specimen 05

Figure 185: Cracking at the corners of the window in Specimen 05 – detail of the bottom left side

Figure 186: Cracking at the corners of the window in Specimen 05 – detail of the bottom right side
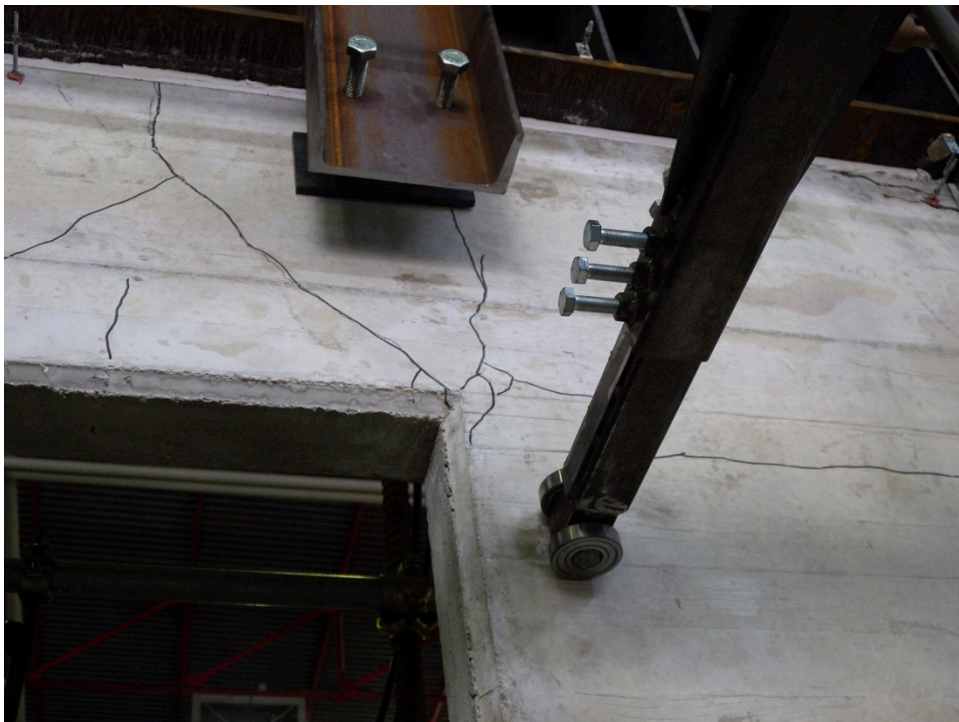

Figure 187: Cracking at the corners of the window in Specimen 05 – detail of the top right side

Figure 188: Cracking at the corners of the window in Specimen 05 – detail of the top left side
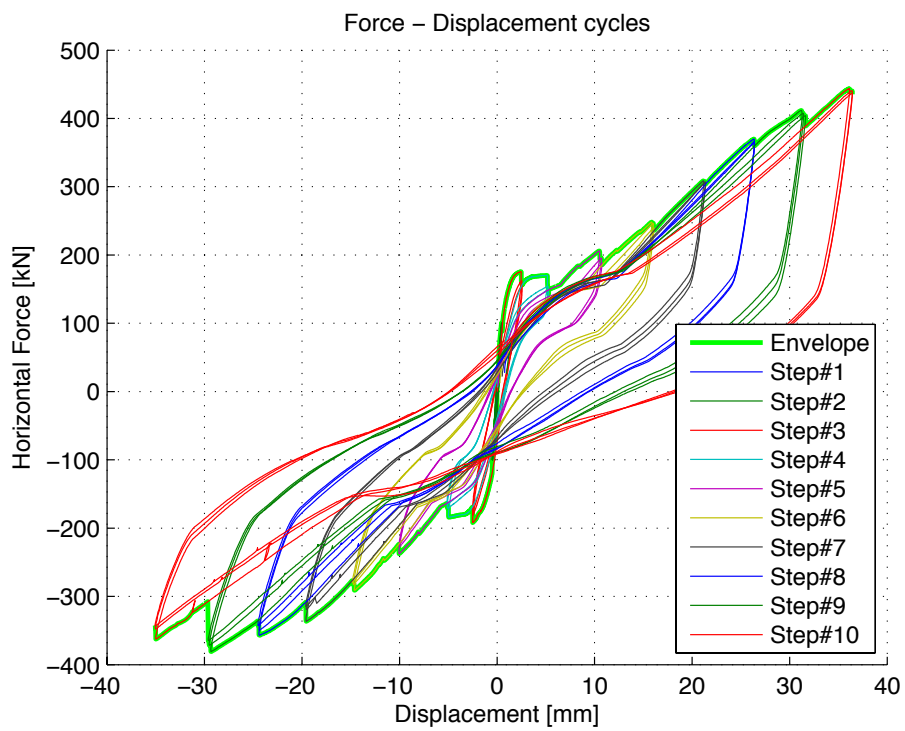

Figure 189: Specimen 06 – base shear vs. top displacement curves
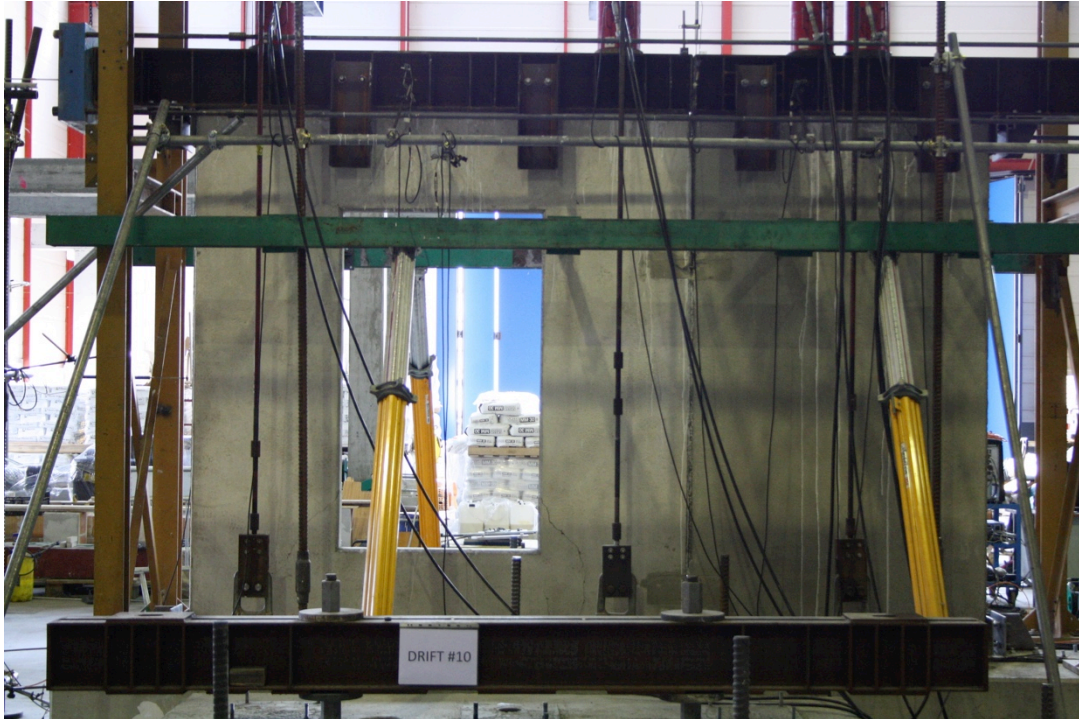
Figure 190: Deformed shape at the end of the test – Specimen 06

Figure 191: Cracking at the corners of the window at the end of the test – Specimen 06

Figure 192: Crack pattern at the corners of the window and buckling of longitudinal bars – Specimen 06

Figure 193: Cracking at the corners of the window in Specimen 06 – detail of the bottom left and right sides

Figure 194: Vertical cracks at the top of the window – Specimen 06

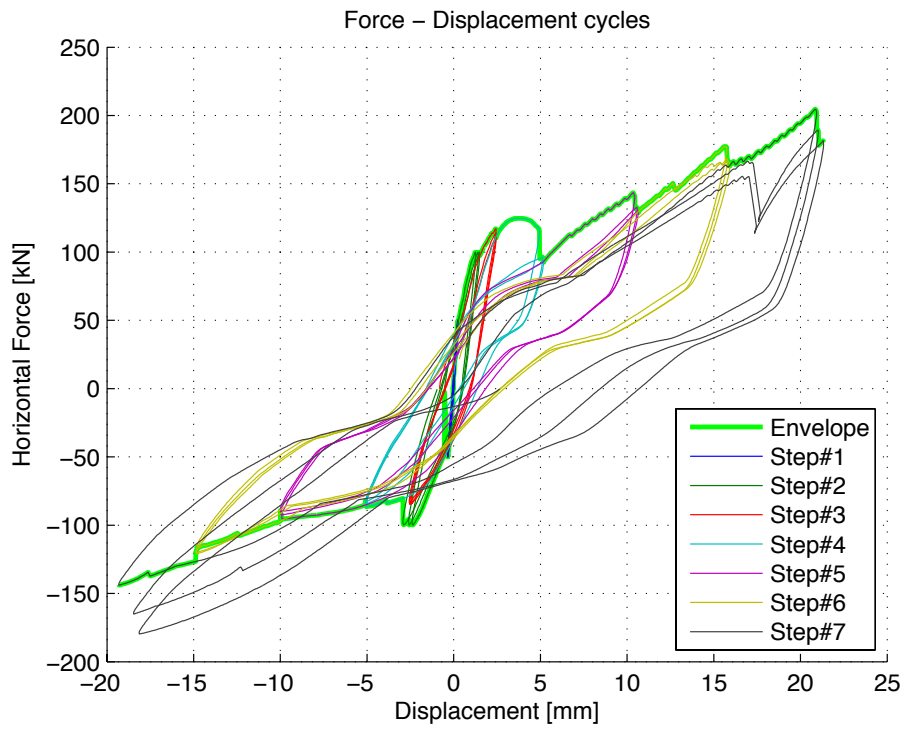**Figure 195: Out-of-plane misalignment and failure of the anchors – Specimen 06**

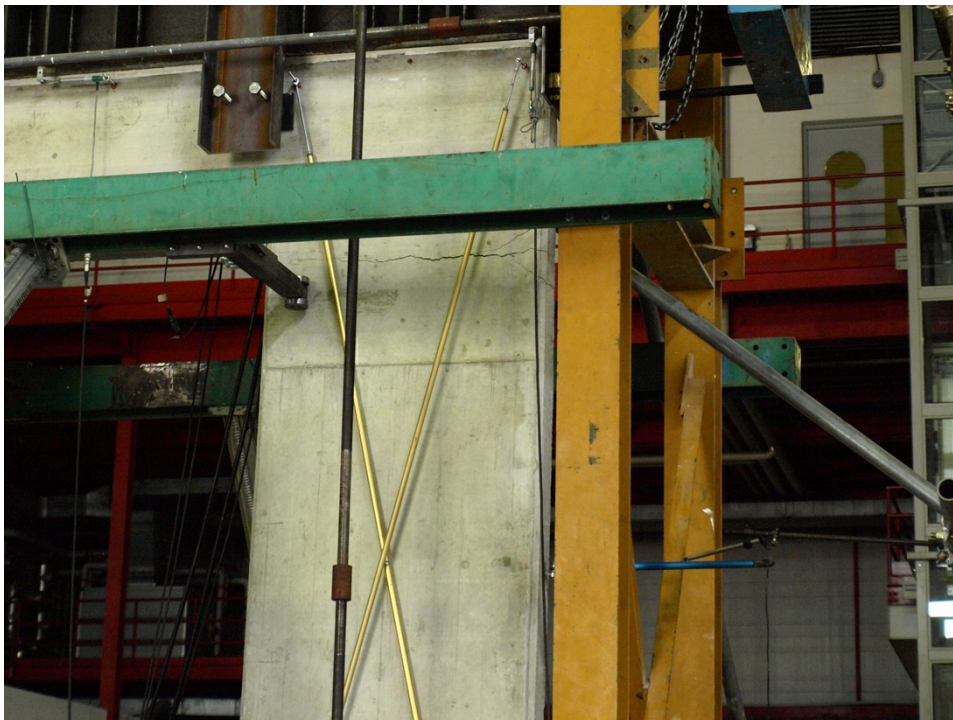**Figure 196: Specimen 07 – base shear vs. top displacement curves**

Figure 197: Incipient horizontal cracks at the corner of the door – Specimen 07
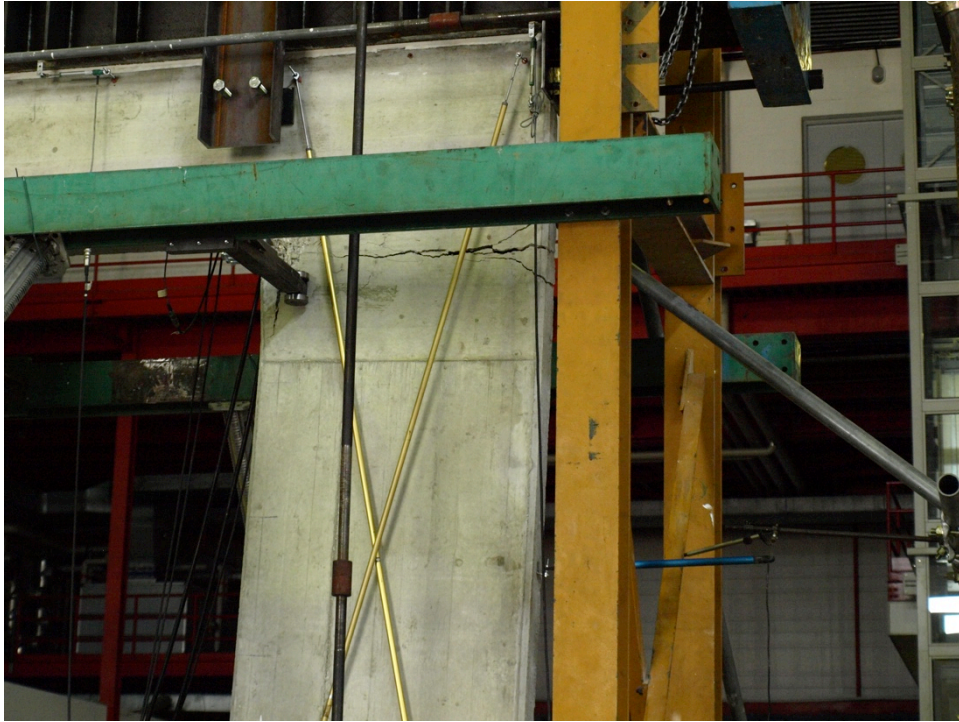
Figure 198: Propagation of horizontal cracks at the corner of the door – Specimen 07

Figure 199: Deformed shape at the end of the test – Specimen 07

Figure 200: Failure of the anchors and detaching of the two panels – Specimen 07

Figure 201: Concrete crushing and spalling at the base of the wall – Specimen 07

Figure 202: Detail of the anchors failure – Specimen 07

Figure 203: Crack and gap opening at the top connection – Specimen 07

Figure 204: Side view of the horizontal crack at the top of the door – Specimen 07

Figure 205: Pounding between the two panels of the assembly – Specimen 07

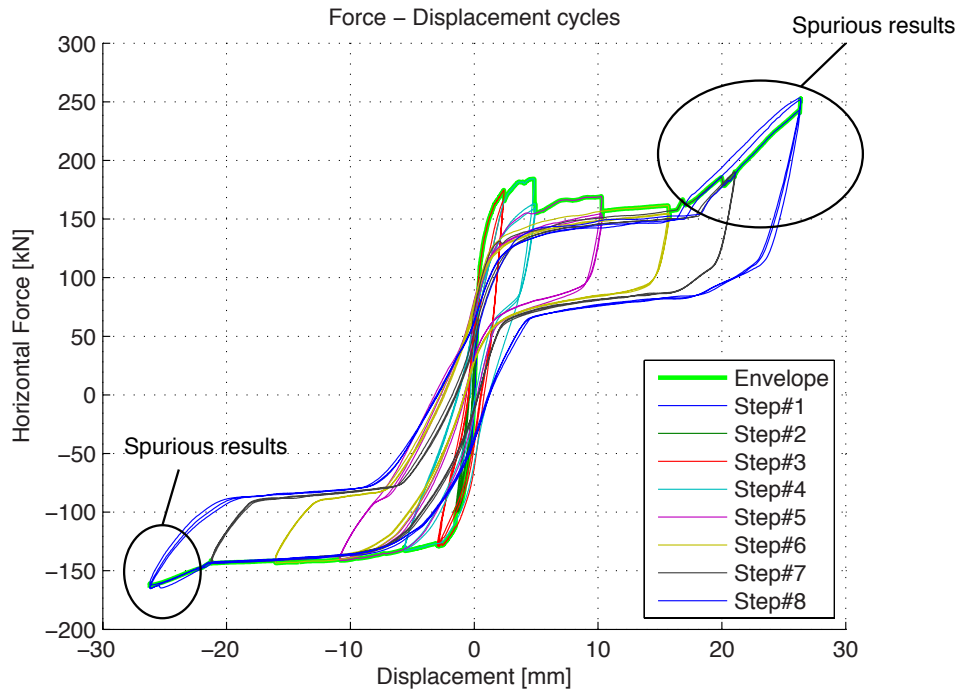**Figure 206: Concrete crushing and buckling of longitudinal bars – Specimen 07**

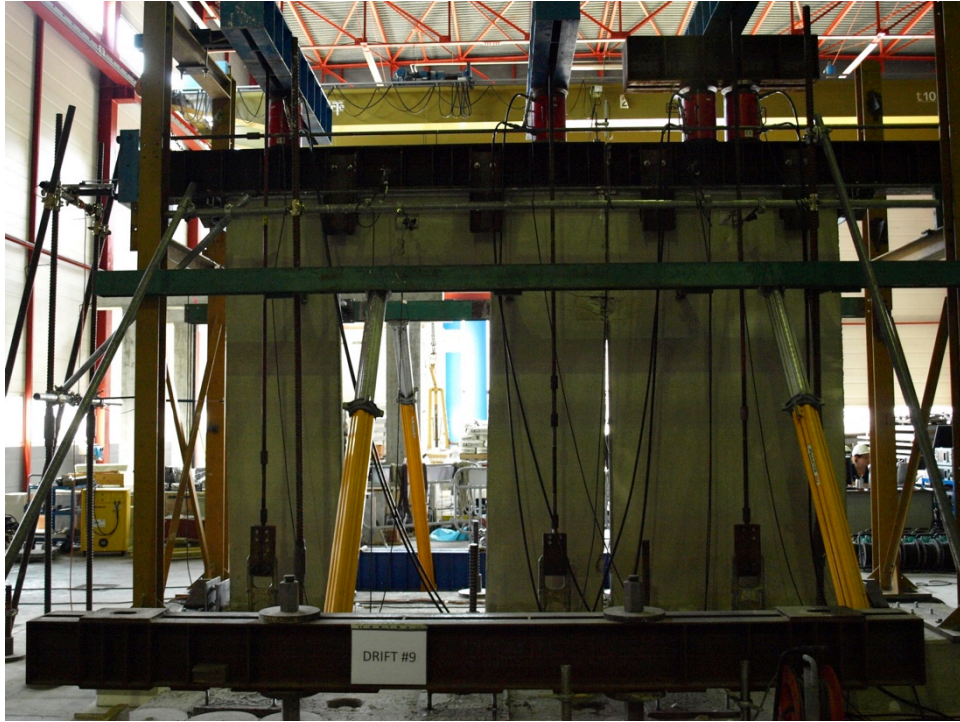**Figure 207: Specimen 08 – base shear vs. roof displacement curves**

Figure 208: Deformed shape of Specimen 08 at the end of the test – detaching of the panels

Figure 209: Rocking and base uplift at the corner of the wall – Specimen 08

Figure 210: Base uplift in Specimen 08 – detail of the propagation along the entire pier

Figure 211: Base uplift along the entire pier of Specimen 08 – opposite side

Figure 212: Horizontal cracks at the corner of the door – Specimen 08

Figure 213: Detaching and pounding at the top and bottom connections – Specimen 08

Figure 214: Failure of the anchors – detail of the connection at the bottom of Specimen 08

Figure 215: Failure of the anchors – detail of the connection at the top of Specimen 08
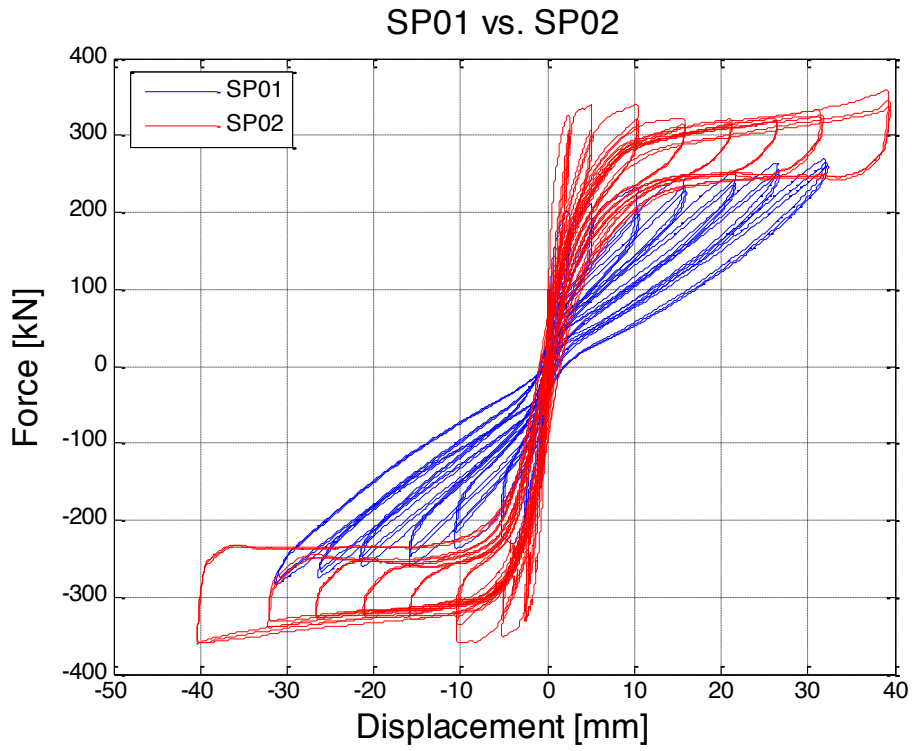
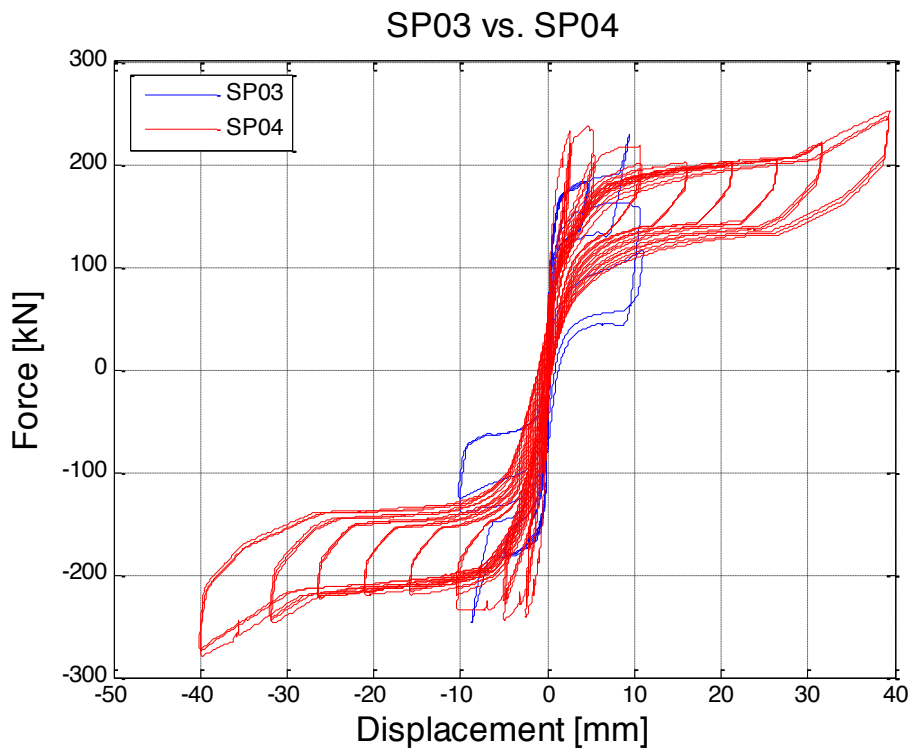**Figure 216: Specimen 01 vs. Specimen 02 – influence of axial load**

Figure 217: Specimen 03 vs. Specimen 04 – sensitivity to axial load
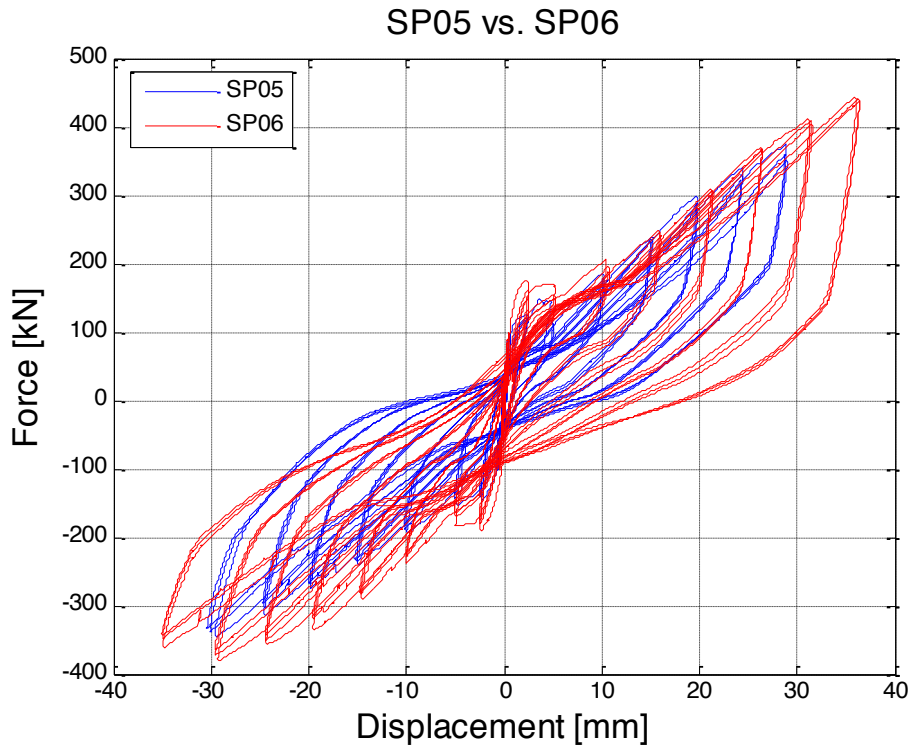
Figure 218: Specimen 05 vs. Specimen 06 – effect of changes in the axial load
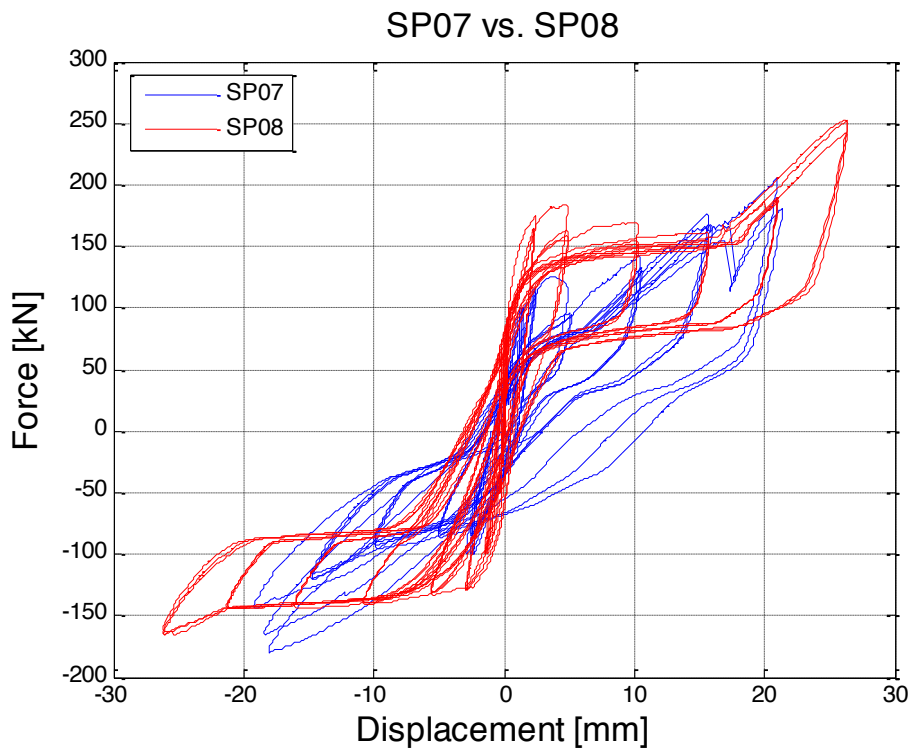

Figure 219: Specimen 07 vs. Specimen 08 – sensitivity to variations in the axial load level

In the framework of this experimental investigation, failure of the test specimens was identified according to three performance criteria that were distinctly defined either at global or local levels:

1. first exceedance of a conventionally fixed drift limit (i.e. 1.5%);
2. first attainment of a conventionally fixed decrease in load bearing capacity (i.e. 20%);
3. first shear-buckling fracture of a mechanical connector in the panel-to-panel joints.

The first occurrence of one of the three ultimate conditions listed above was thus interpreted as a conservative check of the "near collapse" limit state for the panel prototypes under consideration. As expected, all the tested specimens were observed to collapse by the premature shear failure of their connections because of kinematics that attracted unintended forces in poorly detailed joints, primarily constituted by steel dowels and mostly relying on shear friction for the horizontal load transfer between structural members. Therefore, the intrinsic lack of shear and ductility capacity shown by this type of connection system results in a local failure, which in turn implies a global-structural collapse of the tested panel assemblies. These aspects are crucial considerations that can be drawn towards the improvement of their early design, as precast walls may nowadays emulate the response of a cast-in-place construction with lapped reinforcing bars in concreted/grouted joints, or alternatively they may be designed with discrete joints that are capable of dissipating energy through ductile connections or damping devices. Thus, connections can be either (i) strengthened to ensure that the relative displacements/rotations between adjoining wall segments are minimized or (ii) rationally conceived to properly allow for displacement demand rather than to attempt strain and load levels that might be unfeasible, depending on the design target of each specific case-study.

The damage mechanisms observed during the experimental investigation are collected and discussed. As presented in Figure 32 and Figure 33, the behaviour of Specimen 01 was mostly characterized by a rocking response that resulted in panel uplift at its base and failure of the shear connection systems at bottom and top. A similar type of response can also be highlighted for Specimen 02, the prevailing modes of which are summarized in Figure 166, Figure 167, Figure 168 and Figure 169. As before, the experimental results during the last imposed target drift revealed a rocking mechanism with damage at the steel anchors location. The increase of the horizontal capacity observed in Figure 165 was ascribed to the test setup. More in detail, the rocking of the panels induced a rotation of the actuator loading line, hence the applied load measured by the load cell and reported in that figure has a vertical component resulting in a fictitious increment of the specimen lateral capacity. Furthermore, the main observations related to the behaviour of Specimen 03 are shown in Figure 40, Figure 41, Figure 42 and Figure 43. In this case, the test was interrupted due to a premature connection failure which resulted in a pronounced out-of-plane misalignment between the two panels. Figure 176, Figure 177, Figure 178, Figure 179, Figure 180 and Figure 181 point out peculiar aspects of Specimen 04. Even in this case the load picking up recorded in the last steps of this test (see Figure 175) was attributable to an undesirable mechanism which involved the global behavior of the specimen. The failure mechanisms of the steel anchors in combination with moderate concrete spalling/crushing at the base of the walls are the prevailing observations for this assembly.

It can be noted that similar damage modes were collected during the cyclic tests of Specimen 01 and Specimen 02. A visible horizontal crack took place at the base of the wall due to panel uplift and propagated along the depth of each wall segment as a consequence of rocking mechanism, which in turn caused damage of concrete and anchor rods in the top and bottom panel-to-panel

joints. Despite this, such a resisting mechanism, in which joints were reaffirmed to be the weakest link of the system, resulted in fairly symmetric hysteresis loops that were different in shape and character, particularly for post-yielding and unloading regimes of the response. Specimen 01 shows an early yielding followed by a post-yield branch of steep slope, while Specimen 02 presents a flag-shape cyclic curve with larger yield forces and smaller post-yield slopes. This unexpected response was attributed to the unintentional axial load applied to Specimen 01 after 0.2% drift cycles. The axial force did not remain constant during the cycle, in the sense that the peak load planned was reached but this happened gradually during the load step. The problem with the experimental setup was then fixed in order to carry out the rest of the experimental investigation (Specimens 02 to 07).

Therefore, it is worth mentioning that no specific trends can be derived regarding the sensitivity to changes in the axial load that was observed for 200 mm thick panels, as the comparison shown in Figure 216 is affected by the unintended vertical forces applied during the test of Specimen 01. Considering 120 mm thick panels, specimen 04 resisted peak horizontal loads 25-28% higher than those obtained for specimen 03 at the same level of lateral drifts. As highlighted in Figure 217, the evaluation of behavioral changes is limited to the small displacement range because of the premature global collapse of specimen 03 at 0.4% drift cycles. In this range, similar effects/trends can be observed in case of specimens having an opening in their layout, as shown in Figure 218 and Figure 219. A discrepancy in the range 25-29% was indeed determined by comparing Specimen 05 and Specimen 06, and the comparison between Specimen 07 and Specimen 08 resulted in a similar mismatch of 27-30%. Different considerations can be drawn at larger drift amplitudes, as in both cases a difference of about 10% can be computed in terms of peak horizontal force. Thus, it can be noticed that a variation in the imposed axial load causes a difference of about 25-30% in the small displacement range, regardless of the presence of an opening. The comparison between walls with a window (i.e. Specimen 05 versus 06) and walls with a door (i.e. Specimen 07 versus 08) leads to similar results, regardless of the drift range considered. A similar difference was indeed observed for the small drift range (i.e. approximately 25-30%) and for larger drift levels (i.e. roughly 10%).

In Figure 52, Figure 53, Figure 54, Figure 55, Figure 56 and Figure 57, the damage pattern obtained at the end of the test for Specimen 05 are presented. Its base shear vs. top displacement capacity curve shown in Figure 182 reveals a cyclic response characterized by significant hardening. The cracks developed and propagated at the four corners of the window confirmed that a resisting mechanism other than that observed for walls without openings took place in this case. A similar type of response and resisting mechanism was also obtained for the same geometry tested under a different axial load level (i.e. Specimen 06), as collected in Figure 190, Figure 191, Figure 192, Figure 193, Figure 194 and Figure 195. In this case, concrete cracking and crushing with inherent buckling of the longitudinal bars was observed to occur mostly at the bottom left and right corners of the window. By contrast, a more complex response was obtained in case of Specimen 07 (Figure 197, Figure 198, Figure 199, Figure 200, Figure 201, Figure 202, Figure 203, Figure 204, Figure 205 and Figure 206) and Specimen 08 (Figure 208, Figure 209, Figure 210, Figure 211, Figure 212, Figure 213, Figure 214 and Figure 215). In both cases, the classical base uplift resulting from a rocking behaviour was associated with the formation and propagation of horizontal cracks at the corner of the door. In addition, the collapse of the anchors caused a visible detaching of the two panels. Significant concrete crushing at the base of the wall was also observed for Specimen 07 (i.e. Figure 201), while pounding during cyclic loading reversals was observed in case of Specimen 08 (i.e. Figure 213).

6.3 Asymmetric push-pull tests of precast connection systems

In order to detail the response of precast connection systems even further, 4 additional precast panel assemblies were constructed and tested at Eucentre laboratory. As discussed more in detail later on, the experimental investigation consisted of asymmetric push-pull tests in this case. By adopting the framework prepared for tests on full-scale panels, the following paragraphs will collect the main geometrical characteristics and reinforcement layout of this additional set of tests, as well as experimental setup and adopted loading protocol. Finally, capacity curves and damage mechanisms recorded during the experimental activity will be presented and discussed.

6.3.1 Description of precast assemblies

In Table 10, the specimen nomenclature used in the upcoming discussion is given. In addition, the prevailing geometric characteristics of precast panel assembly are collected. The set of asymmetric push-pull tests carried out were performed assuming a cantilevered static scheme, as specified in the following section.

Table 10: panel assemblies – specimen nomenclature and test characteristics

Specimen #	Specimen type	Nomenclature	Height [m]	Length [m]	Width [m]	Static scheme
09	L-20-12	NAM_AddE14-9	1.2	1	1	Cantil.
10	L-20-20	NAM_AddE14-10	1.2	1	1	Cantil.
11	L-12-20	NAM_AddE14-11	1.12	1	1	Cantil.
12	L-12-12	NAM_AddE14-12	1.2	1	1	Cantil.

Furthermore, longitudinal and transverse reinforcement arrangement of each panel used to compose the assemblies tested are summarized in the following Figure 220, Figure 221, Figure 222, Figure 223, Figure 224 and Figure 225. As shown therein, reinforcement layouts in close agreement with those assumed for the full-scale single walls tested were provided in these additional panels. In detail, Ø8 bars were used to detail Specimen 09, Specimen 10, Specimen 11 and Specimen 12.

For what concerns the mechanical properties of concrete and steel bars, further details can be found in Section 6.2 and 6.2.1, as the same type of materials used for the 8 full-scale panels is considered for the 4 precast panel assemblies under investigation in this paragraph. As mentioned in Section 6.2, concrete class C35/45 was used for all specimens, while steel type B450C was considered for what concerns both longitudinal and transverse reinforcement. A series of tensile and compressive characterization tests were conducted and their main results were collected and reported in Table 6, Table 7 and Table 8. A measure of concrete compressive strength at different concrete ageing was provided comparing the values summarized in Table 7 and Table 8.

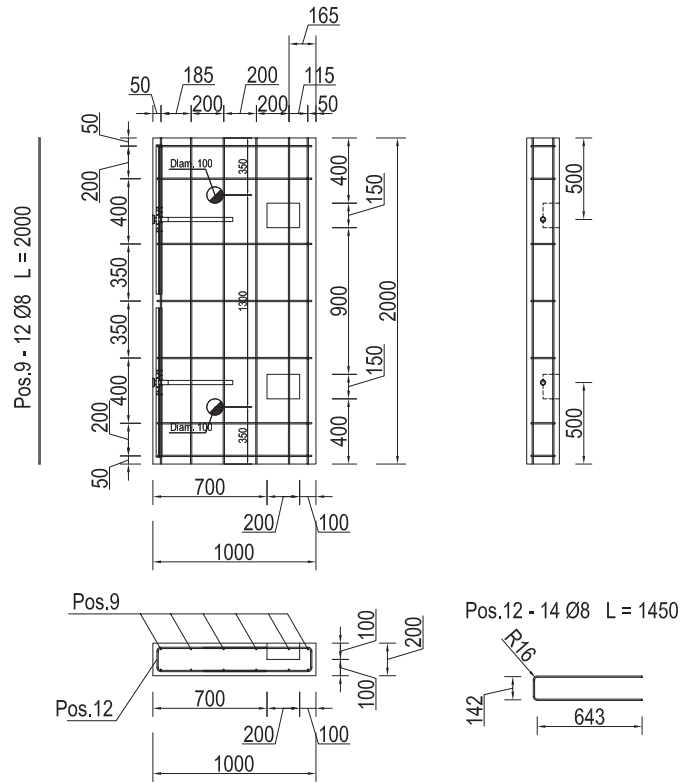Finally, Figure 226 provides a schematic of each specimen when assembled for the test.

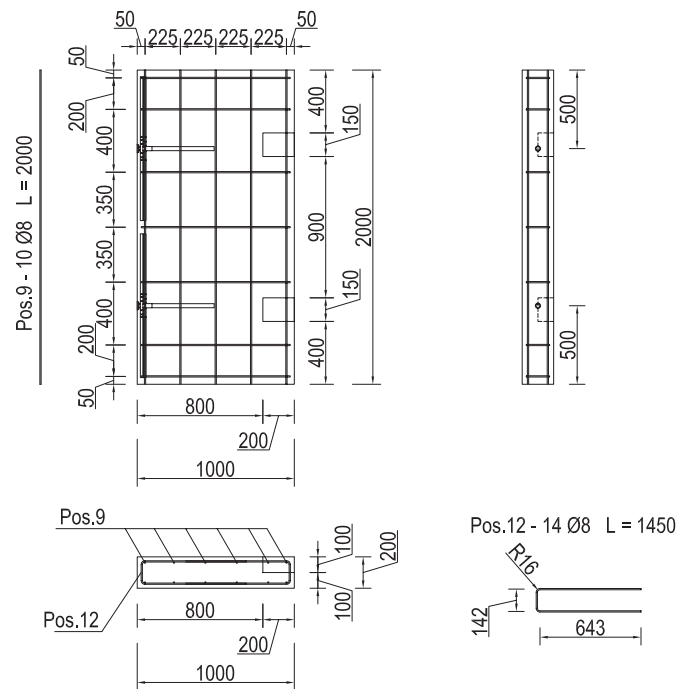**Figure 220: Component Type 5 – geometry and reinforcement layout**

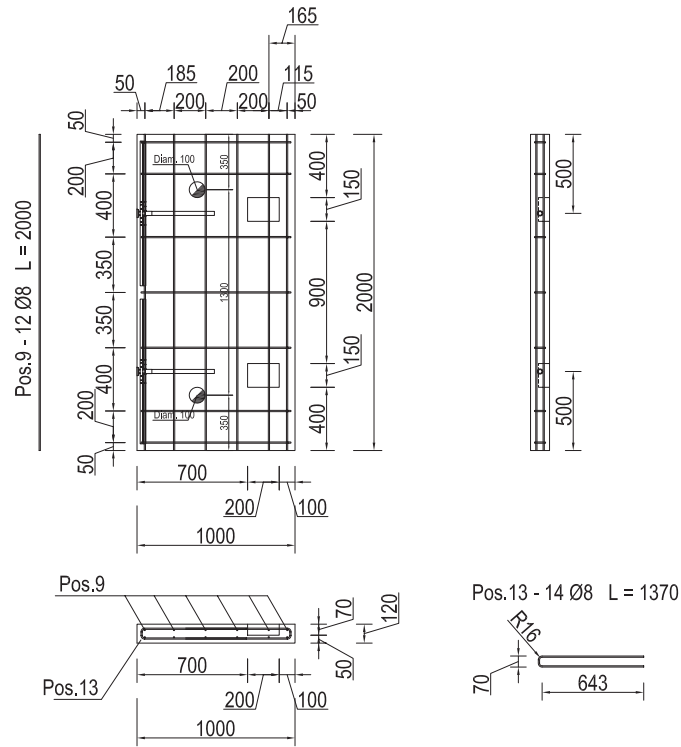**Figure 221: Component Type 6 – geometry and reinforcement layout**

Figure 222: Component Type 7 – geometry and reinforcement layout
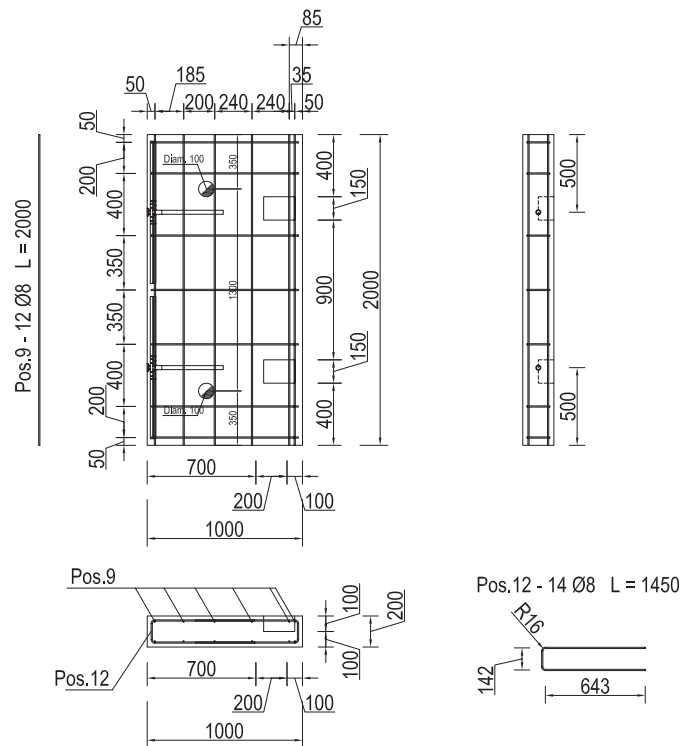

Figure 223: Component Type 8 – geometry and reinforcement layout
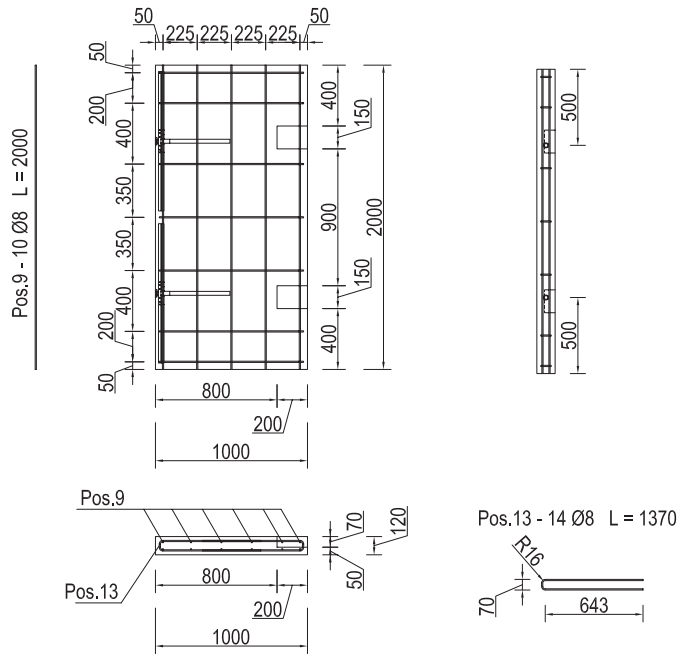
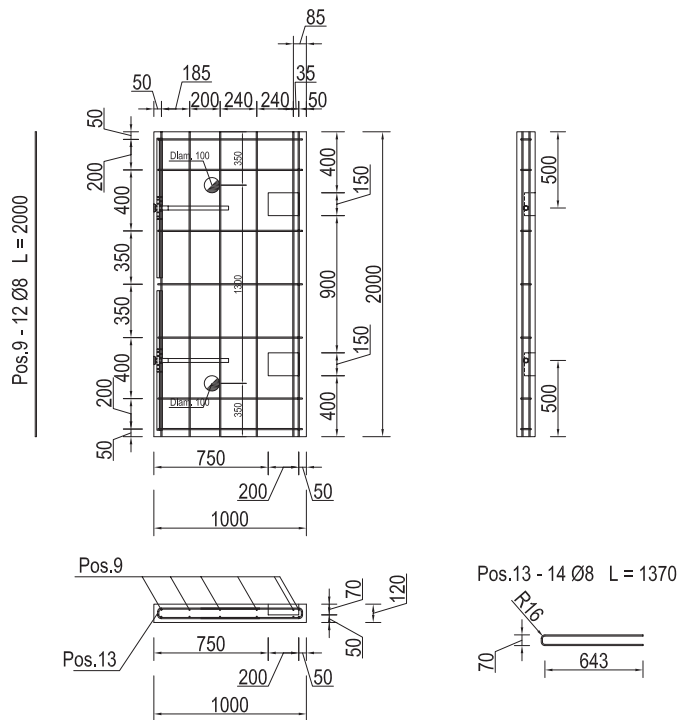**Figure 224: Component Type 9 – geometry and reinforcement layout**

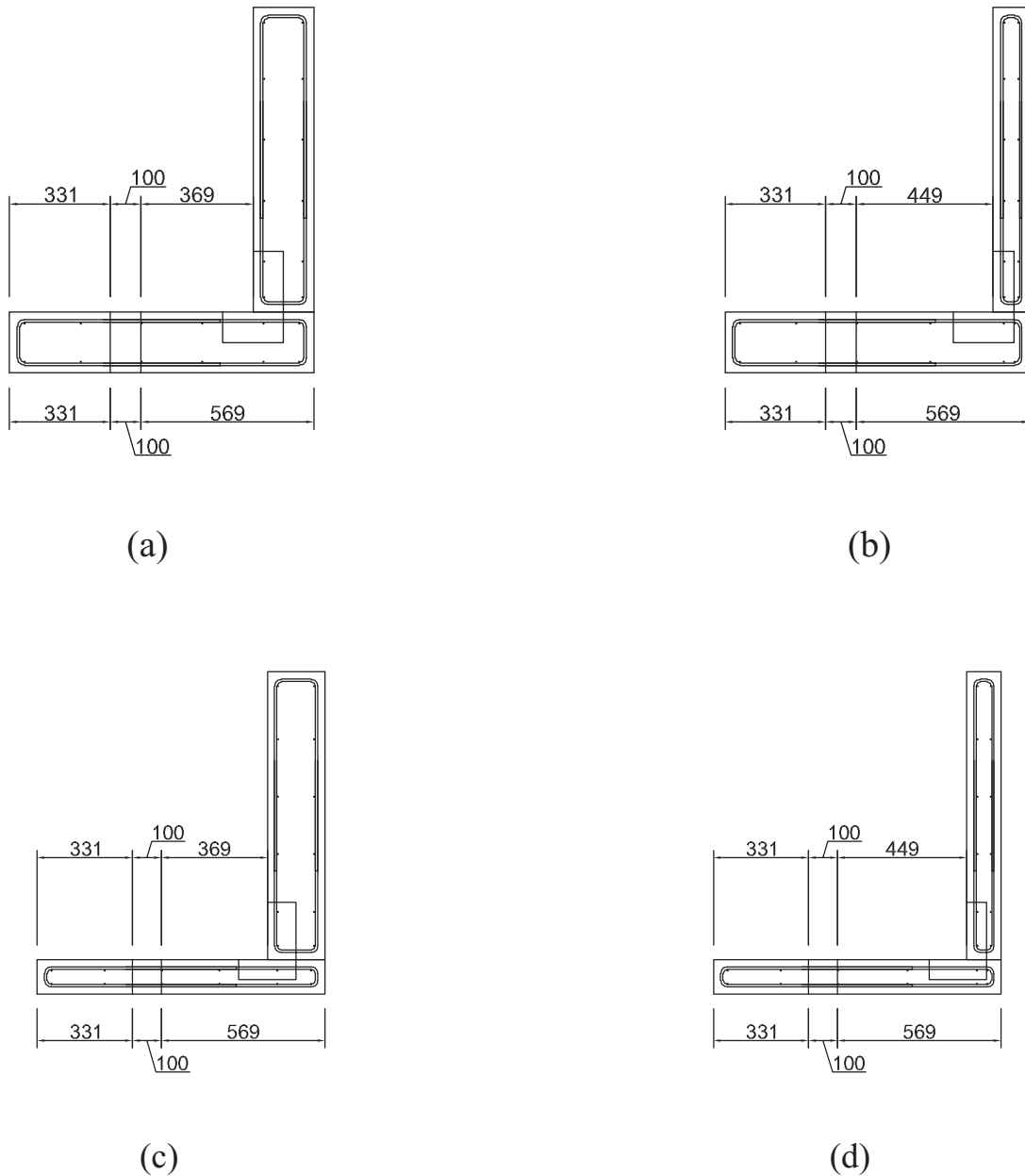**Figure 225: Component Type 10 – geometry and reinforcement layout**

Figure 226: Geometry and reinforcement layout of the assemblies tested for the assessment of connection systems. Schematic of (a) Specimen 09, (b) Specimen 10, (c) Specimen 11 and (d) Specimen 12, respectively.

6.3.2 Test setup and loading protocol

The 4 specimens were tested assuming a single bending configuration without any axial load imposed. A quasi-static cyclic drift history at increasing top displacement levels was applied by means of a horizontal MTS actuator in displacement control. In particular, the experimental loading protocol consisted of a series of asymmetric horizontal top drift targets as reported in Table 11. This table summarizes the asymmetric cyclic reversals applied Specimen 09, Specimen 10, Specimen 11 and Specimen 12. As assumed for the 8 full-scale panels, three cycles per amplitude were planned.

Figure 227 shows a schematic of test setup and instrumentation used for these 4 specimens.
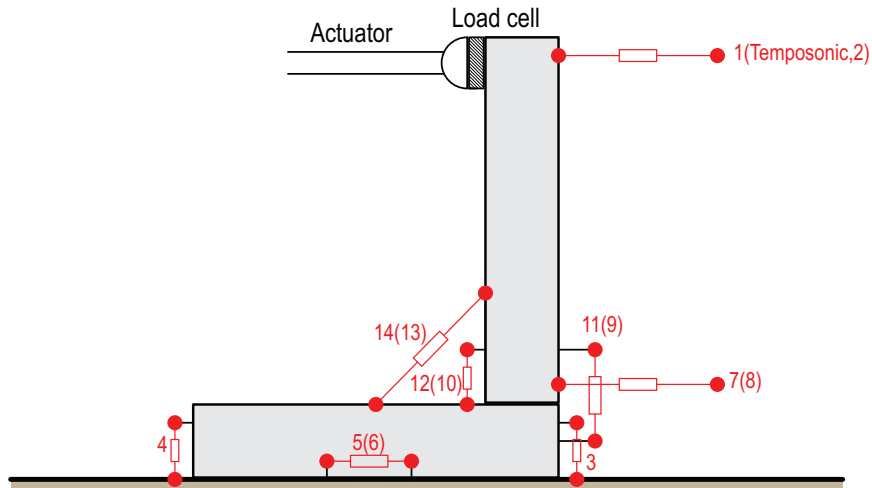
Figure 227: Experimental setup and instrumentation adopted for the set of tests on connection systems

Table 11: experimental loading protocol

Test #	Test Name	Label	Main DoF	Control Type	MAX Ampl.	MIN Ampl.	Loading Speed	Load Shape	Axial Load	Cycles
				(Force or Displ.)	[kN] [mm]	[kN] [mm]	[kN/s] [mm/s]		[kN]	[#]
0	Axial Loading	-	-	-	-	-	-	-	-	-
1	Drift #1	D1	Long	Displ.	1	0	0.025	triang.	-	3
2	Drift #2	D2	Long	Displ.	2	0	0.050	triang.	-	3
3	Drift #3	D3	Long	Displ.	4	0	0.100	triang.	-	3
4	Drift #4	D4	Long	Displ.	6	0	0.150	triang.	-	3
5	Drift #5	D5	Long	Displ.	8	0	0.150	triang.	-	3
6	Drift #6	D6	Long	Displ.	10	0	0.150	triang.	-	3
7	Drift #7	D7	Long	Displ.	15	0	0.150	triang.	-	3
8	Drift #8	D8	Long	Displ.	20	0	0.150	triang.	-	3
9	Drift #9	D9	Long	Displ.	30	0	0.150	triang.	-	3
10	Drift #10	D10	Long	Displ.	40	0	0.200	triang.	-	3
11	Drift #11	D11	Long	Displ.	50	0	0.250	triang.	-	3
12	Drift #12	D12	Long	Displ.	75	0	0.375	triang.	-	3

A series of potentiometers were used to measure absolute and relative displacement at key locations throughout the specimen. The main results obtained are collected and discussed in the following.

6.3.3 Experimental response: data collection and discussion

As done in Section 6.2.3 for the 8 full-scale walls, this paragraph synthesizes the mian observations obtained by the experimental tests performed to specifically investigate the cyclic behaviour of precast connections. In particular, the set of capacity curves recorded for each specimen are

provided hereafter (see Figure 228, Figure 233, Figure 240 and Figure 247), and a series of photos presenting damage patterns and related resisting mechanisms will be presented in the following (i.e. from Figure 229 to Figure 255).

The main aim of this data collection was to characterize the behaviour of this connection system in order to propose simplified modeling approaches capable to include their response when performing FE simulations on prototypes representative of terraced buildings used in the Dutch context.
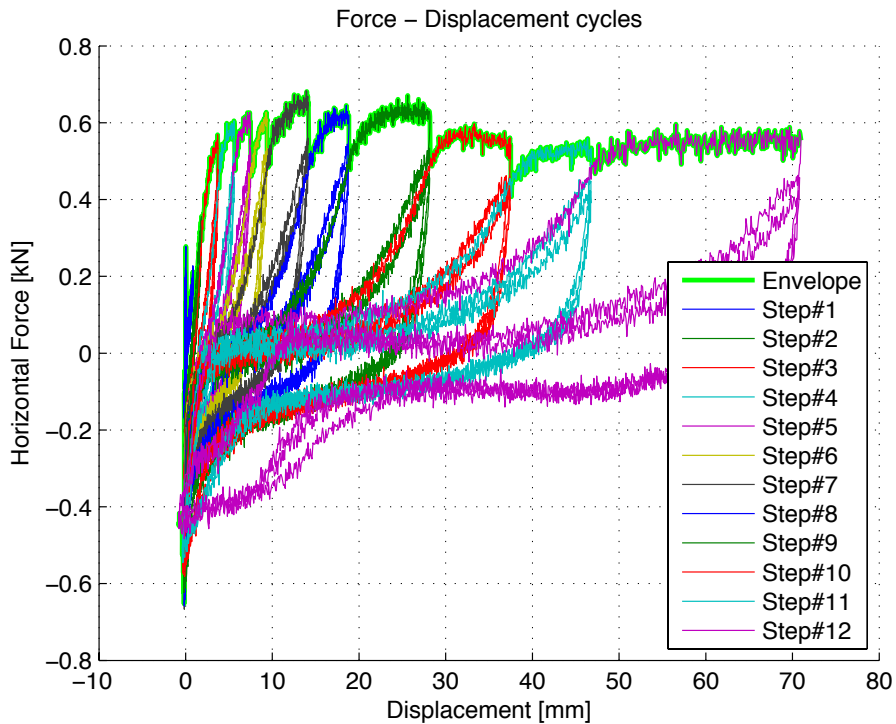

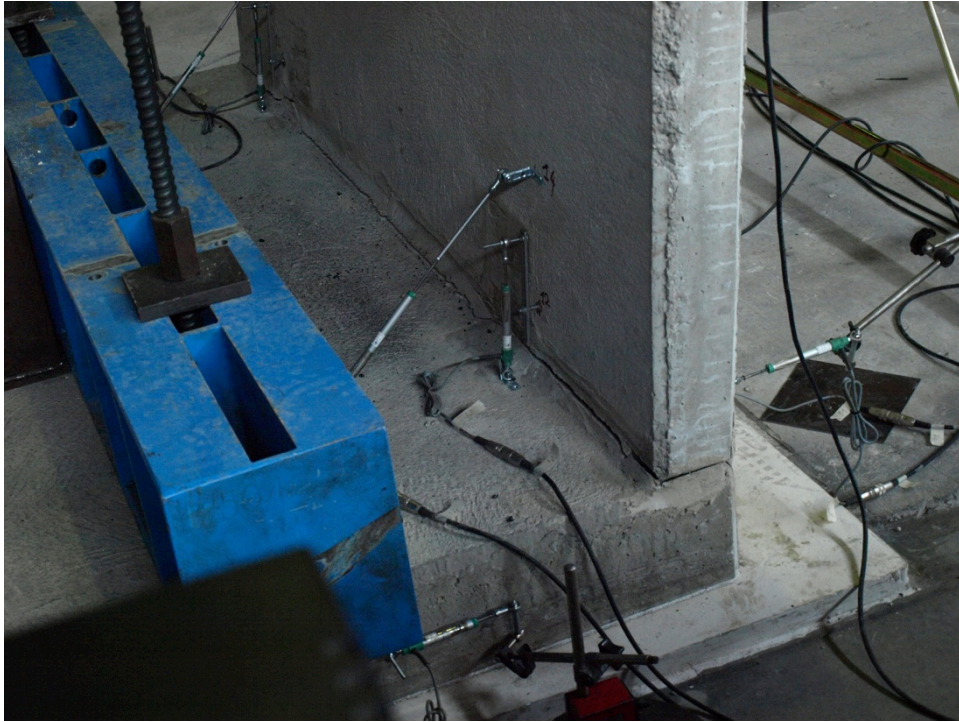**Figure 228: Specimen 09 – capacity curves**

Figure 229: Deformed shape of Specimen 09 at the end of the test – Global view

Figure 230: Rotation at the panels connection – side view of Specimen 09

Figure 231: Damage mechanism at the connection level in Specimen 09 – detail of the crack

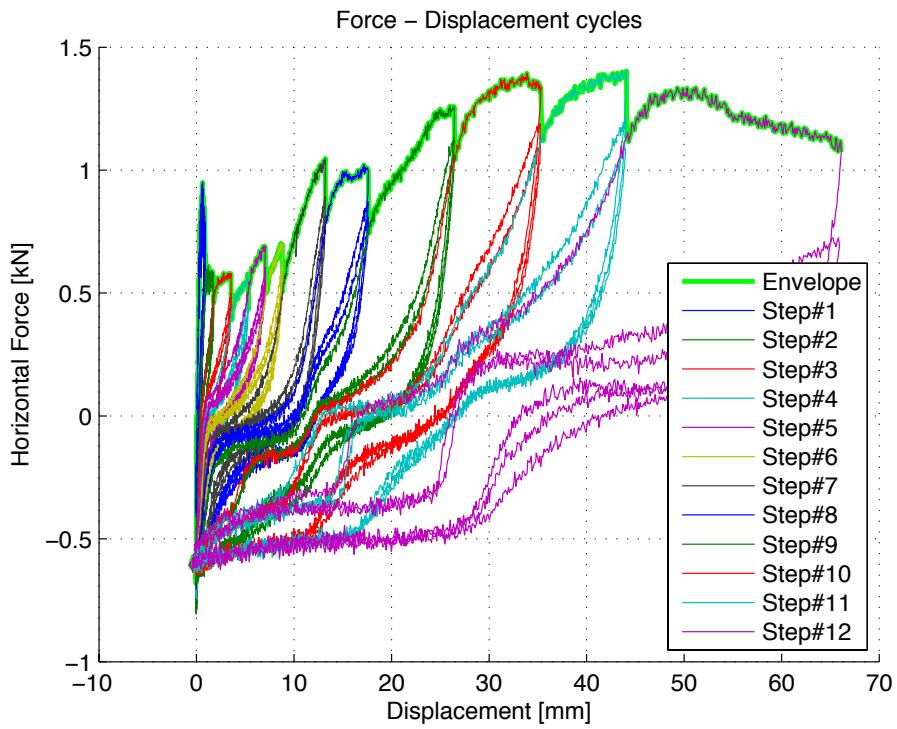**Figure 232: Detail of the mortar at the steel anchor location – Specimen 09**

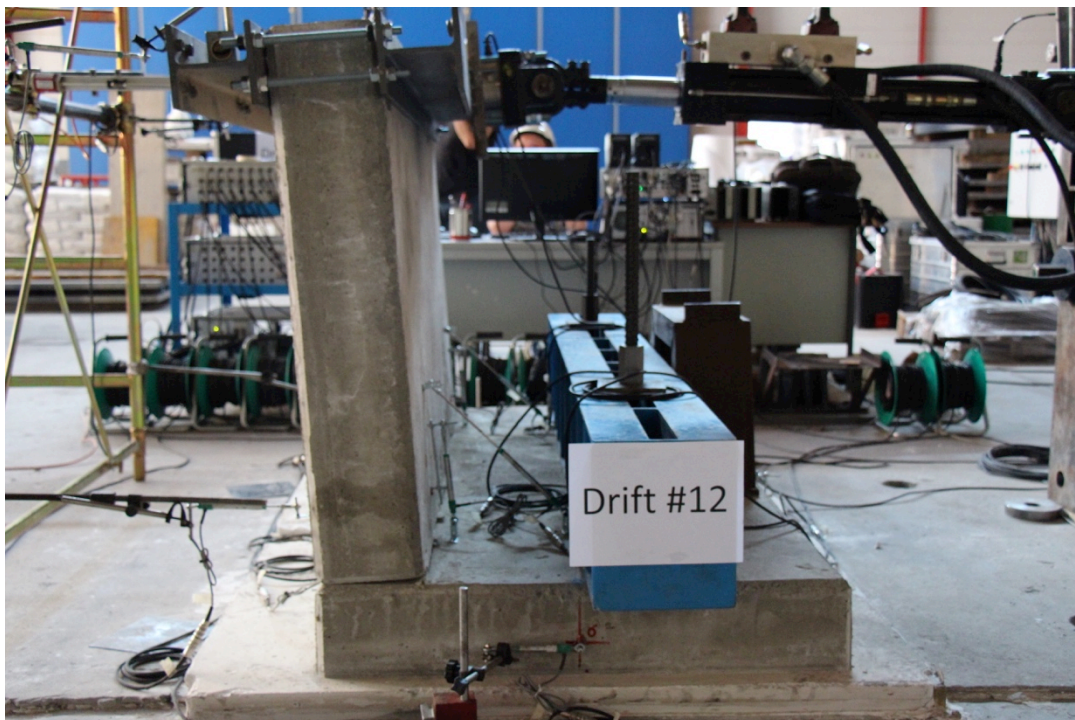**Figure 233: Specimen 10 – capacity curves**

Figure 234: Deformed shape at maximum imposed displacement – Specimen 10

Figure 235: Detail of the crack at the connection level – Specimen 10

Figure 236: Propagation of the crack along the entire width – Specimen 10

Figure 237: Propagation of the crack in correspondence to the connection – Specimen 10

Figure 238: Global view of the damage pattern of panel assembly – Specimen 10

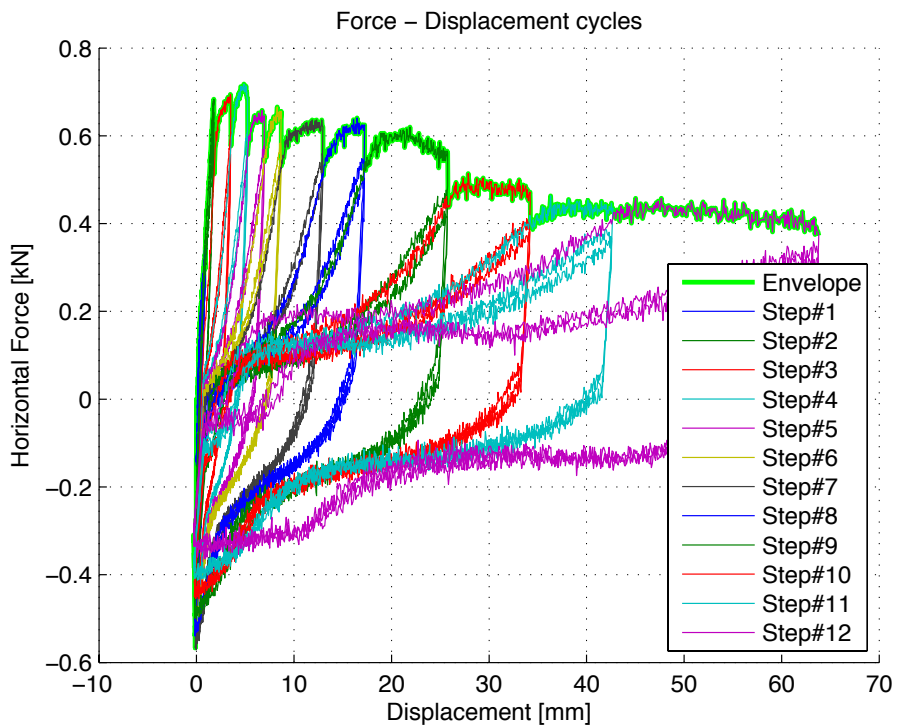**Figure 239: Detail of the crack at the base of panel assembly – Specimen 10**

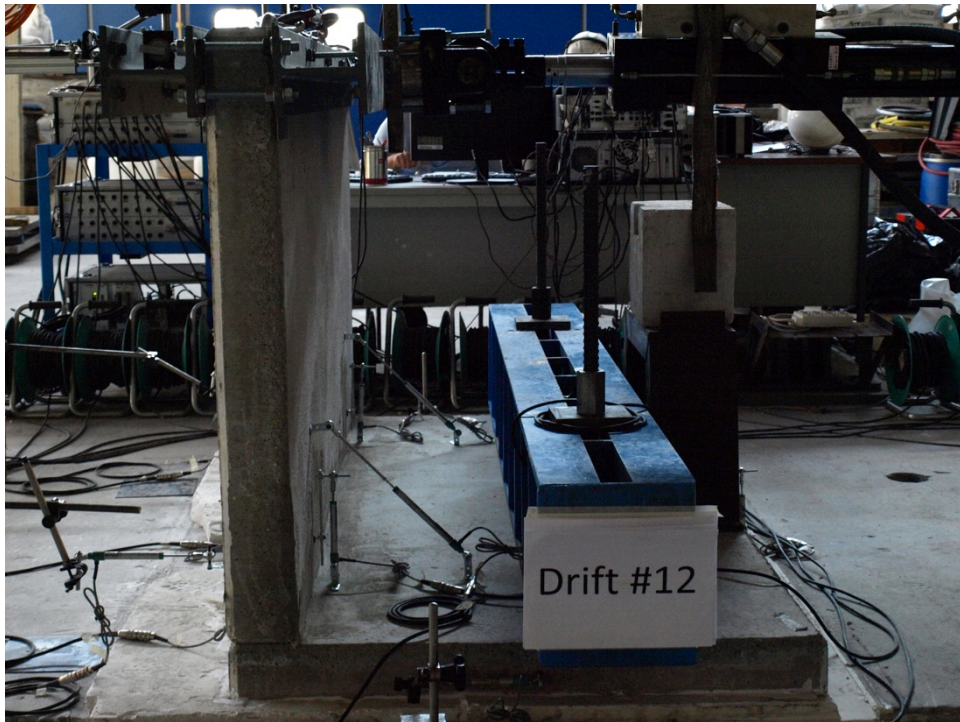**Figure 240: Specimen 11 – capacity curves**

Figure 241: Drift peak imposed during the last cycle of the test – Specimen 11

Figure 242: Side view of the damage at the connection – Specimen 11

Figure 243: Propagation of the crack along the width of panel assembly – Specimen 11

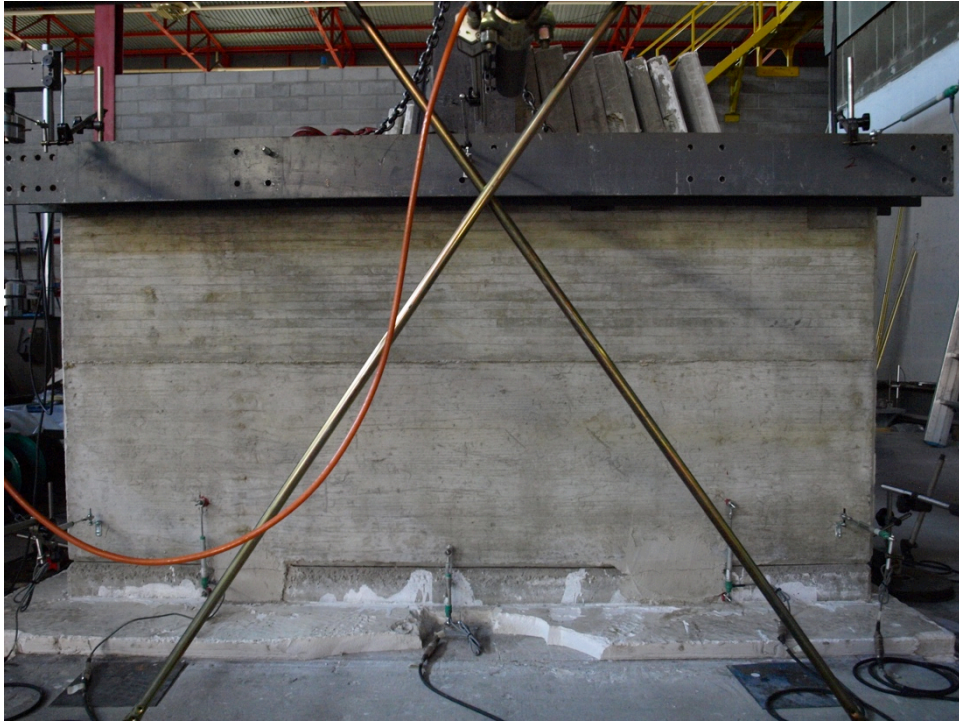**Figure 244: Lateral view of the crack at the base of panel assembly – Specimen 11**

Figure 245: Global view of panel assembly at the end of the test – Specimen 11

Figure 246: Detail of crack propagation along the width – Specimen 11
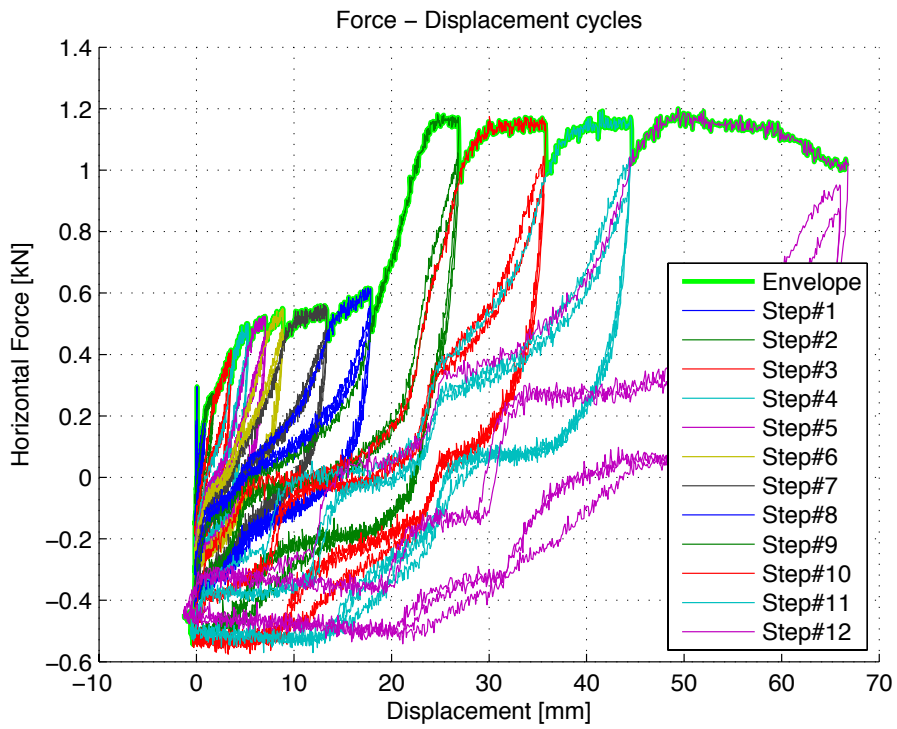
Figure 247: Specimen 12 – capacity curves
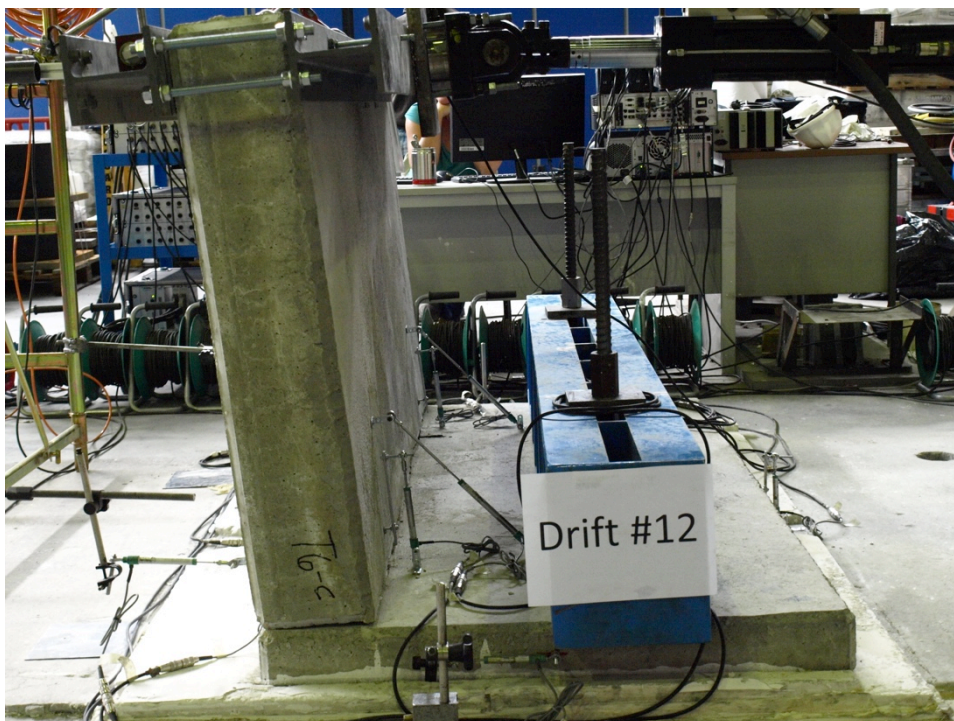
Figure 248: Maximum displacement imposed during the test – Specimen 12

Figure 249: Detail of gap opening at the end of the test – Specimen 12

Figure 250: Detail of gap opening and propagation along the width of Specimen 12 – side view

Figure 251: Crack opening at the connection level – propagation along the width of Specimen 12
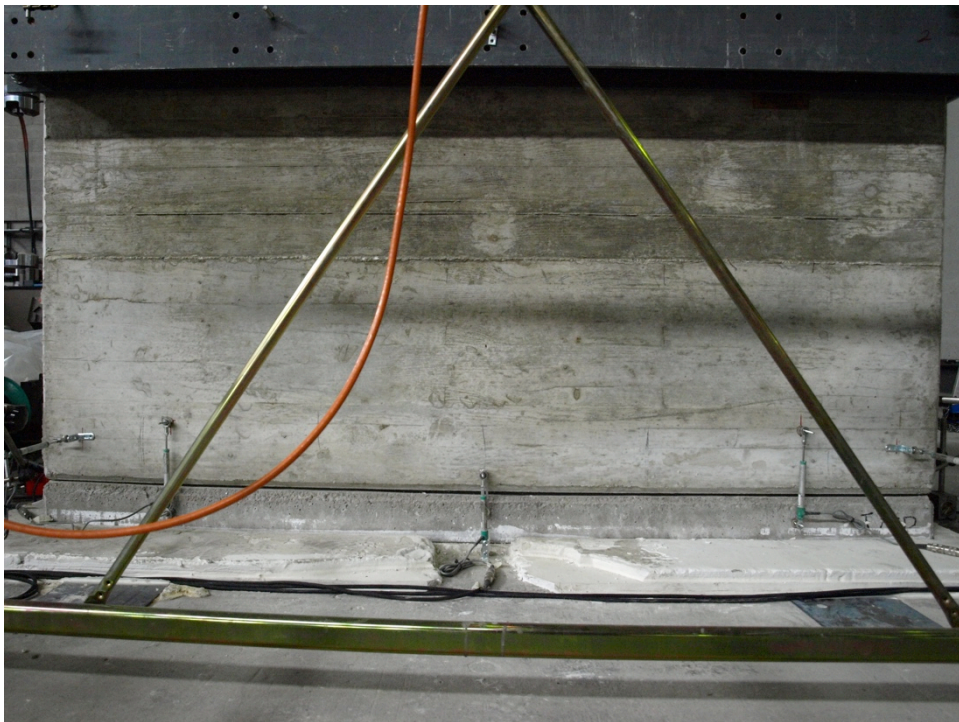

Figure 252: Global view of the damage mechanism at the end of the test – Specimen 12

Figure 253: Detail of detaching between the panels of the assembly – Specimen 12

Figure 254: Minor propagation of cracks in the fixed panel of the assembly – Specimen 12

Figure 255: Detail of crack propagation along the width – Specimen 12

The damage modes collected from Figure 229 to Figure 255 well match the assumption of a pinned connection system. Similarly, the series of capacity curves shown in Figure 228, Figure 233, Figure 240 and Figure 247 are in good agreement with the hypothesis, as an almost negligible bending moment transfer was observed to take place between adjacent panels, regardless their thickness. In particular, moderate capacities in the range 0.7-1.4 kN were obtained experimentally for the assemblies under investigation. In addition to that, the cyclic responses determined are characterized by a low energy dissipation capacity and, in some cases, by evident stiffness and strength degradation. This effect is particularly evident when the ultimate drift target was applied to the connection system.

Hence, the results reported and discussed in this Section will be used in Chapter 7, when calibrating the flexural behaviour of wall-to-wall connection systems thus justifying the assumption used in FE analysis based on which no bending moment transfer was imposed to take place between adjacent panels in correspondence to the steel anchors. More specific information concerning the calibration proposed and validate in compliance with test observations can be found in the upcoming Chapter.

7 Numerical analysis of precast terraced buildings

The main aim of this section is the definition and implementation of specific modeling procedures for quick and accurate seismic response assessment of precast terraced houses typical of past and current Dutch building practice. Once the major assumptions related to the equivalent mechanical representation proposed were identified, the approach was used to predict the experimental response of the 8 full-scale specimens presented in Paragraph 6.2. Hence, a series of pushover analyses were performed and the base shear-roof displacement capacity curves obtained from nonlinear monotonic static simulations were compared to the experimental envelopes presented in Section 6.2.3. After experimental validation, the numerical and modeling outcome of this research on seismic behaviour of reinforced precast concrete panels may be immediately extended and applied to the vulnerability assessment, fragility analysis and strengthening of different structural typologies of precast terraced buildings built with this particular wall-to-wall and wall-to-foundation connection technology.

7.1 Introduction and framework of the investigation

To reproduce the experimental behaviour of the specimens tested at Eucentre laboratory, an equivalent mechanical model, consisting of a set of vertical fiber wall elements in combination with rigid links and nonlinear shear-flexural springs, was constructed in SeismoStruct and, hence, a series of geometrically and materially nonlinear FE simulations were performed in order to validate the numerical approach proposed. Therefore, the response of this structural system with its key components (i.e. wall-to-foundation and wall-to-wall connections) was first studied at a global scale. Even if advantage can be taken of high-definition solid numerical models based on classical principles of nonlinear fracture mechanics in order to investigate the response of precast assemblies, test results are suitable to ensure that all potential modes of failures are accounted in the simplified mechanical representation prepared. Hence, the prevailing characteristics and assumptions related to this spring-based FE idealization will be described and discussed in the following. Furthermore, a direct comparison will be provided between experimental and numerical base shear-top displacement curves to quantify the effectiveness of FE predictions. Finally, numerical curves will be compared to outline behavioral changes in load-bearing capacity and global displacement ductility as a consequence of axial load increments and variations in the geometry (i.e. wall thickness and presence of openings) of these panels, acting as membrane elements (i.e. in-plane shear and axial stresses).

7.2 FE simulations of full-scale single precast panels

As previously mentioned, one of the main objectives of this study is to develop a quick modeling procedure for large-scale nonlinear static analysis of three-dimensional building configurations, combining classical fiber beam-column and spring or multi-spring elements with the FE platform SeismoStruct. In Figure 256, a schematic of the planar representation prepared for seismic response assessment of these lightweight sandwich panels can be observed.
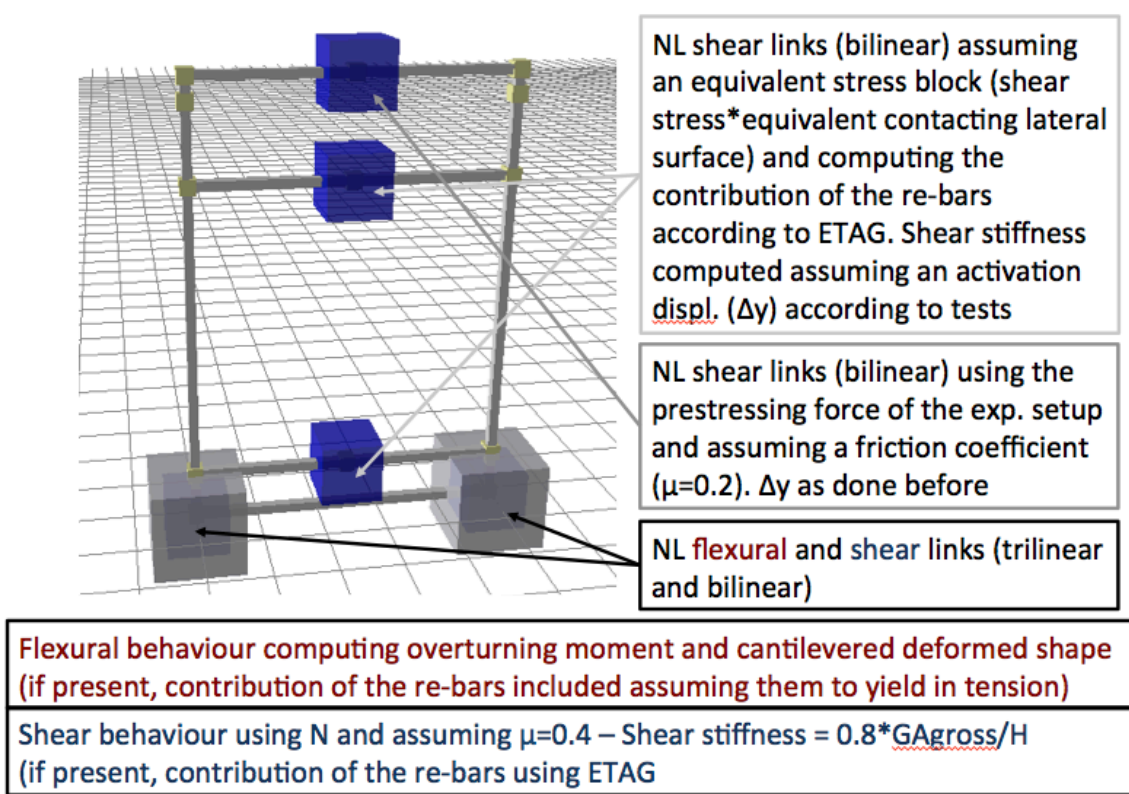
Figure 256: Example of FE representation and assumptions for its calibration

Inelastic fiber beam-column elements were introduced to materialize the geometry of the two panels and then, rigidly connected to each other in correspondence to the steel anchors. A one-to-three correspondence was assumed between structural portions of the panel and model elements along the height in order to place in the model nonlinear springs capable to reproduce the response of wall-to-wall connection systems. Very high stiffness was assigned to rigid members in order to minimize their interaction with the primary elements of the model. Similarly, a nonlinear link was provided at the base of the wall, each of which having specific shear and flexural constitutive laws based on bilinear or trilinear relationships that were used to lump rocking and sliding mechanisms.

The prevailing assumptions introduced for the calibration of this equivalent discrete approach will be specified below.

7.2.1 Modeling approach and computational techniques

The flexural behaviour of the nonlinear spring at the base of each wall was obtained by computing the overturning moment of the system according to basic stability principles. As imposed during the test, a cantilevered deformed shape was assumed to compute the elastic flexural stiffness of the wall system. If present, the contribution of the starter re-bars was included by assuming them to yield in tension. Furthermore, the constitutive law in shear was computed according to basic mechanics of friction. In particular, the shear transfer was determined by multiplying the axial force imposed during the tests times a friction coefficient that was assumed to be equal to 0.4. The shear stiffness of the system was additionally computed by assuming 80% of the gross area of the wall (A_{gross}). In detail, the shear stiffness equals $0.8*G*A_{gross}/H$, where G and H are the shear modulus and height of the wall, respectively. If present, the contribution to shear strength that was provided by the starters

was obtained using ETAG expressions. Even when present, the effects of these bars was found to be minor either in terms of shear or flexural resistance.

While the flexural behaviour of wall-to-wall connections was imposed to be a release in accordance with experimental observations (i.e. no bending moment transfer between adjacent panels), more care was paid to their shear response. In particular, an equivalent stress block-based approach was prepared considering an equivalent portion of the lateral surface as the actual contacting-contacted zone of two adjacent walls. As described in Figure 256, the bilinear constitutive relationship of the nonlinear shear links was obtained assuming an equivalent stress block; an allowable shear stress transferred across the two adjoining walls was obtained on the basis of preliminary detailed models used to calibrate the experimental tests carried out (i.e. 3-4 MPa). Furthermore, the equivalent contact zone across which shear was transferred during rocking mechanism was assumed to be equal to one tenth of the lateral surface of the wall. Finally, the elastic stiffness in shear was determined by assuming a displacement that activates the bilinear branch according to tests (i.e. 2-3 mm). The contribution of the anchors was again computed according to ETAG equations.

Finally, the bilinear constitutive law of the shear link that was introduced where the top beams were imposed not to be continuous in order to force a rocking response of the specimen was again computed using simple friction principles. In detail, the prestressing force of experimental setup was multiplied by a friction coefficient that was assumed in accordance with the mechanical properties of a layer of Teflon that was placed to interrupt the continuity of the top beams (i.e. 0.2).

A classical displacement/rotation-based convergence criterion was adopted to conduct the series of nonlinear static analyses using Hilber-Hughes-Taylor integration scheme to iteratively equilibrate monotonically increased loads.

7.2.2 Monotonic static analysis vs. cyclic pseudo-static tests

The FE idealization proposed was quite effective in reproducing the interaction between shear and flexural response, as presented in Figure 257 where an example of the deformed shape of a panel is collected. In addition, the capacity curves predicted for each specimen are compared to test data in the following plots (i.e. from Figure 258 to Figure 264). The set of base shear-roof displacement capacity curves obtained for the seven specimens tested are then compared in Figure 265. Specimen 01 was omitted therein because of the issue related to the application of the axial load.

As shown in Figure 258, the proposed model was accurate when used to predict the response of the 20 cm thick panels (i.e. Specimen 02). A similar consideration can be drawn for what concerns Specimen 04 (see Figure 260), while a less accurate match is shown in Figure 259 for Specimen 03, the premature failure of which caused the interruption of the test. Quite good estimates were also obtained for specimens presenting a door in their geometry (i.e. Specimen 07 and 08 – see Figure 263 and Figure 264), particularly for Specimen 08 (see Figure 264). By contrast the accuracy of the mechanical FE representation proposed visibly decreased in case of panels with a window (i.e. Specimen 05 and 06 – see Figure 261 and Figure 262), due to a response much more hardened in character.
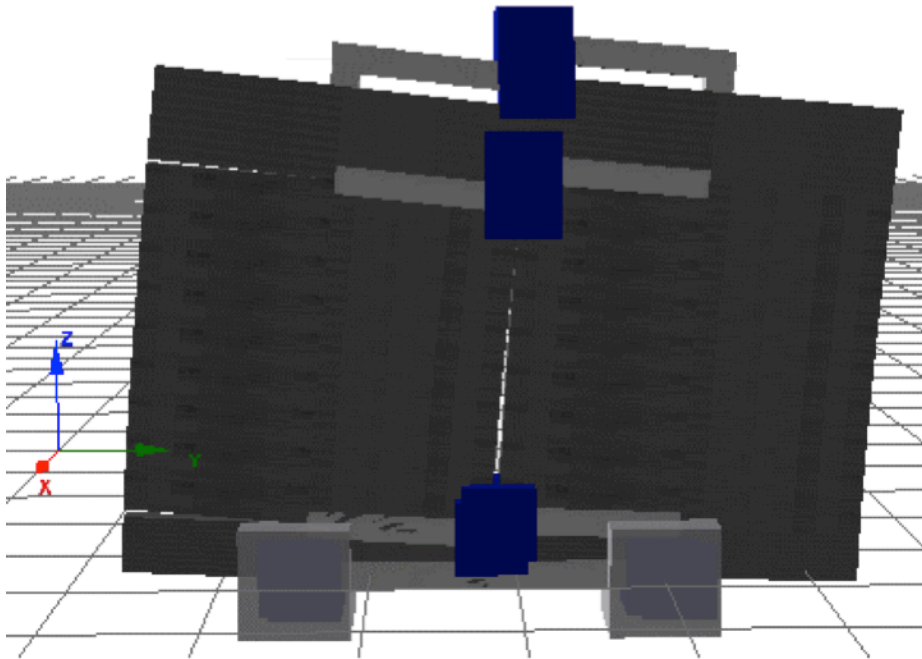
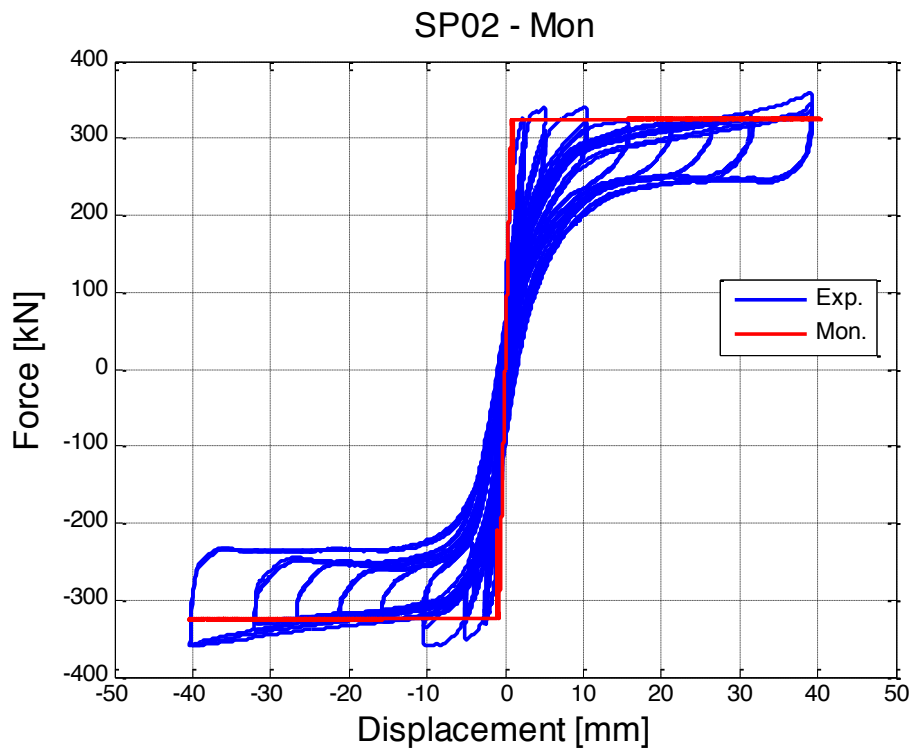**Figure 257: Example of numerical deformed shapes – Specimen 02**

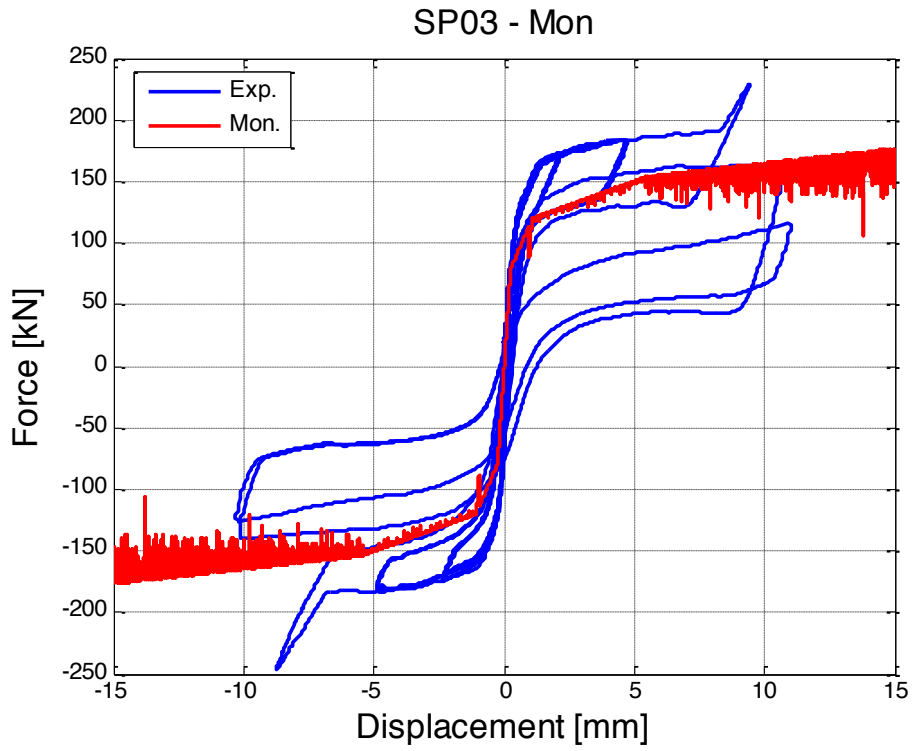**Figure 258: Experimental vs. numerical capacity curves – Specimen 02**

Figure 259: Experimental vs. numerical capacity curves – Specimen 03
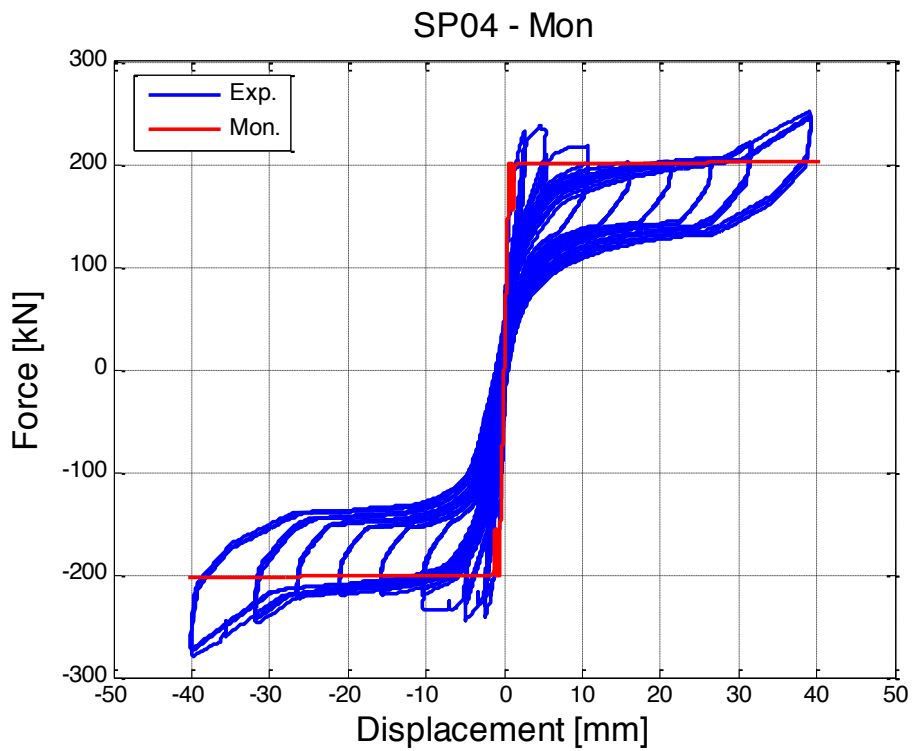

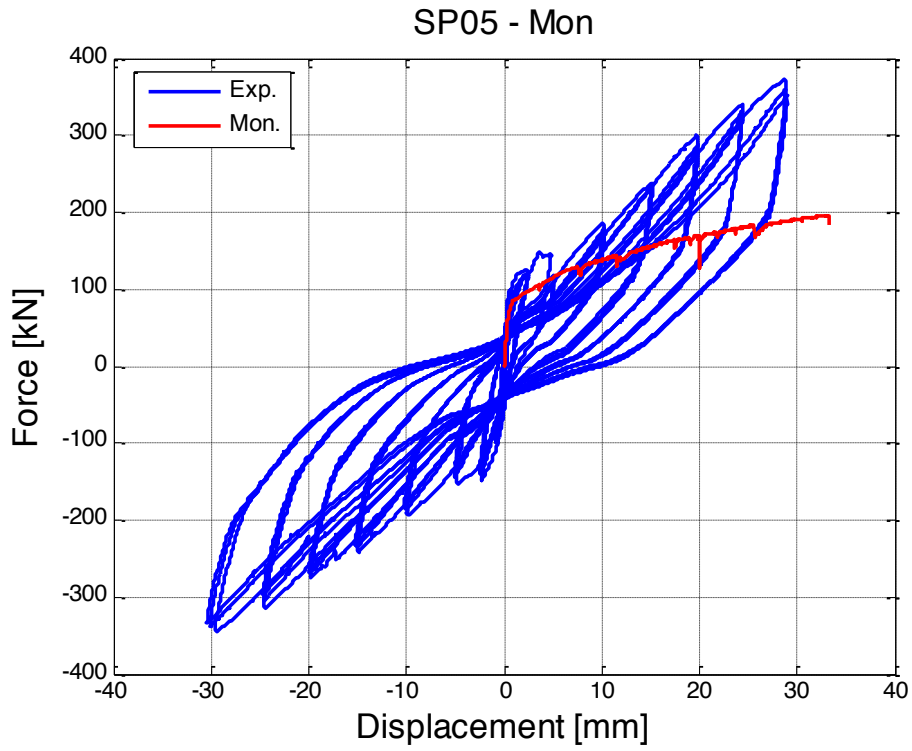**Figure 260: Experimental vs. numerical capacity curves – Specimen 04**

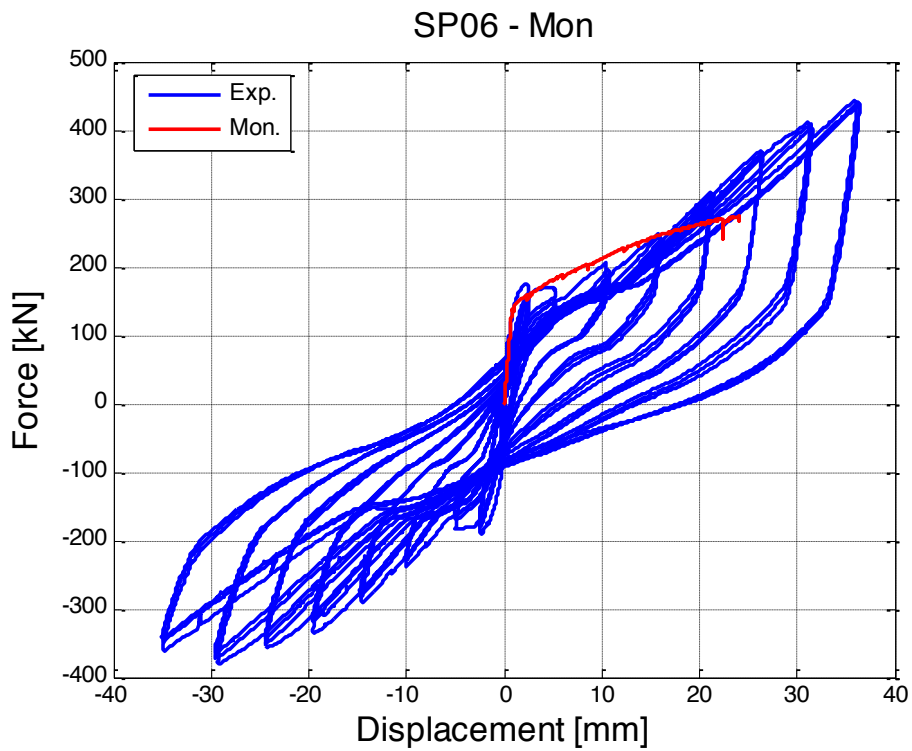**Figure 261: Experimental vs. numerical capacity curves – Specimen 05**

Figure 262: Experimental vs. numerical capacity curves – Specimen 06
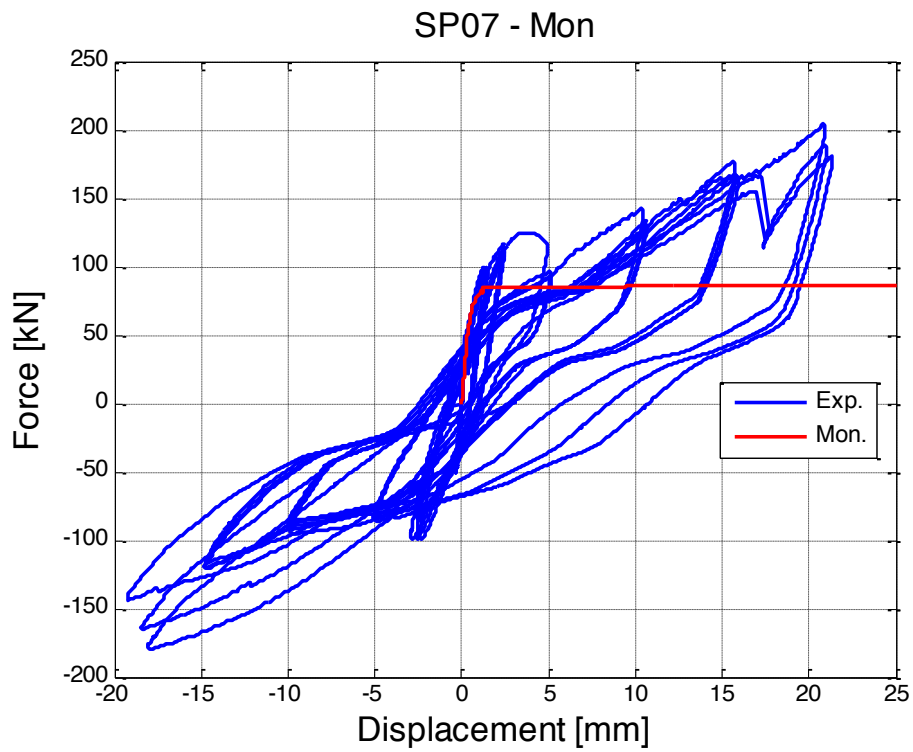
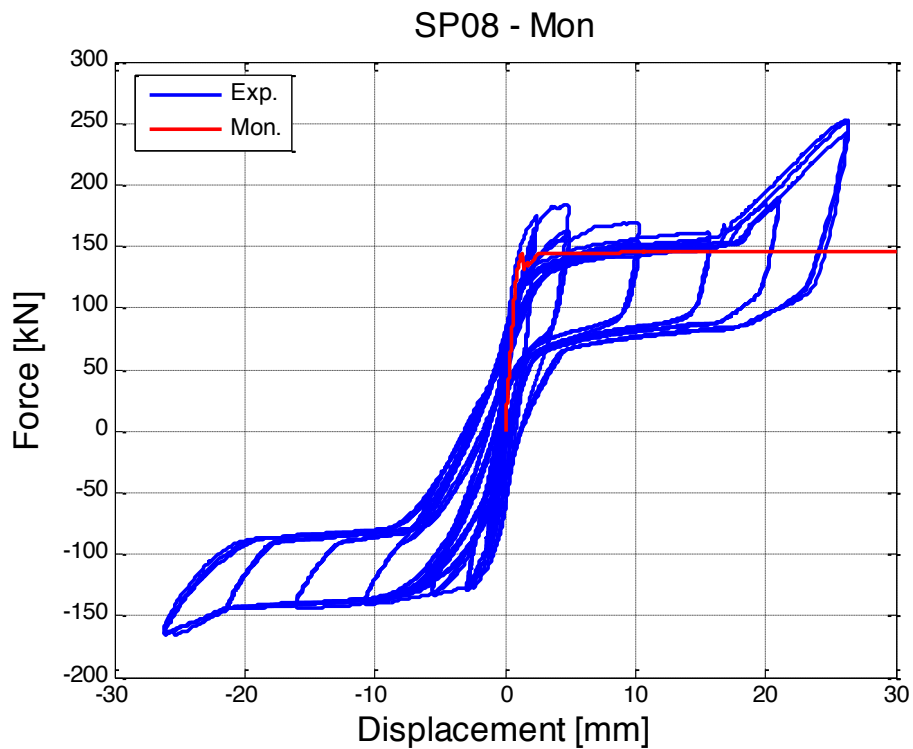**Figure 263: Experimental vs. numerical capacity curves – Specimen 07**

Figure 264: Experimental vs. numerical capacity curves – Specimen 08
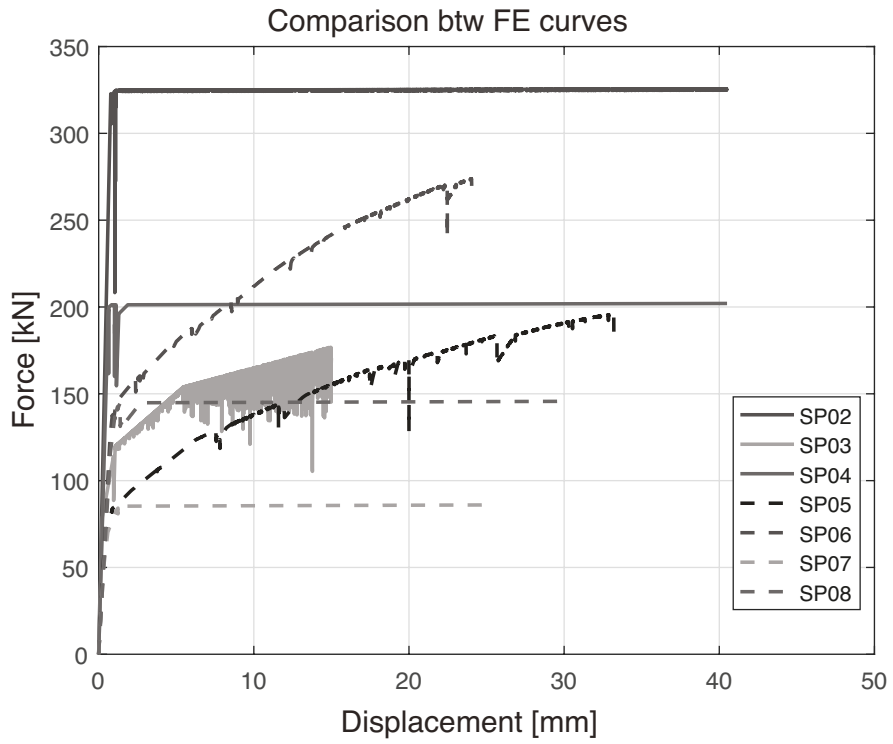
Figure 265: Comparison between numerical capacity curves

8 References

Papers

1. Adalier, K., and O. Aydingun. 2001. Structural engineering aspects of the June 27, 1998 Adana-Ceyhan (Turkey) earthquake. Engineering Structures, V. 23, No.4: pp. 343-355.
2. B.F. Allan, S.K. Chen, R.S. Henry, J.M. Ingham, Experimental testing of precast concrete panel connections, The New Zealand Concrete Industry Conference 2012.
3. Belleri, A., and P. Riva. 2012. Seismic performance and retrofit of precast grouted sleeve connections. PCI Journal, V. 57, No. 1: pp. 97-109.
4. Belleri, A., E. Brunesi, R. Nascimbene, M. Pagani, and P. Riva. 2015. Seismic performance of precast industrial facilities following major earthquakes in the Italian territory. Journal of Performance of Constructed Facilities ASCE, 29(5), 04014135.
5. Belton/Bevlon, Prefab Beton in de Woningbouw, Belton/Bevlon, Woerden,Netherlands, 1997.
6. Bora, C., Oliva, M. G., Dow Nakaki, S., Becker, R. 2007. Development of a Precast Concrete Shear-Wall SystemRequiring Special CodeAcceptance, PCI Journal.
7. Bournas, D. A., P. Negro, and F. J. Molina. 2013a. Pseudodynamic tests on a full-scale 3-storey precast concrete building: Behavior of the mechanical connections and floor diaphragms. Engineering Structures, doi: 10.1016/j.engstruct.2013.05.046.
8. Bournas, D. A., P. Negro, and F. F. Taucer. 2013b. Performance of industrial buildings during the Emilia earthquakes in Northern Italy and recommendations for their strengthening. Bulletin of Earthquake Engineering, doi: 10.1007/s10518-013-9466-z.
9. Brunesi E, Nascimbene R, Bolognini D, Bellotti D. Experimental investigation of the cyclic response of reinforced precast concrete framed structures. PCI Journal 2015; 60(2):57-79.
10. Eligehausen, R., Hoehler, S. M., and Mahrenholtz, P. (2011). Behaviour of Anchors inConcrete at Seismic-Relevant Loading Rates. ACI Structural Journal 108(2): 238-247.
11. Englekirk, R. E. 1982. Overview of ATC seminar on design of prefabricated concrete buildings for earthquake loads. PCI Journal, V. 27, No. 1: pp. 80-97.
12. Englekirk, R. E. 1990. Seismic design considerations for precast concrete multistory buildings. PCI Journal, V. 35, No. 3: pp. 40-51.
13. Englekirk, R. E. 2003. Seismic design of reinforced and precast concrete buildings. Wiley & Sons, New York.
14. Fischinger, M., M. Kramar, and T. Isakovic. 2008. Cyclic response of slender RC columns typical of precast industrial buildings. Bulletin of Earthquake Engineering, V. 6, No. 3: pp. 512-534.
15. Ghosh, S. K., and N. Cleland. 2012. Observations from the February 27, 2010, earthquake in Chile. PCI Journal, V. 57, No. 1: pp. 52-75.
16. Glass, J. 2000. The future forprecast concretein low-rise housing, British Precast Concrete Federation, 2000.
17. Henry, R. and Ingham, J. (2011). Behaviour of tilt-up precast concrete buildings during the 2010/2011 Christchurch earthquakes. Structural Concrete 12(4): 234-240.

18. Holden, T., Restrepo, J., Mander, J. B. 2003. Seismic Performance of Precast Reinforced and Prestressed Concrete Walls Journal of Structural Engineering © ASCE.

19. Iverson, J. K., and N. M. Hawkins. 1994. Performance of precast/prestressed concrete building structures during Northridge earthquake. PCI Journal, V. 39, No. 2: pp. 38-56.

20. Liberatore, L., L. Sorrentino, D. Liberatore, and L. D. Decanini. 2013. Failure of industrial structures induced by the Emilia (Italy) 2012 earthquakes. Engineering Failure Analysis, V. 34: pp. 629-647.

21. Magliulo, G., G. Fabbrocino, and G. Manfredi. 2008. Seismic assessment of existing precast industrial buildings using static and dynamic nonlinear analyses. Engineering Structures, V. 30, No. 9: pp. 2580-2588.

22. Magliulo, G., M. Ercolino, C. Petrone, O. Coppola, and G. Manfredi. 2013. Emilia Earthquake: the Seismic Performance of Precast RC Buildings. Earthquake Spectra, doi: http://dx.doi.org/10.1193/091012EQS285M.

23. McMullin, K. M., Rai, K., Ortiz, M., Kishimoto, T. 2011. Experimental Design and Detailing of a Precast Concrete Test Specimens forBuilding Facade Research, Proceedings of 2011 NSF Engineering Research and Innovation Conference, Atlanta, GA

24. McMullin, K. M., Tai, E. and Ma, T. 2014. Experimental Testing of Precast Concrete Claddingfor Building Facade Systems, San Jose State University.

25. Muguruma, H., M. Nishiyama, and F. Watanabe. 1995. Lessons learned from the Kobe earthquake - a Japanese perspective. PCI Journal, V. 40, No. 4: pp. 28-42.

26. Palermo, M., Ricci, I., Silvestri, S., Gasparini, G., Trombetti, T., Foti, D., Ivorra, S., 2014. Preliminary interpretation of shaking-table response of a full-scale 3-storey building composed of thin reinforced concrete sandwich walls, Engineering Structures 76, 75‑89, Elsevier Ltd.

27. Pavese, A., Bournas, D. A. 2011. Experimental assessment of the seismic performance of a prefabricated concrete structural wall system, Engineering Structures 33, 2049–2062, Elsevier Ltd.

28. Psycharis, I. N., Mouzakis, H. P., 2012. Shear resistance of pinned connections of precast members to monotonic and cyclic loading, Engineering Structures 41, 413–427, Elsevier Ltd.

29. Psycharis, I. N., Mouzakis, H. P., 2012, Assessment of the seismic design of precast frames with pinned connections from shaking table tests, Bull Earthquake Eng, 10:1795–1817, Springer.

30. Restrepo, J. I., Crisafulli, F. J., & Park, R. (1996). Earthquake resistance of structures : thedesign and construction of tilt-up reinforced concrete buildings. Christchurch, N.Z. : Dept. of Civil Engineering, University of Canterbury.

31. Rodríguez, M., and J. Blandón. 2005. Tests on a half-scale two-story seismic-resisting precast concrete building. PCI Journal, V. 50, No. 1: pp. 94-114.

32. Sezen, H., and A. S. Whittaker. 2006. Seismic performance of industrial facilities affected by the 1999 Turkey earthquake. Journal of Performance of Constructed Facilities, V. 20, No. 1: pp. 28-36.

Books

33. FIB (FédérationInternationale du Béton), "Seismic design of precast concrete building structures", Bulletin 27, pp. 262, 2003.

34. FIP - Fédération Internationale de la Précontrainte, "FIP handbook on practical design: Examples of the design of concrete structures", pp. 192, 1990.
35. FIB. 2008. "Structural Connections for Precast ConcreteBuildings." Bulletin 43. Lausanne, Switzerland: fib.

Codes

36. European Committee for Standardisation – EN 1992: (Eurocode 2) Design of concrete structures
37. European Committee for Standardisation – EN 1998: (Eurocode 8) Design of structures for earthquake resistance
38. European Organization for Technical Approvals (EOTA), ETAG 001 Guideline for European technical approval of metal anchors for use in concrete, Annex C: Design methods for anchorages, 2010.
39. U.S. Departement of Homeland Security – FEMA P – 751: NEHRP Recommended Sesimic Provisions for New Buildings and Other Structures, 2009 edition.

Websites

40. www.alvon.nl
41. http://www.calduran.nl/
42. www.calduran.be
43. http://www.crhstructural.nl/
44. www.dycore.nl
45. www.heembeton.nl/